Fuel Consumption Estimation and Analysis of the University of Alberta Fleet Vehicles

by

Amir Ansari

A thesis submitted in partial fulfillment of the requirements for the degree of

Master of Science

Faculty of Engineering Department of Department of Mechanical
University of Alberta

Abstract

This thesis aims to create a platform to estimate and monitor the University of Alberta (UAlberta) fleet vehicles' fuel consumption and Carbon Dioxide (CO_2) emissions. The main objective is to collect and analyze fleet vehicles information to reduce energy consumption and greenhouse gas emissions from university vehicles. To this end, this thesis creates a data collection platform for real-time monitoring and analysis of fleet activity, utilizing onboard diagnostics (OBD) data from each vehicle. By processing the collected data, this thesis seeks to identify the causes of high fuel consumption in the fleet and determine the optimal vehicle type for different applications and driving cycles.

Two machine learning methods, including random forest (RF) and artificial neural network (ANN), were investigated to estimate fuel consumption based on OBD and actual fuel consumption data. The study used data from a Ford Escape plug-in hybrid electric vehicle (PHEV) and a Ford F-350 vehicle during real-world urban and highway driving on a 100-km route. The machine learning models utilized OBD parameters such as engine load, engine speed, intake manifold absolute pressure, air-fuel equivalence ratio, and throttle position. The validation results indicated that the RF model was more accurate than the ANN model, achieving an estimation accuracy of 99% for the Ford Escape PHEV and 100% for the Ford F-350. These findings confirm that utilizing machine learning models can effectively estimate vehicular fuel consumption; thus, these models can be used to monitor fleet vehicles' energy consumption, and design strategies to reduce the fuel consumption from the UAlberta fleet vehicles.

Additionally, this thesis investigated the energy consumption and cost of a conventional vehicle (Ford Escape S) with an internal combustion engine (ICE) and a PHEV (Ford Escape PHEV) from the UAlberta fleet. The vehicles were driven 243 times on a 20-km route in Edmonton, Canada, during 2021 - 2022. The route included both urban and highway areas. The research also explored the impact of ambient temperature (T_{amb}) on the operations and energy consumption of the vehicles, considering different powertrains and electrification levels. This study reveals that for warm start tests, the total energy consumption increased by decreasing the T_{amb} from 32 °C to -24 °C. Modes that entail continuous operation of the electric motor are especially affected. Among the modes, Auto EV (i.e., electric and hybrid electric) mode demonstrated the highest increase in energy consumption, rising by almost 452% when the T_{amb} drops from 29°C to -24°C. Similarly, during cold start tests, there was an increase in energy consumption as the T_{amb} decreased from 29 °C to -18 °C. The mode that showed the highest increase in energy consumption was EV Now (i.e., all-electric) mode, with an increase of 527% by reducing the T_{amb} from 29 °C to -13 °C.

The thesis also examined the effect of start-stop technology on conventional vehicles' energy consumption and operational costs. To conduct the study, three vehicles from the UAlberta fleet were tested, and the effect of start-stop technology was evaluated on four different applications of UAlberta fleet vehicles. The findings indicated that the energy and cost savings achieved by vehicles equipped with start-stop technology could be significant, depending on the vehicle drive cycle and idling percentage, as well as engine size. The fuel savings are anticipated to increase during the cold season operation of fleet vehicles.

INDEX Terms- Instantaneous Fuel Consumption, Machine Learning, Artificial Neural Networks, Random Forest, Real-world Driving Data Powertrain Modes, Energy Consumption, Energy Cost, CO_2 Emissions, Start-Stop Technology.

Preface

This thesis is an original work by Amir Ansari. The research was conducted using various UAlberta fleet vehicles, a brand new model year (MY) 2021 Ford Escape PHEV, and the experimental setup of data collection equipment in the University of Alberta Energy Mechatronics Laboratory (EML) led by Dr. Shahbakhti.

All data in this thesis was collected by myself and analyzed for the conclusions in this thesis. Each chapter is partially based on published or submitted papers in peer-reviewed journals, conference procedures, and technical presentations.

I contributed to Hamidreza Abediasl in " Real-time Fuel Consumption Estimation using Machine Learning and On-board Diagnostics Data " Peer Reviewed Journal Paper [1].

I was the lead author of the Peer Reviewed Journal Paper, contributed by Hamidreza Abediasl in " Ambient Temperature Effects on Energy Consumption and CO_2 Emissions of a Plug-in Hybrid Electric Vehicle "[2], used to write chapter four of this thesis. In that work, I was responsible for doing the driving tests and collecting and analyzing the data.

I was the lead author of the conference proceeding paper, contributed by Hamidreza Abediasl and Parth Pataal Rakeshkomomar in the " Estimating Instantaneous Fuel Consumption of Vehicles By Using Machine Learning And Real-Time On-Board Diagnostics (OBD) Data " article [3].

Also, I contributed to Liu Yang's " Identification of the Driving Cycle for University Fleet Vehicles " article [4] used to write chapter two of this thesis and " Characterizing Driving Behavior and Link to Fuel Consumption for University Campus

Shuttle Minibuses " [5] conference proceeding papers. In that work, I was responsible for doing the driving tests and collecting and analyzing the data.

In addition, I was the lead author of the technical presentation paper, contributed by Hamidreza Abediasl in " Effect of Cold Climate on Energy Consumption of a Plug-in Hybrid Electric Vehicle " [6] used to write chapter four of this thesis.

The University of Alberta Transportation Services, led by Jim Laverty, supported this thesis by assisting in the fuel measurement equipment setup for the tested vehicles.

Random Forest (RF) and Artificial Neural Network (ANN) machine learning models to estimate fuel consumption were developed by me, Parth Rakeshkumar Patel, and Hamidreza Abediasl.

I, along with Everett Stewart and Jashwanth Reddy Sarikonda, developed a software platform for real-time data collection from UAlberta fleet vehicles.

Hamidreza Abediasl reviewed Chapter Five of this thesis and provided feedback to improve results and discussion.

The drive cycles used in Chapter Five of this thesis are based on an extensive study done by Liu Yang (see MSc thesis [5]).

To My Wife and Family

Acknowledgements

I would also like to express my sincere gratitude to Dr. Mahdi Shahbakhti, Associate Professor of Mechanical Engineering at the University of Alberta, for allowing me to participate in the Energy Management and Sustainable Operation (EMSO) project. I thank him for his support and guidance throughout this project.

I would like to express my gratitude to the Campus Sustainability Grant by EMSO that financially supported the experimental and analysis works done in this thesis.

I want to thank my wife, Elahe Nouri, my parents, my sister, and my brother-in-law for their support and patience.

Furthermore, I would like to thank Jim Laverty, Fleet Manager, University of Alberta, and his team for their support throughout my project.

Finally, I would like to thank my colleagues Hamidreza Abediasl and Liu Yang, who contributed to the successful completion of my project.

Amir Ansari October, 2023

Table of Contents

List of Tables

List of Figures

Abbreviations

24/7 Available at any time.

AC Air Conditioning.

AER All-Electric Range.

AGM Absorbed Glass Mat.

ANN Artificial Neural Network.

API Application Programming Interface.

AWD All-Wheel Drive.

B Bank.

CAN Controller Area Network.

CEP Circular Error Probability.

CMEM Comprehensive Modal Emission Model.

CO2 Carbon Dioxide.

CSJ Campus Saint-Jean.

CSV Comma Separated Values.

DC Direct current.

EC Energy Consumption.

ECU Electronic Control Unit.

EFB Enhanced Flooded Battery.

EGR Exhaust Gas Recirculating.

EML Energy Mechatronics Laboratory.

EMSO Energy Management and Sustainable Operation.

EPA Environmental Protection Agency.

EV Electric Vehicle.

FWD Front-Wheel Drive.

GHG Greenhouse Gas.

GNSS Global Navigation Satellite System.

GPS Global Positioning System.

GRNN Generalized Regression Neural Network.

GUI Graphic User Interface.

HAPMS Highways Agency Pavement Management System.

HEV Hybrid Electric Vehicle.

HTTP Hypertext Transfer Protocol.

HVAC Heating, Ventilation and Air Conditioning.

HWFET Highway Fuel Economy Test.

IDE Integrated Development Environment.

i-PTM Integrated Power and Thermal Management.

ICE Internal Combustion Engine.

INL Idaho National Laboratory.

IP Internet Protocol.

ISO International Organization for Standardization.

IST Information Service and Technology.

JSON JavaScript Object Notation.

KNN k-Nearest Neighbors.

KWP2000 Keyword Protocol 2000.

LDV Light-Duty Vehicle.

LF Low Flow.

LRT Light Rail Transit.

MAF Mas Air Flow.

MIL Malfunction Indicator Light.

MY Model Year.

NEDC New European Driving Cycle.

NGS Next Generation Simulation.

NINT National Institute of Nanotechnology.

OBD On-Board Diagnostic.

PDS Power Distribution System.

PHEV Plug-in Hybrid Electric Vehicle.

PID Parameter Identification.

PTC Positive Temperature Coefficient.

PWM Pulse Width Modulation.

RAM Random Access Memory.

RDE Real Driving Emission.

ReLU Rectified Linear Unit.

RF Random Forest.

RFCR Real-world Fuel Consumption Rate.

RMSE Root Mean Square Error.

RPM Revolutions Per Minute.

RTC Real-Time Clock.

S Sensor.

SAE Society of Automotive Engineers.

SD Secure Digital.

SOC State of Charge.

SPC Supervisory Powertrain Controller.

SQL Structured Query Language.

SUV Sports Utility Vehicle.

SVM Support Vector Machine.

TMS Thermal Management System.

TWC Three-Way Catalyst.

UAPS University of Alberta Protective Service.

UDDS Urban Dynamometer Driving Schedule.

VPM Variable Pulse Modulation.

VRP Vehicle Routing Problems.

VSC Visual Studio Code.

VSP Vehicle Specific Power.

VT-Micro Virginia Tech Microscopic.

Wi-Fi Wireless Fidelity.

List of Symbols

Variables

$\dot{F}$ Mass flow rate of gasoline (kg/s)

η Fuel conversion efficiency (-)

λ Air-fuel equivalence ratio (-)

$\tilde{x_s}$ Normalized data

T_D Total distance required to achieve an ROI for the PHEV (km)

x Original data

XSE_A Energy costs for Auto EV powertrain mode (¢/km)

XSE_L Energy costs for EV Later powertrain mode (¢/km)

XSE_N Energy costs for EV Now powertrain mode (¢/km)

Z_A Difference in energy costs between the Ford Escape S and Auto EV powertrain mode (¢/km)

Z_L Difference in energy costs between the Ford Escape S and EV Later powertrain mode (¢/km)

Z_N Difference in energy costs between the Ford Escape S and EV Now powertrain mode (¢/km)

gCO2/kWh CO2 emission intensity

LHV_g Lower heating value of gasoline (MJ/kg)

NO_x Nitrogen Oxides (ppm)

P_b Engine brake power (W)

P_g Gasoline output power (W)

R^2 Coefficient of determination

S_e Engine speed from OBD (Rad/s)

T_e Estimated engine torque from OBD (Nm)

XS Energy cost for the Ford Escape S (¢/km)

Chapter 1

Introduction

This chapter provides the background information, literature review, scope, and goals of this thesis.

1.1 Motivation

The University of Alberta (UAlberta) manages a fleet of more than 180 vehicles, including sedans (compact and intermediate), sports utility vehicles (SUVs), trucks, vans, and buses. These vehicles are used for various purposes, such as passenger transportation, cargo transportation, police/security operations, and other applications.

The fleet consumes approximately 205,000 liters of fuel annually, emitting 564,291 kg of Carbon Dioxide (CO_2) greenhouse gases (GHG).

The powertrains of the fleet vehicles consist of conventional (gasoline and diesel), hybrid electric vehicles (HEV), and plug-in hybrid electric vehicles (PHEVs). Therefore, the university fleet vehicles include a mix of different types of vehicles with varying levels of fuel conversion efficiency and emissions profiles.

Each vehicle in the fleet is assigned to a specific application, such as passenger vans, cargo vans, police/security vehicles, passenger sedans/SUVs, trucks (crew and cargo), and buses. To this end, the fleet is diverse regarding vehicle types and usage scenarios, catering to different operational needs and requirements.

Intelligent management of the university fleet vehicles presents opportunities for implementing strategies to improve fuel conversion efficiency, reduce emissions, and optimize vehicle usage based on their specific applications. Some of these strategies may include:

i) Identification of energy-saving opportunities by identifying inefficient driving patterns, identifying unnecessary idling times, optimizing routes, and exploring alternative fuels or technologies.

ii) Short-term and long-term fleet renewal plan development to maximize the fleet's transport efficiency and reduce fuel consumption. This involves vehicle replacement strategies, exploring alternative fuel options, and implementing vehicle technologies that improve fuel efficiency.

iii) Real-time monitoring of fuel consumption to provide feedback to drivers and fleet managers on fuel usage patterns and areas for improvement. This involves using telematics, Global Positioning System (GPS), and other technologies to collect and analyze real-time fuel consumption data.

iv) Developing practical and reliable methods for estimating fuel consumption and tailpipe emissions of fleet vehicles, using available sensor data, vehicle parameters, and other relevant information to estimate fuel consumption and emissions in real time accurately.

v) Fleet operational cost reduction by exploring strategies to reduce fleet operating costs through optimum fleet assignments and other operational strategies. This may involve developing tools or software for fleet management to optimize fleet operations and reduce costs.

Figure 1.1 illustrates different factors influencing a vehicle's energy consumption and CO_2 emission. This thesis investigates the effect of vehicle technology and the environment (winter vs summer) on vehicular energy consumption and CO_2 emission. In particular, this thesis aims to provide contributions in the following areas:

1. Establishment of a framework to estimate fuel consumption from each individual

vehicle in the university fleet, using available On-Board Diagnostic (OBD) data.

2. Assessment of ambient temperature (T_{amb}) on the performance of vehicles with different levels of electrification.

3. Effect of start-stop technology on fuel and cost savings from university vehicles. This helps the university fleet manager to make an informed decision for including or excluding the start-stop option and associated cost in the future purchases of the university vehicles based on their applications.

In the following section, a review of the literature in the three contribution areas of this thesis is provided.

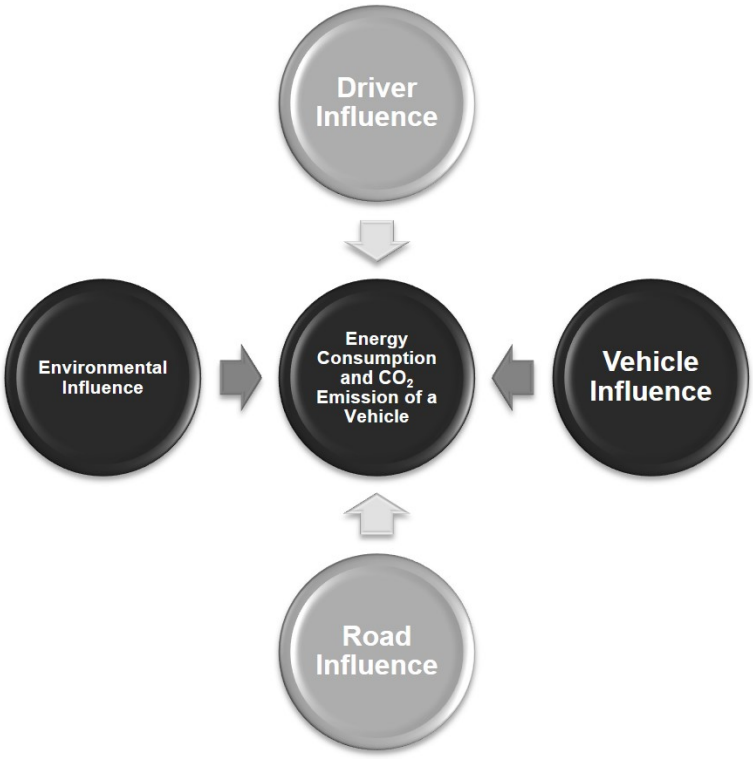

Figure 1.1: The factors that influence on energy consumption and CO_2 emission of a vehicle. The dark circles show the areas for the focus of this thesis.

1.2 Literature Review

1.2.1 Fuel Consumption Estimation of Fleet Vehicles

Different vehicle technology types can affect a fleet's energy consumption, operational costs, and CO_2 emissions. Figure 1.2 illustrates the distribution of Light-Duty Vehicle (LDV) sales by technology or fuel in the United States [7]. The data shows that gasoline-powered vehicles are still the most commonly used technology, followed by HEVs. Over the past few years, electric vehicles (EVs) have become increasingly popular due to the technology development and the substantial decline in the costs of batteries [8].

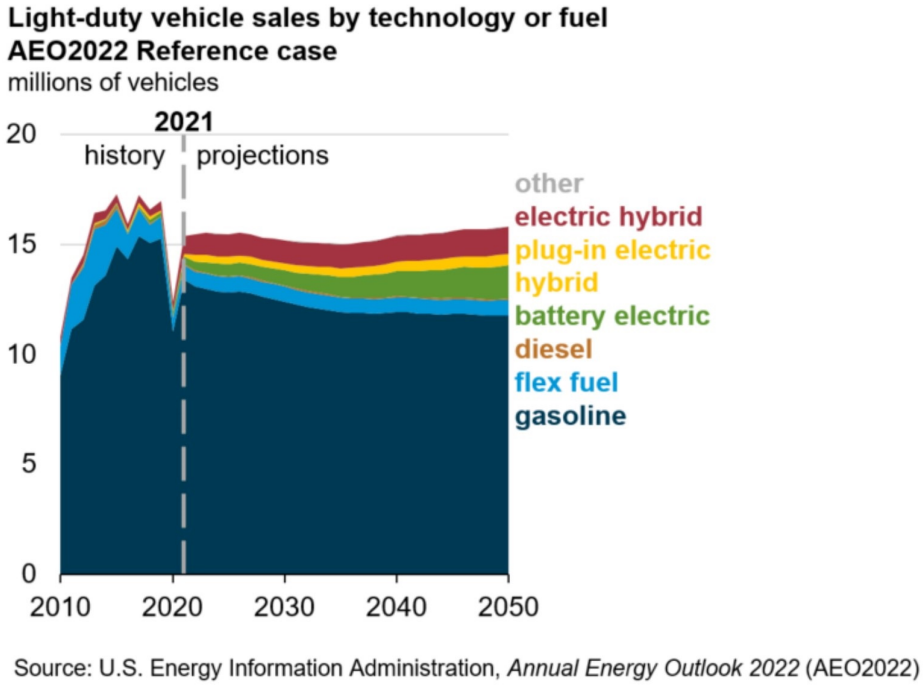

Figure 1.2: LDV sales by technology or fuel in the U.S. [7]

A model for fleet management was developed in [9] based on an efficient and high-precision fuel consumption estimation. The model used information about the elevation variations and destination of the trip, weather conditions, vehicle characteristics, and driver's behavior. The model can be used to find the most economical itinerary for fleet vehicles.

As part of the transportation fleet to cover different market sections, companies are interested in having vehicles that suit the type of goods transported, which means a fleet with vehicles of varying load and capacity. A multi-objective model based on Tchebycheff methods was developed in [10] for Vehicle Routing Problems (VRP). Vehicle capacities, costs, and emissions were the factors considered in the model to minimize the total internal costs, CO_2 and Nitrogen Oxides (NO_x).

Instantaneous vehicle speed influences emissions and fuel consumption. Analyzing the acceleration, cruising, deceleration, and idling based on time, distance, and average fuel consumption and emission factors showed that the aggressive modes are more polluting than steady-speed driving modes. In addition, driving at a low speed (i.e. V$<$ 32 km/h)[11] contributes to a high percentage of total emissions. Minimizing vehicle stops in urban areas to smooth driving, acceleration, and deceleration will help to reduce fuel consumption and emissions [12].

Individualized machine learning methods were developed based on the distance for fuel consumption of heavy vehicles. Vehicle speed and road grade are the parameters that were used to produce a predictive neural network model. This method can be deployed for each vehicle in a fleet to optimize fuel consumption over the whole fleet [13].

A fuel consumption machine learning model was developed to choose the route based on road geometry. Support Vector Machine (SVM), Random forest (RF), and Artificial Neural Network (ANN) models were used. The data set was from the collected data of the fleet truck's telematics system and the road, vehicle characteristic data from the Highways Agency Pavement Management System (HAPMS) of Highways England. Results showed that the RF model has the highest accuracy for fuel consumption prediction of the fleet trucks [14].

An approach was developed for estimating truck fuel consumption based on a Generalized Regression Neural Network (GRNN) model. The proposed model was compared with the Vehicle Specific Power (VSP) model, the Virginia Tech Microscopic

(VT-Micro) model, and the Comprehensive Modal Emission Model (CMEM). The result showed the model has a strong performance in predicting fuel consumption [15].

Fuel consumption of a vehicle depends on the vehicle and external factors. However, some factors may not be available for the fuel consumption analysis. The machine learning model was developed by learning the patterns in data for these cases. Based on the results, the RF technique produced a more accurate prediction than gradient boosting and neural networks [16].

A Real-world Fuel Consumption Rate (RFCR) model was developed to estimate the fuel consumption of 201 brands of vehicles in 34 cities in different areas of China. According to the results, the use of manual transmission and the reduction of the use of air conditioning (AC) can reduce the energy consumption of the investigated vehicles [17].

Instantaneous fuel consumption was estimated by using smartphones and an OBD-II data logger. To this end, two models were used. Powertrain-based model, based on the engine's fuel injection rate, and vehicle dynamics-based model, regarding the mechanical work applied on a vehicle. The results showed the average difference between the models' estimation and the actual fuel consumption was about 6% [18].

In Brazil, a mobile application was developed to encourage the reduction of fuel consumption. The application used fuzzy logic and vehicle data was read from an OBD-II Bluetooth device (ELM 327). The collected parameters were analyzed, and the instantaneous fuel consumption was estimated. On real-world tests, an accuracy of more than 85% was obtained [19].

A modal was developed in [20] to estimate the energy/emissions of the vehicle based on sparse mobile sensor data. Acceleration, deceleration, cruising, and idling are considered driving modes. The vehicle energy/emissions factors are estimated based on operating mode distributions reconstructed by a rate of 1 Hertz (Hz). When the Next Generation Simulation (NGS) data set is compared with the linear interpolation

model, NGS performs better on vehicle energy/emissions estimation.

1.2.2 Effect of Ambient Temperature on Energy Consumption of Conventional Vehicles and PHEVs

The shift towards EVs and HEVs for light-duty applications is well documented [21, 22]. Using electricity produced from sustainable sources leads to no emissions from EVs (Tailpipe emissions). Therefore, these types of vehicles have significant environmental benefits such as zero tailpipe emissions, easy driving, particularly in stop-start, quiet driving, and economical fuel costs.

PHEVs have an electric motor and an internal combustion engine (ICE), and their CO_2 emissions depend on the proportion of driving done in all-electric mode versus using the ICE. Longer All-Electric Range (AER) can result in higher electric driving percentages and lower overall CO_2 emissions. However, the energy consumption and CO_2 emission reduction of these vehicles in extremely cold T_{amb} is understudied.

Figure 1.3 illustrates the global average temperature during winter in the Northern Hemisphere, revealing that a significant portion of the world's population experiences temperatures below -7 °C. In North America, the Federal Test Procedure (FTP) is used for emission certification and fuel economy tests of LDVs, the coldest temperature covered in the cold phase of the FTP being 20 °F (approximately -7 °C) [23]. Similarly, the European Real Driving Emission (RDE) test covers T_{amb} as low as -7 °C [24]. Many Canadian cities experience temperatures below -7 °C during winter. This thesis reports the energy consumption and CO_2 emission results of a PHEV with different levels of electrification in T_{amb} as low as -24 °C.

Battery electric powertrains have the potential to significantly reduce air pollutant emissions generated by combustion and lower CO_2 emissions, primarily when powered by renewable energy sources. However, the effectiveness of electric powertrains in reducing CO_2 emissions depends on multiple factors, including the carbon intensity of electricity production at the source and the real world performance of the vehicle.

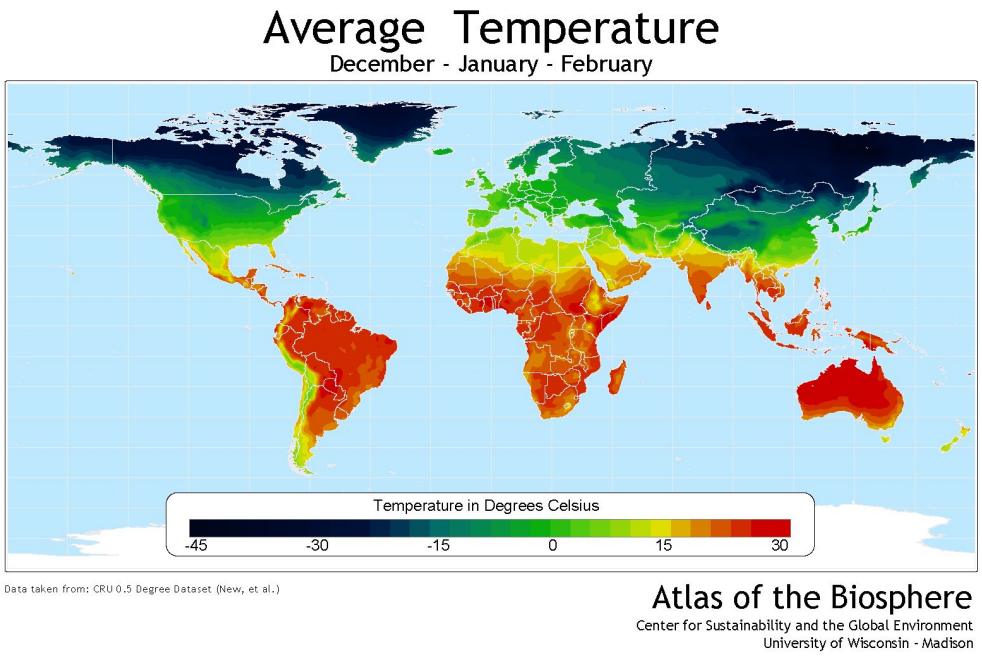

Figure 1.3: Global average temperature of December, January, and February [23]

Reducing CO_2 emissions from shifting towards electric powertrains may be limited in regions with predominantly carbon-intensive electricity production. The carbon intensity of electricity production varies geographically and is influenced by the mix of energy sources used for electricity generation in different regions. For example, in Alberta, Canada, where only 15% of electricity is generated from renewable and zero-carbon sources of energy [25], the benefits of electric powertrains compared to ICEs need to be carefully studied, particularly considering the extreme winter conditions in Alberta.

The fuel cost of driving an electric vehicle depends on the cost of electricity per kilowatt-hour (kWh) and the vehicle's energy efficiency. In addition, the fuel cost of a conventional vehicle with an ICE depends on the costs of gas and fuel consumption. According to the Idaho National Laboratory (INL) comparison of energy costs per mile for electric and gasoline-fueled vehicles in the U.S. (Figure 1.4), the fuel for an electric vehicle with an energy efficiency of 3 miles (4.83 km)/kWh costs about 3.3

¢/mile, when electricity costs 10 ¢/kWh [26].

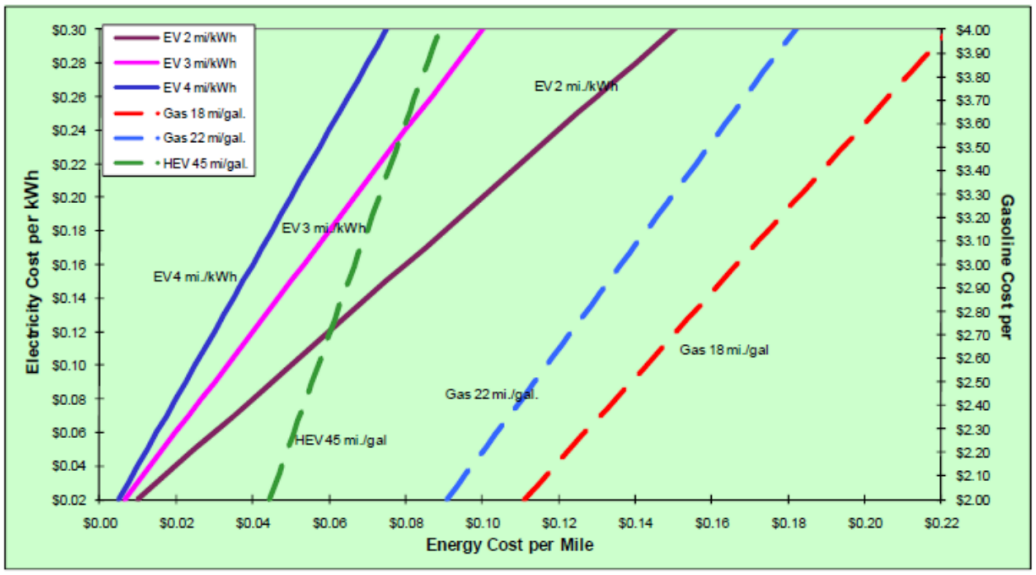

Figure 1.4: Comparing energy costs per mile for electric and gasoline-fueled vehicles based on INL data [26]

A study conducted in [27] developed an engine model that can predict the influence of cold battery and engine temperatures on the fuel and electric consumption of a power-split PHEV with a Prius powertrain. The engine model considers engine utilization history and starting temperature to calculate engine fuel rate. According to the results, the cold temperature significantly impacts engine efficiency and battery power restrictions, resulting in higher fuel and electrical energy consumption for a PHEV.

Low ambient temperatures have a negative effect on powertrain performance, charging time, distance range, and costs. In the study by Ghobadpour, et.al.[28], the effect of cold temperatures on the performance of the PHEV components, road conditions, and charging infrastructure was studied to improve efficiency and energy consumption. The study found that PHEVs were a better choice than EVs for cold climates.

PHEVs are generally considered to produce lower levels of pollution than conventional passenger vehicles. However, a study on a Euro 6 parallel PHEV in T_{amb} of -7

°C and 23 °C shows that the PHEVs can emit similar or even higher levels of emissions and pollutants compared to Euro 6 conventional gasoline and diesel vehicles [29].

A model year (MY) 2012 Chevrolet Volt PHEV was tested in a T_{amb} range of -25 °C to 25 °C in Winnipeg, Canada. The results confirm that energy consumption has an inverse relationship with T_{amb}. At T_{amb} -3 °C to -5 °C, the electric travel range was less than half of the baseline range, and electrical energy consumption was more than double [30].

The energy consumption of PHEVs increases when operating in cold temperatures due to low powertrain efficiency and the extra energy required for battery thermal conditioning and cabin heating. Figure 1.5 shows the average energy consumption of the best-selling vehicles at various T_{amb} [31].

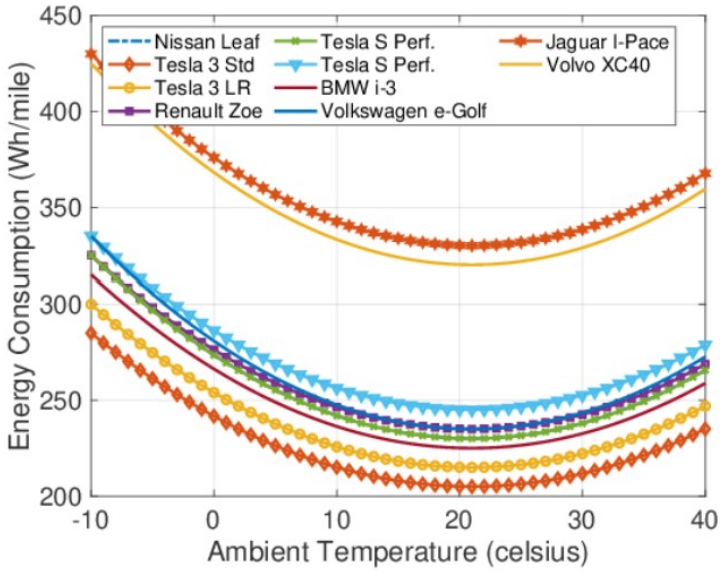

Figure 1.5: Average energy consumption of top-selling vehicles under varying T_{amb} [31]

The hybrid functions of an HEV depend on T_{amb}. These functions, like auto-stop/start and brake regeneration, are unavailable in extremely cold climates. A Thermal Management System (TMS) to warm up the battery quickly without any additional hardware is a cost-efficient solution [32].

Extremely cold climate operations have a negative effect on the available energy of the PHEV's Li-ion battery and experience degradation mechanisms. A non-isothermal equivalent circuit battery model was developed in [33] for cold starts in extremely low temperatures. The model can be used for thermal management and increasing the performance and persistence of battery energy.

A method was demonstrated in [34] for quantifying energy use and emissions of a MY2013 Toyota Prius plug-in. The vehicle was equipped with a portable emission measurement system. VSP-based modal average energy use and emission rates. The results show that the PHEV operating in charge-depleting mode has better energy efficiency and lower emission rates than same-sized conventional light-duty gasoline vehicles.

Battery performance varies throughout the temperature range specific to automotive applications. A dynamic battery model was developed in [35] based on current and temperature for battery voltage. According to the results, a significant performance increase can be achieved by including temperature influences in the models.

An integrated power and thermal management (i-PTM) scheme was developed in [36] to optimize power split, engine thermal management, and cabin heating. Based on data collected from a 2017 Prius HEV, the heating requirement influences optimal power management and energy consumption behavior. The study has shown that integrating power and thermal optimization has the potential to save up to 6.85% fuel.

The battery charge in PHEVs is designed to be consumed during a drive cycle. Sometimes, a drive cycle distance range exceeds a PHEV's AER. In these situations, as ICE starts to work, the vehicle produces emissions by changing the powertrain mode, and optimization of the vehicle's performance becomes a priority for energy-saving purposes. A method was developed to synthesize a supervisory powertrain controller (SPC) that adjusts the engine on/off, gearshift, and power-split strategies to optimize fuel consumption for known travel distances [37].

1.2.3 Effect of Start-Stop Technology on Energy Consumption and Costs

Start-stop technology is an alternative for reducing energy consumption with low cost and high effectiveness. One of the most significant advantages of this technology is installing it on traditional powertrain systems. Start-stop systems are not a new development. The early versions arrived in the 1980s [38], but they are now more developed and commonplace. Figure 1.6 shows the schematic of the start-stop system.

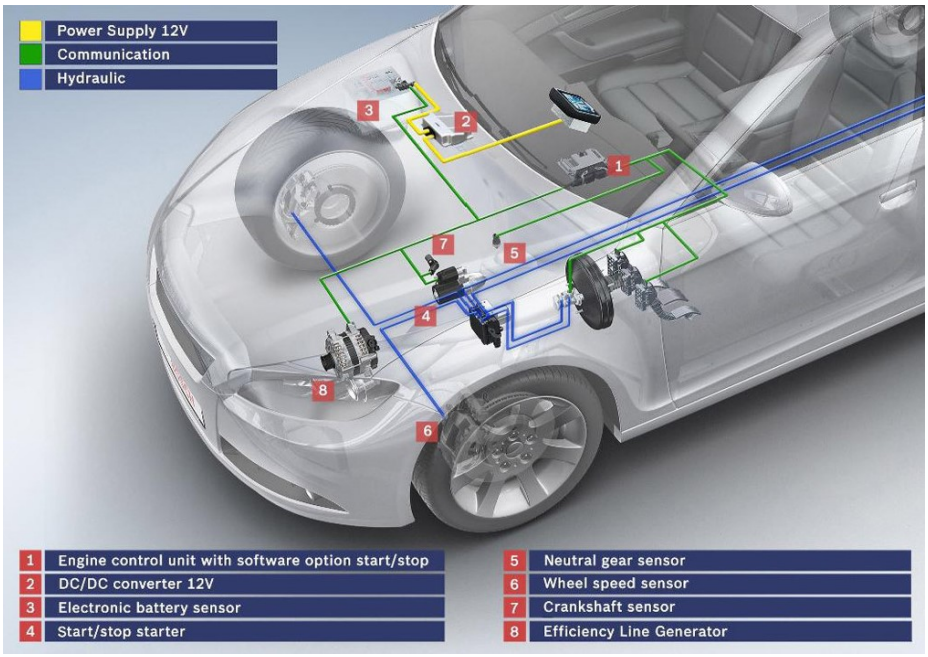

Figure 1.6: The start-stop system components [38]

The system is equipped with various sensors that monitor parameters such as the vehicle's speed, brake pedal position, clutch pedal position (in manual transmissions), battery status, and engine temperature. The start-stop system uses these sensors to detect when the vehicle comes to a complete stop, for example, at a traffic light or in heavy traffic.

The system ensures that the transmission is in neutral or the clutch is disengaged, in case of manual transmissions, and also checks whether the brake pedal is depressed. If both conditions are met, the system automatically shuts off the engine to conserve

fuel and reduce emissions. The system continuously monitors the battery state to ensure that there is sufficient power to restart the engine. In case of low voltage, the system may not shut off the engine or may restart the engine to recharge the battery.

When the driver releases the brake pedal or, depresses the clutch (in manual transmissions) or accelerates, the engine stop-start system will restart the engine. To do this, the starter motor will be engaged to crank the engine, and then the fuel and air mixture will be reignited to resume combustion. The transition between engine shutdown and restart is designed to be smooth and unobtrusive, so the driver usually does not notice the engine stopping and starting. While the engine is off, the vehicle's power steering, brakes, and other essential systems are still operational.

The start-stop system was tested over the New European Driving Cycle (NEDC). The results showed a fuel saving rate of up to 8.31% [39].

In the study done by Ma, et.al. [40], during a cold start test, the idling start-stop function of the first idling segment under NEDC conditions did not work normally. This was because the coolant temperature was too low at that time, which did not reach the threshold required to trigger the idling start-stop operation.

It should be considered that using the start-stop function for situations like a red light for less than 5 seconds is not beneficial because the fuel consumed by using the engine start-stop technology is more than when the engine idles for the same period [41].

The research contributed by Abas et al. in [42], in Malaysia at T_{amb} of 34.7 °C, showed that the average fuel saved by the start-stop system was about 20.7%. Then, the test was repeated, considering the cabin comfort temperature of 16 °C, which was the coldest demand using the air conditioning system. This led to energy saving dropped to 11%.

1.3 Aim and Scope

The primary aims and scope of this thesis are:

- Investigating the fuel consumption of the UAlberta fleet vehicles to reduce energy consumption.

- Measuring a vehicle's actual instantaneous fuel consumption in the real world requires costly equipment. In this thesis, a framework is proposed to estimate the fuel consumption of individual vehicles in the university fleet, utilizing available On-Board Diagnostic (OBD) data and machine learning models.

- The University of Alberta's fleet, with more than 180 vehicles, is in Edmonton—a city with extremely cold temperatures down to -40 °C in winter, and warm weather up to 35 °C in summer. In this thesis, the effect of T_{amb} on the performance and energy consumption of conventional (ICE) vehicles versus the electrified operating modes are investigated. The results reveal valuable insights into the impact of T_{amb} on various powertrain options, identifying fuel consumption patterns and ideas for energy-saving for UAlberta fleet vehicles.

- Analysing the effect of start-stop technology on energy consumption and operational costs of conventional vehicles in UAlberta fleet vehicles. To this end, three vehicles with varying engine sizes were selected from the UAlberta fleet: a Ford Escape S, a Chevrolet Silverado 1500, and a Ford Econoline 450. The fuel saving by using start-stop technologies in these three vehicles was studied for four UAlberta fleet vehicle applications by considering their distinct drive cycles.

1.4 Thesis Outline

The thesis is organized into six chapters, including an introduction, experimental setup, fuel consumption estimation of UAlberta fleet vehicles, effect of ambient temperature on energy consumption of a vehicle, effect of start-stop technology on energy consumption and costs, and conclusion. The structure and workflow of the thesis are

shown in Figure 1.7, and the resulting publications are also listed.

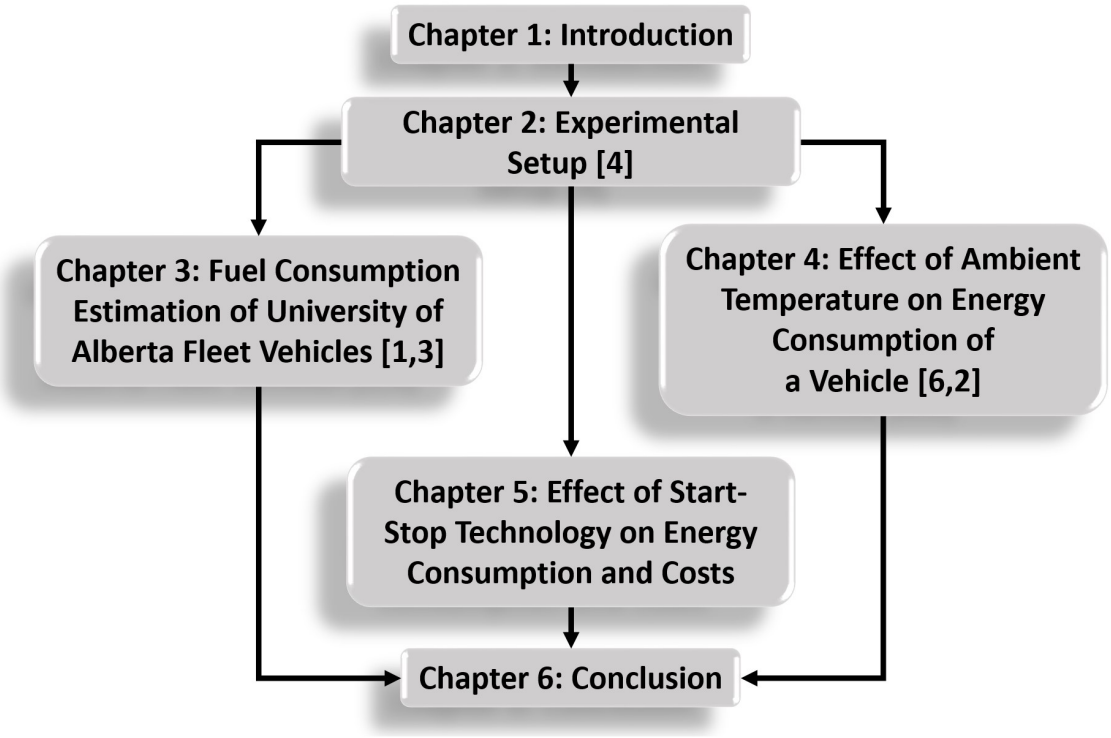

Figure 1.7: Thesis flow including chapters and resulting publications

The experimental setup chapter provides a detailed description of the research design, the methods used for collecting vehicle OBD data, and the equipment setup. It also explains the development of a software platform for real-time monitoring, highlighting opportunities for energy-saving, pattern recognition, and driving cycle optimization to reduce fleet operational costs and CO_2 emissions.

In chapter three, different practical and reliable methods to estimate the instantaneous fuel consumption of fleet vehicles were studied. Two RF and ANN machine learning methods were developed using real-world OBD data.

Investigating the effect of T_{amb} on energy consumption, costs, and CO_2 emission is described in chapter four. A Ford Escape PHEV was tested in different weather conditions in the T_{amb} range of -24 °C to 32 °C.

Chapter five investigates the impact of start-stop technology on the fleet vehicles of the University of Alberta. To determine the fuel savings of the vehicles, three UAlberta fleet vehicles were selected, and the drive cycles of four university vehicle application areas were considered.

Finally, chapter six summarizes the study's key findings and conclusions drawn from analyses of the experimental results, discusses their implications, and provides recommendations for future research and practice.

Chapter 2

Experimental Setup

This chapter explains the experimental setups designed to collect the required data for this thesis. Overall, two types of data are collected: i) On-Board Diagnostic (OBD) data using Controller Area Network (CAN) data loggers on different UAlberta fleet vehicles, and ii) Instantaneous fuel consumption data by installing a fuel flow meter. The following sections explain each of the data collections.

2.1 Vehicle OBD Data Collection

The OBD systems have been mandatory in the United States and Canada for all passenger vehicles and light to medium-duty trucks since 1996 [43], and the OBD-II standard was established to ensure that vehicles comply with emission standards. OBD-II monitors various systems related to engine and exhaust after-treatment system operation to detect and report any malfunctions that may impact tailpipe emissions.

OBD-II utilizes different signal protocols to communicate information from the OBD system to external devices. These protocols are explained in Figure 2.1. Via OBD-II, a large number of vehicle engine operational parameters become publicly available by using OBD data loggers. This thesis uses OBD data for performance analysis of the university vehicles.

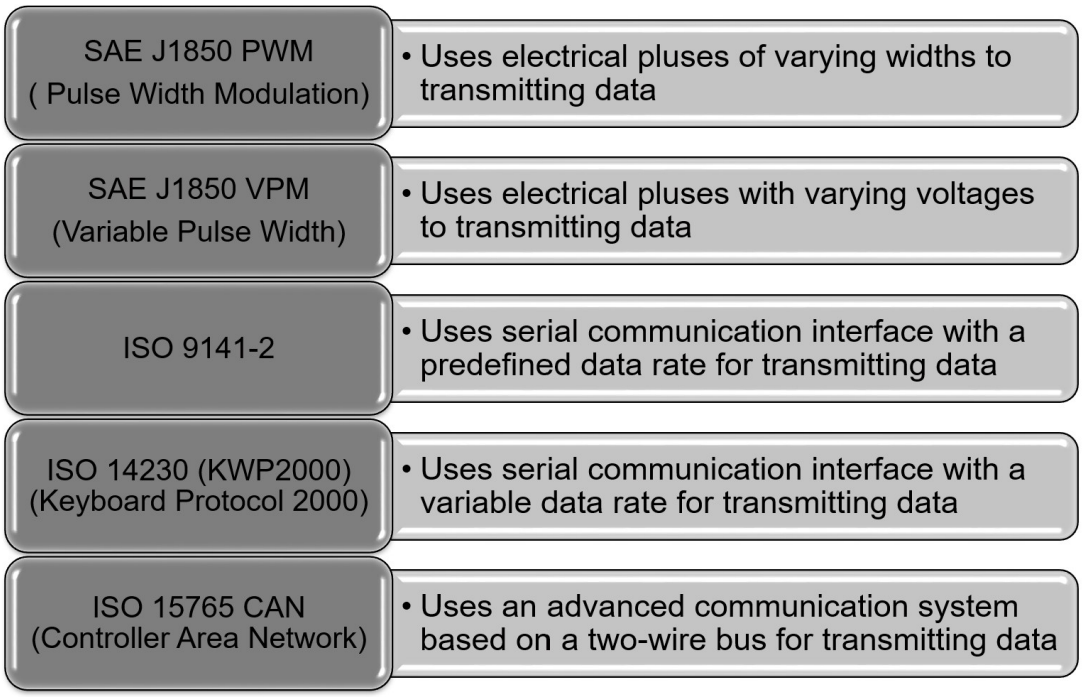

Figure 2.1: OBD-II signal protocols

2.1.1 OBD Data Logger

The OBD data can be accessed using an OBD scanner or a CAN data logger. CAN data loggers help collect OBD data over extended periods, such as for research or fleet management. They are typically small, portable devices that can be connected to the OBD port in the vehicle. The data logger continuously records information from the OBD system, such as vehicle speed, engine speed, and fuel consumption, and stores it in its memory for later analysis. Data loggers are especially useful for monitoring vehicle performance and identifying potential issues. In addition, data loggers can be equipped with Wireless Fidelity (Wi-Fi) or cellular connection for continues data transfer to the cloud or server for fleet vehicles' management. This thesis uses the Freematics CAN data logger One+ Model B (Figure 2.2).

Wi-Fi Option

In the Wi-Fi mode of the Freematics CAN data logger, the device collects data while the vehicle is in motion but has no live connection to a server. Instead, the collected

(a) The Freematics CAN data logger One+ Model B

(b) The Freematics CAN data logger installed on OBD port of a vehicle

Figure 2.2: The Freematics CAN data logger used for this study

data is stored on an internal Secure Digital (SD) card. The device must connect to a Wi-Fi network to access the collected data and use Hypertext Transfer Protocol (HTTP) Application Programming Interface (API) commands. However, there are limitations with the Wi-Fi mode as the device needs to have access to specific internet routers located at limited locations, such as fuelling stations, which are associated with the University of Alberta. These limitations suggest that the device may have restricted access to the internet and that data retrieval may only be possible in specific locations with the required network infrastructure.

Cellular Option

The cellular option of the Freematics CAN data logger allows for real-time monitoring and data transmission, which is beneficial for fleet management. However, it's important to remember that cellular coverage can be limited in certain areas, especially in remote locations, which may affect the ability to transmit data in real time.

The availability and reliability of cellular coverage can vary depending on location, network provider, and environmental conditions. In remote or rural areas, cellular signal strength may be weaker or unavailable, impacting the device's real-time ability to transmit data. It's essential to consider these limitations when relying on cellular

connectivity for data transmission and fleet management and have contingency plans for situations where cellular coverage may be limited or unavailable.

The alternative option is to store the data locally on the device and transfer it later when cellular coverage is available or using satellite communication.

This data logger (Figure 2.2a) is a small device that can be easily installed into the OBD port of a vehicle (Figure 2.2b). It can collect various data types, including Global Positioning System (GPS) location, vehicle speed, engine speed, engine load, and other Parameter Identifications (PIDs) defined by the OBD-II standard. This device has an internal 16 GB SD card for data storage and can be connected to a database server via Wi-Fi or cellular network to upload the data.

The technical specifications of the Freematics CAN data logger One+ Model B are shown in Table 2.1.

Table 2.1: Specifications of the Freematics CAN data logger used in this study

Parameter	**Value**
Random Access Memory (RAM) configuration	520 KB IRAM + 8 MB PSRAM
Real-Time Clock (RTC)	External 32 K
Cellular module	Integrated 4G LTE module
Global Navigation Satellite System (GNSS)	Integrated M8030 10 Hz GNSS module and antenna
External I/O	2x GPIO for digital I/O, analog input, serial UART etc.
Co-Processor features	Vehicle ECU interfacing GNSS data processing
Horizontal Pos. Accuracy	2.0m Circular Error Probability (CEP)

The Freematics CAN data logger uses open-source code and can be programmed using the Arduino Integrated Development Environment (IDE) or other programs such as Visual Studio Code (VSC), making it highly customizable for specific tasks.

This allows users to modify the behavior of the logger by writing and uploading their code, giving them greater flexibility and control over the data collection process.

To address the concern of potential battery drain during the operation of the Freematics device in Edmonton's cold winter conditions, a standby and startup code was defined in the Freematics program. This code allows the device to be put into standby mode when not actively collecting data, which can help conserve battery power.

When the Freematics device is in standby mode, it typically draws a lower current of 10 milliamperes (mA) than its normal operating mode of 150 mA. By putting the device into standby mode during periods of inactivity, such as when the vehicle is not in use or when data collection is not required, the device's power consumption can be reduced, potentially helping to mitigate battery drain issues. This can protect the battery from over-discharge damage and ensure the device's reliable performance.

When the device detects movement or the vehicle is turned on, it wakes up from standby mode and resumes its data collection and transmission functions. This ensures that data is only collected when the vehicle is in use, reducing unnecessary power consumption and data storage.

2.1.2 Data Server

The data logger records a minimum of 2 MB of data per hour of operation, and each vehicle may operate for 4 hours per day. This results in a minimum of 8 MB of data per vehicle daily. With a fleet of 180 vehicles, the total data generated daily would be 1,440 MB, or approximately 1.5 GB (1 GB = 1,024 MB). Therefore, the system should be capable of handling the transfer of a minimum of 1.5 GB of data per day from the UAlberta fleet's data loggers. This would require sufficient bandwidth and storage capacity in the system to accommodate the data transfer and storage needs, ensuring efficient and smooth operation without data loss or performance issues. It is also essential to consider the system's scalability and flexibility to handle potential

future data volume increases.

A computer server was set up in the National Institute of Nanotechnology (NINT) building, located at the University of Alberta, to serve as both a network server and a database. This computer is operational 24/7 and is designed to collect data continuously. The data collected include GPS and OBD data recorded from vehicles. The collected data, including vehicle location, speed, engine parameters, and other relevant data from the OBD system. The collected data is automatically sent to the network server and uploaded to the database. This allows for efficient and automated data management, storage, and retrieval. Using a dedicated computer as a network server and database helps ensure the collected data is securely stored and readily accessible for analysis and further processing.

2.1.3 Data Collection, Transfer, and Processing

The designed fleet data collection system uses an OBD data logger to record various vehicle parameters, such as vehicle speed, engine speed, coolant temperature, and other relevant data.

Parameter Identifications (PIDs)

The specific set of PIDs available for a particular vehicle will depend on various factors, such as the make and model of the vehicle, the year it was manufactured, and the type of OBD scanner being used. Some PIDs may be standard across all vehicles, while others may be unique to specific makes or models.

The device is capable of collecting up to 21 PIDs with a sample rate of 1 Hz. However, the sampling rate decreases if more PIDs are added. This is because the logger has to request and receive data for each PID, and the more PIDs that are collected, the longer it will take to complete an entire data collection cycle.

The number of PIDs collected by the Freematics OBD data logger affects the sampling rate, as shown in Figure 2.3. Data was collected from four different vehicles

using the Freematics OBD data logger. These vehicles included a model year (MY) 2010 Ford Econoline E150, a MY2012 Dodge Ram 1500, a MY2011 Hyundai Sonata, and a MY2017 Chevrolet Express.

Collecting 20 PIDs from both the Dodge Ram 1500 and the Chevrolet Express took almost 0.6 seconds and 0.7 seconds, respectively. Increasing to 30 PIDs increased the sampling period to almost 1.5 seconds for both vehicles. The Ford Econoline E150 took the longest sampling period, at 2.8 seconds, to collect 50 PIDs. The Hyundai Sonata with 46 PIDs took 2.6 seconds, while the Chevrolet Express and Dodge Ram 1500 with 49 and 48 PIDs respectively took almost 2.5 seconds.

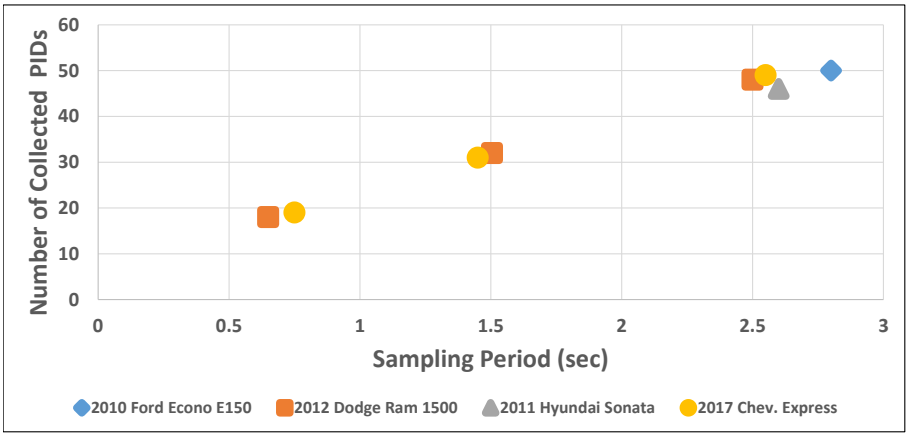

Figure 2.3: The link between the number of PIDs and possible sampling period using Freematics OBD data loggers

It is common for the number of available PIDs to vary between different vehicles. In this case, the maximum number of PIDs collected was 54 from the UAlberta fleet vehicles (Tables 2.2, 2.3). However, the parameters available varied considerably between different vehicles. These PIDs include data such as vehicle speed, Mass Air Flow (MAF) rate, throttle position, engine speed, and many others.

Table 2.2: The list of PIDs collected from UAlberta fleet vehicles in this study (part1)

No.	Parameter	Unit
1	Calculated engine load	%
2	Engine coolant temperature	°C
3	Short term fuel trim Bank 1	%
4	Long term fuel trim Bank 1	%
5	Short term fuel trim Bank 2	%
6	Long term fuel trim Bank 2	%
7	Fuel pressure (gauge pressure)	kPa
8	Intake manifold absolute pressure	kPa
9	Engine speed	rpm
10	Vehicle speed	km/h
11	Timing advance	° before TDC
12	Intake air temperature	°C
13	Mass air flow (MAF) sensor	g/s
14	Throttle position	%
15	O_2 Sensors present (in 2 banks)	-
16	O_2 Sensor 1 - voltage & short term fuel trim	V & %
17	O_2 Sensor 2 - voltage & short term fuel trim	V & %
18	O_2 Sensor 5 - voltage & short term fuel trim	V & %
19	O_2 Sensor 6 - voltage & short term fuel trim	V & %
20	Run time since engine start	s
21	Time run with Malfunction Indicator Light (MIL) on	min
22	O_2 Sensor 1 air-fuel equivalence ratio & voltage	ratio & V
23	Commanded Exhaust Gas Recirculating (EGR)	%
24	Commanded evaporative purge	%
25	Fuel tank level input	%
26	Warm-ups since codes cleared	-
27	Distance since codes cleared	km

Table 2.3: The list of PIDs collected from UAlberta fleet vehicles in this study (part2)

No.	Parameter	Unit
28	Evap. system vapor pressure	Pa
29	Absolute barometric pressure	kPa
30	O_2 Sensor 1 air-fuel equivalence ratio & current	ratio & mA
31	O_2 Sensor 2 air-fuel equivalence ratio & current	ratio & mA
32	O_2 Sensor 5 Air fuel equivalence ratio & current	ratio & mA
33	Catalyst temperature: Bank 1, Sensor 1	°C
34	Catalyst temperature: Bank 2, Sensor 1	°C
35	Catalyst temperature: Bank 1, Sensor 2	°C
36	Monitor status of this drive cycle	-
37	Control module voltage	V
38	Absolute load value	%
39	Air-fuel equivalence ratio	ratio
40	Relative throttle position	%
41	Ambient air temperature	°C
42	Absolute throttle position B	%
43	Accelerator pedal position D	%
44	Accelerator pedal position E	%
45	Commanded throttle actuator	%
46	Distance traveled with MIL on	km
47	Time since trouble codes cleared	min
48	Fuel type	-
49	Ethanol fuel	%
50	Long term trim O_2 sensor, Bank 1, Bank 3	%
51	Long term trim O_2 sensor, Bank 1, Bank 3	%
52	Engine oil temperature	°C
53	Actual engine - percent torque	%
54	Engine reference torque	N.m

Figure 2.4 shows the data collection process by Freematics data loggers. The Freematic OBD data loggers were used to collect data from UAlberta fleet vehicles (Figure 2.4a). The capability of transmitting data to the server via cellular was the advantage of this type of OBD data logger.

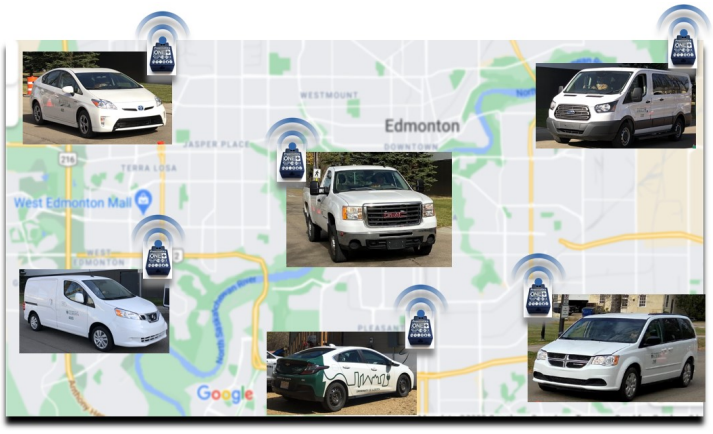

(a) The Freematics CAN data logger connected to UAlberta fleet vehicles

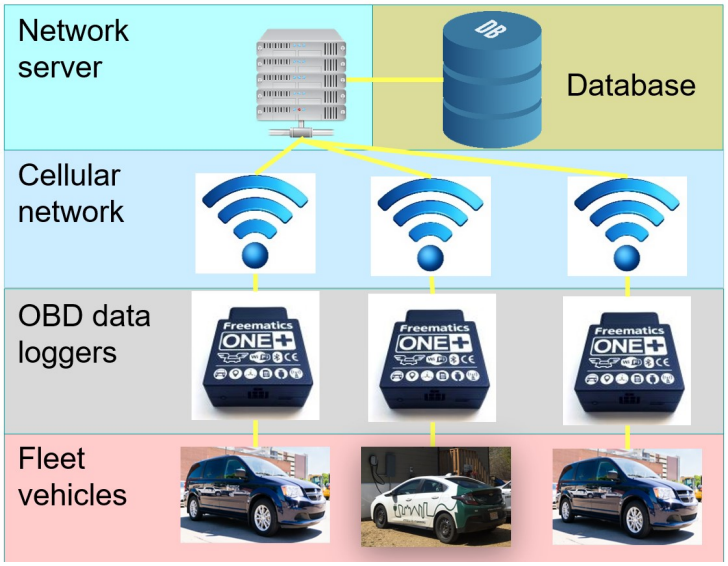

(b) Schematic of data collection

Figure 2.4: Schematic of data collection and transmitting to the server

As shown in (Figure 2.4b), by leveraging the cellular connectivity of the Freematics data loggers, the collected data from the UAlberta fleet vehicles can be transmitted to the network server in real-time, enabling live monitoring and analysis. At the same time, it can be stored in the database. This allows for prompt identification of any

issues, monitoring of vehicle performance, and the potential for timely interventions or decision-making based on the analyzed data.

A software platform was designed that consisted of both a back-end and a front-end component. The back-end was responsible for handling the processes involved in collecting data from vehicles and storing it in the database. The front-end was focused on providing a Graphic User Interface (GUI) for visualization and live data monitoring. The schematic of the data collection platform is shown in Figure 2.5.

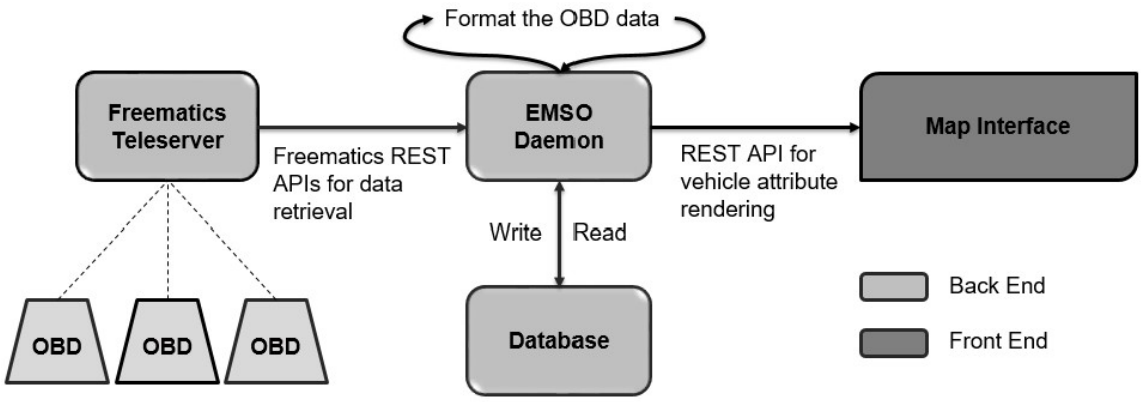

Figure 2.5: The schematic of the data collection platform used in this thesis

Data Collection Platform (Back-End)

Figure 2.6 illustrates the schematic of the back-end process. Following this back-end process, the collected data from the OBD scanner is effectively transferred and stored in a database on the computer. This allows for further data analysis, modeling, and utilization for various purposes, such as estimating fuel consumption or conducting other data-driven investigations.

The OBD data logger collects data from the vehicle's OBD port and records it as a Comma-Separated Values (CSV) file on an SD card stored inside the device. The collected data from the SD card is transferred to a server in the NINT building. This data transfer is facilitated by programs such as Teleserver.exe, HubDataRetriever.exe,

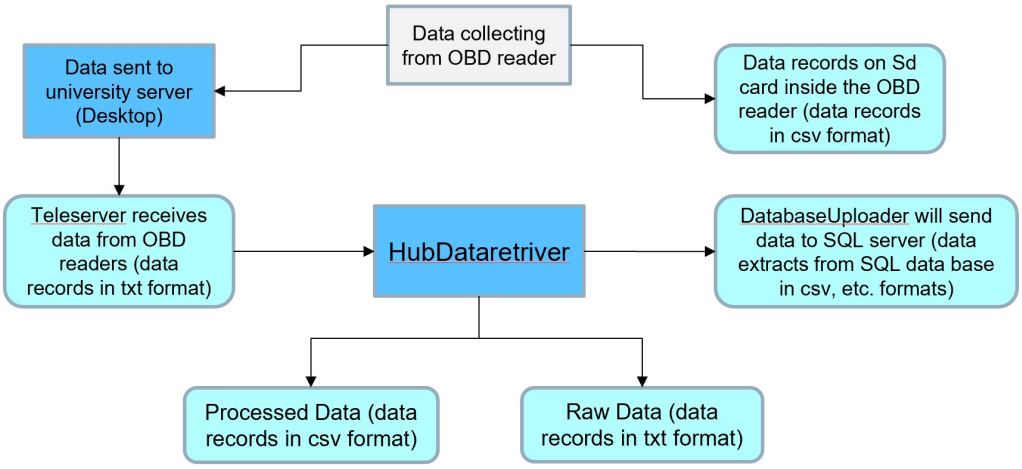

Figure 2.6: The schematic of the back-end software for the data collection platform used in this thesis

and DatabaseUploader.exe, which are designed for transferring data from OBD readers to the Structured Query Language (SQL) server and need to be run on the server constantly.

Teleserver

Data from OBD devices is transmitted to the computer and stored using the Freematics Hub server. The data is stored on the server in TXT format, which can be retrieved later using API commands. This program bridges the OBD scanners and the server, allowing real-time data transfer at regular intervals.

HubDataRetriever

The HubDataRetriever program uses API commands to communicate with the Freematics Hub, a device that acts as a central hub for collecting data from various connected devices. The API commands allow the program to identify the devices connected to the hub. Once the devices are detected, the program determines which devices are active and ready to transmit data. This step helps identify the devices from which data will be collected. The program collects the most recent period of data from the active devices. It communicates with each device using the appropriate API commands to retrieve the data they have recorded. The collected data may include sensor readings,

GPS data, or any other relevant information captured by the connected devices.

After collecting the data, the program saves it as a raw text file in the "RawData" folder. The raw data file contains the unprocessed, original data obtained from the devices. This allows for further analysis or processing if required. The program uses the "DATAscanner.exe" file, which is an executable or script, to process the raw data. This processing step applies specific algorithms or transformations to the raw data, converting it into a structured format suitable for further analysis or visualization. Once the data is processed, the program saves it as a CSV file in the "Processed Data" folder. The CSV format enables easy data manipulation and compatibility with various software tools and applications.

DatabaseUploader

This program is designed to monitor the ProcessedData folder for any new files created, modified, or deleted. This is accomplished using a file system watcher, which can detect changes to the file system in real-time. When a new file is detected in the ProcessedData folder, the program sends a series of SQL commands to the SQL server to upload the processed data into the database. This involves parsing the CSV file and inserting the data into the appropriate tables and columns in the SQL database. By automating this process, the DatabaseUploader program allows for efficient and reliable data transfer from the ProcessedData folder to the SQL database. This can save time and reduce the risk of errors when manually uploading data to the database.

The three "Teleserver.exe", "HubDataRetriever.exe", and "DatabaseUploader.exe", programs used for transferring the collected data from the OBD readers to the SQL server, are set up to run automatically in case the university desktop restarts. This means that the programs will start running independently without requiring manual intervention. If any of these three programs crash, the RestartOnCrash software will be used to restart them automatically. This ensures that the data transfer process is not interrupted and all collected data is uploaded to the SQL server as expected. The software also has a "show log" tab that can be used to view the time of the crash,

which can help troubleshoot any issues that may arise.

Ensuring the security and protection of databases storing sensitive data is indeed crucial. To address the concern of unrecognized Internet Protocol (IP) addresses attempting connections to the database server, access to the server has been limited to only defined IP addresses. This is a standard security measure known as IP whitelisting or IP filtering. IP whitelisting involves specifying a list of approved IP addresses from which connections to the database server are allowed. Any connection attempts from IP addresses not included in the whitelist are denied, effectively blocking unauthorized access attempts. By implementing IP whitelisting, the database server only accepts connections from devices with IP addresses explicitly defined and approved. Limiting access to the server to defined IP addresses reduces the risk of unauthorized access, as only authorized users with recognized IP addresses can access the database. This helps to prevent data breaches, theft of sensitive information, and other security threats.

Figure 2.7 indicates that only authorized OBD data loggers with specific IDs (such as ID: A0HLZJ1U and ID: A0HNZYJ0) have been granted access to the database server. On the other hand, unauthorized devices with IDs like ID: A0HNZK3J and ID: A0HN8K3U were denied access.

To maintain the security and integrity of the designed database, it is essential to review and update the IP whitelist regularly. This will ensure that only authorized devices are granted access and that any unapproved or unnecessary devices are promptly removed. Additionally, monitoring database access regularly and keeping security measures up-to-date to protect against potential threats is crucial. Implementing measures such as encryption, user authentication, and data backups can further enhance database security and ensure its integrity over time.

Once the data is uploaded to the database, it can be accessed by authorized personnel for further analysis. Data analysis techniques can include pattern recognition, driving cycle identification, and other data-driven approaches to identify energy-

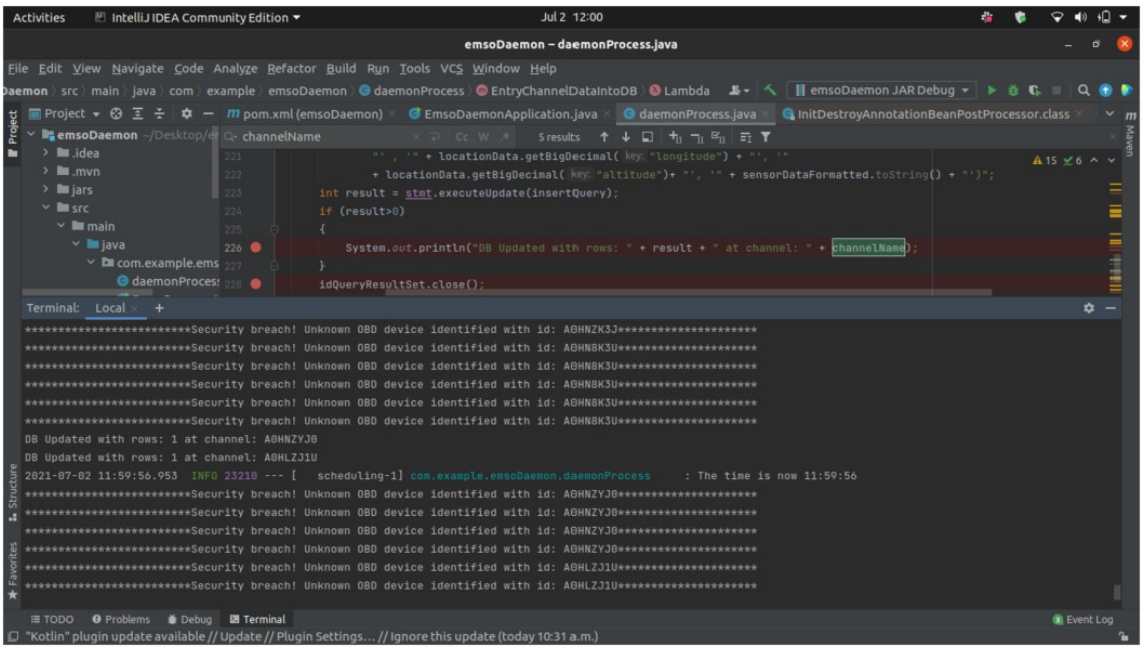

Figure 2.7: The server IP filtering

saving opportunities, optimize fleet operations, and develop strategies for reducing fuel consumption and GHG emissions.

The transferred data is stored in an SQL database on the server. SQL is a widely used database management system that allows efficient and organized structured data storage in a relational database. Once the data is stored in the SQL database, it can be processed, analyzed, and queried. SQL provides powerful tools for data manipulation, including querying, filtering, and aggregating data to derive insights or generate reports.

It can be extracted as a CSV file from the SQL database to analyze the data further. These extracted data can be used for advanced analyses, visualization, reporting, or integration with other systems or models (Figure 2.8).

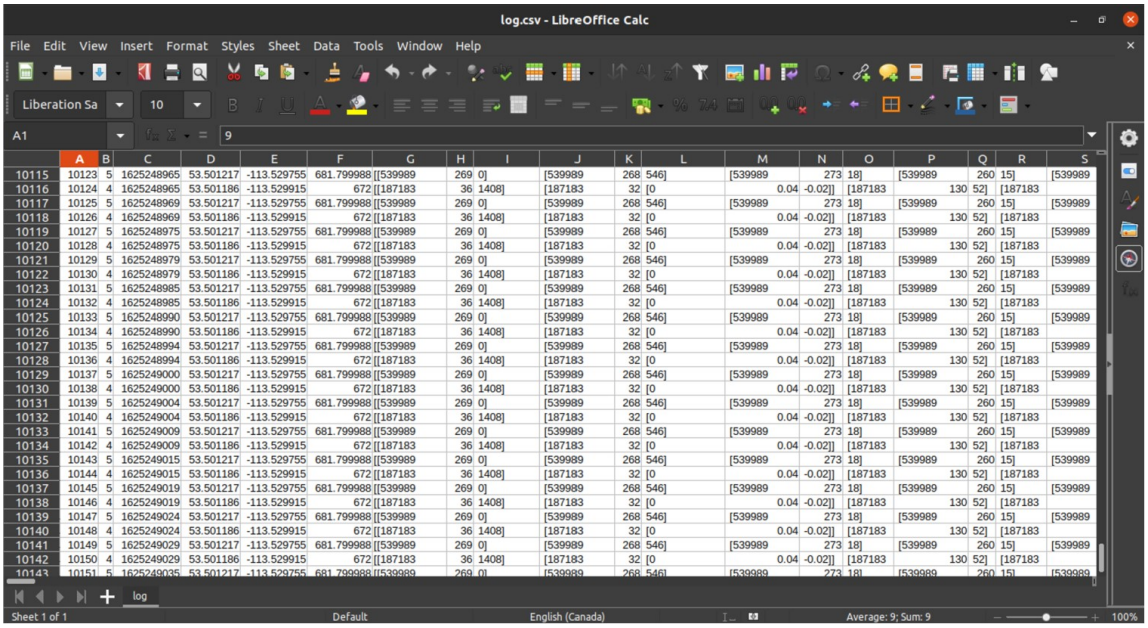

Figure 2.8: The back-end of the data collection platform used in this thesis

Data Collection Platform (Front-End) and Live Monitoring

In the data collection platform, the front-end component includes the usage of Freematics Hub as the telemetry and data server software. It facilitates the collection and real-time upload of OBD and GPS data from the OBD data loggers. The OBD data loggers, connected to the vehicles, transmit the collected OBD and GPS data to the Freematics Hub. This data is uploaded to the server in real-time using a Wi-Fi or cellular connection. Real-time data upload ensures that the most recent data is available for monitoring and analysis. To ensure data is uploaded whenever the OBD devices have access to DEVNet, Freematics Hub should be running continuously. This ensures that data is not lost or missed due to server downtime or other issues. Maintaining an uninterrupted connection with the OBD data loggers makes the data collection process reliable and consistent.

Freematics Hub is designed to be compatible with Windows and Linux operating systems. It is lightweight server software that can be easily deployed on the chosen platform. The operating system's choice depends on the deployment environment's specific requirements and preferences. Freematics Hub provides an interface for mon-

itoring and managing the collected data. This interface lets users view real-time data, configure settings, and manage storage and retrieval. It may include visualizations, data filtering, device management, and system status monitoring. The Freematics Hub interface (Figure 2.9) contains a dashboard and a map view, where the information of the vehicles is presented.

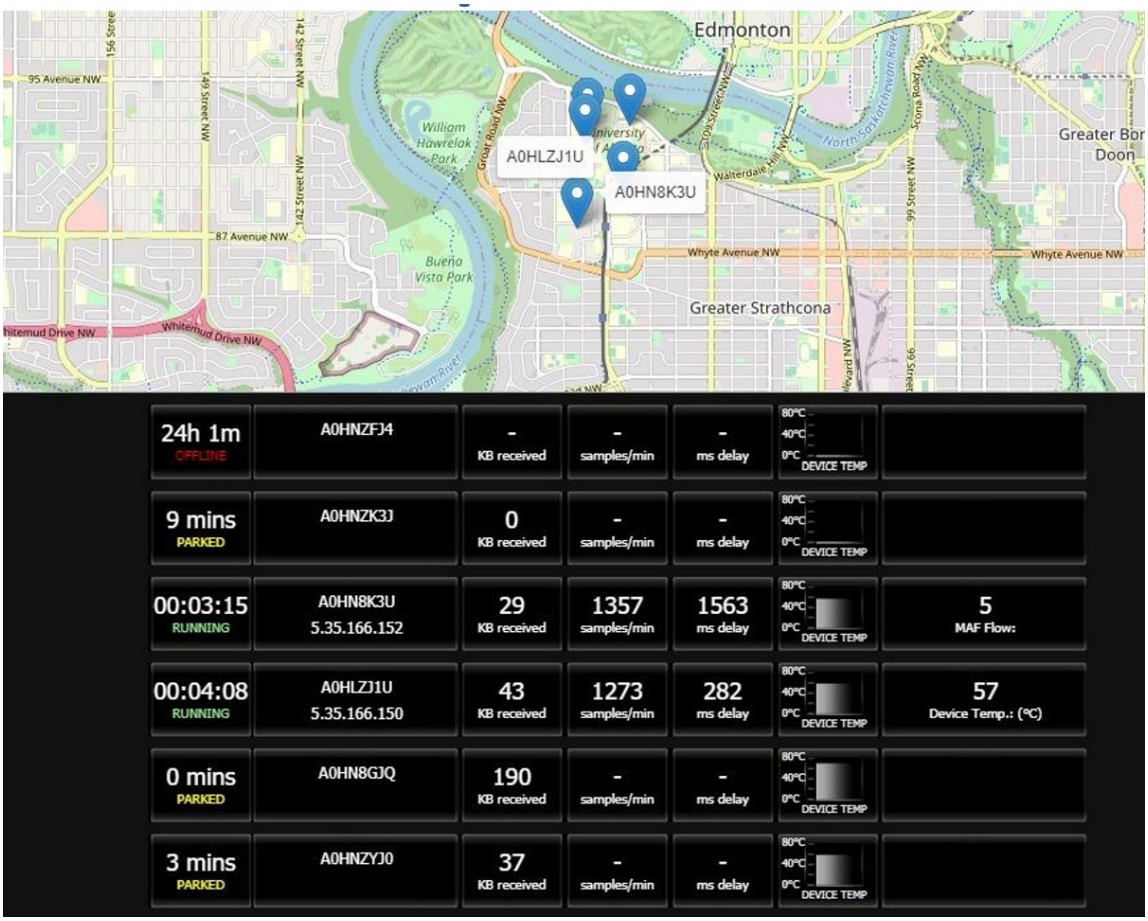

Figure 2.9: Freematics Hub interface

The interface displays the vehicles as individual markers on a map, indicating their locations. Additionally, real-time data such as vehicle speed, engine speed, fuel level, coolant temperature, or any other relevant PIDs the vehicle provides can be shown on the dashboard. The interface provides interactive features, allowing users to zoom in or out on the map, select specific vehicles for detailed information, or apply filters to focus on particular data or vehicles of interest. This provides a comprehensive

view of the real-time data collected from the vehicles and facilitates monitoring and analysis of their performance and operational parameters.

2.2 Fuel Measurement Data Collection

Instant fuel consumption of selected vehicles was measured by installing an ultrasonic fuel flow meter. The data was used for i) fuel consumption analysis (e.g., for start-stop technology assessment) and ii) developing machine learning models to estimate the instantaneous fuel consumption of a vehicle using real time OBD data. Here, the installation of the fuel flow meter and special dual-channel high frequency CAN data logger to collect vehicle data are explained. The schematic of data collection by the CANedge2 data logger is shown in Figure 2.10.

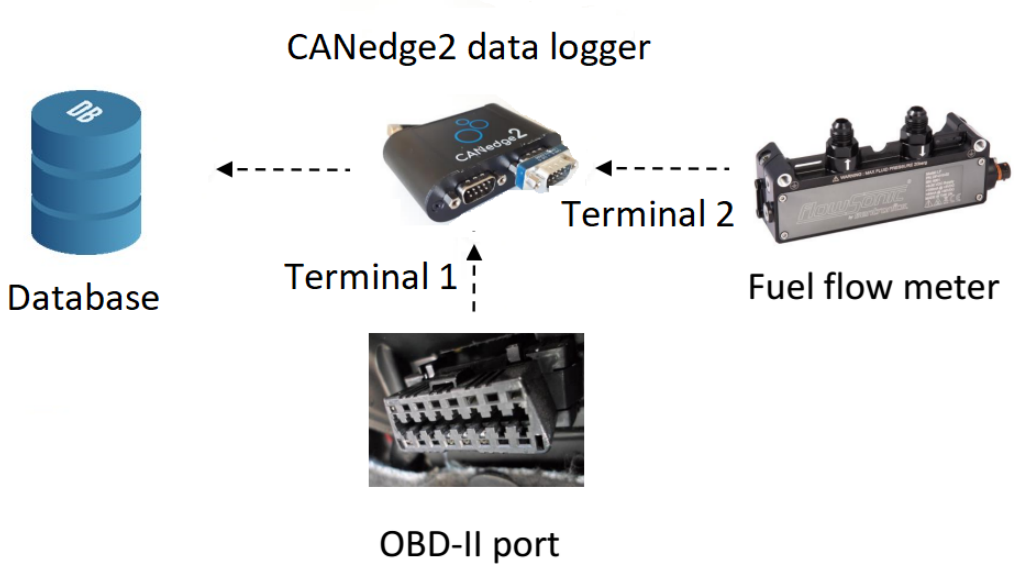

Figure 2.10: Schematic of data collection by the CANedge2 data logger used in this thesis

A CANedge2 data logger was used in this thesis to collect data from the vehicle OBD and the fuel flow meter simultaneously. The collected data contains actual fuel consumption and the related vehicle's OBD PIDs. This combined dataset can be

used to train machine learning models to learn the relationship between the vehicle's PIDs and the corresponding fuel consumption.

2.2.1 Sentronics FlowSonic Low Flow (LF) Ultrasonic Flow Meter

A fuel flow meter is a device specifically designed to measure the flow rate of fuel passing through it. It provides precise measurements of the amount of fuel consumed by the vehicle. The fuel flow meter is installed in the vehicle's fuel line, between the fuel tank and the engine. As the fuel flows through the flow meter, it measures the volume or weight of fuel passing through per unit of time. This information is then recorded to calculate the vehicle's actual fuel consumption. The actual fuel consumption data is used for validating the machine learning models developed for estimating fuel consumption and analyzing the effect of T_{amb} on the energy consumption of a vehicle.

The Sentronics fuel flow meter (Figure 2.11) was selected for its flexibility of use with gasoline and diesel engines and absence of any physically moving components. Ultrasonic fuel flow meters use ultrasonic waves to measure fuel flow without mechanical parts. This means they are more reliable and durable than traditional flow meters with moving parts since they don't impose any restrictions on the fuel [44].

Figure 2.11: Sentronics flowSonic LF ultrasonic flow meter

This device has a measurement range of 0-1,000 ml/min, with an accuracy of 0.25% of the reading and a resolution of 0.01 ml/min. The sensor can measure cumulative and instantaneous fuel volume and mass and can be configured to sample data at rates up to 10 Hz. To increase the accuracy of collected data, the flow meter was set to collect data with a sample rate of 5 Hz. The technical specifications of the Sentronics fuel flow meter are shown in Table 2.4.

Table 2.4: Specifications of the fuel flow meter used in this thesis

Parameter	**Value**
Measurement uncertainty	+/- 0.5 % of reading
Repeatability	+/- 0.15 % of reading
Fluid temperature range	-20 to +120 °C
T_{amb} range	-40 to +120 °C
Measurement flow range	8 – 4,000 ml/min
Measurement rate	Up to 2.2 kHz
Electrical supply voltage	8 V DC to 30 V DC
Fluid Compatibility	Petrol, diesel, bio-diesel, ethanol, methanol

The settings of the flow meter were configured using a GUI application. This flow meter was installed on the vehicle's fuel line, enabling it to measure real-time fuel consumption accurately. Figures 2.12 and 2.13 illustrate the installation of the fuel flow meter on the fuel line of the UAlberta fleet vehicles.

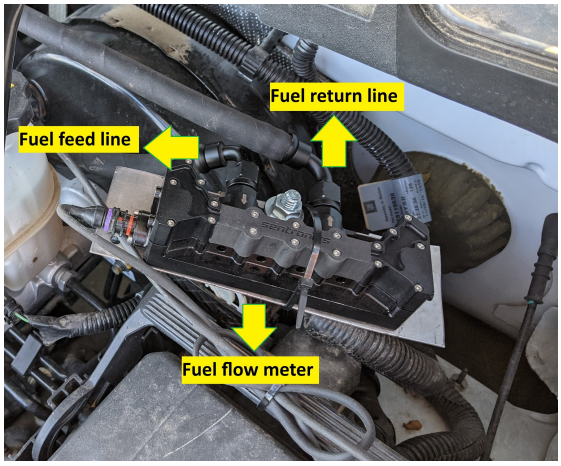

(a) Chevrolet Silverado 1500

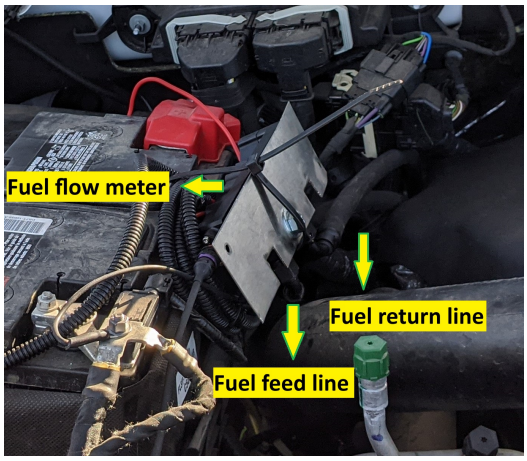

(b) Ford Expedition

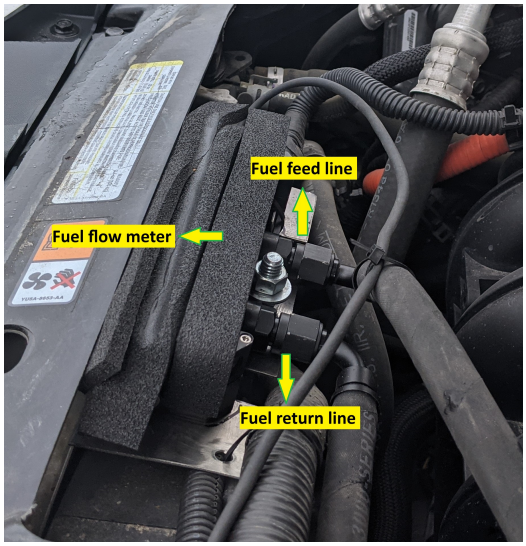

(c) Ford Fusion Hybrid

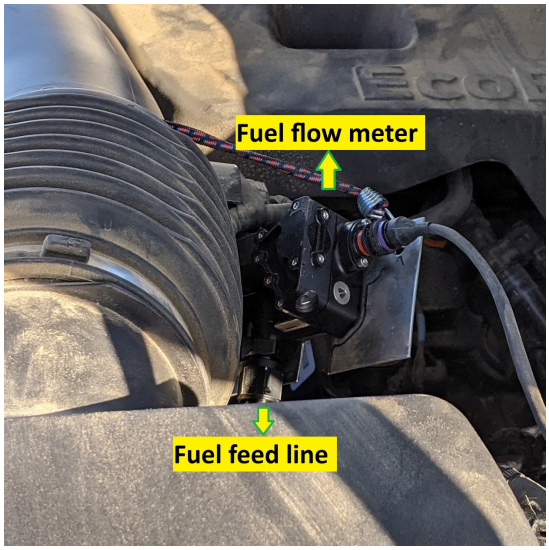

(d) Ford F-150

Figure 2.12: Sentronics ultrasonic fuel flow meter installed on UAlberta fleet vehicles (Part 1)

Table 2.5 shows the list of vehicles on which the Sentronics fuel flow meter was installed to measure fuel consumption. The vehicles were chosen from the UAlberta fleet vehicles, with varying engine sizes and technology.

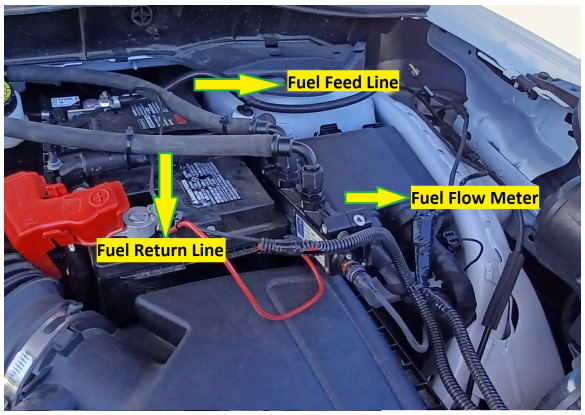

(a) Ford Escape S

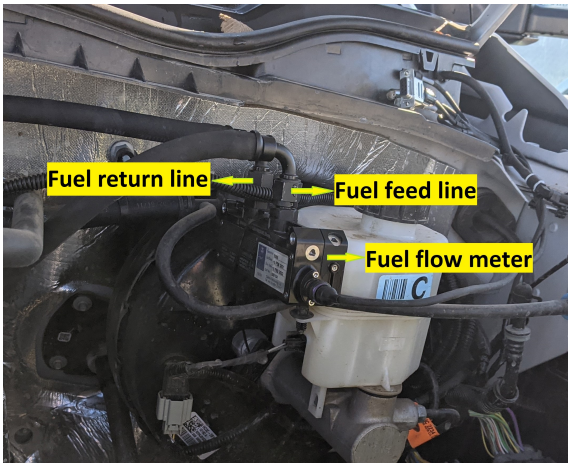

(b) Ford F-350

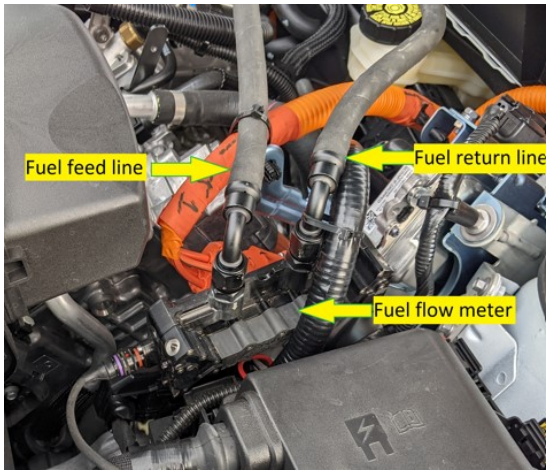

(c) Ford Escape PHEV

Figure 2.13: Sentronics ultrasonic fuel flow meter installed on UAlberta fleet vehicles (Part 2)

Table 2.5: Sentronics ultrasonic fuel flow meter installed on UAlberta fleet vehicles

No.	Vehicle	Model Year	Engine Size / Type
1	Ford Escape PHEV	2021	2.5 L / Atkinson-Cycle I-4
2	Ford Escape S	2021	1.5 L / Eco Boost
3	Ford F-350	2021	6.2 L / Tuned Intake
4	Ford F-150	2021	3.5 L / Eco Boost
5	Ford Expedition	2019	3.5 L / Twin Turbocharged
6	Ford Fusion Hybrid	2010	2.5 L / I-4 Engine
7	Chevrolet Silverado 1500	2016	4.3 L / Eco Tec3

2.2.2 CSS Electronics CANedge2 data logger

The CSS Electronics CANedge2 data logger (Figure 2.14) was used in this thesis to collect data from the vehicle OBD and the fuel flow meter simultaneously (Figure 2.10). The collected data contains actual fuel consumption and the related vehicle's OBD PIDs.

Figure 2.14: CSS electronics CANedge2

The technical specifications of the CSS Electronics CANedge2 data logger are shown in Table 2.6.)

Table 2.6: Specifications of the CSS Electronics CANedge2 data logger used in this thesis

Parameter	**Value**
Storage	Extractable industry grade micro SD-card (8-32 GB)
Transceiver	Compliant with CAN Protocol Version 2.0 Part A, B and ISO 11898-1
Common mode input voltage	±30V
Data rates	Up to 5 Mbps
Channel 1 voltage supply range	+7.0V to +32V DC
Secondary port output supply	Channel 2, fixed 5V up to 1.5A
Consumption	1W
Operating temperature:	-25 °C to +70 °C
Weight	100 g

Terminal 1 of the CANedge2 was connected to the OBD port of the vehicle, powering up the device and enabling the collection of vehicle PIDs. These PIDs represent various parameters and sensor readings from the vehicle's internal systems, such as engine speed, vehicle speed, throttle position, etc.

In addition to the OBD data, terminal 2 of the CANedge2 captured flow meter data. The flow meter measures the actual fuel consumption of the vehicle. By simultaneously recording the OBD PIDs and flow meter data, it becomes possible to correlate the vehicle's operational characteristics with its actual fuel consumption.

The CANedge2 OBD data logger saved recorded data in an SD card in MP4 format. The Assammdf software was used to automatically synchronize and extract data into a CSV file (Figure 2.15).

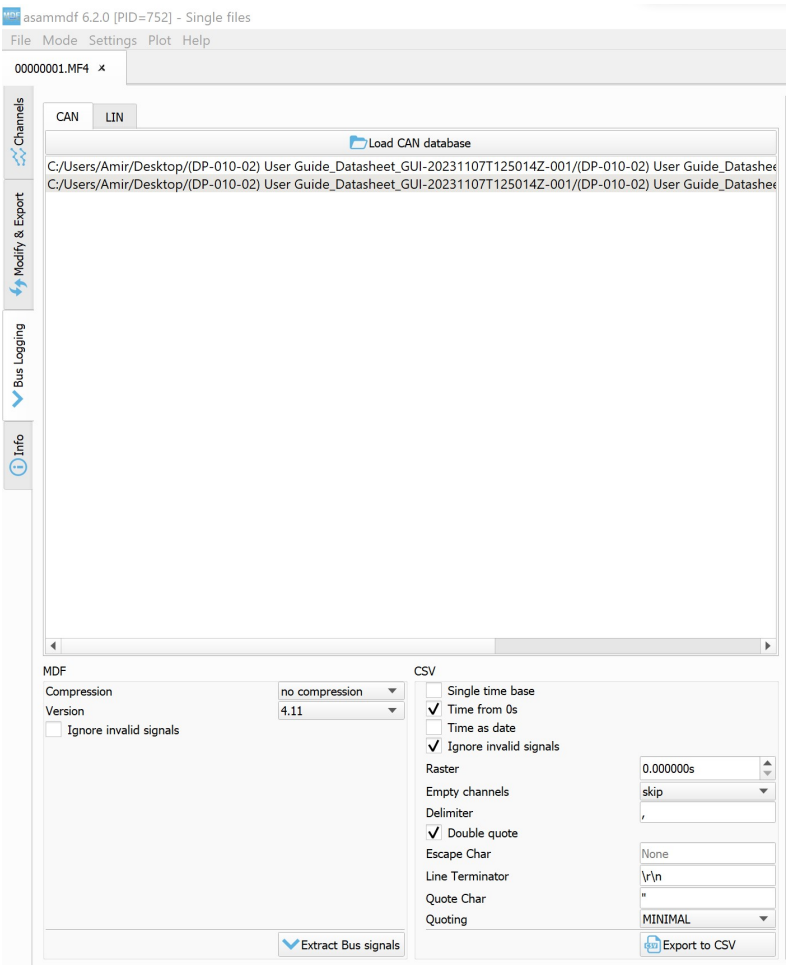

Figure 2.15: Assammdf software used in this thesis

Details of how to set up CANedge2 are explained in Appendix (B.2).

Figure 2.16 shows the engine speed, vehicle speed, and fuel consumption time series of the Ford Escape PHEV during an urban drive cycle with a maximum speed of 80 km/h.

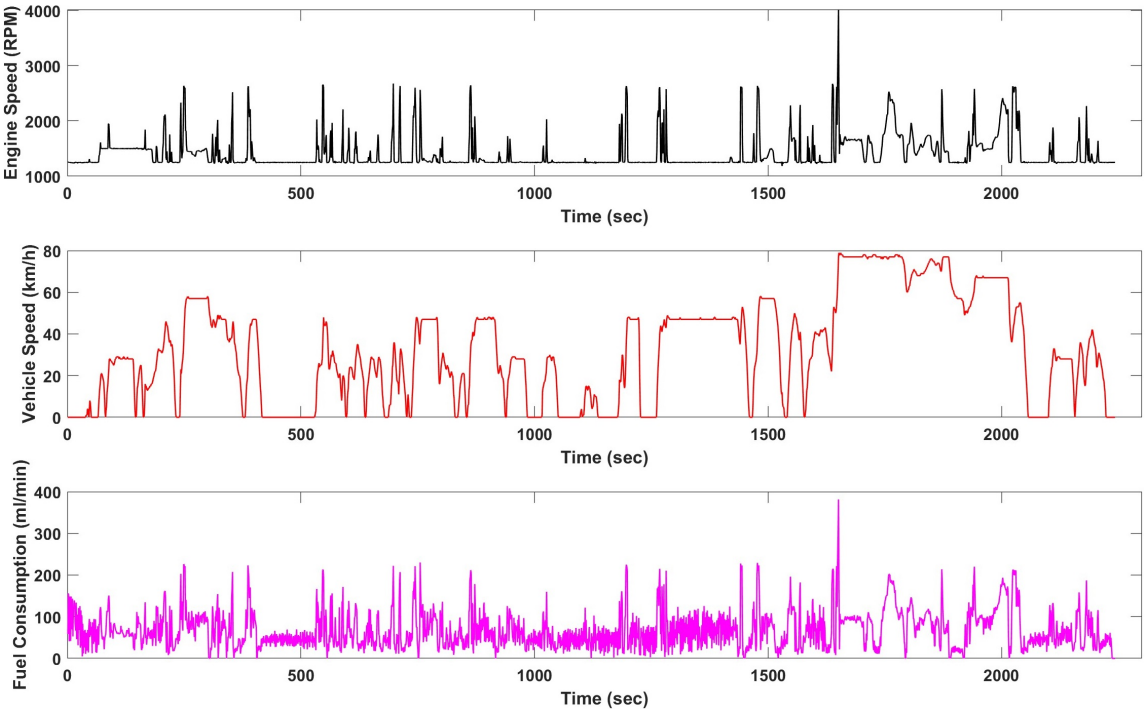

Figure 2.16: Ford Escape PHEV engine speed, vehicle speed, and fuel consumption time series

As can be seen in Figure 2.16, the engine maintained a speed of around 1200 RPM while the vehicle speed remained constant. The fuel consumption was generally below 100 ml/min but increased during acceleration and decreased during deceleration.

Figure 2.17 shows the time series of engine speed, vehicle speed, and fuel consumption for the Ford Escape S during an urban drive cycle with a maximum speed of 80 km/h.

According to plots in Figure 2.17, the engine speed was around 1600 RPM during the constant vehicle speed. The vehicle was equipped with start-stop technology, leading the engine to turn off during the stops.

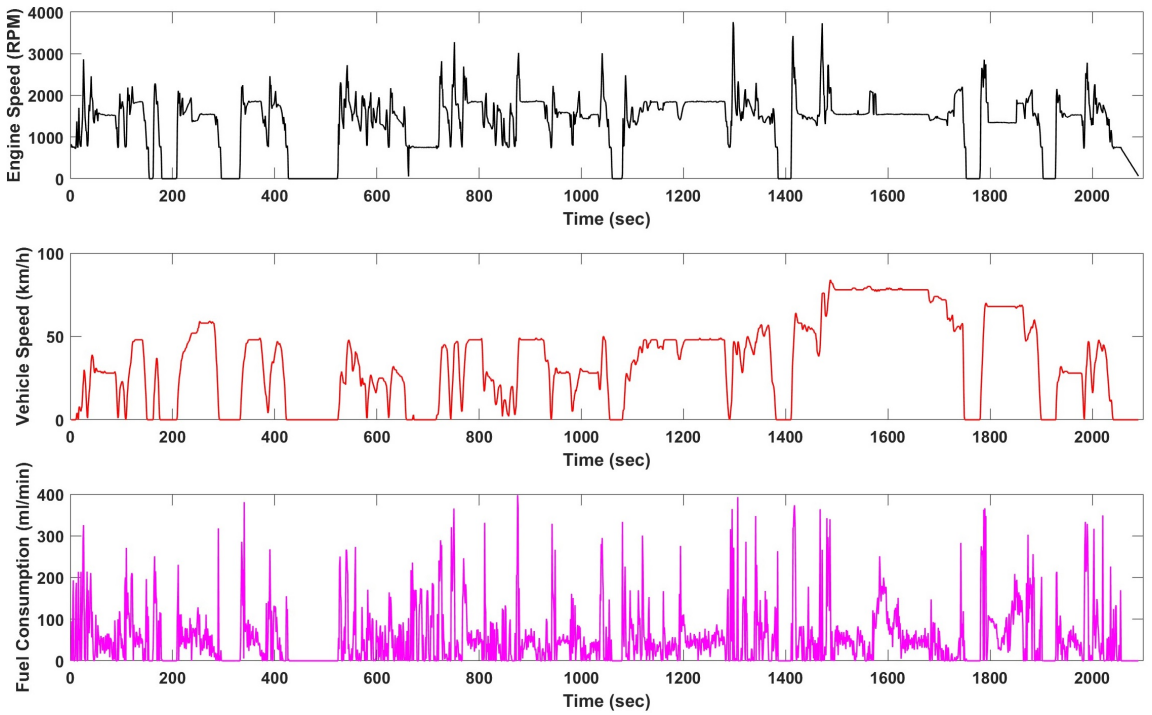

Figure 2.17: Ford Escape S engine speed, vehicle speed, and fuel consumption time series

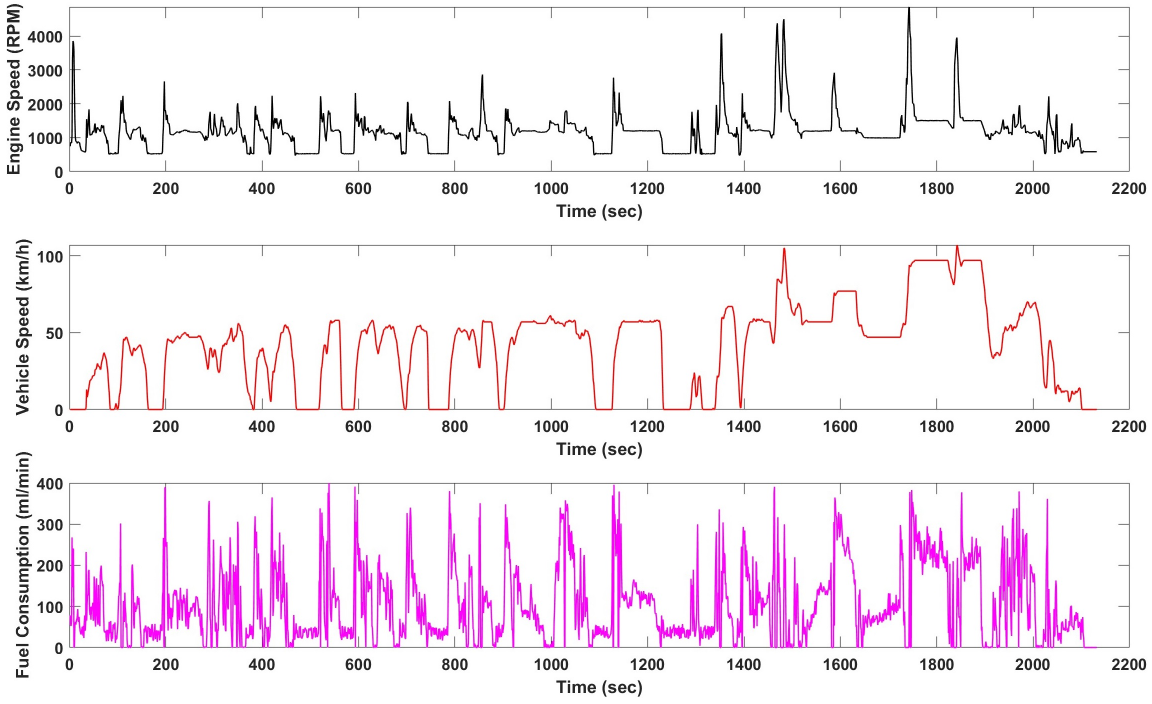

Figure 2.18: Ford F-350 engine speed, vehicle speed, and fuel consumption time series

Figure 2.18 shows the time series for engine speed, vehicle speed, and fuel consumption of the Ford F-350 during a drive cycle that includes both highway (with a speed limit of 100km/h) and urban (with a speed limit of 60 km/h) driving.

The Ford F-350 had a larger engine compared to both the Ford Escape PHEV and model S, resulting in higher fuel consumption. This can be observed by comparing the fuel consumption time series of the three vehicles. The fuel consumption rate was between 200 ml/min to 300 ml/min while the vehicle was driven at its highest drive cycle speed, with approximately 100 km/h. This resulted in the highest fuel consumption among all three vehicles at a constant speed.

Chapter 3

Fuel Consumption Estimation of University of Alberta Fleet Vehicles

3.1 University of Alberta fleet vehicles overview

Figure 3.1: University of Alberta South campus transportation service

The University of Alberta's fleet of 180+ vehicles causes significant greenhouse gas emissions due to its annual fuel consumption of 205,000 liters. This leads to the emission of 564,291 kg of CO_2 annually, contributing to climate change and negatively impacting the environment and human health.

By using machine learning models to estimate fuel consumption based on real-time data from data loggers, the University of Alberta can gain valuable insights into its fleet's performance and identify areas for improvement in fuel efficiency.

Analyzing this data can better understand the fleet's energy consumption pat-

terns, which is crucial for identifying opportunities to transition to low-emission vehicles. Comparing the energy consumption of conventional gasoline vehicles with low-emission alternatives like electric vehicles (EVs) or hybrid vehicles will provide valuable information for making informed decisions on fleet replacements or additions. This showcases the university's commitment to sustainability and aligns with broader global efforts to combat climate change and reduce greenhouse gas emissions.

The primary objective of this thesis is to develop a reliable and accurate method for monitoring the instantaneous fuel consumption of these vehicles using On-Board Diagnostic (OBD) data.

The study employs Random Forest (RF) and Artificial Neural Network (ANN) models to accomplish these goals. These are machine learning techniques used to model and predict instantaneous fuel consumption using real-time OBD data.

RF model is an ensemble learning method that combines multiple decision trees to improve prediction accuracy and reduce overfitting. It is well-suited for regression tasks like predicting fuel consumption, as it can handle complex relationships between the input features (e.g., vehicle speed, engine speed, throttle position) and the output variable (fuel consumption).

On the other hand, ANNs are computational models inspired by the human brain's neural networks. They consist of interconnected nodes (neurons) organized into layers, with each neuron performing simple computations. Neural networks are powerful tools for capturing non-linear relationships in data and have been successfully used in various applications, including fuel consumption prediction.

By utilizing these machine learning methods on real-time OBD data, the study aims to develop a robust and accurate model that can reliably predict fuel consumption for the university's fleet vehicles. This predictive capability will significantly benefit fleet management decisions, such as identifying areas of improvement in driving behavior, optimizing routes, and selecting appropriate vehicles for specific tasks.

The new contributions of this thesis are pretty significant and address important

aspects of fuel consumption estimation using machine learning models.

i) Actual Measurement of Instantaneous Fuel Consumption: It is essential to consider the usage of actual measurement of instantaneous fuel consumption to provide accurate and reliable data for training machine learning models. This approach ensures that the data used for modeling is as close to real-world fuel consumption as possible, improving the accuracy of the predictions. By avoiding reliance on indirect estimations or extrapolations, the results will be more trustworthy and representative of actual fuel consumption patterns.

ii) Real-Time OBD Data and Wide Operating Conditions: Incorporating real-time OBD data alongside accurate fuel consumption measurements is an excellent approach. OBD data can provide valuable information about the vehicle's performance, emissions, and operating conditions. Combining this data with fuel consumption measurements allows for a more comprehensive analysis. It enhances the machine learning models' accuracy across various driving scenarios, including critical factors like cold starts and non-stoichiometric conditions.

iii) Ultrasonic Fuel Flow Meter for Ultra Low-Volume Fuel Flow Operation: An ultrasonic fuel flow meter is a novel and valuable addition. This technology allows for precise measurement of ultra-low-volume fuel flow operations, particularly useful for modern vehicles with high fuel efficiency and reduced fuel consumption. The high sampling frequency of 5Hz ensures that the models capture fine-grained variations in fuel consumption, leading to more nuanced and accurate predictions.

iv) Fuel Consumption Data from Modern Vehicles: Including fuel consumption data from two MY2021 modern vehicles is highly relevant and adds to the applicability of the research. Modern vehicles often feature advanced fuel-saving technologies, and understanding their fuel consumption patterns is essential for making informed decisions about fleet composition and future vehicle choices. Having data from current vehicles helps bridge the gap between research and real-world applications.

Overall, the contributions of this thesis address critical aspects of fuel consumption

estimation, considering real-world scenarios and modern vehicles. The methodologies employed provide accurate, high-quality data for training machine learning models, which can have broader implications for improving fuel efficiency and reducing greenhouse gas emissions in the University of Alberta's fleet.

3.2 Experimental Procedure

3.2.1 Tested Vehicles

In this part of the thesis, two MY2021 vehicles with different powertrain systems were selected from the University of Alberta (UAlberta) fleet vehicles for testing. A Ford F-350 (full-size pickup truck) with a conventional 6.2-liter gasoline engine (Figure 3.2) and a Ford Escape PHEV (compact SUV) equipped with a 2.5-liter gasoline engine and an electric motor, allowing the vehicle to operate on both electric power and gasoline power. The study aims to investigate the instantaneous fuel consumption of the PHEV model and the conventional gasoline-powered truck.

Figure 3.2: The Ford F-350 used in this thesis

The specifications of the tested Ford F-350 are shown in Table 3.1.

Table 3.1: Specifications of the Ford F-350

Vehicle Specification	
Model Year	2021
Vehicle Body Style	Pickup Truck
Fuel Type	Gasoline
Engine Type	6.2 L
Engine Rated Power	287 kW @ 5,750 RPM
Engine Torque	583 N.m @ 3,800 RPM
Compressor Ratio	9.8:1
Induction System	Naturally Aspirated, Tuned Intake
Transmission Type	10-Speed Automatic
Vehicle Base Curb Mass	3,042 kg

The Ford Escape PHEV (Figure 3.3) used in this study allows the assessment of vehicle energy consumption under different modes of operation: i) Pure electric, ii) hybrid electric, and iii) pure combination engine operations using the same vehicle platform.

Figure 3.3: The Ford Escape PHEV used in this study

Table 3.2 shows the tested Ford Escape PHEV specifications.

Table 3.2: Specifications of the Ford Escape PHEV

Vehicle Specification	
Vehicle Body Style	Compact SUV
Fuel Type	Gasoline / Battery
Engine Type	2.5 L Aluminum Block and Head, Atkinson-Cycle I-4
Engine Rated Power (Using 93 Octane Fuel)	123 kW @ 6,250 RPM
Total System Power (Hybrid and Plug-in Hybrid)	149 kW @ 6,250 RPM
Engine Torque	210 N.m @ 4,500 RPM
Engine Compressor Ratio	13.0:1
Engine Induction System	Naturally Aspirated
Transmission Type	Electronic Continuous Variable Transmission
High Voltage Battery	Approximately up to 450 Volt DC, Liquid cooled lithium ion battery
High Voltage Battery Capacity	14.4 kWh
Vehicle Base Curb Mass	1,762 kg
EPA Gasoline Fuel Consumption	5.8 L/100 km City/Hwy Combined
EPA Electricity + Gasoline Fuel Consumption	2.2 L_e/100 km City/Hwy Combined
EPA Electricity Energy Consumption	19.9 kWh/100 km City/Hwy Combined

It has a 123 kW ICE and a total power (Hybrid and Plug-in Hybrid) of 149 kW. The vehicle is equipped with a 14.4 kWh Li-ion battery, and according to Environmental Protection Agency (EPA) data, based on 45% highway and 55% city driving [45], its energy consumption is 19.9 kWh/100 km. The claimed all-electric range (AER) of the vehicle based on EPA is 61 km in the T_{amb} range of 20 °C to 30 °C [46]. The vehicle mileage was 820km before the study and 10,150 km after completion.

3.2.2 Test Driving Route

The selected comprehensive driving test route (Figure 3.4) covers a variety of driving conditions to ensure a thorough evaluation of the university fleet vehicles. The route length is 100 km, and completing it takes approximately 1 hour and 33 minutes. By collecting OBD data from the vehicles during this comprehensive route, the university can gain valuable insights into fuel consumption patterns and identify opportunities for improvement in various driving scenarios.

Figure 3.4: The driving route in this study

Starting from the University of Alberta Transportation Service at South Campus,

the route includes diverse scenarios that can impact fuel efficiency.

i) Residential Areas: The route passes through residential areas where the maximum speed limit is 40 km/h. These areas typically involve frequent stops and starts due to traffic lights, intersections, and pedestrian crossings. Fuel consumption tends to increase in such areas due to frequent acceleration and deceleration.

ii) City Areas: The route also covers city areas with speed limits ranging from 40 km/h to 100 km/h. This includes typical urban roads where drivers encounter moderate traffic, traffic signals, and varying road conditions. Driving in these areas can present challenges in maintaining fuel efficiency due to constant speed changes and traffic congestion.

iii) Road Grade Changes: The route incorporates road segments with grade changes (uphill and downhill sections). Driving on inclines can increase fuel consumption, while downhill sections might allow for some fuel-saving opportunities.

iv) Highway Areas: The route includes highway sections with an increase in the maximum speed limit. Highways generally offer smoother driving conditions, but maintaining high speeds for extended periods can also impact fuel efficiency.

The data collected from this route can be used in conjunction with the RF and ANN methods mentioned earlier to develop accurate models for predicting fuel consumption based on real-time OBD data.

3.2.3 Data Collection and Fuel Consumption Measurement

The schematic of the data collection procedure is shown in Figure 3.5.

The CANedge2 data logger was used to collect and store CAN bus data from the vehicle's OBD-II port and fuel flow meter. In this case, the OBD reader was connected to the OBD port of the vehicle to collect OBD data, while the fuel flow meter was connected to the other terminal of the OBD reader to collect fuel flow CAN data.

The OBD data was collected at a sample rate of 2 Hz, which means the data was recorded two times per second. This data included a variety of parameters, such as

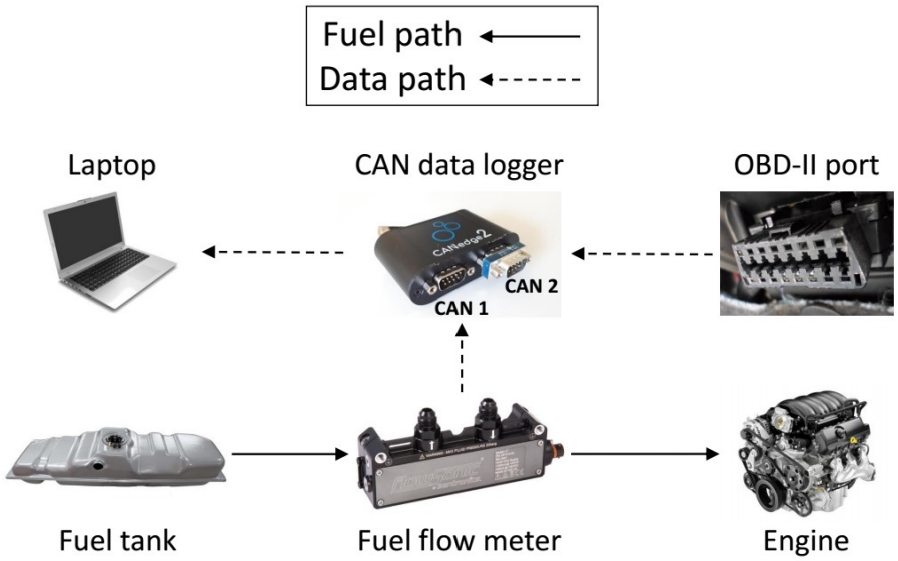

Figure 3.5: Schematic of fuel consumption data collection process

engine speed, vehicle speed, throttle position, and more (Table 3.3).

Table 3.3: The main PIDs collected by CANedge2 data logger

Parameter	**Unit**
Vehicle Speed	km/h
Engine Speed	RPM
Engine Load	%
Engine Coolant Temperature	°C
Exhaust Catalyst Temperature	°C
Short Fuel Trim	-
Long Fuel Trim	-
Intake Manifold Absolute Pressure	kPa
Throttle Position	%
Air/Fuel Equivalence Ratio	-

The fuel flow meter data were collected at a sample rate of 5 Hz. This data would provide information about the amount of fuel being consumed by the engine.

By syncing the OBD data with the fuel flow meter data, it is possible to gain

insights into the vehicle's transient performance and fuel conversion efficiency at different speeds and load conditions. For example, one could use this data to calculate the vehicle's fuel economy or identify areas where the engine may be operating inefficiently.

The data collected from the vehicles using the CANedge2 data logger was recorded in the MF4 format and stored on an SD card inside the device. To analyze and work with the data, the Asammdfgui software (which is a software tool used for processing, analyzing, and visualizing data from various sources) was used to convert the MF4 files to CSV format. This CSV format is commonly used for storing and manipulating tabular data, making it easier to work with and analyze.

3.2.4 Instantaneous Fuel Consumption Estimation Models

Machine learning models were developed to estimate the instantaneous fuel consumption of the vehicles in the fleet based on OBD data. These models were designed to work in real time and were tailored to the specific parameters available from each vehicle's OBD data logger. Since different vehicles may have other public parameters available via OBD, the models were designed to consider the availability of the relevant PIDs in the OBD data.

Selected Features

In order to train the selected models, the OBD parameters should be selected carefully, ensuring that they are readily available in all vehicles and directly impact the engine's instantaneous fuel consumption. The selected parameters include engine load, engine speed, intake manifold absolute pressure (MAP), throttle position, air-fuel equivalence ratio, and engine coolant temperature, which are listed in Table 3.4. Engine load, throttle position, and intake manifold pressure are all linked together and help to include the effect of intake air mass flow rate in the model. It was found that the combination of these three variables was more effective than including only one of

them for accurate estimation of instantaneous fuel consumption.

During the cold phase, i.e., when the engine coolant hasn't reached the fully warmed-up condition, fuel consumption is more significant for shorter trips. This is because it accounts for a larger fraction of the overall trip time and distance. Thus, it's vital to include the cold start phase in the training data for urban driving fuel consumption models. To represent engine temperature, coolant temperature from OBD data is used in the training process.

By training machine learning models to predict fuel consumption based on these parameters, it will be possible to estimate fuel consumption accurately and in real time, which can be helpful for monitoring and optimizing fleet performance.

Table 3.4: Parameters used as inputs to machine learning models

Parameter	**Unit**
Engine Speed	RPM
Engine Load	%
Intake Manifold Absolute Pressure	kPa
Throttle Opening	%
Air/Fuel Equivalence Ratio	-
Engine Coolant Temperature	°C

Four machine learning methods were investigated to estimate fuel consumption in fleet vehicles, including RF, ANN, SVM, and K-Nearest Neighbors (KNN). RF model is a standard machine-learning algorithm known for its ability to handle high-dimensional data sets and complex relationships between features. It works by constructing multiple decision trees and combining their predictions to produce a final output. One advantage of the RF model is that it is resistant to over-fitting and can handle many features without normalizing the data [47]. ANN is another common machine learning algorithm for handling non-linear relationships between features. ANNs work by modeling the relationship between input and output data using in-

terconnected nodes that simulate the behavior of neurons in the brain [48]. This allows them to capture complex patterns and relationships in the data, making them well-suited for predicting fuel consumption in fleet vehicles. After initial analysis, RF and ANN methods were found to offer the highest accuracy, and thus, the study focuses on presenting the results for these two methods. Overall, both RF and ANN models have their strengths and weaknesses, and the choice of which method to use may depend on factors such as the complexity of the data, the number of features available, and the desired level of accuracy.

Artificial Neural Network (ANN) Model

An ANN is a machine-learning model inspired by the structure and functioning of the human brain. It is a deep learning algorithm that can be used for various tasks, such as classification, regression, pattern recognition, and more. ANNs are widely used in artificial intelligence and have successfully solved complex problems across multiple domains.

An ANN consists of interconnected artificial neurons organized in layers. There are three primary types of layers. i) Input Layer: This layer receives the raw data as input. Each neuron in the input layer represents a feature or attribute of the data. ii) Hidden Layers: These layers are placed between the input and output layers and play a crucial role in learning complex patterns from the data. The number of hidden layers and the number of neurons in each hidden layer can vary depending on the complexity of the problem. iii) Output Layer: The final layer of the network, which produces the output. The number of neurons in the output layer depends on the type of problem.

The connections between neurons are represented by weights, which determine the strength of the links. During training, the ANN adjusts these weights to learn patterns and relationships in the data. The process of adjusting the weights is known as backpropagation, and it involves minimizing a loss function that quantifies the

difference between the predicted output and the actual target values. Each neuron in the ANN typically applies an activation function to the weighted sum of its inputs. The activation function introduces non-linearity to the model, enabling it to learn complex relationships in the data. Standard activation functions include sigmoid, tanh, and Rectified Linear Unit (ReLU).

The ANN is trained using a process called supervised learning, where it is presented with a labeled dataset (input data along with corresponding target outputs). The network iteratively adjusts its weights during training using optimization techniques like gradient descent and variants. The objective is to minimize the error between the predicted outputs and the actual target outputs. Once the ANN is trained on a sufficiently large and diverse dataset, it can expect new, unseen data with reasonable accuracy.

An ANN model with one hidden layer was used for this study. The model was developed using Table 3.5 parameters. During the training and validation of the model, the optimal number of nodes was determined.

Table 3.5: Parameters of the designed ANN model

Parameter	**Value**
Number of Hidden Layers	1
Activation Function for the Hidden Layer	Relu
Solver for Weight Optimization	Adam
Learning Rate	0.001
Numerical Stability Criteria	10^{-8}
Maximum Number of Iterations	200

The ANN model used in this thesis was sensitive to the range of feature values. This is a common issue with many machine learning algorithms, including neural networks. When the range of feature values is too extensive, it can cause the model to give too much importance to certain features and ignore others, leading to inaccurate

predictions. The data was normalized before training the ANN model to address this issue. Normalization is a technique used to scale the range of feature values to a standard range. Equation (3.1) shows the general formula for normalizing a feature:

$$\tilde{x_s} = \frac{x - min(x)}{max(x) - min(x)} \tag{3.1}$$

where $\tilde{x_s}$ represents the normalized data which is between 0 and 1, x is the original data, $\min(x)$ is the minimum value of feature x, and $\max(x)$ is the maximum value of component x. By applying this formula to each element in the dataset, all features are scaled to the same range, which can improve the performance of the ANN model.

Random Forest (RF) model

RF model is a machine-learning algorithm used for classification and regression tasks and is known for its high accuracy, robustness, and ability to handle complex data without overfitting. It creates a multitude of decision trees during the training process and combines their predictions to make a final decision. Each decision tree in the forest is constructed independently, using a random subset of the training data and features. This randomness and diversity in the trees contribute to the model's effectiveness. The critical concepts of the RF model include:

i) Bagging, a technique where multiple subsets of the training data are created by random sampling with replacement. Each subset is used to train a separate decision tree. This process introduces diversity in the training data and helps in reducing over-fitting.

ii) For each decision tree, only a random subset of features is considered for splitting at each node. This further increases the diversity among the trees and helps improve the model's generalization.

iii) During prediction, the outputs of all the decision trees in the forest are com-

bined. The final prediction is determined by a majority vote from the individual trees for classification tasks. For regression tasks, the final prediction is the average of the individual tree predictions.

For this study, an RF model was developed based on the parameters shown in Table 3.6. The number of decision trees can significantly impact the performance of the model. The optimal number of decision trees is determined using cross-validation. The objective is to find the right balance between having enough trees to capture the complexity of the data while avoiding over-fitting. Generally, having a more significant number of decision trees can lead to better performance, but it also increases the computational cost and can lead to over-fitting.

Table 3.6: Parameters of the designed RF model

Parameter	**Value**
Split Criterion Function	Squared Error
Minimum Number of Samples to Split	2
Minimum Number of Samples for Leaf Node	1

The collected data was split into two parts to develop and evaluate the machine learning models. This method applies to both ANN and RF models, and the same process was followed. The first part, which consisted of 70% of the total data, was used for training and validation using a 5-fold cross-validation method. Four parts were used for training, and the remaining was used for validation. This is a specific type of cross-validation called "k-fold cross-validation," where the data is divided into k subsets, and the model is trained and validated k times, with a different subset used for validation each time. This allows for a more robust evaluation of the model's performance by using different subsets of the data for training and validation. The remaining 30% of the data was held out for testing the final models after training and validation. This data was not used during the training or validation process and was used to evaluate the performance of the last models on unseen data. During

testing on a desktop computer with 32 GB RAM and a core i7-9700 processor, it was observed that the RF and ANN models took approximately 56 msec and 72 msec to run respectively for about 90 seconds of operation. If the amount of data is reduced, the training duration will be shorter. In addition, there were no noticeable differences in the training duration between the RF and ANN models.

3.3 Results and Discussion

In order to have an accurate fuel consumption model, it is essential to cover a wide range of engine speeds and loads in the training data. Machine learning models can learn to accurately predict fuel consumption across a wide range of operating conditions. Engine speed and load are two of the most critical factors that can help describe the engine's operating points.

Engine speed (RPM) is a critical factor in determining fuel consumption because it affects the amount of air that enters the engine, which in turn affects the amount of fuel that is burned, assuming maintaining a constant air-fuel ratio. Load, typically measured as a percentage of the engine's maximum torque output, is also significant because it affects the amount of work the engine is doing and, therefore, the fuel required to support the requested engine load.

The engine operation points of both tested vehicles over the drive cycle (Figure 3.4) are shown in Figure 3.6. As mentioned earlier, the Ford Escape PHEV is a plug-in hybrid electric vehicle with a gasoline engine and an electric motor. In certain operating conditions, the vehicle can rely solely on electric power, which limits the range of data points and engine operating conditions when the gasoline engine is not being used. The number of points would be fewer due to the selective usage of the gasoline engine (Figure 3.6a). On the other hand, the Ford F-350 is powered exclusively by a gasoline engine. As a result, the engine operating range for the Ford F-350 is broader and covers a more comprehensive range of driving conditions compared to the Ford Escape PHEV (Figure 3.6b).

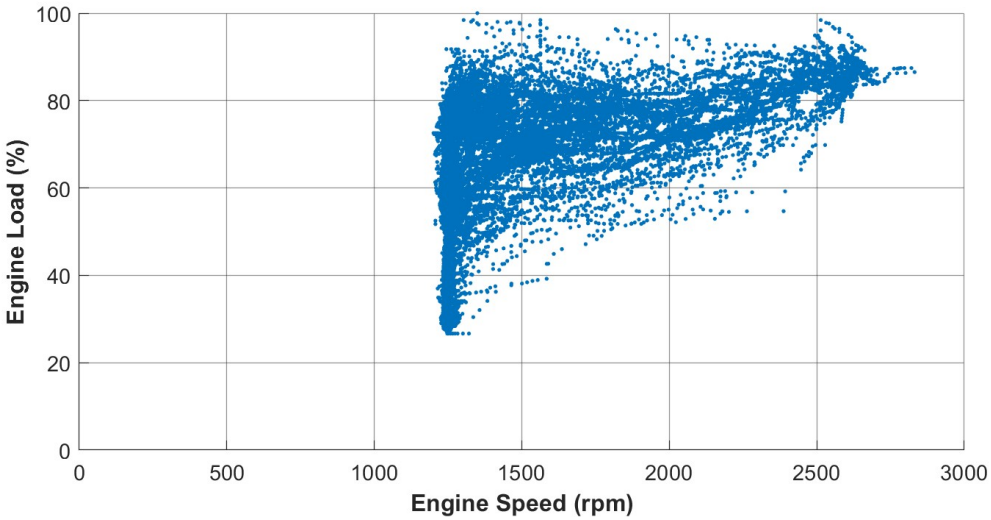

(a) Ford Escape PHEV

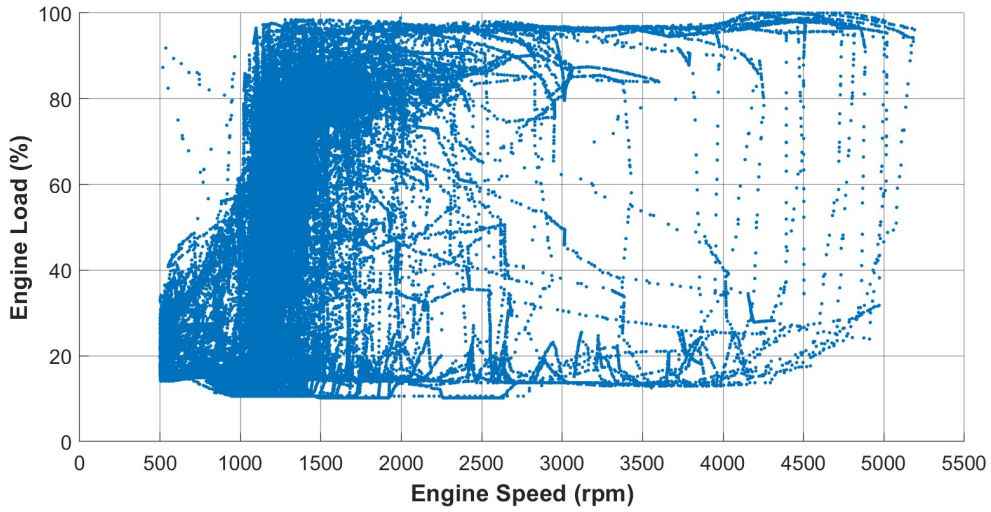

(b) Ford F-350

Figure 3.6: Engine operation map (engine speed vs. engine load) for two tested vehicles

The range of input parameters variation for both RF and ANN models is presented in Table 3.7.

The time series of vehicle speed and instantaneous fuel consumption shown in Figure 3.7 indicate that driving behavior and operating conditions significantly impact fuel consumption. During acceleration, the instantaneous fuel consumption increases considerably as the engine works harder to generate more power. The similar speed

Table 3.7: The range of input parameters variation for both RF and ANN models

Parameter	**Ford Escape PHEV Min-Max**	**Ford F-350 Min-Max**
Engine Speed	1200 - 2831 RPM	500 - 5190 RPM
Engine Load	27 - 100 %	12 - 100 %
Intake Manifold Absolute Pressure	29 - 92 kPa	15 - 92 kPa
Throttle Opening	16 - 55 %	6 - 90 %
Air/Fuel Equivalence Ratio	0.83 - 1.30	0.79 - 1.47
Engine Coolant Temperature	21 - 105 °C	82 - 88 °C

profiles of both vehicles suggest that they were driven in identical driving conditions. However, the minor variations in the fuel consumption graphs of the two vehicles could be attributed to variances in driving behavior, traffic conditions, or other related factors.

As shown in Table 3.8, the validation results of the ANN model are acceptable for both vehicles, with a slightly lower Root Mean Square Error (RMSE) for the Ford Escape PHEV compared to the Ford F-350. This suggests that the ANN model can accurately estimate fuel consumption for various driving conditions and different vehicle types.

Table 3.8: Result of ANN fuel consumption model Cross validation

Parameter	**Ford F-350**	**Ford Escape PHEV**
Hidden Layer Size	160	260
RMSE (g/min)	18.88	7.38
R^2	0.97	0.96

Table 3.9 lists the RF model cross-validation results. The optimization of the hidden layer size for each model is an essential step in developing accurate fuel consump-

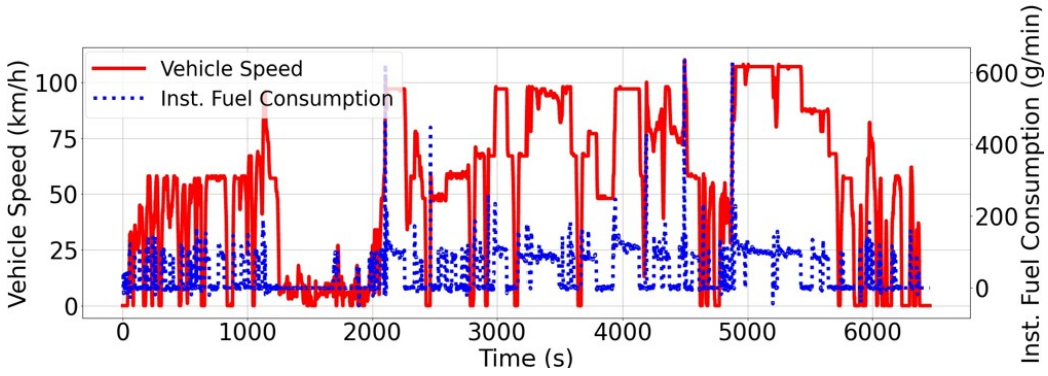

(a) Ford Escape PHEV

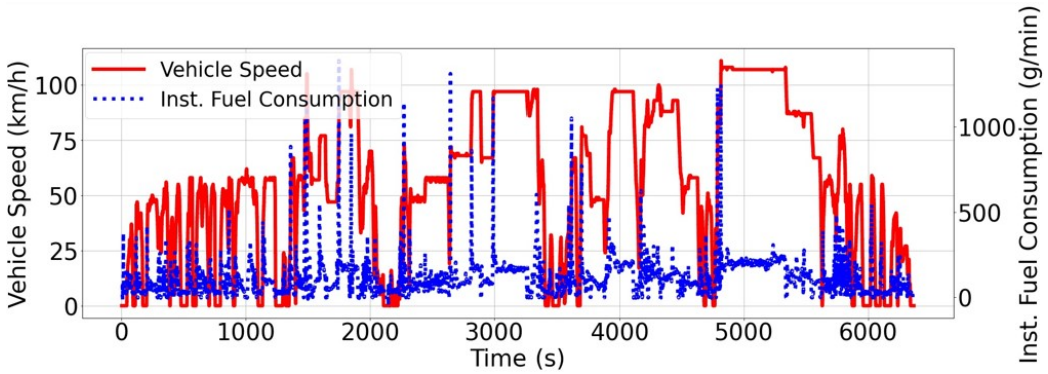

(b) Ford F-350

Figure 3.7: Time series of vehicle speed and fuel consumption

tion models. Minimizing the RMSE of the estimated fuel consumption, the hidden layer size can be optimized to provide the best balance between model complexity and accuracy.

Table 3.9: Results of RF fuel consumption model cross-validation

Parameter	**Ford F-350**	**Ford Escape PHEV**
No. of Decision Trees	110	60
RMSE (g/min)	12.47	4.27
R^2	1.00	0.99

It is important to note that the RMSE values for both RF and ANN models are relatively low, indicating that both models can accurately estimate fuel consumption for the two vehicles. However, the RF model performs slightly better than the ANN

model.

Table 3.10: Results of the fuel consumption models on the test dataset

Model	Vehicle	RMSE	R^2
ANN	Ford F-350	21.21	0.97
ANN	Ford Escape PHEV	9.07	0.96
RF	Ford F-350	11.01	1.0
RF	Ford Escape PHEV	6.096	0.99

The ANN and RF models' predictions are compared to fuel consumption measurements via scatter plots for both vehicles in Figures 3.8 and 3.9, respectively.

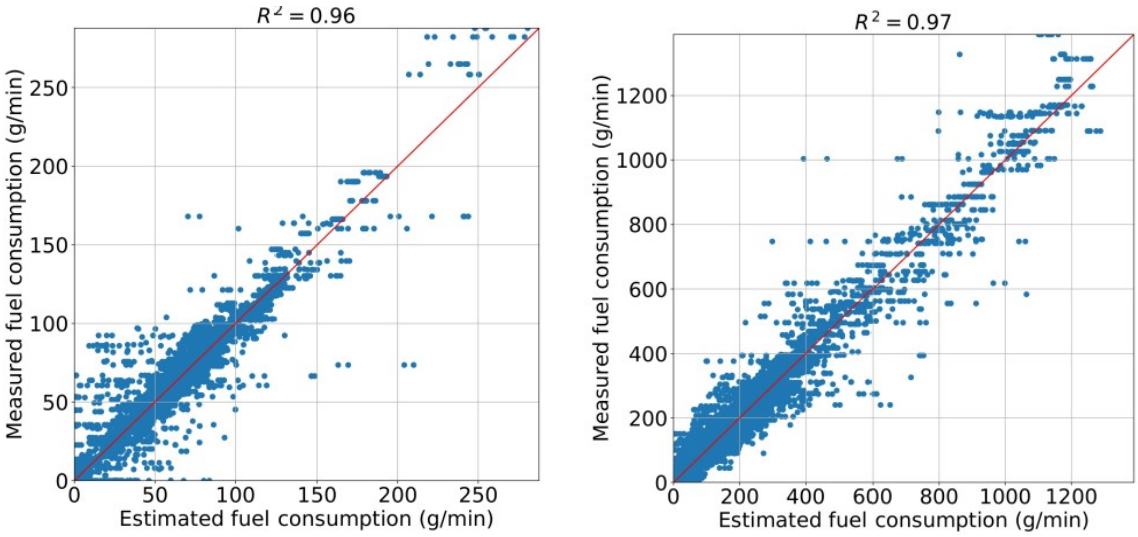

(a) Ford Escape PHEV (b) Ford F-350

Figure 3.8: Performance of the developed ANN model for estimating instantaneous fuel consumption

The closer the points are to the diagonal line, the more accurate the model's predictions are. In this case, based on the higher estimation accuracy and the closer alignment of points to the diagonal line on the scatter plot, it is concluded that the RF model is a better fit for the data. The RF model performs better in predicting fuel consumption for both vehicles, with an accuracy of accuracy of 100%, while it's 99% for the Ford Escape. Compared to the ANN model. The ANN model can estimate

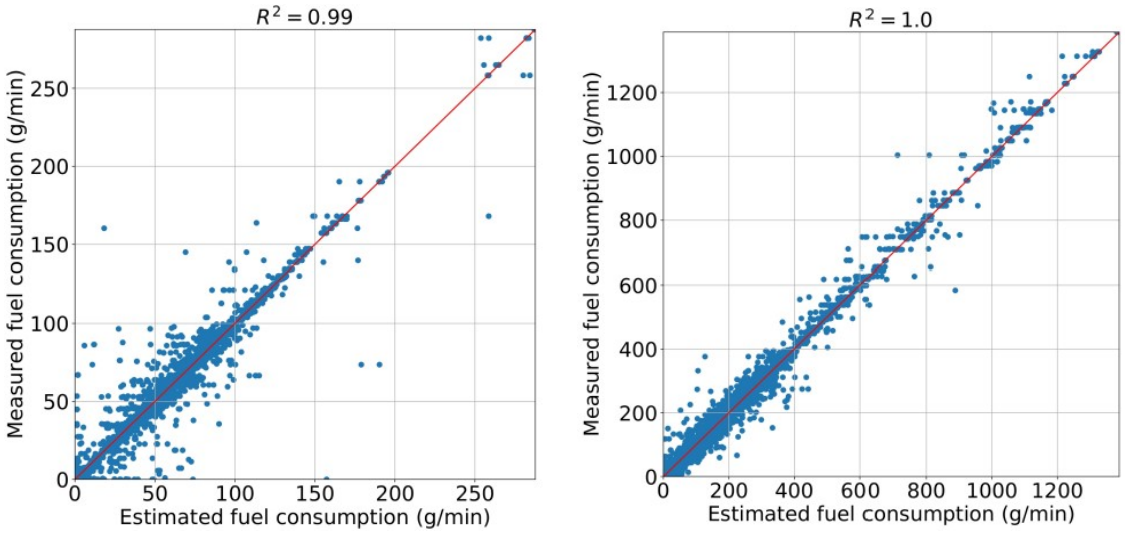

(a) Ford Escape PHEV (b) Ford F-350

Figure 3.9: Performance of the developed RF model for estimating instantaneous fuel consumption

Ford F-350 fuel consumption with an accuracy of 97%, while it's 96% for the Ford Escape. Both methods have acceptable accuracy for instantaneous fuel consumption estimation of the fleet vehicles.

Two ANN and RF machine learning models were developed to estimate the instantaneous fuel consumption of vehicles using OBD data. The actual fuel consumption was measured using an ultrasonic flow meter. In Figure 3.10, the models' estimated fuel consumption values were compared with the actual fuel consumption for a selected portion of a driving cycle.

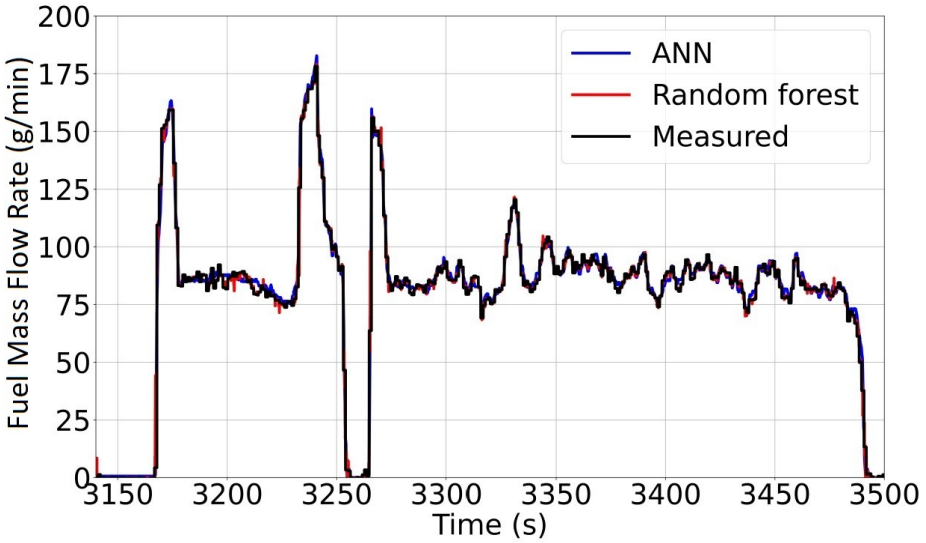

(a) Ford Escape PHEV

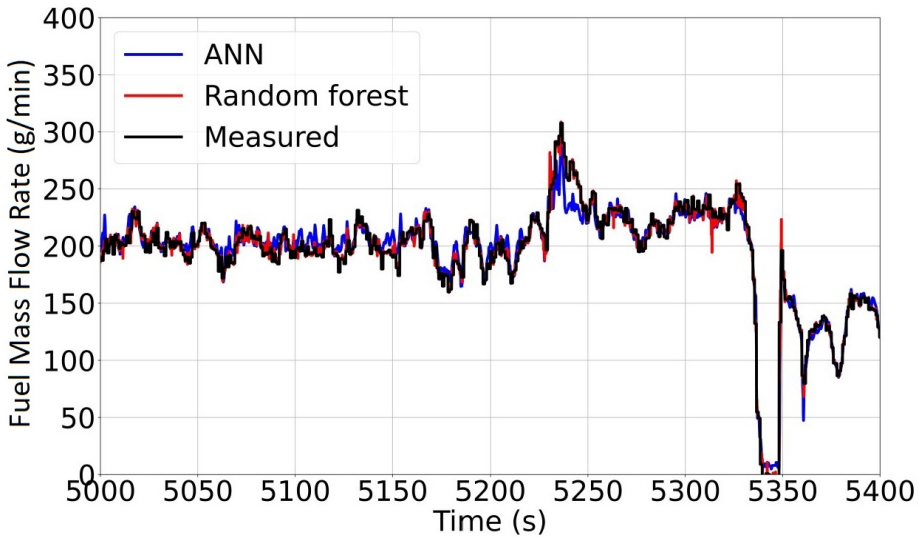

(b) Ford F-350

Figure 3.10: Comparing the estimation models

Looking at part of the drive cycle in Figure 3.10, the RF model deviates less from the actual values. Overall, the performance of the machine-learning models on the Ford Escape PHEV is slightly better than the Ford F-350. This comparison aims to assess the accuracy and performance of the machine learning models in predicting fuel consumption. By plotting the estimated fuel consumption against the actual fuel consumption, it can visually observe how well the models' predictions align with the

real-world measurements.

Chapter 4

Effect of Ambient Temperature on Energy Consumption of a Vehicle

This chapter studies the effect of T_{amb} on the energy consumption of three different powertrain types. These include pure internal combustion engine (ICE), hybrid electric, and pure electric operations. To properly compare the three powertrain types, a single vehicle with the possibility to run in each of these three powertrain modes is selected. To this end, this study is centered on a Ford Escape PHEV.

This chapter will compare energy consumption and Carbon Dioxide (CO_2) emissions under different driving conditions and powertrain modes. Transitioning to low-emission vehicles, such as EVs or hybrids, can significantly reduce the overall greenhouse gas emissions from the university's fleet. Electric vehicles, in particular, produce zero tailpipe emissions when charged with electricity from renewable sources, making them a desirable option for sustainable transportation. In real-world driving conditions, energy consumption and CO_2 emissions of a vehicle are affected by various factors (Figure 4.1).

Generally, the energy consumption and CO_2 emissions of road vehicles of all powertrain modes increase in lower ambient temperature (T_{amb}). Previous studies have shown that the increase in energy consumption ranges between 20% to 100% compared to normal operating temperatures [49]. In Electric Vehicles (EVs), a large portion of this increase is due to cabin heating [49]. In ICE vehicles, the wasted heat

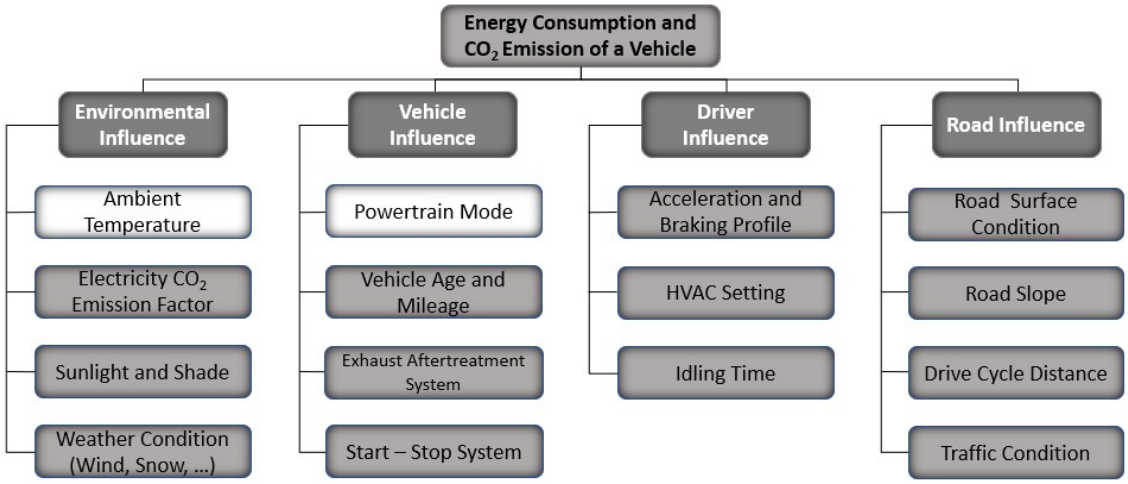

Figure 4.1: Major influencing factors on energy consumption, and CO_2 emissions of a vehicle. White blocks show the focus areas of this study.

from the combustion engine is usually used to provide cabin heating energy; thus, EVs are more affected by energy consumption increase in cold climates [50, 51]. In PHEVs, an optimal TMS is essential to increase energy efficiency by maintaining the vehicle components at an optimum temperature [28].

A real-driving test of a PHEV on three different urban, rural, and freeway routes showed that the initial battery state of charge (SOC) could change tailpipe CO_2 emissions and fuel consumption up to 40%. The powertrain mode of the vehicle between charge depleting (or EV) and charge sustaining (or HEV) is based on SOC [52]. In another real-driving PHEV study, the distance-specific energy consumption of the charge-depleting mode, compared with the charge-sustaining mode, was 45% lower. Still, the CO_2 emission was 50% higher due to the electricity generation carbon intensity [53].

Another PHEV was driven on different routes to assess energy consumption and emissions in different powertrain modes. Based on current electricity generation efficiency and transmission loss, the PHEV operating in charge-depleting mode is less energy efficient than the charge-sustaining mode for the energy mix of any U.S. state. However, the charge-depleting mode is more energy efficient than the comparably

sized conventional light-duty gasoline vehicle [34].

Among driving behavior and trip condition factors, the T_{amb} had the most decisive influence on the specific energy consumption of an EV in real-world driving data, doubling it by changing the temperature from 20 °C to 0 °C [54]. In another study, a PHEV was driven in a cold climate city with charge-depleting powertrain mode in different T_{amb}. At temperatures lower than -3 °C, the travel range did not change much, while it almost halved from 18 °C to -3 °C [30].

Testing a Chevrolet Volt PHEV in different T_{amb} showed a high dependency of energy consumption on the T_{amb} in both urban and highway driving conditions. The least energy was consumed during the operation from 20 °C to 25 °C. In the charge-sustaining mode in extreme winter temperatures (-25 °C), it consumed 20% - 30% more fuel than at 22 °C. In charge depleting mode, at around 0 °C, vehicle electricity consumption increased by 50% and 100% for highway and city driving, respectively [55]. In another study on a Chevrolet Volt PHEV in a T_{amb} range of -26 °C to 25 °C in Winnipeg, Canada, it was shown that the electric travel range is half of the baseline condition in temperatures below -4 °C. The engine was turned on more frequently as the temperature declined [30].

A PHEV and a range-extended battery electric vehicle (BEV_X) were examined for their AER in cold temperatures. PHEV's range decreased from 20.1 km at 23 °C to 15.5 km at -7 °C (25%). For BEV_X, the reduction was from 123.9 km to 73.5 km (40%) [29]. Several vehicles with different powertrain systems, such as conventional, hybrid electric, PHEV, and battery electric vehicles (BEV), were investigated for fuel and energy consumption. The test temperatures were 20 °F (-6.67 °C), 72 °F (22.22 °C), and 95 °F (35 °C) with 850 W/m^2 of emulated radiant solar energy and the tests were on the Urban Dynamometer Driving Schedule (UDDS), Highway Fuel Economy Test (HWFET), and US06 drive cycles, maintaining the cabin temperature on 72 °F (22.22 °C) during warm and cold temperatures. For the PHEV, the maximum increase in energy consumption is in the cold start UDDS test at 20 °F (-6.67 °C)

relative to 72 °F (22.22 °C), with a 60% increase in charge sustaining and a 100% increase in charge depleting modes [56].

Table 4.1 shows the summary of previous studies on the effect of powertrain mode and T_{amb} on PHEV energy consumption and CO_2 emissions.

Table 4.1: Summary of previous studies on the effect of powertrain mode and T_{amb} on PHEV energy consumption and CO_2 emissions

Reference No.	**T_{amb}**	**Powertrain Mode**	**Data Type**
[52]	Not studied	Charge depleting/sustaining	Real driving
[53]	Not studied	Charge depleting/sustaining	Real driving
[34]	Not studied	Charge depleting/sustaining	Real driving
[54]	0 °C to 30 °C	EV	Real driving
[55]	-27 °C to 37 °C	Charge depleting/sustaining	Real driving
[30]	-26 °C to 25 °C	Charge depleting	Real driving
[29]	-7 °C, 23 °C	EV	Chassis dynamo meter
[56]	-6.7 °C, 22.2 °C, 35 °C	Charge depleting/sustaining	Chassis dynamo meter

The main new contributions from this part of the study in this thesis include

(i) Analysis of the effect of T_{amb} on energy consumption and CO_2 emissions of an electrified vehicle for extremely cold temperatures, as low as -24 °C. This provides insights into the challenges of electrified vehicles in cold climates and helps understand the impact of temperature on their energy efficiency and emissions.

(ii) Real-world data collection of actual fuel consumption measurements of a modern PHEV for urban and highway driving conditions across a wide range of T_{amb}, ranging from -24 °C to 32 °C. This experimental data provides valuable information for understanding the real-world performance of PHEVs in different temperature conditions.

(iii) Measurement of actual fuel and energy consumption of the vehicle in different powertrain modes, including using the ICE, electric motor, and hybrid mode. This provides a comprehensive understanding of the energy usage of PHEVs in different operating modes, which can help optimize their energy management strategies.

(iv) Identification of the optimal powertrain mode for PHEVs based on T_{amb} and initial battery SOC to minimize energy consumption and CO_2 emissions.

4.1 Experimental Procedure

A Ford Escape PHEV was driven for 4300 km and repeated a specific test route 213 times in different climate conditions with T_{amb} ranging from -24 °C to 32 °C. Investigations include studying the variations in energy consumption and efficiency for different powertrain modes, including pure electric, hybrid electric, and IC Engine operations. The collected data were processed and analyzed.

The vehicle was equipped with an ultrasonic flow meter to measure the fuel consumption, and the battery energy usage was collected from the vehicle's telematics. Data was collected from the vehicle's ECU and fuel flow meter to ensure the accuracy of the measurements.

A camera was used during the tests to record the vehicle's operation (Figure 4.2) from the vehicle's instrument cluster display for further analysis. This data included the vehicle's speed, engine coolant temperature, powertrain mode, power usage/charge, T_{amb}, and trip summary, which can be used to better understand the vehicle's behavior under different weather conditions and powertrain modes.

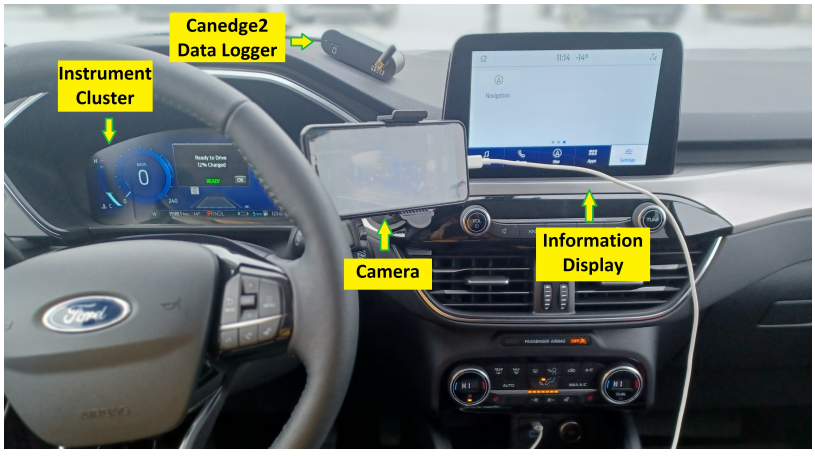

Figure 4.2: Recording from the vehicle's instrument cluster display

Analyzing the video footage and the collected data from the ultrasonic flow meter

and ECU can be used to identify specific driving behaviors, such as aggressive acceleration or braking, which can significantly impact the vehicle's energy consumption. Additionally, the camera footage was used to validate the accuracy of the collected data and ensure that the vehicle was operating as expected. This can help identify any potential issues or inconsistencies in the data and ensure the reliability of the study's findings.

4.1.1 Powertrain Modes of Ford Escape PHEV

The Ford Escape PHEV used in this thesis had four different powertrain modes, allowing the driver to choose the electrification level based on needs and preferences. These four modes are briefly explained in the following:

I. Auto EV Mode

The Auto EV mode is the default powertrain mode of the vehicle, providing an automatic use of battery power during the drive. This mode stays in electric mode when possible and runs the engine when more power is needed. This mode is suitable for longer trips where the battery may not be sufficient to cover the entire distance.

II. EV Now Mode

The EV Now mode provides a pure electric experience in which the battery and electric motor power the vehicle. This mode is suitable for short trips or driving in urban areas with a high density of charging infrastructure. It was recommended not to use this mode when towing a trailer. Because the electric drive system was not designed for towing.

III. EV Charge Mode

The EV Charge mode allows the vehicle to use the ICE to generate electricity, which is used to charge the high-voltage battery while driving. However, the battery cannot be charged to 100% using this mode, and it is limited to a maximum SOC of

77%. Once the battery SOC reaches this level, the engine and electric motor work sequentially to maintain the SOC in the range of 75% - 78%. This mode is suitable for situations where the battery is depleted and there is no access to charging infrastructure.

IV. EV Later Mode

In EV Later mode, the vehicle operates in a charge-sustaining mode, using the engine to maintain the battery's SOC. The electric motor is used to power the vehicle until the battery's SOC drops to 2% to 3% less than the target SOC, at which point, the engine starts to run and charge the battery until it reaches 1% to 2% above the target SOC. This mode is helpful for drivers who want to save their electric range for specific times, such as driving in urban areas or during traffic congestion, and switch to electric mode when needed.

The Ford Escape PHEV used for this study was equipped with regenerative braking, which converts kinetic energy into electric energy and stores it in the 14.4 kWh battery when applying the brakes or coasting. This feature helps to increase the vehicle's overall efficiency and reduce energy consumption during driving. Table 4.2 specifies the active components for each powertrain mode.

Table 4.2: Active components in different powertrain modes of the studied vehicle

Components (Function)	**Powertrain Modes**			
	Auto EV	**EV Now**	**EV Later**	**EV Charge**
High Voltage Electric Motor (Provides Traction to the Vehicle)	Yes	Yes	Yes	No
Gasoline Engine (This Engine Operates Similarly to Non-Hybrid Vehicles)	No	No	Yes	Yes
Charge Unit (Charges the High Voltage Battery)	No	No	Yes	Yes

The powertrain mode can be changed by a button (Figure 4.3a), and the current running mode is displayed in the vehicle's instrument cluster display (Figure 4.3b). These features allow the driver to easily switch between different powertrain modes and keep track of the current mode during driving. This can help the driver optimize energy consumption and reduce vehicle emissions based on the driving conditions and their preferences.

(a) Button for changing powertrain mode

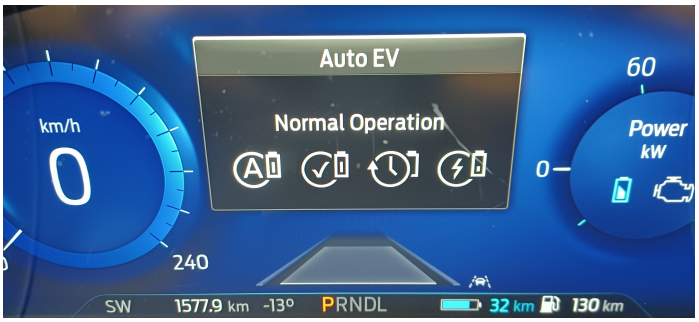

(b) Ford Escape instrument cluster display

Figure 4.3: Powertrain mode selection

The vehicle was equipped with a Positive Temperature Coefficient (PTC) electric heater, which heats the coolant to provide the passenger compartment with consistent heat. A PTC electric heater is an electrical device that uses a material with a PTC of resistance. As the temperature increases, the material's resistance also increases. When an electrical current passes through the material, it heats up and provides warmth. In the case of the vehicle, the PTC electric heater heats up the coolant that flows through the vehicle's heating system, providing warmth to the passenger compartment.

4.1.2 Test's Driving Route

A test route was selected to cover a broad range of driving conditions. The route was a 20-km stretch that took approximately 35 minutes to complete (Figure 4.4). It begins at the University of Alberta's South Campus and goes through residential and commercial areas before returning to the South Campus via the Whitemud Dr

highway. The selected route (with a distance of 20 km) is less than the PHEV charge depletion range of 61km at a T_{amb} range of 20 °C - 30 °C. This indicates that the vehicle's hybrid battery could power the vehicle throughout the test without recharging.

Figure 4.4: The driving route in this study

The selected route for testing the PHEV includes a significant number of intersections with traffic lights (31), stop signs (13), and pedestrian crossing lights (6), which can affect the duration of the test. The study recorded test duration ranging from 29.5 to 42 minutes, indicating that traffic conditions were inconsistent across all tests.

In order to increase the accuracy of the results, the study excluded 14 tests due to heavy traffic or construction on the test route. Additionally, tests with a duration of more than 38.5 minutes were excluded to avoid bias in the data. By removing tests affected by external factors and setting a time limit, the study aimed to ensure that the test conditions were consistent across all trials.

4.1.3 Test Procedure

For this study, all powertrain modes of the Ford Escape PHEV powertrain modes were tested. These modes include Auto EV, EV Now, EV Later, and EV Charge.

In EV Charge mode, the hybrid battery's SOC was set to zero percent, meaning that the ICE was used to charge the battery up to 77%. For the other powertrain modes (Auto EV, EV Now, and EV Later), the SOC was set to 77% ± 1% at the beginning of the tests.

The study also included both cold start and warm start tests, which indicates that the tests were conducted under different conditions to evaluate the performance of the PHEV in various scenarios.

In order to increase the accuracy of the tests, the cabin Heating, Ventilation, and Air Conditioning (HVAC) setting was kept constant across all tests. Specifically, the HVAC temperature was set to 25 °C, and the fan speed was set to the second speed. Table 4.3 lists the initial conditions for the Ford Escape PHEV tests.

Table 4.3: The initial condition followed for Ford Escape PHEV tests

Powertrain Mode	**SOC at the beginning of the Test**	**Coolant Temperature for Cold Starts**	**HVAC Setting**
Auto EV	77% ± 1%	Same as T_{amb}	25 °C / Fan Speed set on 2 level
EV Now	77% ± 1%	Same as T_{amb}	25 °C / Fan Speed set on 2 level
EV Later	77% ± 1%	Same as T_{amb}	25 °C / Fan Speed set on 2 level
EV Charge	0%	Same as T_{amb}	25 °C / Fan Speed set on 2 level

The Ford Escape PHEV was driven through the selected test route in different weather conditions, with T_{amb} ranging from -24 °C to 32 °C.

The driving on the test route was repeated 213 times, with 14 tests excluded to

avoid bias in the data. This leads to a total of 199 tests used in this study. The total driving distance covered during these tests was 4300 km, a considerable distance that can provide a large dataset for analysis in this thesis. The study also considered seasonal weather and driving conditions variations because the tests were conducted over nine months, from January to September 2022.

For this study, a minimum of 41 tests were conducted for each powertrain mode operation out of 199 total tests (Table 4.4). This ensured obtaining a large enough dataset for each powertrain mode operation.

Table 4.4: Overview of the conducted Ford Escape PHEV tests

Powertrain Mode	**No. of Total Tests**	**No. of Cold Starts**
Auto EV	48	12
EV Now	53	21
EV Later	55	11
EV Charge	41	8
Total	199	53

Additionally, 53 of the 199 tests were cold start tests, which allowed this study to evaluate the PHEV's performance during cold starts. Cold starts can significantly affect a PHEV's energy consumption and efficiency, as the battery and engine need extra energy to reach their working operating temperatures.

The fuel flow meter remained attached to the fuel line of the vehicle throughout the entire duration of the tests. The 12V battery of the vehicle powered the flow meter. Still, in the first stages of the tests, the connection between the flow meter and the battery was fixed, which caused the battery to drain, especially in extremely cold weather. The power cord was changed to a portable one to prevent this issue, allowing the flow meter to be connected and disconnected more easily between tests. This approach helped prevent the battery from draining and ensured that the fuel consumption measurements were accurate and reliable.

A CANedge2 data logger collected data from the vehicle's fuel flow meter and OBD port. The data was then recorded on an SD card in MF4 format. Asammdfgui software was used to convert the MF4 file to CSV format to analyze the data.

4.1.4 Electric Energy Consumption Measurement

The data on battery energy consumption was obtained from various sources, such as vehicle telematics and the dashboard display. The Ford Escape PHEV had a hybrid battery with a capacity of 14.4 kWh, and the SOC level was shown on the dashboard. To fully charge the battery at a public charging station with 3.2 kW power currency it took roughly 4.5 hours. Additionally, the battery's usable capacity was approximately 84% of the total 14.4 kWh capacity. Figure 4.5 shows the details of electric energy consumption measurement.

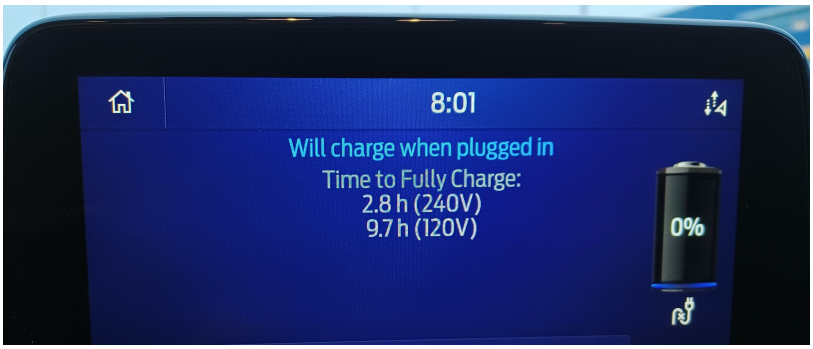

(a) SOC status shown on vehicle's display

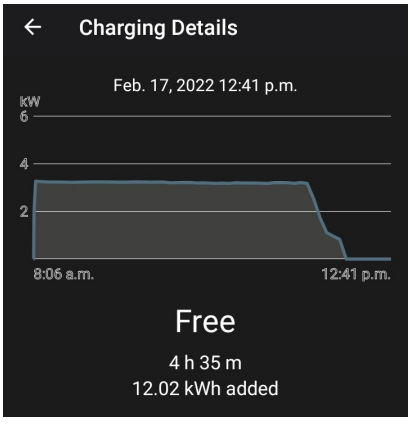

(b) Charging details

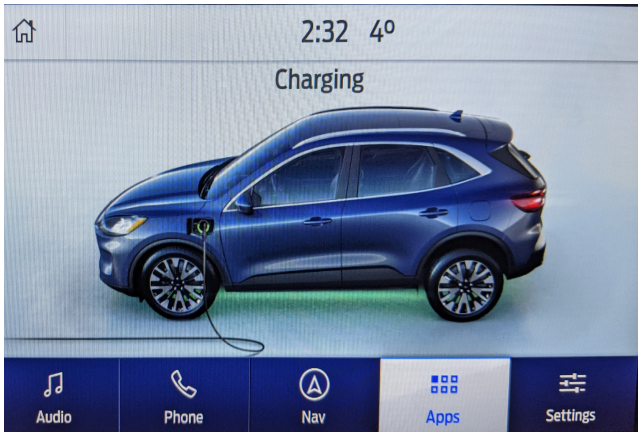

(c) Vehicle Status Shown on Vehicle's Display

Figure 4.5: Electric energy consumption measurement

To calculate the total energy consumption of the Ford Escape PHEV, we need to convert the units of gasoline and electricity into a common unit, such as kilowatt-hours (kWh). Equation 4.1 illustrates the gasoline power output measurement.

$$P_{\mathrm{g}} = LHV_{\mathrm{g}} \times \dot{F} \tag{4.1}$$

where P_g is gasoline output power in W, LHV_g is the lower heating value of gasoline and with the value of 44 MJ/kg [57], and $\dot{F}$ is the mass flow rate of gasoline being consumed in kg/s.

Data Collection

The CANedge2 data logger allows synchronizing data collected from different sources using a common time stamp. In this case, the data from the OBD port and the fuel flow meter were synchronized through the CANedge2 data logger to provide accurate and reliable data for analysis. This helped to ensure that the results obtained from the study could be used to draw valid conclusions about the vehicle's dynamic performance under different driving conditions.

The selected OBD parameters collected from the vehicle control units are listed in Table 4.5.

Table 4.5: The PIDs collected by CANedge2

Parameter	**Unit**
Vehicle Speed	km/h
Engine Speed	RPM
Engine Load Percentage	%
Engine Coolant Temperature	°C
Catalyst Temperature	°C
Ambient Air Temperature	°C
Cumulative Fuel Consumed	mL
Instantaneous Fuel Consumed	mL

In addition, the Ford Escape PHEV provides information about the powertrain, electric energy consumption, and trip summary on its screen and instrument cluster display. These parameters are shown in Table 4.6.

Table 4.6: Parameters collected from the screen and instrument cluster display of the vehicle

Parameter	**Unit**
State of Charge of the Battery	%
Test Duration	Sec
Total Test Distance	km
Total ICE Used Distance	km
Total Electric Used Distance	km

4.2 Results and Discussion

4.2.1 Ambient Temperature Coverage

The T_{amb} coverage for all powertrain modes of the Ford Escape PHEV is shown in Table 4.7.

Table 4.7: T_{amb} coverage in Ford Escape PHEV tests

Powertrain Mode	**Min Temperature (°C)**	**Max Temperature (°C)**
Auto EV	-24	29
EV Now	-22	29
EV Later	-23	28
EV Charge	-24	32

The T_{amb} ranged from -24 °C to 32 °C for the whole set of tests. 36% of the tests were done in T_{amb} less than 0 °C.

4.2.2 Energy Consumption

The energy consumption of the tested vehicle depends on a variety of factors. T_{amb} is a significant factor that affects an electrified vehicle's energy consumption. In colder temperatures, the car's electrical heater by heat pump requires energy to warm up the cabin and run the defroster, which can increase energy consumption. In PHEV, the IC engine might mainly run in extreme cold conditions to support cabin heating due to the electric heater's limited capacity or the car's heat pump. In contrast, in hot weather, the car's AC system requires substantial energy to cool down the cabin and avoid high temperatures in the high-voltage battery. These increase energy consumption. The compressor in the AC system requires energy to operate, and the battery may be used to power the AC.

Energy consumption can vary depending on whether the vehicle starts in cold or warm conditions. During a cold start, the engine and other vehicle components require additional energy to warm up to their optimal operating temperatures [58]. This includes warming up the engine coolant, battery, exhaust after-treatment system, and other powertrain parts. Additionally, the battery may require additional energy to power the starter motor and other systems during a cold start. This increased energy consumption during cold starts leads to low fuel conversion efficiency and high tailpipe emissions since the exhaust after-treatment system requires time to reach the required operating temperatures, i.e., 300 °C – 400 °C. This time is called light-off time, and this increases as the vehicle's cold start temperature decreases.

In addition, test duration impacts a vehicle's energy consumption during testing. Traffic conditions, including the presence of intersections and traffic lights, can affect the time it takes to complete a test. This can lead to higher energy consumption due to low-speed operation and frequent declaration and acceleration, while not 100% of regeneration braking energy can be captured. The percentage of available regenerated energy that can be captured ranges from 80% to 84% in hybrid vehicles and from 16%

to 70% in electric vehicles [59], [60]. The test route itself can have an impact on energy consumption. For example, crossing a Light Rail Transit (LRT) line or encountering other obstacles that require the vehicle to slow down or stop can increase idle time and decrease overall efficiency.

Driving behavior is another important factor significantly impacting a vehicle's energy consumption. Different driving behaviors, such as accelerating quickly or driving at high speeds, can increase energy consumption and reduce vehicle propulsion efficiency. On the other hand, driving behaviors that are more fuel-efficient, such as maintaining a steady speed or using cruise control, can help reduce energy consumption and improve overall efficiency.

Cruise control was used in most parts of the tests done in this study. However, the need to accelerate quickly to merge into a lane, as in the case of the entrance to Whitemud Dr, increased instantaneous energy consumption for those situations. This is because the engine must work harder to accelerate the vehicle, which requires more fuel to be burned.

Finally, weather conditions and the time of day a test was conducted also impacted a vehicle's energy consumption. In rainy or snowy conditions, using windshield wipers was necessary to maintain visibility, which could increase energy consumption. Similarly, headlights were required on cloudy days or during nighttime hours for safety reasons, which could also increase energy consumption.

Energy Consumption of Different Powertrain Modes

The energy consumption of all powertrain modes of the Ford Escape PHEV is determined and presented in Figure 4.6.

The vehicle's energy consumption as a function of T_{amb} for Auto EV, EV Now, EV Later, and EV Charge powertrain modes are presented separately in Figure 4.7.

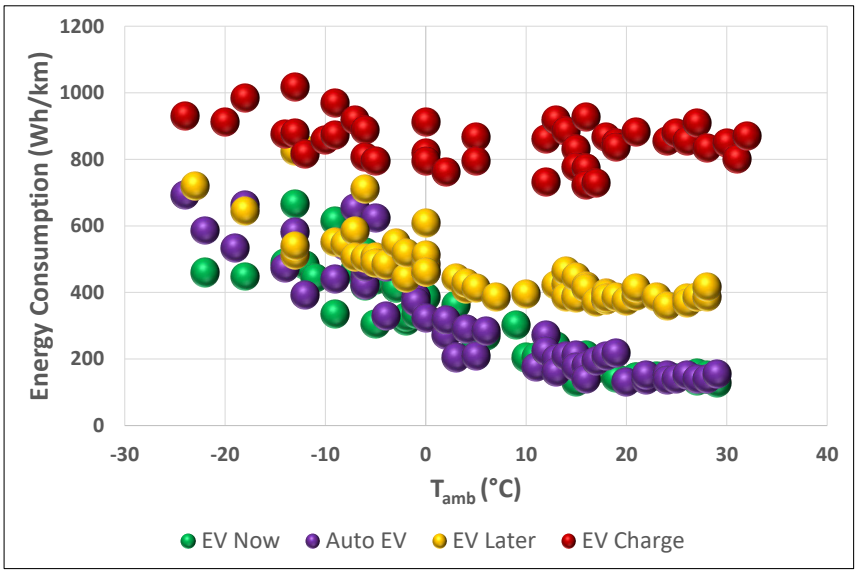

Figure 4.6: The Energy consumption of all powertrain modes of the Ford Escape PHEV

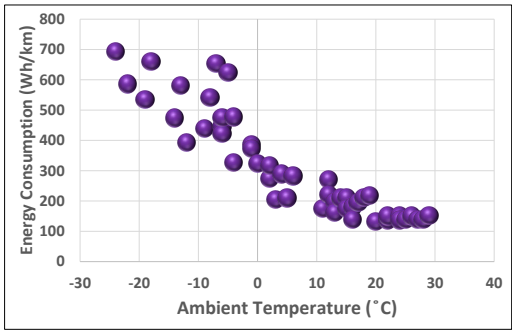

(a) Auto EV mode

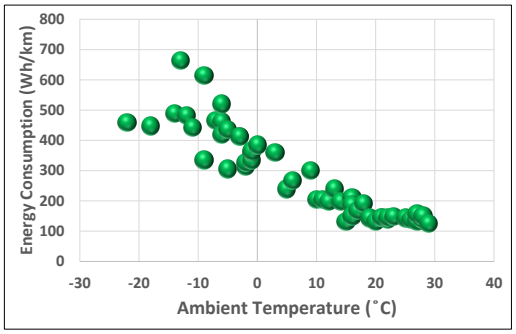

(b) EV Now mode

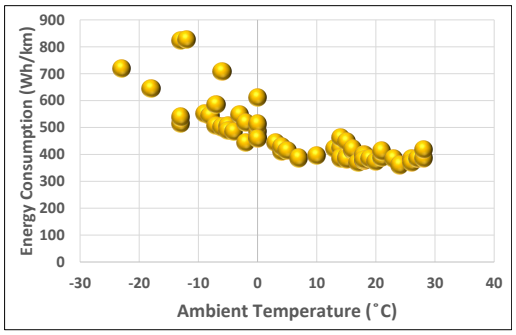

(c) EV Later mode

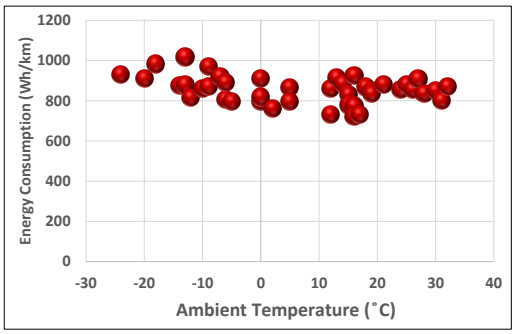

(d) EV Charge mode

Figure 4.7: Energy consumption of the vehicle as a function of T_{amb} for four different powertrain modes

In cold ambient temperatures (T_{amb} below 0 °C), the energy consumption of specific EV modes like Auto EV, EV Now, and EV Later increased, indicating that these modes required more energy to operate compared to warmer temperatures. This phenomenon is expected because colder temperatures can negatively impact battery performance and overall vehicle efficiency.

Colder temperatures can affect battery performance by reducing its ability to deliver power efficiently. The chemical reactions within the battery that generate electricity become less efficient at lower temperatures, resulting in reduced energy output. Additionally, battery internal resistance increases in the cold, further limiting its performance. As a result, more energy is needed to achieve the same level of performance as in warmer conditions.

In terms of overall vehicle efficiency, colder temperatures impact the efficiency of electric motors and other components due to increased friction and fluid viscosity. Tire performance might also be affected, as they tend to have reduced grip on icy or snowy surfaces, requiring more energy to maintain the same speed and control.

The EV Charge mode, however, does not show noticeable changes in energy consumption in cold temperatures. This is because the energy that would have been wasted in traditional ICE vehicles as heat is being repurposed to provide cabin heating. This is an energy-efficient approach, as the waste heat from the engine coolant is utilized to warm up the cabin, reducing the need for additional energy consumption just for cabin heating. As a result, the EV Charge mode's energy consumption remains relatively stable in colder temperatures. The differences in energy consumption in lower temperatures are due to overall vehicle efficiency.

The range of T_{amb} that the vehicle was tested under is shown in Table 4.8, including the minimum and maximum energy consumption values.

The energy usage for the EV Charge mode was the highest, with a consumption rate of 1,017 Wh/km. On the other hand, the energy consumption for the EV Now mode was the least, with a consumption rate of 126 Wh/km. The difference between

Table 4.8: The T_{amb} range and the minimum and maximum energy consumption of the tested vehicle

Drive Mode	**T_{amb}(°C)**		**EC (Wh/km)**	
	Min	**Max**	**Min**	**Max**
Auto EV	-24	29	132	692
EV Now	-22	29	126	664
EV Later	-23	28	360	828
EV Charge	-24	32	723	1,017

the two modes was quite significant, with EV Charge mode using almost eight times more energy than EV Now mode for the same route. This highlights the importance of selecting the appropriate powertrain mode based on specific driving conditions and requirements, as it dramatically impacts the vehicle's energy consumption and efficiency.

Dividing the fuel tests into cold and warm starts is a common practice in automotive testing to improve the accuracy of results. In automotive testing, tests where coolant and catalyst temperatures are the same as the T_{amb} are typically considered cold start tests. These tests are essential because they allow for measuring emissions and fuel consumption during engine startup, which can be a significant source of emissions and energy consumption. On the other hand, warm starts are conducted after the engine has been running and the vehicle has been operating for some time, allowing for a measurement of the engine's performance under typical operating conditions.

Energy Consumption of the Tested Vehicle During Cold Start Tests

For this study, the equipment installation was critical in ensuring the accuracy and reliability of the cold start tests. Any fault in the installation process led to errors or interruptions in the data collection, rendering the test results unusable. When the ICE is turned on, it generates a significant amount of heat in a short period, which

causes the coolant and catalyst temperatures to rise quickly. It is also interesting to note that even at very low T_{amb} (e.g., -20 °C), the cooling down process of a warmed-up vehicle was quite time-consuming. This underscores the importance of careful installation of equipment.

Figure 4.8 highlights the three-way catalyst (TWC) warm-up times for the tested vehicle's powertrain modes with continuous operation of the ICE (Auto EV and EV Now powertrain modes).

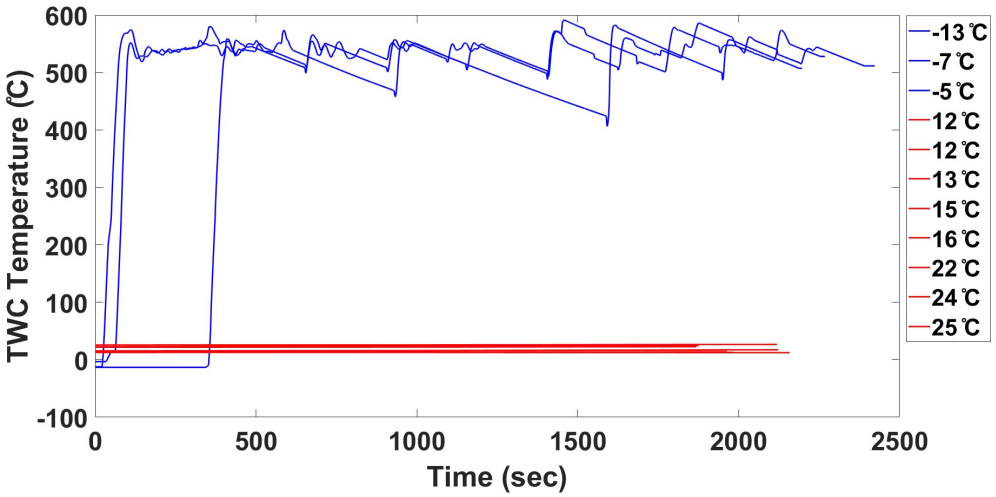

(a) Auto EV mode

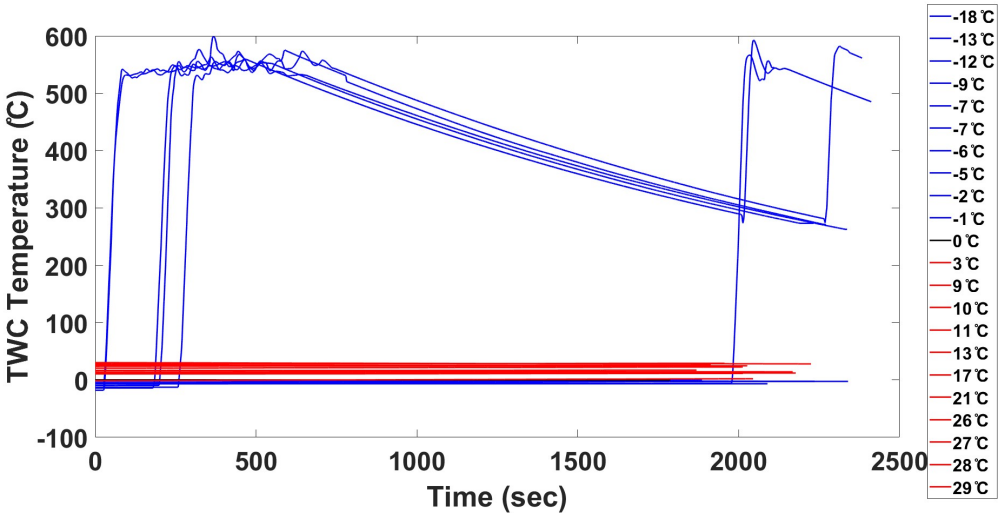

(b) EV Now mode

Figure 4.8: The TWC warming up time of the tested vehicle (for modes without continuous operation of the ICE)

Figure 4.9 illustrates the TWC warm-up times for modes with continuous operation of the ICE (EV Later and EV Charge powertrain modes) of the tested vehicle.

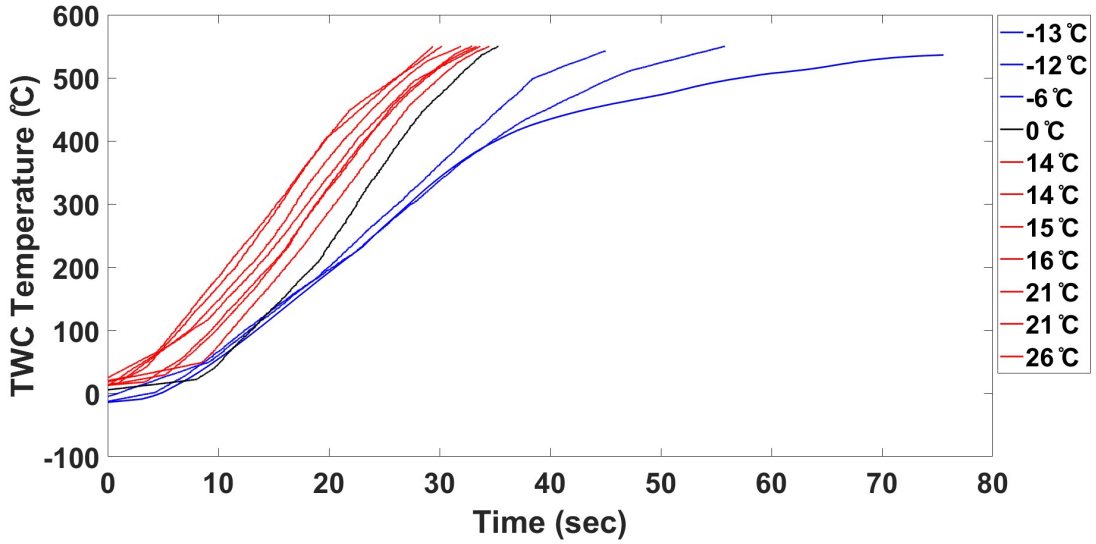

(a) EV Later mode

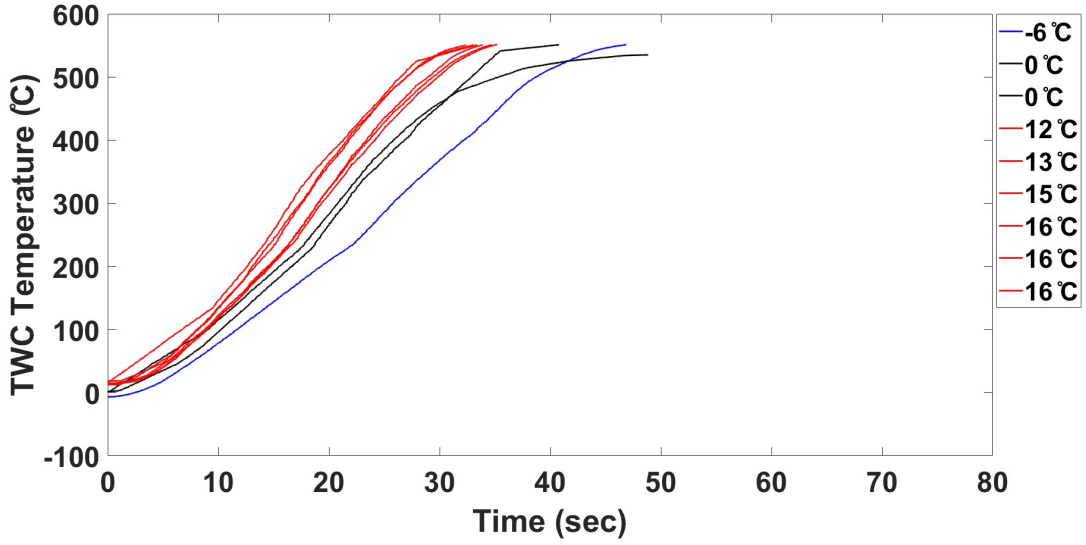

(b) EV Charge mode

Figure 4.9: The TWC warming up time of the tested vehicle (for modes with continuous operation of the ICE)

The data shown in Figure 4.10 indicates the difference in engine coolant warm-up times for modes without continuous operation of the ICE (Auto EV and EV Now powertrain modes).

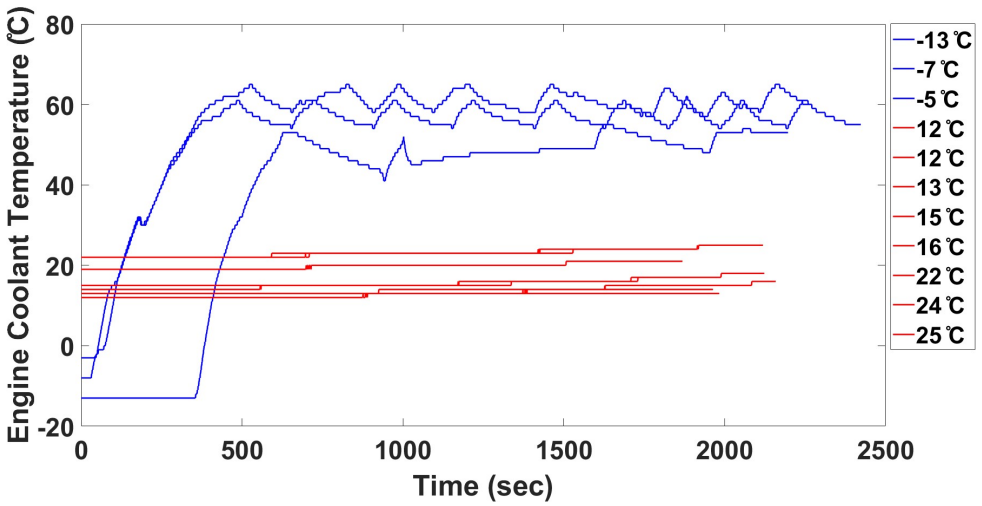

(a) Auto EV mode

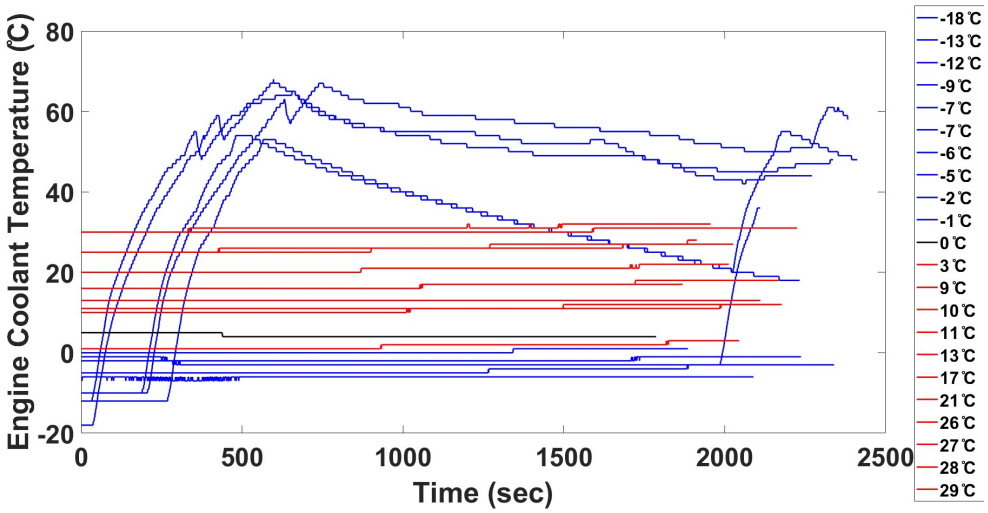

(b) EV Now mode

Figure 4.10: The engine coolant warm-up duration of the tested vehicle (for modes without continuous operation of the ICE)

Figure 4.11 indicates the difference in engine coolant warm-up duration for EV Later and EV Charge powertrain the tested vehicle's modes of the tested vehicle.

The TWC temperature increased at a faster rate compared to the engine coolant temperature. This difference in warm-up duration is not surprising, as the engine coolant has a much larger thermal mass than the catalyst and, therefore, takes longer to heat up. In the powertrain modes where the ICE was not constantly active, the tested vehicle did not fully warm up until the end of the tests, as depicted in Figures

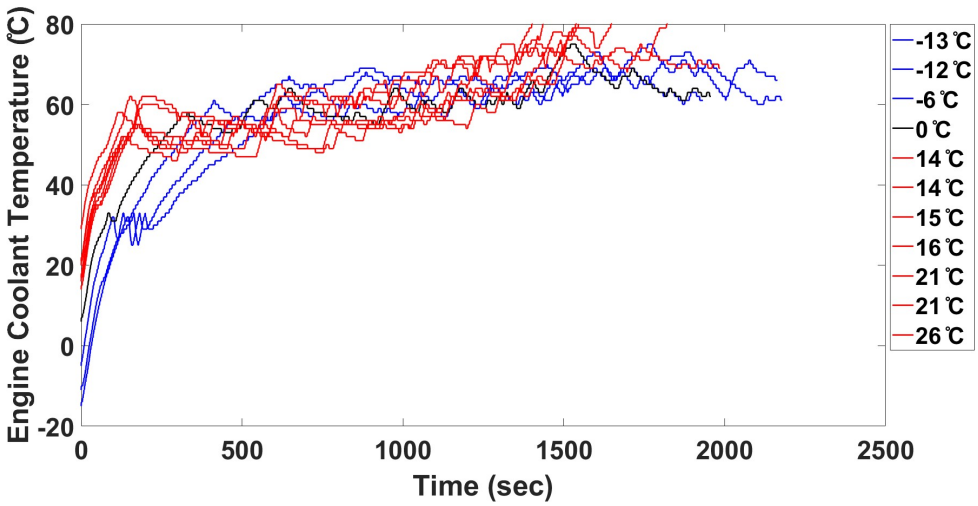

(a) EV Later mode

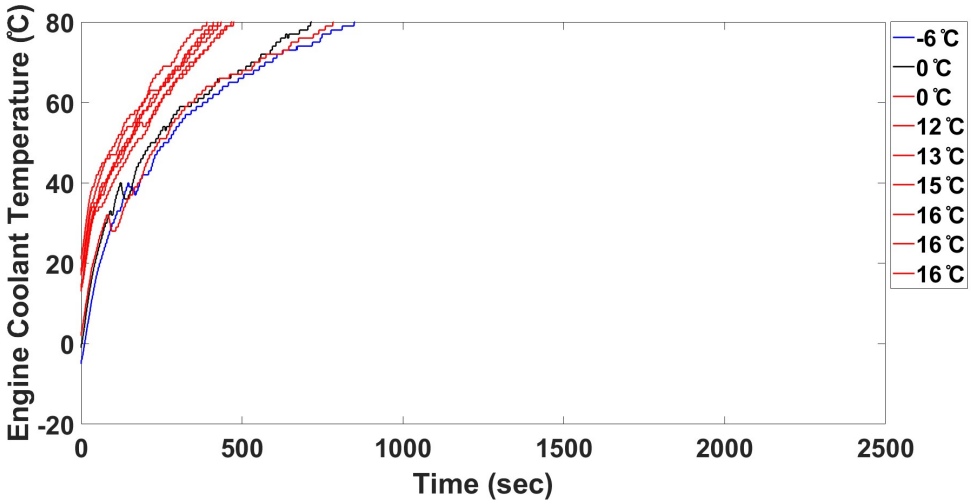

(b) EV Charge mode

Figure 4.11: The engine coolant warm-up duration of the tested vehicle (for modes with continuous operation of the ICE)

4.8 and 4.10. Furthermore, the T_{amb} noticeably impacts the warm-up duration. In Figure 4.11, it is evident that the time required for the engine coolant to warm up was nearly twice as long at lower T_{amb} compared to higher T_{amb}.

Figure 4.12 illustrates the energy consumption of all powertrain modes of the tested vehicle during cold start tests. The energy consumption for each of the four powertrain modes of the vehicle during cold start tests is shown separately in Figure 4.13.

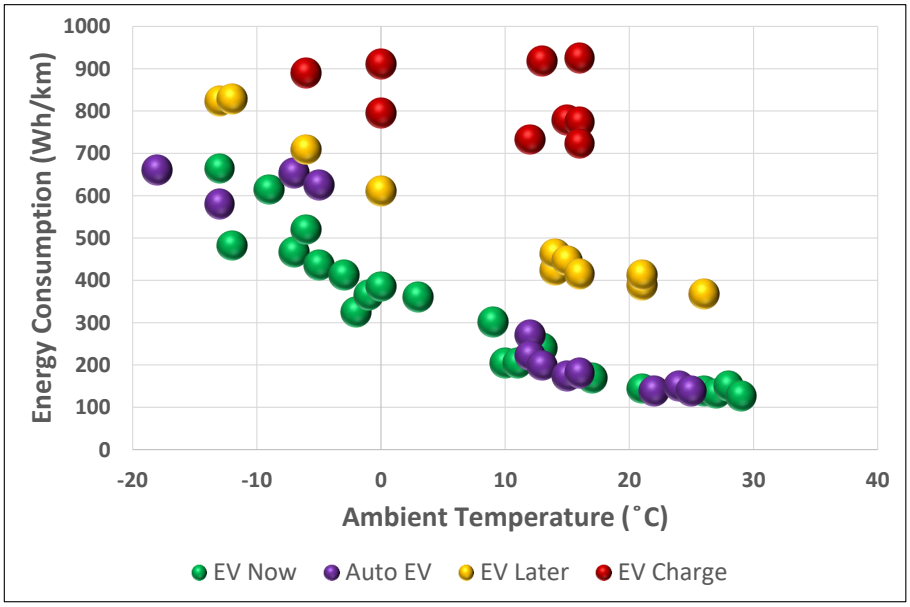

Figure 4.12: The energy consumption of all powertrain modes during cold start tests

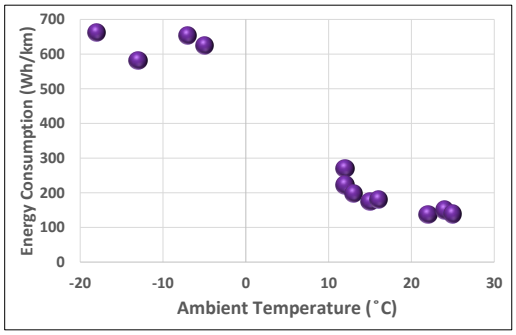

(a) Auto EV mode

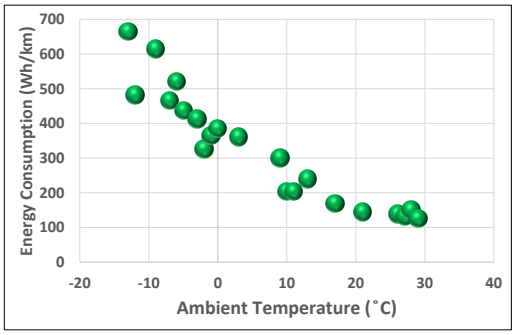

(b) EV Now mode

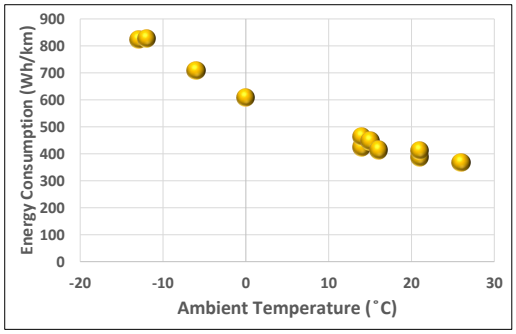

(c) EV Later mode

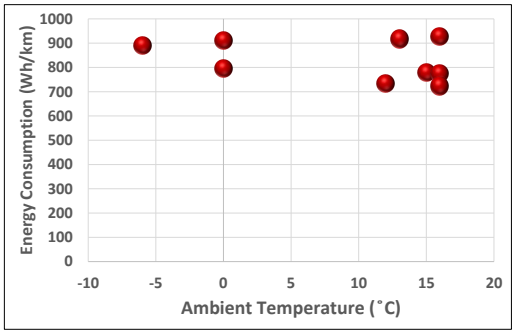

(d) EV Charge mode

Figure 4.13: The energy consumption of different powertrain modes during cold start tests

The energy consumption during cold start tests and the effect of T_{amb} on them are shown in Table 4.9.

Table 4.9: The energy consumption of different powertrain modes during cold start tests

Powertrain Mode	**Min T_{amb} (°C)**	**EC (Wh/km)**	**Max T_{amb} (°C)**	**EC (Wh/km)**	**EC Change(%)**
Auto EV	-18	661	25	138	479
EV Now	-13	664	29	126	527
EV Later	-13	823	26	368	224
EV Charge	-6	889	16	926	-4

According to the results for cold start tests, the T_{amb} in cold start tests has a significant impact on the energy consumption of the EV Now, Auto EV, and EV Later modes but has little effect on the energy consumption of the EV Charge mode.

Specifically, for the EV Now mode, decreasing the T_{amb} from 29 °C to -13 °C resulted in more than a 5-fold increase in energy consumption. Similarly, changing the temperature from 25 °C to -18 °C for the Auto EV mode increased energy consumption by about 479%. The energy consumption of the EV Later mode almost doubled from 26 °C to -13 °C. On the other hand, the energy consumption of the EV Charge mode was almost constant across different T_{amb}, around 900 Wh/km. This is because in this mode, the engine is primarily used to charge the battery, and the energy consumption is less affected by changes in T_{amb}.

Energy Consumption of the Tested Vehicle During Warm Start Tests

When the engine is started, it takes some time for the coolant to reach its optimal temperature, typically around 80 °C to 85 °C. The engine coolant is responsible for absorbing heat generated by the engine and transferring it to the radiator, where it can be dissipated to the ambient air. Once the coolant reaches its optimal temperature, the engine can operate efficiently, with reduced emissions and improved fuel efficiency.

The catalyst temperature is also an essential factor in reducing emissions. The catalytic converter is designed to operate at high temperatures, typically between 500 °C and 550 °C for the Ford Escape PHEV, to effectively reduce pollutants in the exhaust gases.

Figure 4.14 illustrates the energy consumption of all powertrain modes of the tested vehicle during warm start tests.

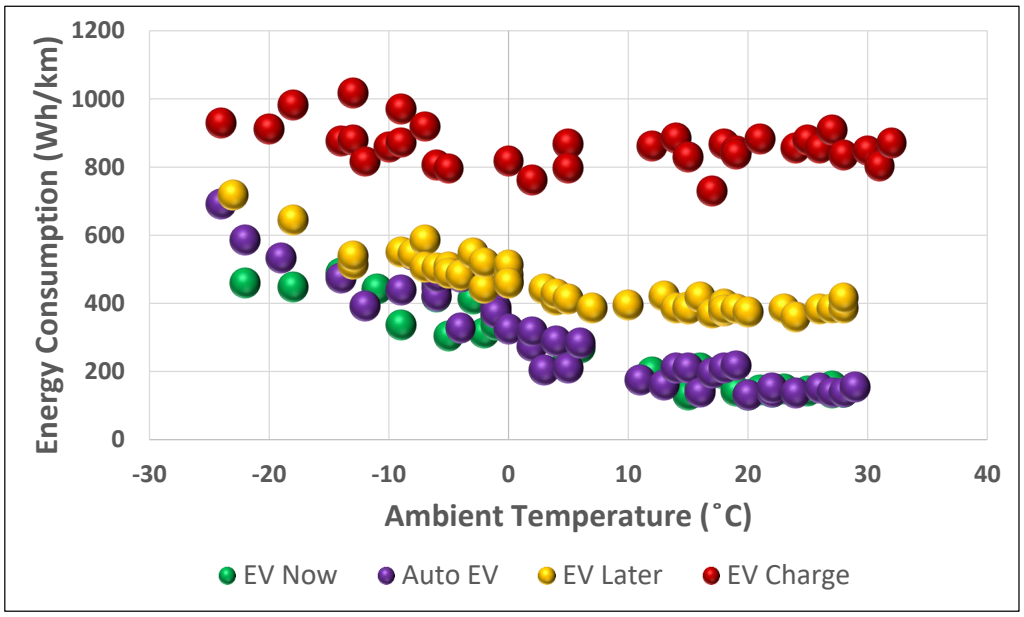

Figure 4.14: The energy consumption of all powertrain modes during warm start tests

The energy consumption for each of the four powertrain modes of the vehicle during warm start tests is shown separately in Figure 4.15.

In general, energy consumption for all powertrain modes is expected to be lower during warm start tests compared to cold start tests due to the higher temperature of the engine and catalyst. Same as cold start tests, the highest energy consumption was for EV Charge mode with the minor effect of T_{amb}. The energy consumption pattern for the other three modes is the same, where the energy consumption increased by decreasing the T_{amb}.

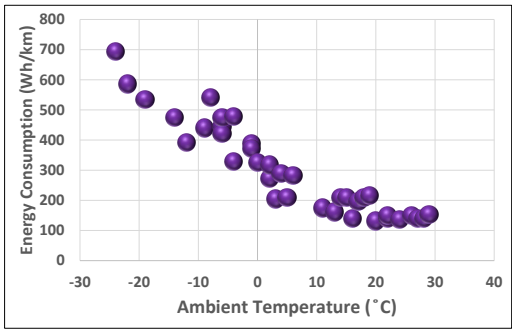

(a) Auto EV mode

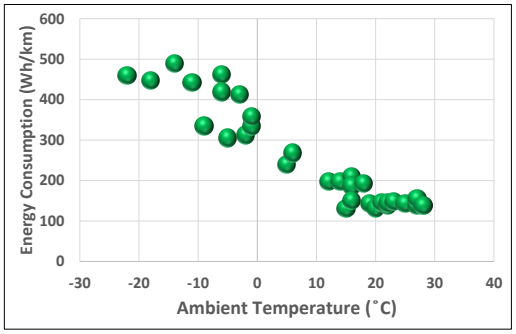

(b) EV Now mode

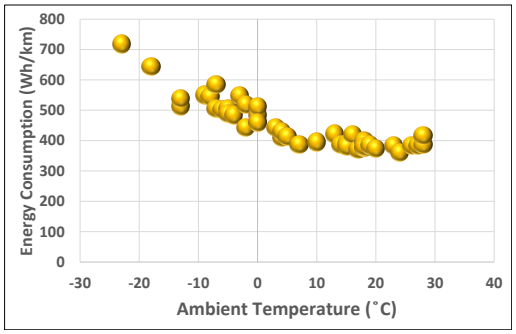

(c) EV Later mode

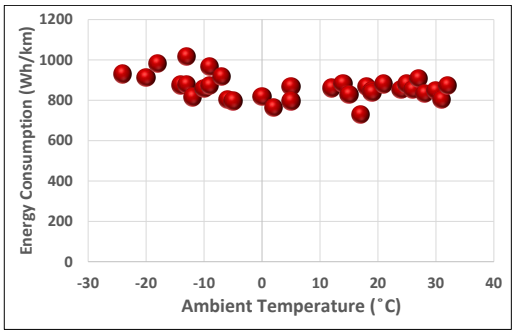

(d) EV Charge mode

Figure 4.15: The energy consumption of different powertrain modes during warm start tests

Table 4.10 shows the energy consumption of different power train modes of the Ford Escape PHEV and the effect of T_{amb} on them.

Table 4.10: The energy consumption of different powertrain modes during warm start tests

Powertrain Mode	**Min T_{amb} (°C)**	**EC (Wh/km)**	**Max T_{amb} (°C)**	**EC (Wh/km)**	**EC Change(%)**
Auto EV	-24	692	29	153	452
EV Now	-22	460	28	138	333
EV Later	-23	718	28	386	186
EV Charge	-24	930	32	871	107

According to the results, for warm start tests, the highest effect of T_{amb} was observed on the Auto EV mode, with a 4.5 times increase in energy consumption by

changing the temperature from 29 °C to -24 °C. Similarly, the energy consumption of the EV Now mode increased threefold by decreasing the T_{amb} from 28 °C to -22 °C. The EV Later mode also doubled energy consumption by reducing the T_{amb} from 28 °C to -23 °C. Interestingly, no significant changes were observed for the EV Charge mode, with only a 107% increase in energy consumption.

4.2.3 Fuel Conversion Efficiency

Fuel conversion efficiency refers to the effectiveness with which energy is extracted from a given fuel source and converted into practical work or desired outputs while minimizing energy losses. The engine load was used to calculate the fuel conversion efficiency for the powertrain modes in which the ICE was used to run the vehicle and charge the hybrid battery. The two modes with the highest utilization of the ICE were EV Charge and EV Later.

To calculate the fuel conversion efficiency for powertrain modes involving the ICE, ECU data obtained through OBD is incorporated. The calculation of fuel conversion efficiency is outlined as follows.

$$\eta = \frac{P_{\mathrm{b}}}{P_{\mathrm{g}}} \tag{4.2}$$

where η is fuel conversion efficiency, P_b is engine brake power in W, calculated in Equation 4.3, and P_g is gasoline output power in W, calculated in Equation 4.1.

$$P_{\mathrm{b}} = T_{\mathrm{e}} \times S_{\mathrm{e}} \tag{4.3}$$

where P_b is engine brake power in W, T_e is estimated engine torque from OBD in N.m, S_e is engine speed from OBD in Rad/s.

The gasoline output power was calculated by Equation 4.1.

The engine map plots for EV Later mode in minimum and maximum tested T_{amb} are shown in Figure 4.16.

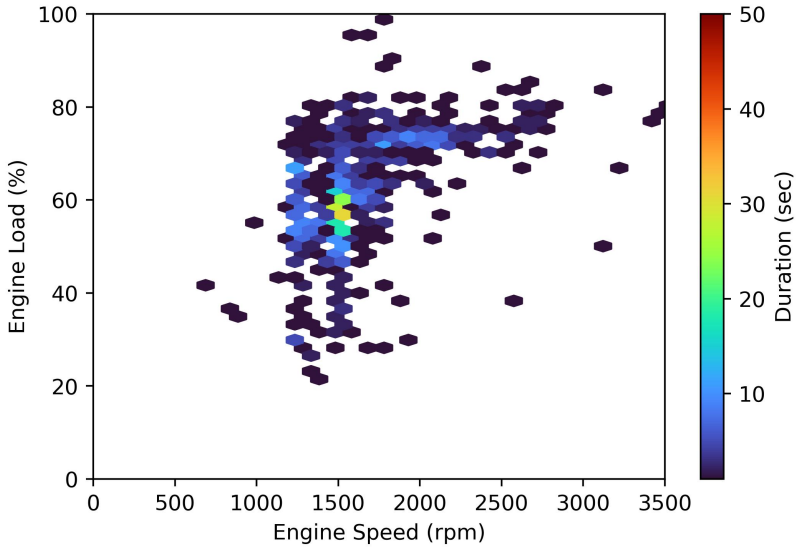

(a) EV Later at T_{amb} of -23 °C

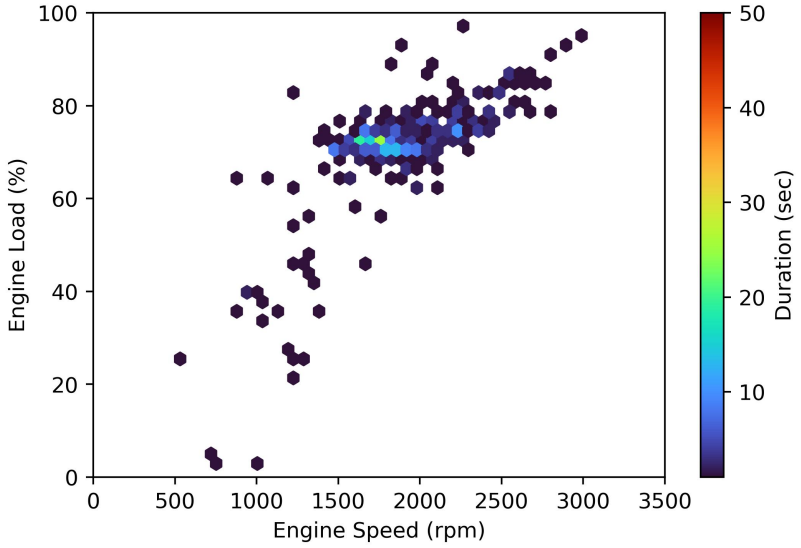

(b) EV Later at T_{amb} of 28 °C

Figure 4.16: The engine map for EV later mode of the tested vehicle

As shown in Figure 4.16, the engine load during the EV Later mode was predominantly within the range of 40% to 80% when the T_{amb} was -23 °C. However, for T_{amb} of 28 °C, the engine load was between 60% and 80%.

The engine map plots for EV Charge mode in minimum and maximum tested T_{amb}

are shown in Figure 4.17.

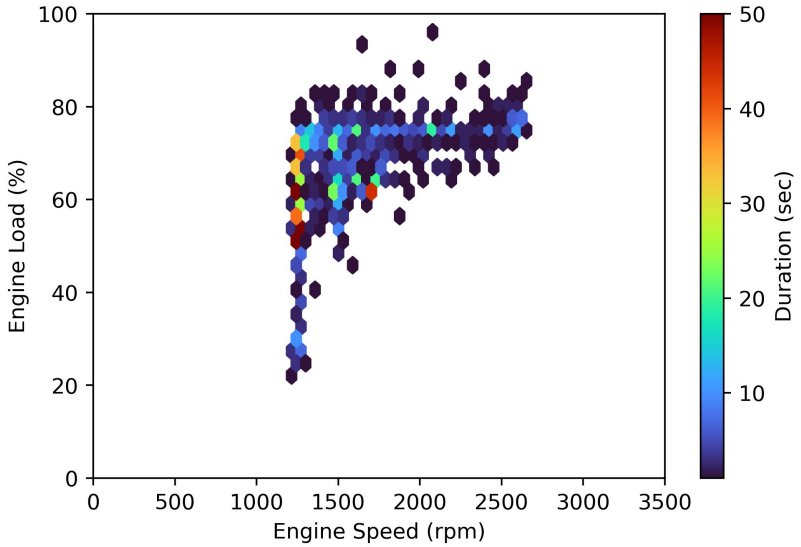

(a) EV Charge at T_{amb} of -24 °C

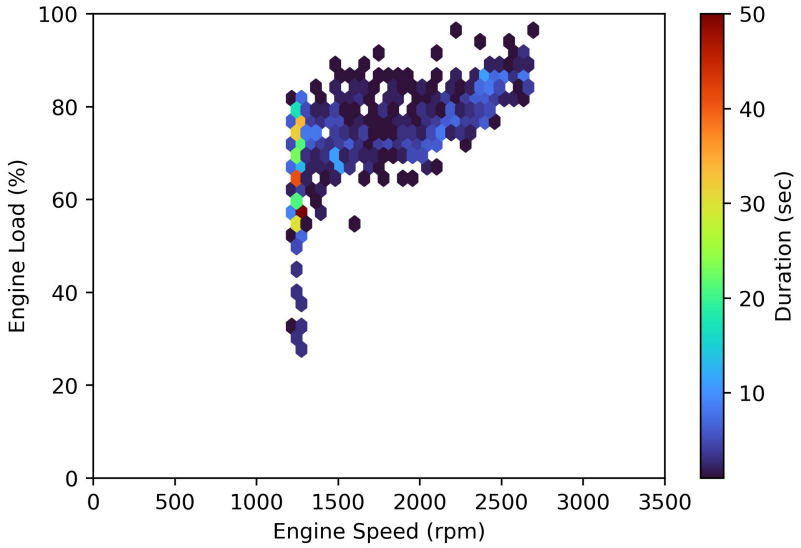

(b) EV Charge at T_{amb} of 32 °C

Figure 4.17: The engine map for EV later mode of the tested vehicle

According to the plots in Figure 4.17, there were no noticeable changes in the engine load for the EV Charge mode across the minimum and maximum tested T_{amb}.

The fuel conversion efficiency for EV Later mode in minimum and maximum tested

T_{amb} are shown in Figure 4.18.

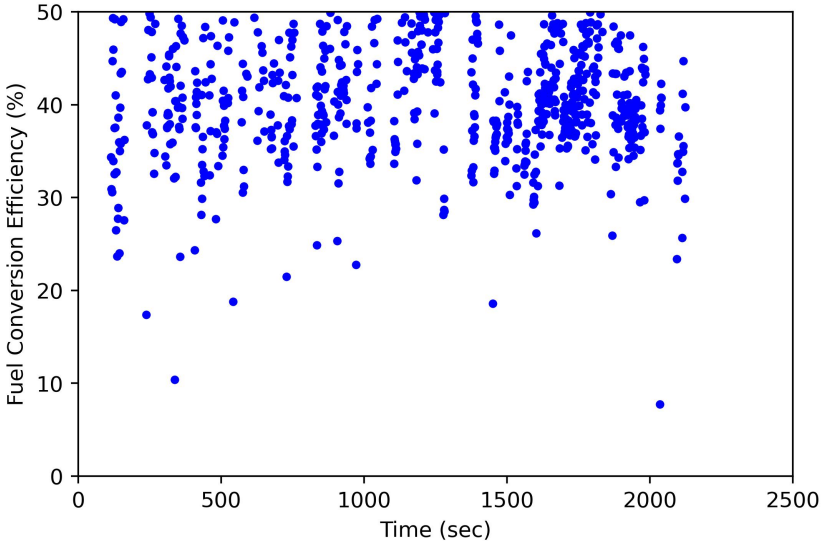

(a) EV Later at T_{amb} of -23 °C

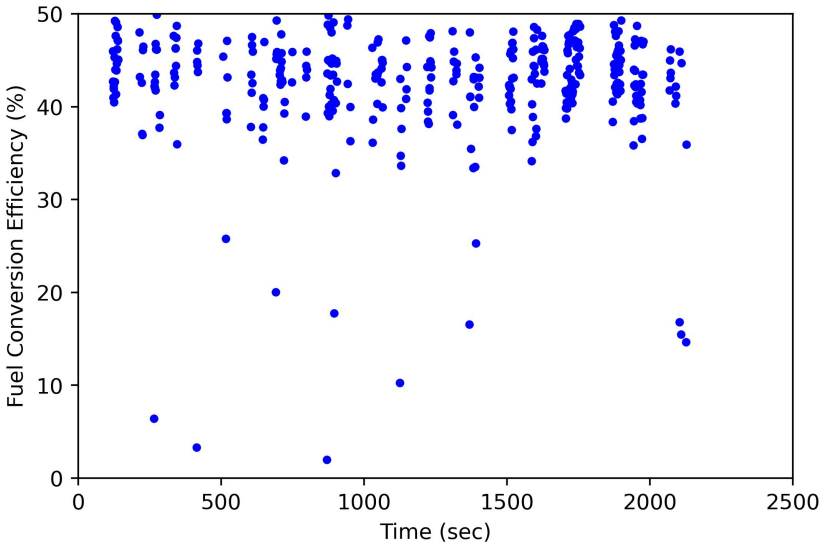

(b) EV Later at T_{amb} of 28 °C

Figure 4.18: The fuel conversion efficiency for EV later mode of the tested vehicle

The average fuel conversion efficiency for the EV Later mode at a T_{amb} of -23 °C is 39.9%, while it increases to 42.4% at a T_{amb} of 28 °C. This represents a 5.8% increase in the average fuel conversion efficiency.

The fuel conversion efficiency for EV Charge mode in minimum and maximum tested T_{amb} are shown in Figure 4.19.

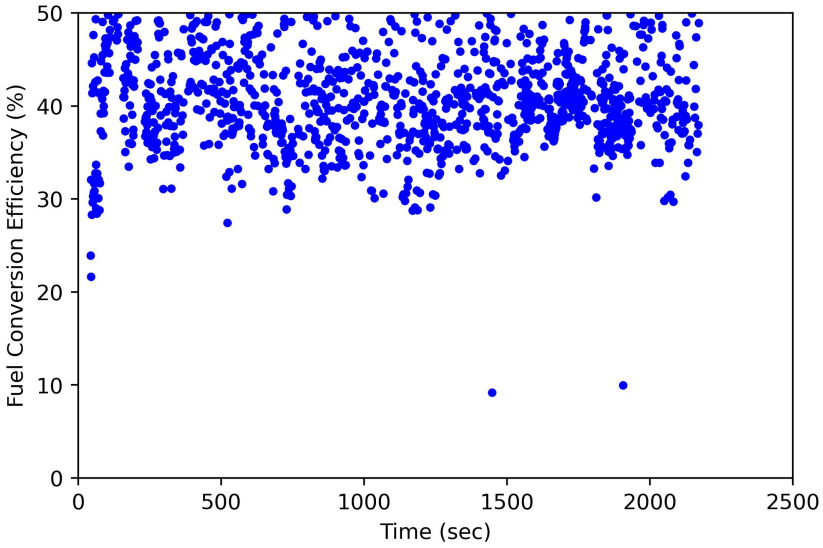

(a) EV Charge at T_{amb} of -24 °C

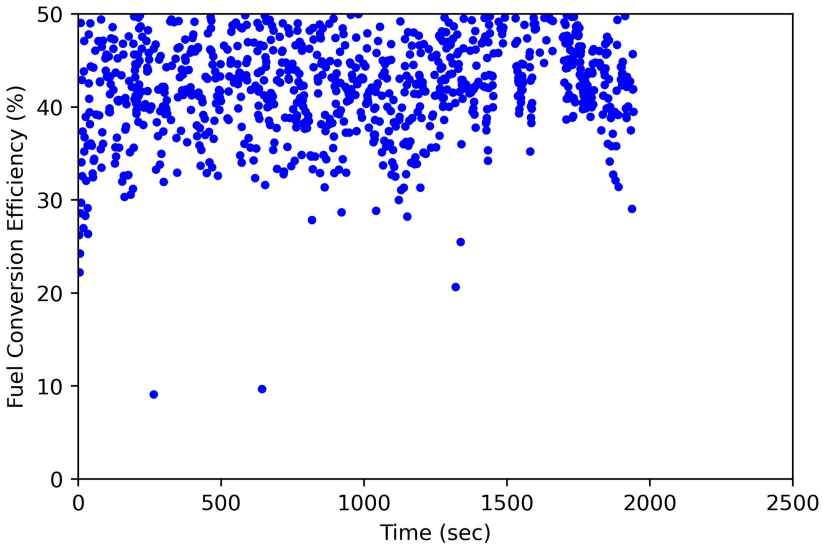

(b) EV Charge at T_{amb} of 32 °C

Figure 4.19: The fuel conversion efficiency for EV later mode of the tested vehicle

Similarly, for the EV Charge mode, the average fuel conversion efficiency at a T_{amb} of -24 °C is 40.4%, while it increases to 41.8% at a T_{amb} of 32 °C. This indicates a

3.5% increase in the average fuel conversion efficiency.

The duration of fuel conversion for EV Later mode in minimum and maximum tested T_{amb} are shown in Figure 4.20.

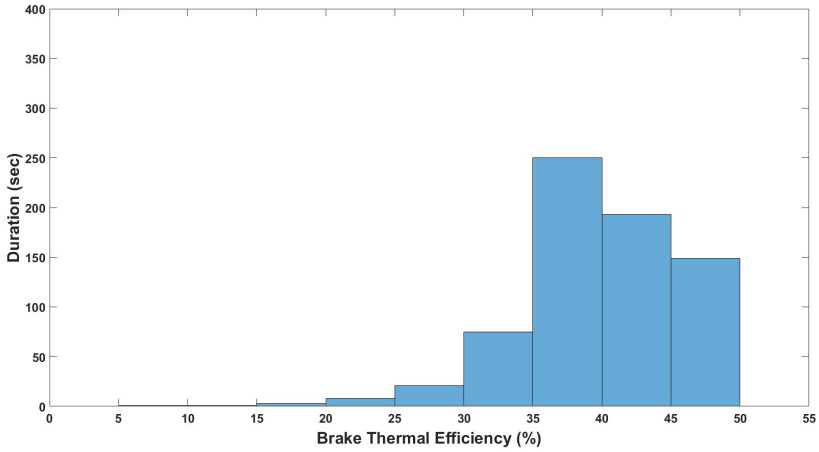

(a) EV Later at T_{amb} -23 °C

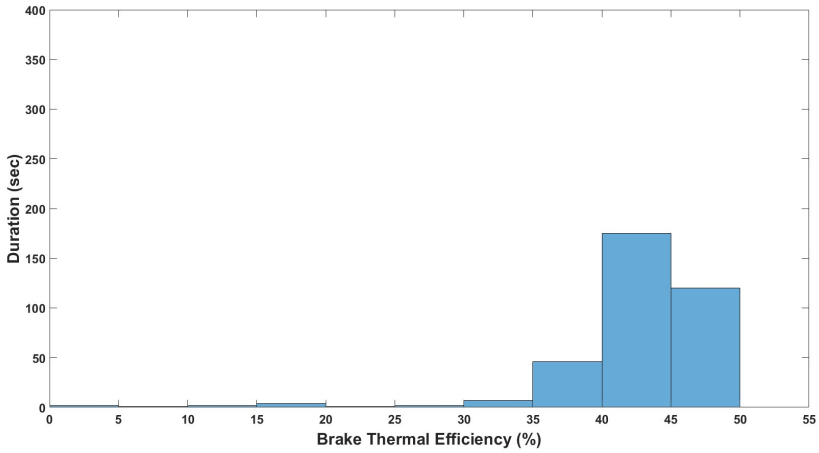

(b) EV Later at T_{amb} 28 °C

Figure 4.20: Duration of fuel conversion efficiency of EV Later mode for the tested vehicle

Based on Figure 4.20 for EV Later mode, the most extended duration is observed for the fuel conversion efficiency range of 35% to 40% at T_{amb} of -23 °C. However, at T_{amb} of 28 °C, the highest duration occurs for the range of 40% to 45%.

The duration of fuel conversion efficiency for EV Charge mode in minimum and maximum tested T_{amb} are shown in Figure 4.21.

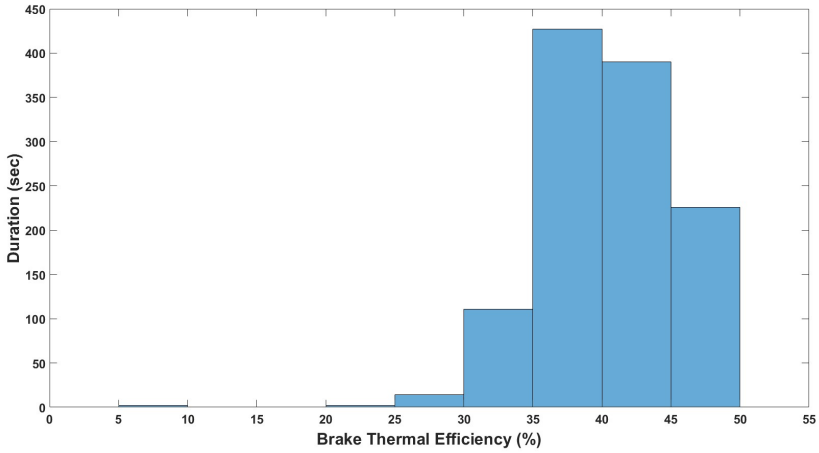

(a) EV Charge at T_{amb} -24 °C

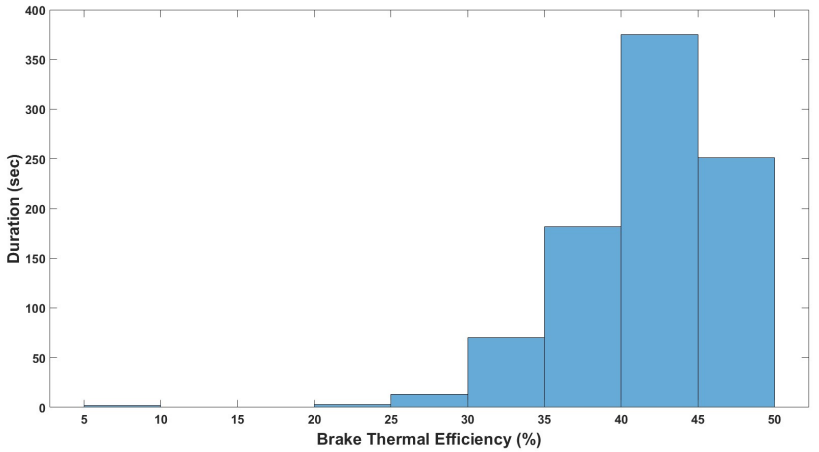

(b) EV Charge at T_{amb} 32 °C

Figure 4.21: Duration of fuel conversion efficiency of EV Charge mode for the tested vehicle

As shown in Figure 4.21, for EV Charge mode, the most extended duration is observed for the fuel conversion efficiency range of 35% to 40% at T_{amb} of -24 °C. However, at T_{amb} of 32 °C, the highest duration occurs for the range of 40% to 45%.

According to the results, the fuel conversion efficiency for both EV Later and EV charge modes was increased by increasing the T_{amb}.

Ford Escape PHEV charging equipment

The 2021 Ford Escape PHEV came with standard charging equipment J1772 that is compatible with most public charging stations. The vehicle came equipped with a level 1 charger port that could be plugged into a regular 110-volt household outlet. This option would take about 10 to 11 hours to fully charge the battery from 0% SOC of starting charge. The vehicle was equipped with a level 2 setup with a 240-volt charging port to charge faster. It took around 3.5 hours to charge the vehicle fully [61]. Figure 4.22 shows the various types of charging equipment available for the Ford Escape PHEV.

(a) Level 1 AC 110-volt charging port

(b) Level 2 AC 220-volt charging port

(c) Level 2 AC 220-volt charging station

Figure 4.22: The various types of charging equipment available for the Ford Escape PHEV

The Ford Escape PHEV had the option to adjust the charging level for the plug-in mode. The minimum setting for the charging level was 50%, and it could be increased in increments of 10%. For the tests in the study, the charging level was set to 80%, which was the closest option to the required 77% needed to start the tests.

Energy Costs

Gas price is an important factor in fleet vehicle costs, return on investment (ROI) on PHEVs, and fleet management's extended plans for renewing the vehicles. When assessing the cost-effectiveness of PHEVs within a fleet, it's essential to consider gas prices. PHEVs have a significant advantage in that they rely more on electricity than gasoline, leading to considerable reductions in fuel expenses.

Various factors influence the expense of charging a PHEV. The battery's size and discharge level impact the energy required to charge it. There are multiple methods to charge a PHEV, which include commercial charging stations that generally charge a fee for every kilowatt-hour (kWh) of electricity consumed. Home charging stations with 110-240 V supply can follow the same model or charge a fixed rate per charging session.

Additionally, the battery can be charged using the ICE of the vehicle. Installing home charging stations can be highly convenient for fleet vehicles, especially since they can be set up at the exact parking location where they are stored overnight. In certain situations, it could be feasible to benefit from lower electricity costs by charging devices during nighttime or utilizing sustainable energy sources like home-based solar panels.

Gas Price in Edmonton (12.10.2022)

The cost of gasoline differs significantly due to various factors, such as worldwide oil prices, supply and demand, and local taxes and regulations. Fluctuations in gas prices significantly affect the cost of operating and maintaining fleet vehicles, especially those that run on traditional gasoline engines. Fleet managers need to monitor gas prices

and consider alternative options, such as PHEVs, to help reduce costs and increase efficiency. The past year has seen a range of gasoline prices, with a minimum of 126.7 ¢/L and a maximum of 190.0 ¢/L (Figure 4.23).

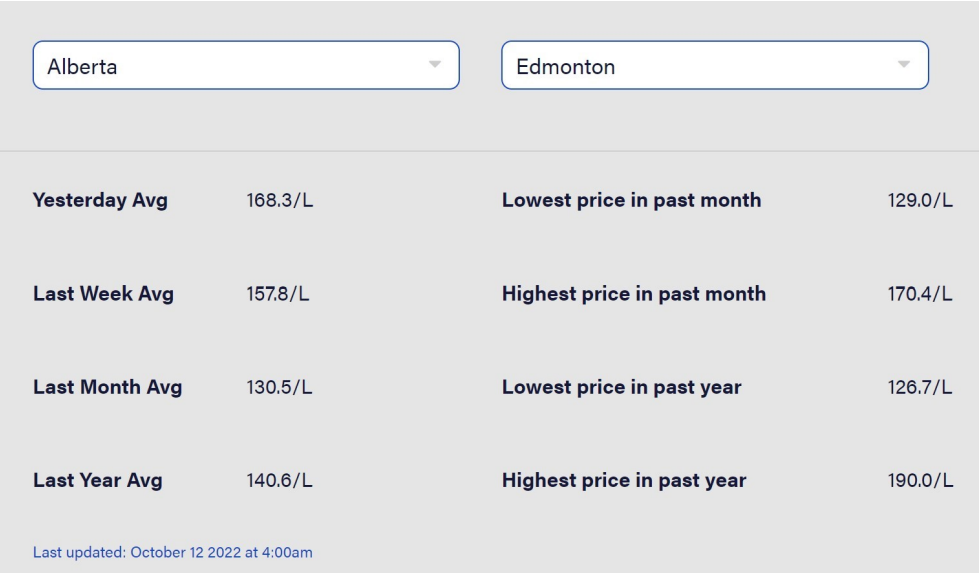

Figure 4.23: Edmonton's regular gas price summary (12.10.2022)

The data presented in Figure 4.24 indicates that gasoline prices in Alberta and Edmonton were comparable to each other but significantly different from the average cost of gasoline in Canada [62].

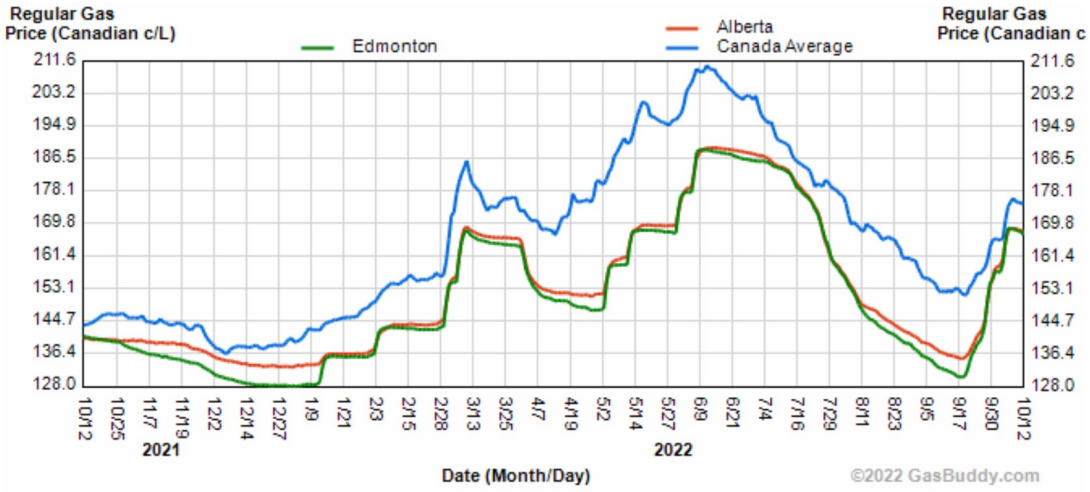

Figure 4.24: 12-month average retail regular gas price chart (12.10.2022)

Edmonton Retail Regular Gas Price Map

Figure 4.25 indicates the gas station and the prices of regular gas [63].

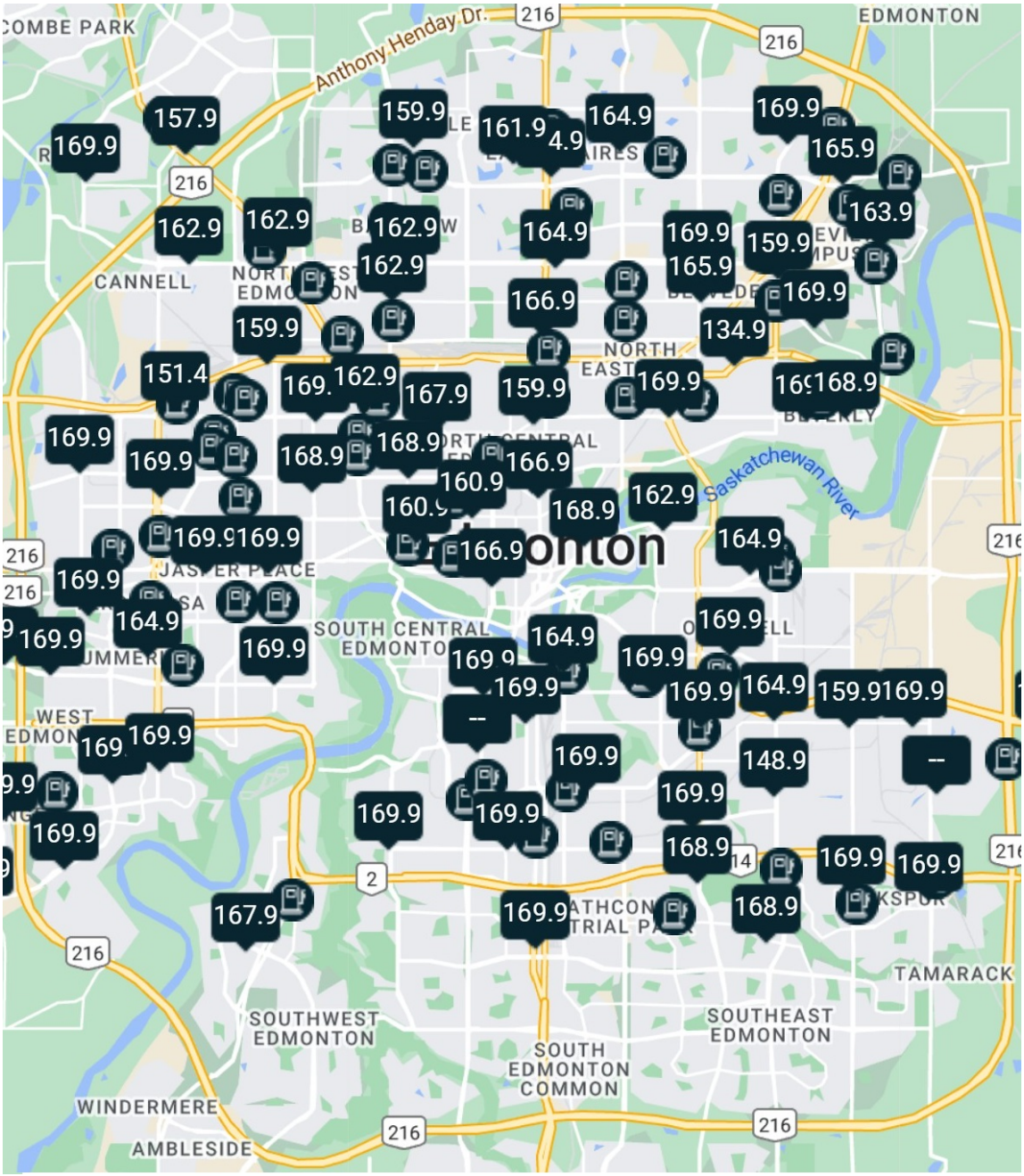

Figure 4.25: Edmonton retail regular gas price on (12.10.2022)

Commercial Charge Station in Edmonton

A commercial charge station is an option to charge a PHEV. The cost of charging a vehicle is determined by two factors: the energy fee and the parking fee. These fees

can either be free or charged on an hourly basis. Figure 4.26 shows the locations of commercial charging stations in Edmonton [64].

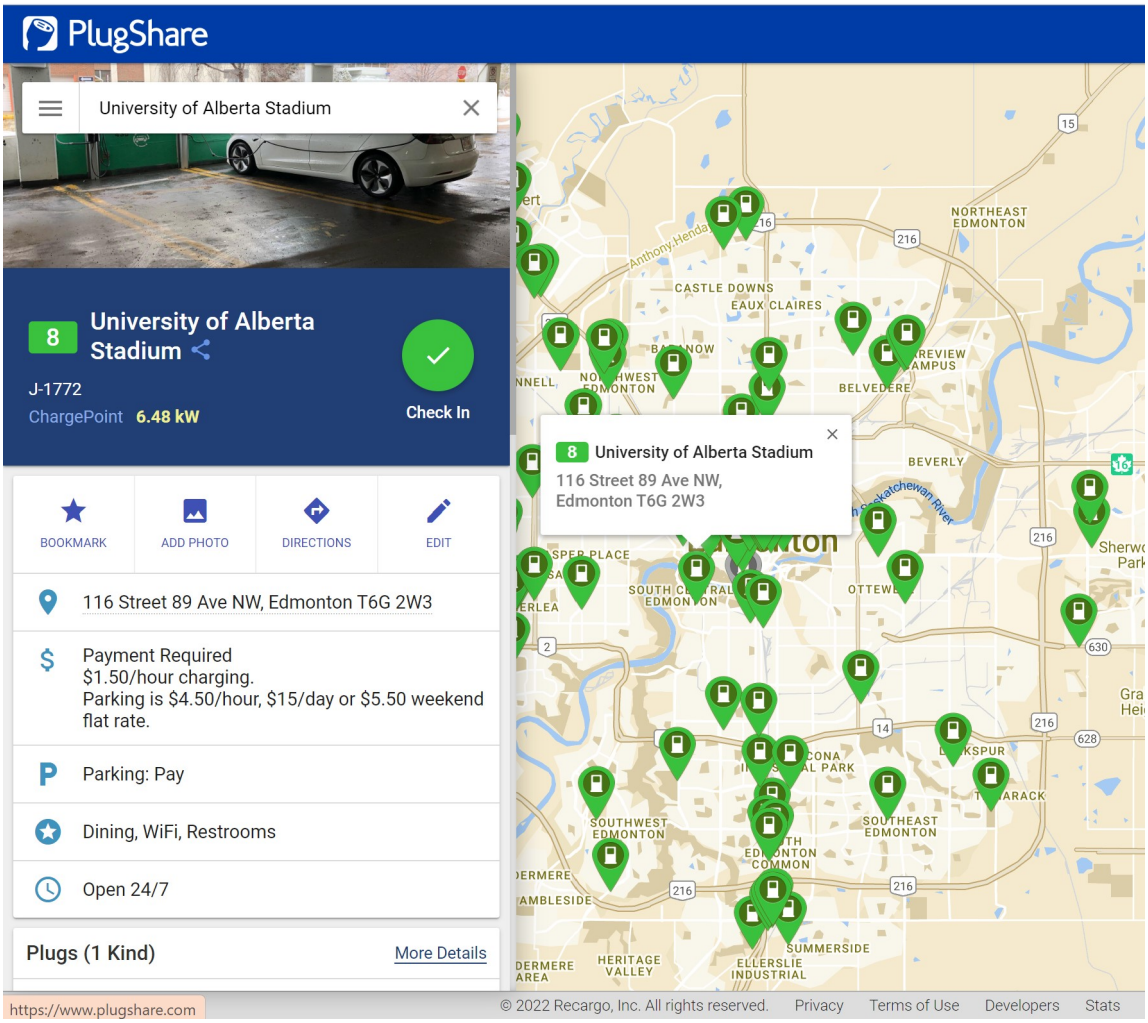

Figure 4.26: Commercial charge station in Edmonton [64]

Ford Escape PHEV Energy Costs

According to information from the University of Alberta's transportation service, one kWh of electricity costs 10 cents. The average gas price from last year was 140.6 ¢/L. The energy cost calculations in this thesis were based on these prices.

Figure 4.27 illustrates the energy cost of all powertrain modes of the Ford Escape PHEV. The energy cost for each of the four powertrain modes of the vehicle is shown separately in Figure 4.28

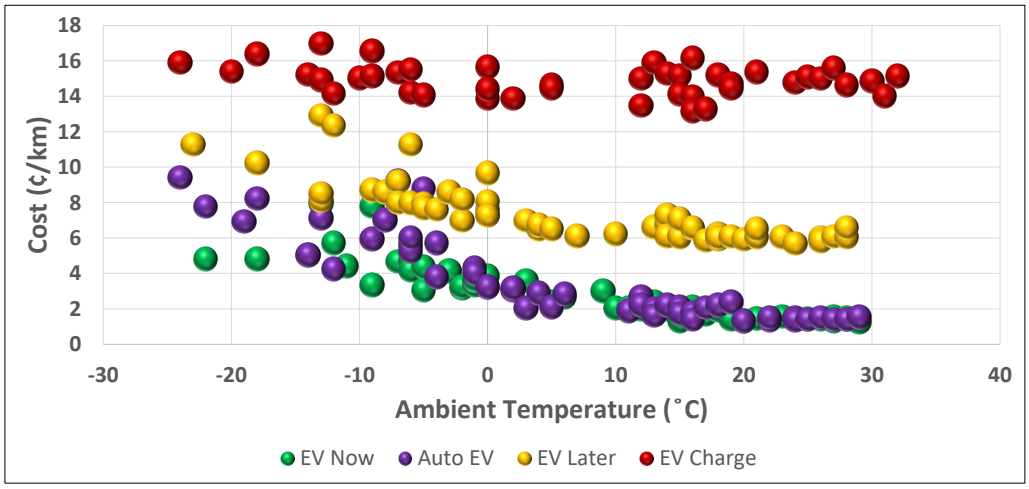

Figure 4.27: The energy cost of all powertrain modes for the tested vehicle

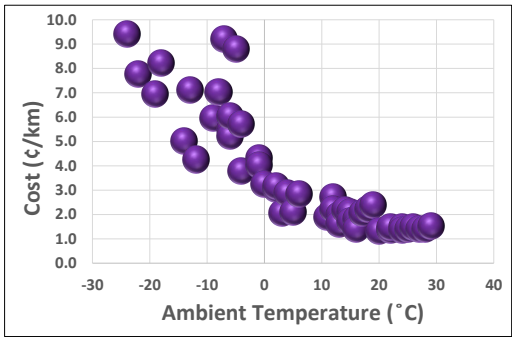

(a) Auto EV mode

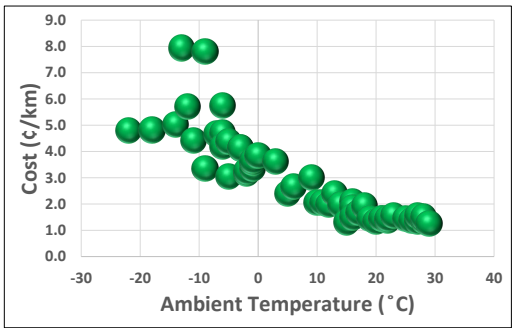

(b) EV Now mode

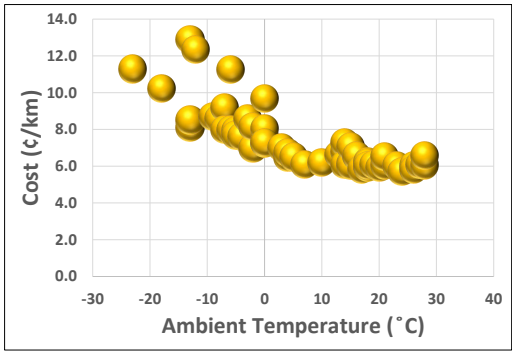

(c) EV Later mode

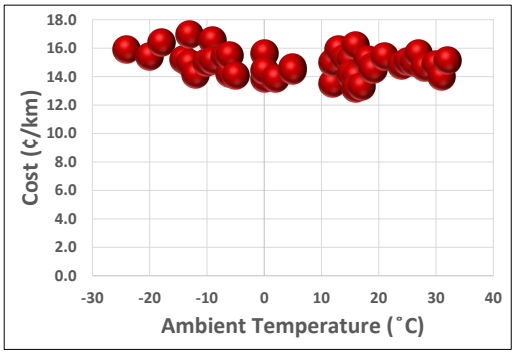

(d) EV Charge mode

Figure 4.28: The energy cost of different powertrain modes for the tested vehicle

According to the results, the energy cost for the powertrain modes with continuous ICE operation was higher than that of the electric motor. This was because gasoline tends to be pricier than electricity, and utilizing the ICE engine results in greater

gasoline consumption. Therefore, it makes sense that EV Charge mode was the costliest, as it relies solely on the ICE. Then, the EV Later mode with a combination of ICE and the electric motor was the second rank, as it used the ICE more frequently than the other modes. Finally, Auto EV and EV Now mode costs were lower and almost near each other, as they rely primarily on the electric motor.

Table 4.11 shows the energy expenses of the Ford Escape PHEV under various powertrain modes, at both minimum and maximum T_{amb}.

Table 4.11: The energy costs of various powertrain modes for the tested vehicle

Test Type	**Min T_{amb} (°C)**	**Energy Cost (¢/km)**	**Max T_{amb} (°C)**	**Energy Cost (¢/km)**
Auto EV	-24	9.4	29	1.5
EV Now	-22	4.8	29	1.3
EV Later	-23	11.3	28	6.1
EV Charge	-24	15.9	32	15.2

The results found that the EV Charge mode incurred the highest cost at T_{amb} of -24 °C, amounting to 15.9 ¢/km. T_{amb} had minimal impact on this mode, costing 15.2 ¢/km at 32 °C. However, for the EV Later mode, the energy cost nearly doubled from 6.1 ¢/km to 11.3 ¢/km as the T_{amb} dropped from 28 °C to -23 °C.

At T_{amb} of 29 °C, the EV Now mode demonstrated the most efficient energy usage, costing only 1.3 ¢/km. Although the cost increased 3.5 times, it remained lower than the other modes. In comparison, the Auto EV mode experienced the highest increase in energy cost compared to other modes, with the cost per kilometer rising from 1.5 ¢/km to 9.4 ¢/km.

Ford Escape PHEV CO_2 Emission

Many companies with large fleets of vehicles, especially those running on conventional ICE, produce significant amounts of CO_2 emissions. These emissions contribute to global warming and climate change. As a result, there is a growing emphasis on

reducing CO_2 emissions from these fleets. Some companies are prioritizing emission reduction over cost reduction when it comes to their fleet operations. Environmental concerns, sustainability goals, regulatory pressures, and customer demand for eco-friendly practices drive this shift in focus. While reducing costs remains essential, there is a growing recognition that environmental responsibility can enhance a company's reputation and long-term viability.

PHEVs combine electric and ICE propulsion systems. The amount of CO_2 emissions generated by a PHEV depends on the energy sources used to generate the electricity that charges its battery and the efficiency of its combustion engine. The CO_2 intensity of producing a kWh of electricity is vital to determining the total emissions associated with PHEVs. The choice of electricity sources to charge PHEVs significantly impacts the overall emissions of a company's fleet. Charging PHEVs using electricity from renewable sources can substantially reduce the fleet's carbon footprint compared to charging from fossil-fuel-intensive sources.

Furthermore, T_{amb} also affects CO_2 emissions of PHEVs. When the temperature is low, a PHEV's ICE needs to run longer to maintain the required cabin temperature, which results in higher emissions. For this purpose, the production of CO_2 emission by the Ford Escape PHEV was investigated as a part of the study.

The graph in Figure 4.29 shows a decreasing trend in the emission intensity of electricity generation in Alberta from 1990 to 2020. In 1990, the emission's intensity was around 950g of CO_2 per kWh, and by 2020, it decreased to 590g of CO_2 per kWh [65]. This trend indicates that electricity generation methods in Alberta are becoming cleaner and more environmentally friendly.

The last 12 months intensity values show that the average CO_2 intensity of electricity generation in Alberta was 457 gCO_2/kWh [25]. This indicates that the emission intensity of electricity generation in Alberta continues to decrease. This is good news for reducing the overall CO_2 emissions of PHEVs that rely on electricity as a power source. The CO_2 intensity of electricity generation in Alberta during the period of

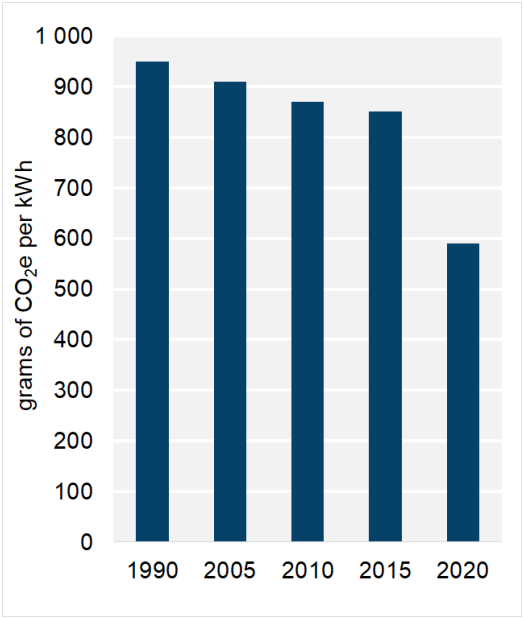

Figure 4.29: Emissions intensity of electricity generation

this study is shown in Figure 4.30.

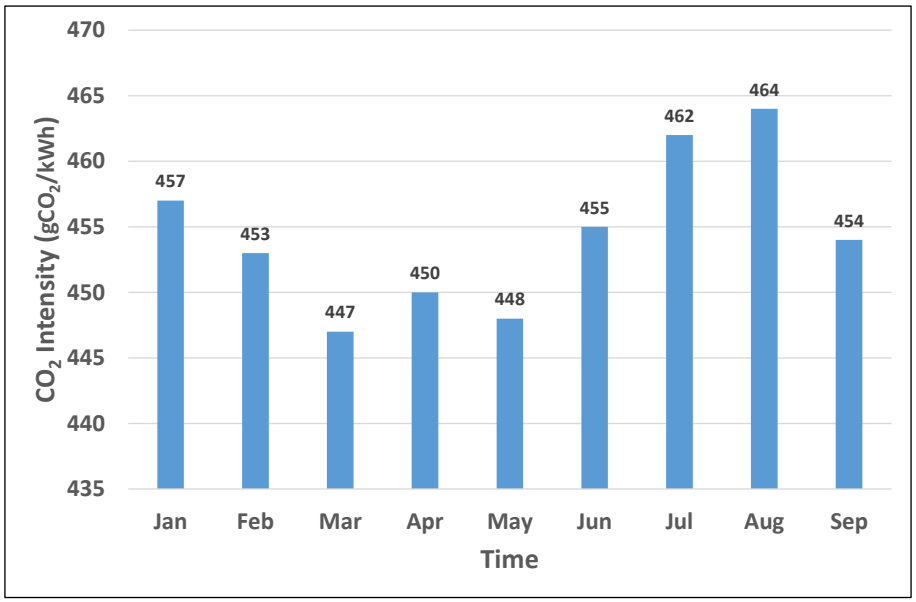

Figure 4.30: The CO_2 intensity of electricity generation for Alberta during the period of this study [25]

Figure 4.31 shows the CO_2 emissions of all powertrain modes of the Ford Escape PHEV. The CO_2 emission for each of the four powertrain modes of the vehicle is

shown separately in Figure 4.32. The results are based on the CO_2 intensity value of electricity generation in Alberta.

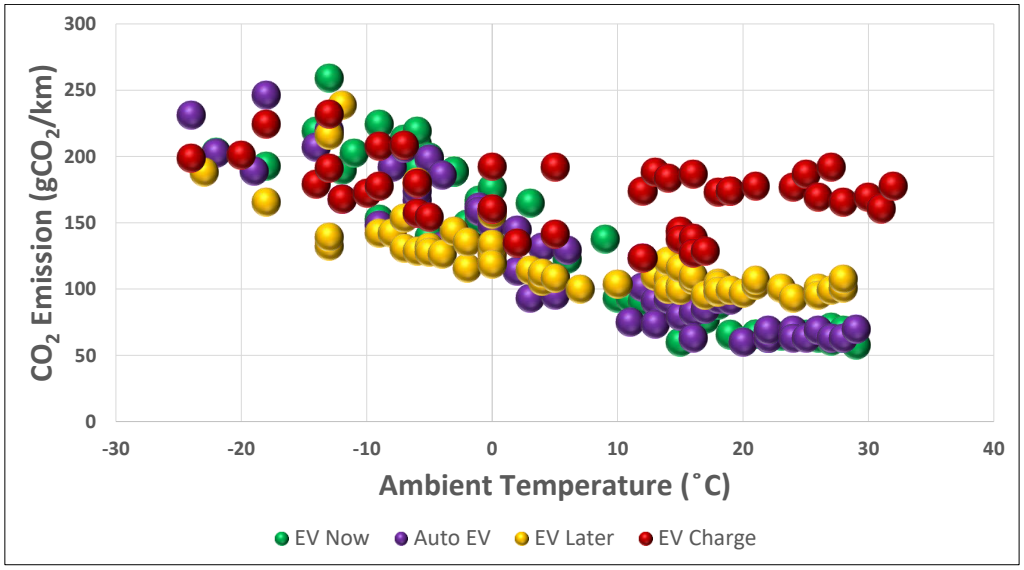

Figure 4.31: CO_2 emission of different powertrain modes of the tested vehicle based on Alberta CO_2 intensity value

According to the results, the intensity of CO_2 emissions for all powertrain modes was increased by decreasing the T_{amb}, as cold weather has a negative impact on the performance of the batteries and increasing the reliance on the ICE in hybrid vehicles or a more significant drain on the hybrid battery, ultimately resulting in increased CO_2 emissions.

The CO_2 emissions for all powertrain modes of the Ford Escape, based on Alberta's CO_2 intensity value, during the minimum and maximum tested T_{amb}, are presented in Table 4.12.

The highest recorded CO_2 emissions occurred during the use of Auto EV mode in T_{amb} of -24 °C, with nearly 231 g/km. On the other hand, the lowest emissions occurred during EV Now mode at T_{amb} of 29 °C, with just 58 g/km. When switching to EV Now mode, decreasing the T_{amb} from 29 °C to -22 °C caused CO_2 emissions to increase by almost 3.5 times. This is because the vehicle relies more on electric power in the Auto EV and EV Now modes. As the battery's efficiency has reduced

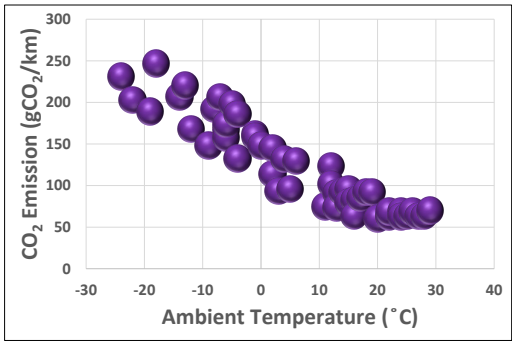

(a) Auto EV mode

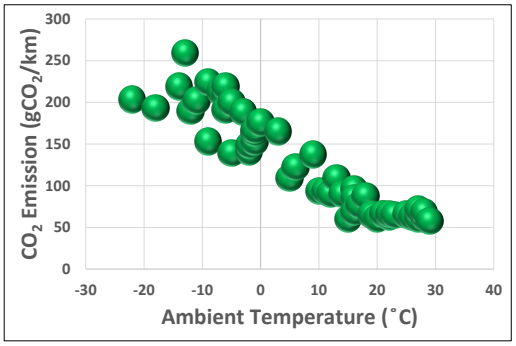

(b) EV Now mode

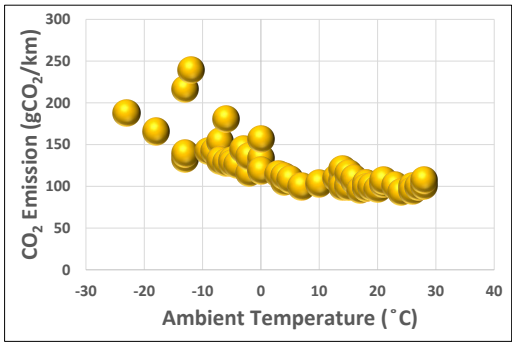

(c) EV Later mode

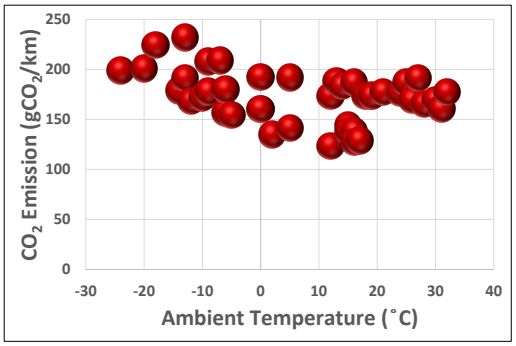

(d) EV Charge mode

Figure 4.32: CO_2 emission of the tested vehicle based on Alberta CO_2 intensity value

Table 4.12: CO_2 emission of different powertrain modes for the tested vehicle based on Alberta CO_2 intensity value

Test Type	**Min T_{amb} (°C)**	**CO_2 Emission (gCO_2/km)**	**Max T_{amb} (°C)**	**CO_2 Emission (gCO_2/km)**
Auto EV	-24	231	29	70
EV Now	-22	203	29	58
EV Later	-23	188	28	101
EV Charge	-24	199	32	177

in extremely cold weather and the battery drained faster, the ICE needed to work more extended periods to run the vehicle and charge the battery, leading to higher emissions.

Similarly, in EV Later mode, reducing the T_{amb} from 28 °C to -23 °C resulted in

CO_2 emissions almost doubling from 101 g/km to 188 g/km. However, when EV Charge mode was used, the impact of T_{amb} on CO_2 emissions was minimal, with only a 12% increase since the EV Charge mode relies more on the ICE to run the vehicle and charge the battery.

The CO_2 emissions of PHEVs are directly affected by the CO_2 intensity of the electricity used to charge their batteries. Suppose the electricity comes from a clean energy source such as solar, wind, hydroelectric, or nuclear power. In that case, the CO_2 emissions associated with charging the batteries will be significantly lower than electricity generated from fossil fuels like coal, oil, and natural gas. Therefore, using clean energy sources to power PHEVs is a vital strategy to reduce the environmental impact of transportation and combat climate change.

Manitoba and Quebec are both provinces in Canada that have a high proportion of electricity generated from clean energy sources, such as hydroelectric power. As a result, the CO_2 intensity of electricity in these provinces is relatively low compared to other regions that rely more heavily on fossil fuels for electricity generation. According to the latest data from the Canadian National Inventory Report (NIR), the CO_2 intensity of electricity in Manitoba is 1.2 gCO_2/kWh, while in Quebec, it is 1.9 gCO_2/kWh. These values are significantly lower than the national average CO_2 intensity of electricity in Canada, which is currently around 200 gCO_2/kWh [25].

The CO_2 emission for different powertrain modes of the Ford Escape PHEV based on Manitoba CO_2 intensity Value is shown in Figure 4.33.

Like Alberta, T_{amb} has a greater effect on CO_2 emissions in powertrain modes with high use of the electric motor, particularly at T_{amb} below 0 °C. Using a cleaner energy source for electricity production, the CO_2 emissions of PHEVs can be significantly reduced, even in extreme temperatures.

The CO_2 emissions for all powertrain modes of the Ford Escape, based on Manitoba's CO_2 intensity value, during the minimum and maximum tested T_{amb}, are presented in Table 4.13.

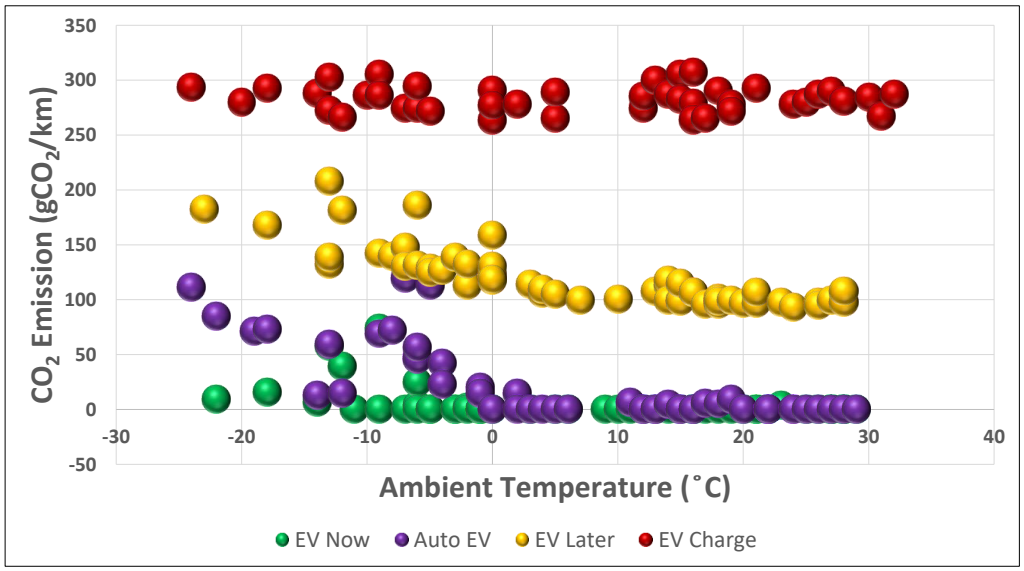

Figure 4.33: CO_2 emission of different powertrain modes of the tested vehicle based on Manitoba CO_2 intensity value

Table 4.13: CO_2 emission of different powertrain modes of the Ford Escape PHEV based on Manitoba CO_2 intensity Value

Test Type	**Min T_{amb} (°C)**	**CO_2 Emission (gCO_2/km)**	**Max T_{amb} (°C)**	**CO_2 Emission (gCO_2/km)**
Auto EV	-24	111	29	0
EV Now	-22	10	29	0
EV Later	-23	183	28	108
EV Charge	-24	294	32	287

The results show that the Ford Escape PHEV had the lowest CO_2 emissions when using the Auto EV and EV Now modes, regardless of T_{amb}, which was extremely cold or warm. However, the highest CO_2 emissions were observed when using the EV Charge mode, followed by the EV Later mode. These findings were due to clean Manitoba's electricity generation; as long as the electric motor powered the vehicle, the CO_2 emissions were at the lowest.

4.2.4 Comparison of Energy Consumption, Costs, and CO_2 Emission of a PHEV .Vs Conventional Vehicle

This part of the study aimed to compare the energy consumption, costs, and CO_2 emissions of a Ford Escape PHEV with a conventional Ford Escape with an IC Engine (Figure 4.34) under similar conditions. The testing conditions of the study were conducted in a T_{amb} range of -4 °C ± 1 °C to 14 °C to capture the impact of T_{amb} on the performance of both the Ford Escape PHEV and the conventional Ford Escape S. T_{amb} affects vehicles' energy consumption, costs, and emissions, impacting the powertrain's efficiency, battery performance, and fuel consumption.

Figure 4.34: The Ford Escape S (on the left) and the PHEV (on the right) used in this study

The specification of the Ford Escape S is shown in Table 4.14.

The engine and flow meter installed location on the Ford Escape S are shown in Figure 4.35.

The fuel test procedures used for the Ford Escape S were the same as those used for the Ford Escape PHEV, as described in the previous chapter. The test was repeated 32 times, with 30 of the tests being deemed acceptable. Additionally, The tests have

Table 4.14: Specifications of the Ford Escape S used in this study

Vehicle Specification	
Model Year	2021
Vehicle Body Style	Compact SUV
Fuel Type	Gasoline
Engine Type	1.5 L Eco Boost
Engine Rated Power	135 kW @ 6,000 RPM
Engine Torque	258 N.m @ 3,000 RPM
Compressor Ratio	10.0:1
Induction System	Turbocharged
Transmission Type	8-Speed Automatic
Vehicle Base Curb Mass	1,496 kg
Fuel Consumption Rate	7.8 L/100 km city/hwy

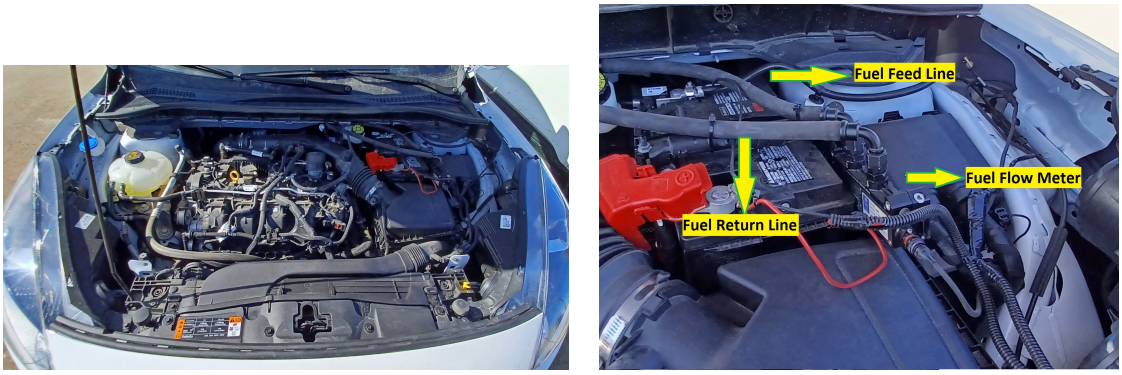

(a) Ford Escape S engine (b) Fuel flow meter installed on fuel line

Figure 4.35: Ford Escape S used in this study

been divided into cold and warm starts to evaluate how the vehicle performs under different starting conditions, as starting a vehicle in cold T_{amb} impacts fuel efficiency and emissions. Table 4.15 shows the Ford Escape S tests overview.

4.2.5 Energy Consumption of Ford Escape S

The energy consumption of the Ford Escape S in the T_{amb} range of 0 °C to 4 °C for cold start and -4 °C to 14 °C for warm start tests are shown in Figure 4.36.

Table 4.15: Ford Escape S fuel tests overview

Type of the Test	No. of Tests
Cold Start	7
Warm Start	23
Total	30

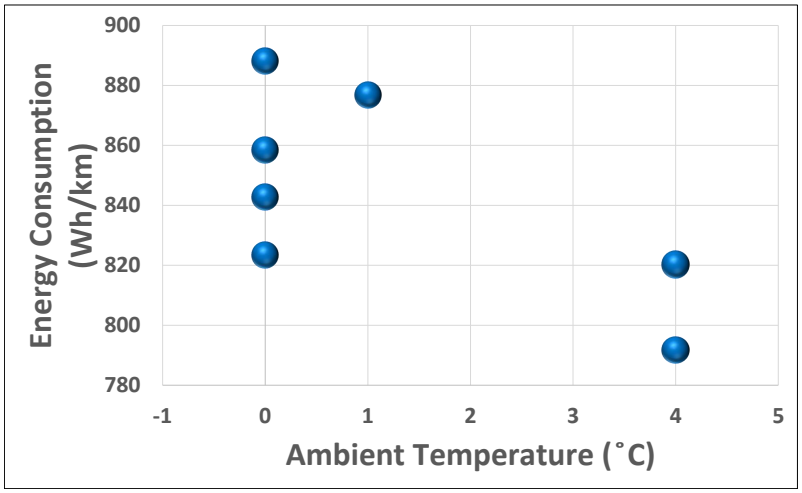

(a) Cold start tests

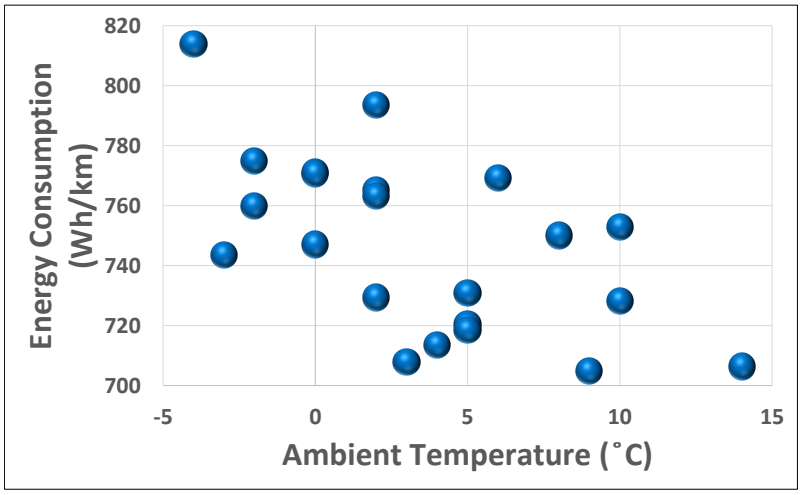

(b) Warm start tests

Figure 4.36: Energy consumption of the Ford Escape S

Table 4.16 shows the energy consumption of the Ford Escape S in minimum and maximum T_{amb} tests and their changes.

Based on the results provided, the energy consumption of the Ford Escape S was

Table 4.16: Energy consumption of the Ford Escape S

Test Type	Min T_{amb} (°C)	EC (Wh/km)	Max T_{amb} (°C)	EC (Wh/km)	EC Change(%)
Cold Start	0	888	4	792	12
Warm Start	-4	814	14	706	15

significantly impacted by the T_{amb} during both cold and warm starts. For the cold start tests, the energy consumption increased by 12% from T_{amb} 4 °C (792 Wh/km) to 0 °C (888 Wh/km). This was due to increased rolling resistance and decreased engine efficiency in colder temperatures. For the warm start tests, the energy consumption increased by 15% from T_{amb} 14 °C (706 Wh/km) to -4 °C (814 Wh/km). This indicates that even in warmer temperatures, the vehicle's energy consumption was still impacted by T_{amb}, albeit to a lesser extent than in the cold start tests.

Energy Consumption Comparison

The energy consumption of the Ford Escape PHEV and model S in the T_{amb} of -5 °C to 14 °C ± 1 °C is shown in Figure 4.37.

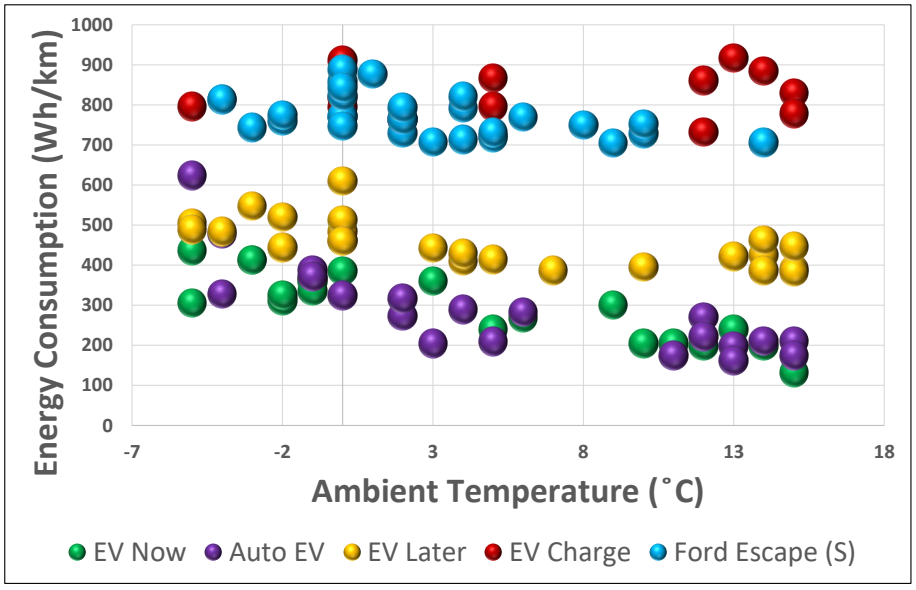

Figure 4.37: Energy consumption of Ford Escape S Vs. PHEV

As shown in Figure 4.37, at lower T_{amb}, the energy consumption of the model S was comparable to that of the EV Charge mode of the PHEV. However, as the T_{amb} increased, the energy consumption of the PHEV became higher than that of the S. The other three powertrain modes of the PHEV (Auto EV, EV Now, and EV Later) consumed less energy compared to the S, particularly at higher T_{amb}. This is because the PHEV can rely more on its electric motor in those modes and consume less fuel, whereas the model S has only the ICE and no electric motor.

Figure 4.38 shows the average and standard deviation of energy consumption for both vehicles.

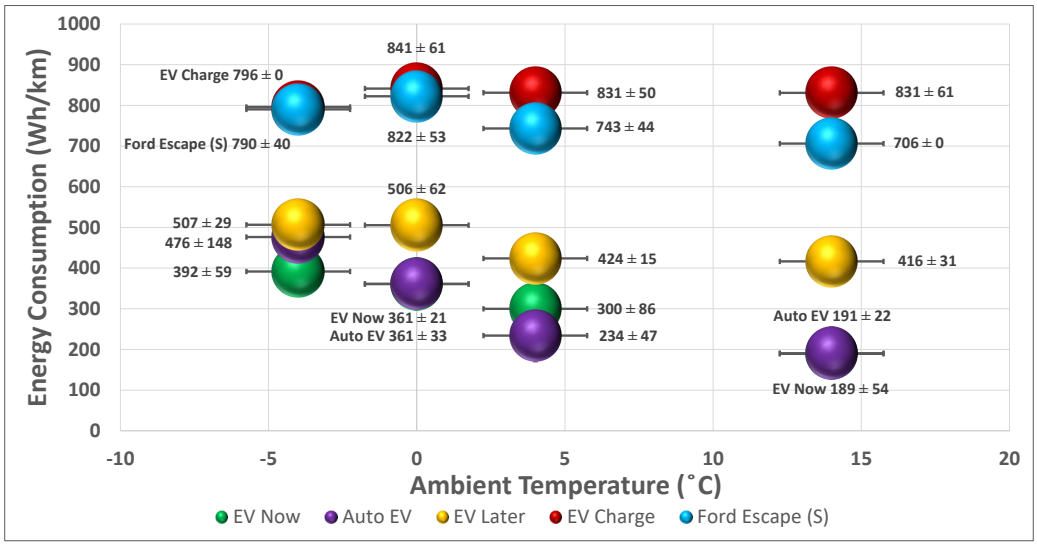

Figure 4.38: Average energy consumption of Ford Escape S Vs. PHEV

The energy consumption of the Ford Escape S and all powertrain modes of the PHEV at the minimum and maximum tested T_{amb} is shown in Table 4.17.

The T_{amb} significantly affects the energy consumption of the PHEV, particularly in the Auto EV and EV Now modes. The results suggest that at a T_{amb} of -4 °C ± 1 °C, the energy consumption in these modes was doubled compared to that at 14 °C. However, for the S, the effect of T_{amb} on energy consumption was very low. The energy consumption only increased by 15% when the temperature decreased from 14 °C to -4 °C ± 1 °C.

Table 4.17: Energy consumption of Ford Escape S Vs. PHEV

Powertrain Mode	Min T_{amb} (°C)	Energy Consumption (Wh/km)	Max T_{amb} (°C)	Energy Consumption (Wh/km)
Auto EV	-4 ± 1	403	14 ± 1	210
EV Now	-4 ± 1	392	14 ± 1	197
EV Later	-4 ± 1	484	14 ± 1	425
EV Charge	-4 ± 1	796	14 ± 1	778
ICE [S]	-4 ± 1	814	14 ± 1	706

Energy Cost Comparison

As previously mentioned, the study used an average gasoline price of 140.7 ¢/L and a cost of 10 ¢/kWh for electricity for its calculations. Based on this information, the cost of the various powertrain modes of the Ford Escape PHEV and model (S) is shown in Figure 4.39.

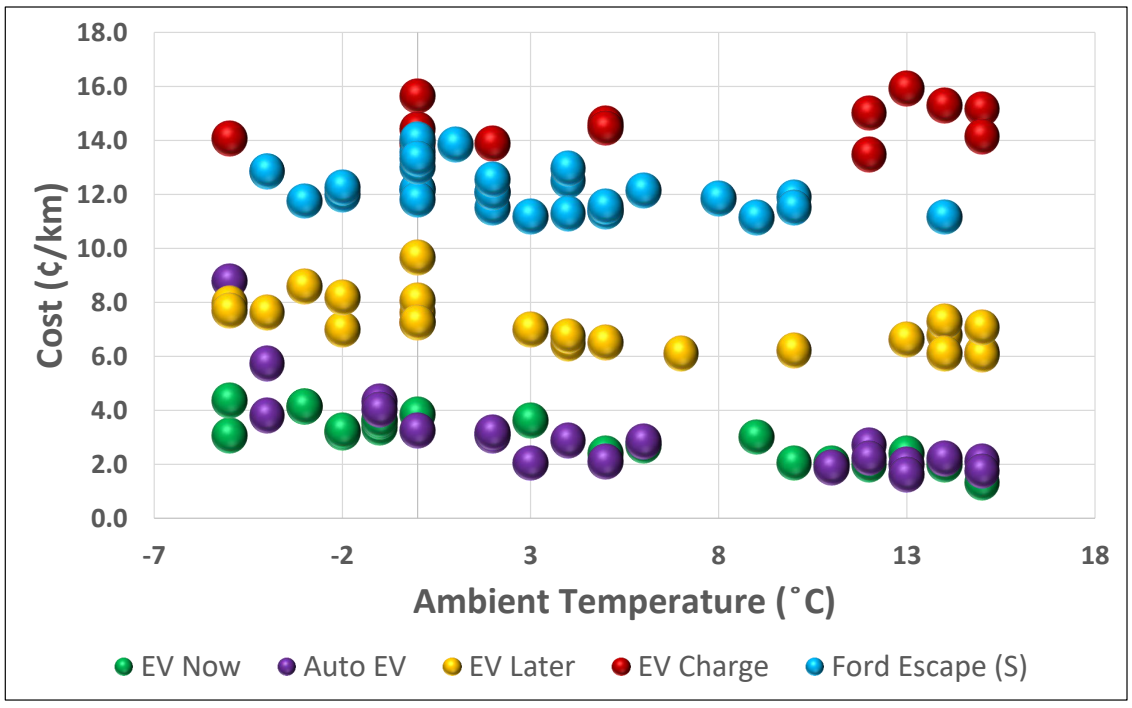

Figure 4.39: Energy cost of Ford Escape S vs. PHEV

The energy costs of all powertrain modes of the Ford Escape S and PHEV at the minimum and maximum tested T_{amb} based on the considered price of gasoline and electricity are shown in Table 4.18.

Table 4.18: Comparison of energy cost for Ford Escape S Vs. PHEV

T_{amb}	Energy Cost (¢/km)				
	Auto EV	**EV Now**	**EV Later**	**EV Charge**	**S**
-4 ± 1 °C	8.8	3	7.9	14.1	12.8
4 ± 1 °C	2.1	2.4	6.5	14.5	11.4
14 ± 1 °C	2.2	2	6.7	15.3	11.2

The study found that the EV Now mode of the PHEV had the lowest cost at T_{amb} of -4 °C ± 1 °C, costing 3 ¢/km. This cost was significantly lower than the cost for model S, which was over four times higher at the same T_{amb}. At T_{amb} of 14 °C ± 1 °C, the cost of the EV Now mode was 2 ¢/km, which was also lower than the cost for the S model. The difference in cost between the two vehicles was even more significant at this T_{amb}, with the model S costing almost six times more than the PHEV. The cost difference between the PHEV and model S was more significant at warmer T_{amb}, where the PHEV's electric-only modes were more efficient and had a lower energy cost. In contrast, the model S relied solely on gasoline, which was more expensive than electricity. Therefore, the PHEV was more cost-effective and had lower energy costs in modes using the electric motor.

CO_2 Emission Comparison

The study measured the CO_2 emissions for different Ford Escape PHEV powertrain modes and the model S. The CO_2 intensity used in the calculations was based on the average for Alberta in the previous year, which was 457 gCO_2/kWh.

The study results are presented in Figure 4.40, which shows the CO_2 emissions for both vehicles.

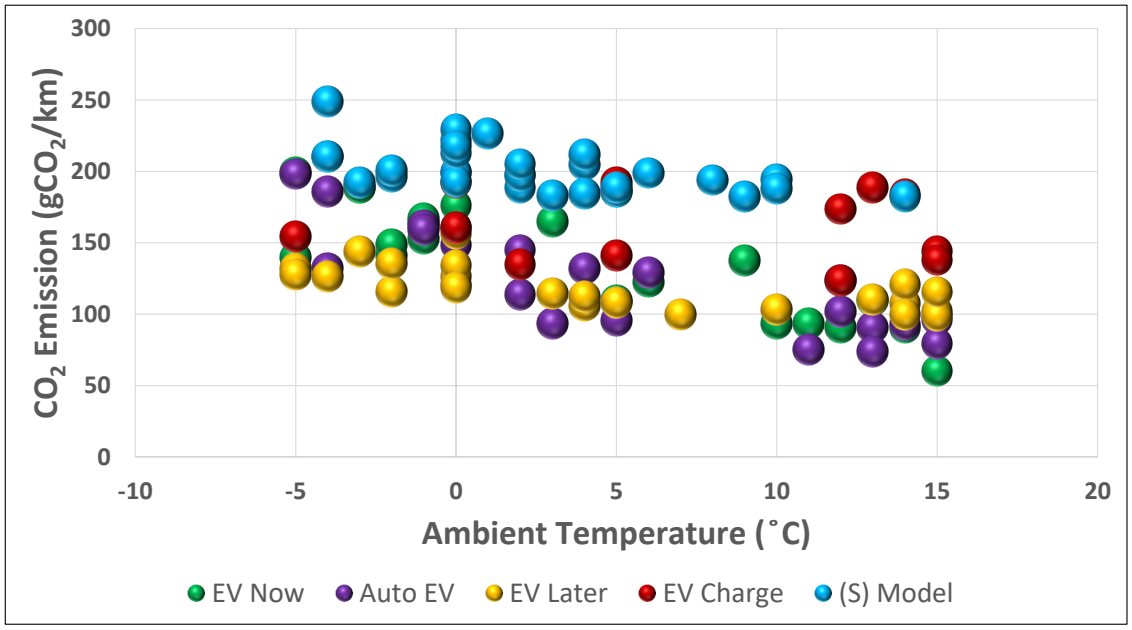

Figure 4.40: Ford Escape S Vs. PHEV CO_2 emission

Figure 4.41 shows the average and standard deviation of CO_2 emissions for both vehicles.

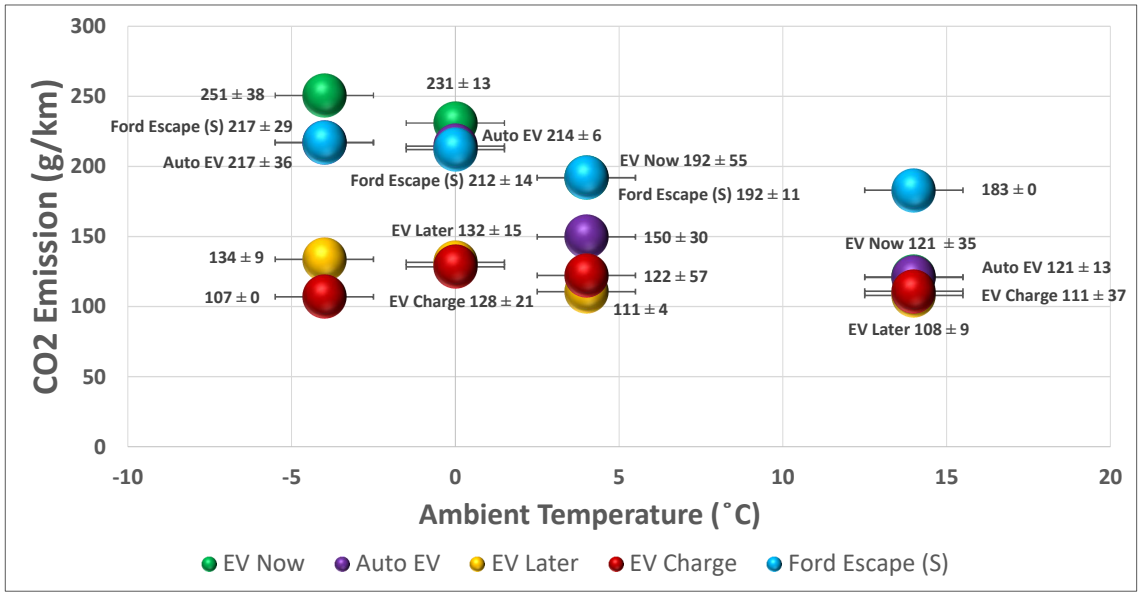

Figure 4.41: Average CO_2 emission comparison of Ford Escape S Vs. PHEV

The CO_2 emission of all powertrain modes of the Ford Escape PHEV and model

S at the minimum and maximum tested T_{amb} are shown in Table 4.19.

Table 4.19: Comparison of CO_2 emission for Ford Escape S vs. PHEV

T_{amb} (°C)	CO_2 Emission (gCO_2/km)				
	Auto EV	**EV Now**	**EV Later**	**EV Charge**	**S**
-4 ± 1	198	200	132	154	210
4 ± 1	96	109	108	141	186
14 ± 1	60	126	99	138	183

The T_{amb} significantly impacted the CO_2 emission of the Auto EV and EV Now modes of the Ford Escape PHEV. On the other hand, the T_{amb} had a lesser effect on the EV Later and EV Charge modes of PHEV. Same as energy consumption, the CO_2 emission for the model S had a slice change by changing the T_{amb}. Overall, the amount of CO_2 emission for the powertrain modes that used the electric motor was much affected by T_{amb}; on the other hand, the powertrains with continued use of ICE were less sensitive to changes T_{amb}.

4.2.6 Return of Investment (ROI)

The ROI is a standard financial metric used to evaluate the profitability of an investment, and it can be calculated by dividing the net profit or savings by the initial investment. In the context of vehicles, ROI can be affected by various factors, including the upfront cost of the vehicle, fuel or energy fees, maintenance costs, and resale value. PHEVs, which have both an electric motor and a combustion engine, can offer potential fuel savings and lower emissions than conventional vehicles. However, they typically have a higher upfront cost.

Ford Escape PHEV and Ford F-150 Lightning were alternatives for the UAlberta fleet of SUVs and 1/2-tonne trucks for this study. The impact of energy costs and T_{amb} on ROI was researched. This analysis has considered the cost of electricity and gasoline, factors such as T_{amb}, and the distance traveled. Furthermore, since the

selected applications of the UAlberta fleet driving cycles were in the city, the ROI was investigated based on the city cycles.

The price of a Ford Escape S with ICE was 32,444 Canadian dollars at the time of this study, while the price of a PHEV (SE) model was 43,394 Canadian dollars.

The Ford F-150 Lightning is an all-electric pickup truck. As an EV, the Ford F-150 Lightning has the potential to offer significant fuel cost savings compared to the traditional ICE model, with a price difference of 25,114 C$. (The price of a Ford F-150 Lightning XLT at the time of this study was 73,750 C$ while it was 48,636 C$ for the XLT with ICE).

The F-150 XLT with ICE consumed 13.8 L/100km in city cycles. As one liter of gasoline contains the energy equivalent to 8.9 kWh of electricity [66], the energy consumption for F-150 XLT with ICE was 1,228 Wh/km for the city. On the other hand, the F-150 Lightning XLT consumed 275 Wh/km in the city [67].

The ROI Based on Total Distance

The disparity in energy cost for the Ford Escape S with an ICE and Auto EV (Equation 4.4), EV Now (Equation 4.5), and EV Later (Equation 4.6) powertrain modes of the Ford Escape PHEV were calculated.

$$XS–XSE_A = Z_A(¢/km) \tag{4.4}$$

$$XS–XSE_N = Z_N(¢/km) \tag{4.5}$$

$$XS–XSE_L = Z_L(¢/km) \tag{4.6}$$

where XS is the base parameter and represents the energy cost for the Ford Escape S, XSE_A, XSE_N, and XSE_L represent the energy costs for Auto EV, EV Now, and EV Later powertrain modes of the Ford Escape PHEV (SE), respectively. Z_A,

Z_N, and Z_L represent the difference in energy costs between the Ford Escape S and Auto EV, EV Now, and EV Later powertrain modes of the Ford Escape PHEV (SE), respectively.

The ROI based on total distance (km) for Auto EV, EV Now, and EV Later powertrain modes of the Ford Escape PHEV (SE) were calculated by Equation 4.7:

$$T_D(km) = 1,095,000(¢)/Z(¢/km) \tag{4.7}$$

T_D is the total distance required to achieve an ROI for the PHEV, and the value of 1,095,000 (¢) represents the difference in cost between the Ford Escape S and the PHEV.

The total distance required to achieve an ROI (T_D) was calculated three times based on the minimum, average, and maximum gasoline prices in Edmonton in 2022. This approach has allowed the study to account for the potential variability in gasoline prices over time and provide a range of estimates for the total distance required to achieve an ROI for the PHEV.

Furthermore, the EV Charge mode was not calculated because it was not considered beneficial, and a PHEV's purpose is to use the electric motor to save fuel and reduce costs.

The energy costs for the Ford Escape S and the PHEV at T_{amb} of (-4 °C ± 1 °C), (0 °C ± 1 °C), (4 °C ± 1 °C), and (14 °C ± 1 °C) are shown in Tables 4.20, 4.21, 4.22 and 4.23 respectively.

The results showed that the Ford Escape S had the highest energy cost at the T_{amb} of -4 °C ± 1 °C with the cost of 16.9 ¢/km; on the other hand, the lowest was for the EV Now mode at the T_{amb} of 14 °C ± 1 °C with the cost of 1.6 ¢/km.

Overall, the energy costs for the Ford Escape S were between 15.1 ¢/km to 16.9 ¢/km while it was 1.6 ¢/km to 3.6 ¢/km for the EV Now mode, 2 ¢/km to 5.5 ¢/km for Auto EV mode and 8.4 ¢/km to 10.7 ¢/km for EV Later mode of the Ford Escape

Table 4.20: The energy costs of the two tested vehicles used in this study at the T_{amb} of -4 °C ± 1 °C

Powertrain Mode	**Based on Min Gas Price (¢/km)**	**Based on Ave Gas Price (¢/km)**	**Based on Max Gas Price (¢/km)**
Auto EV	4.6	4.8	5.5
EV Now	3.6	3.6	3.6
EV Later	7.2	8.0	10.7
ICE [S]	11.2	12.5	16.9

Table 4.21: The energy costs of the two tested vehicles used in this study at the T_{amb} of 0 °C ± 1 °C

Powertrain Mode	**Based on Min Gas Price (¢/km)**	**Based on Ave Gas Price (¢/km)**	**Based on Max Gas Price (¢/km)**
Auto EV	3.8	3.9	4.1
EV Now	3.5	3.5	3.5
EV Later	6.9	7.6	10.3
ICE [S]	10.9	12.1	16.3

Table 4.22: The energy costs of the two tested vehicles used in this study at the T_{amb} of 4 °C ± 1 °C

Powertrain Mode	**Based on Min Gas Price (¢/km)**	**Based on Ave Gas Price (¢/km)**	**Based on Max Gas Price (¢/km)**
Auto EV	2.3	2.3	2.3
EV Now	2.4	2.4	2.4
EV Later	6.0	6.7	9.0
ICE [S]	10.2	11.3	15.3

Table 4.23: The energy costs of the two tested vehicles used in this study at the T_{amb} of 14 °C ± 1 °C

Powertrain Mode	**Based on Min Gas Price (¢/km)**	**Based on Ave Gas Price (¢/km)**	**Based on Max Gas Price (¢/km)**
Auto EV	2.0	2.0	2.0
EV Now	1.6	1.6	1.6
EV Later	5.6	6.2	8.4
ICE [S]	10.1	11.2	15.1

PHEV. Based on these, it's evident that the energy costs for the PHEV powertrain modes were generally lower than those for the Ford Escape S with an ICE, regardless of the T_{amb}.

The fuel consumption of conventional gasoline cars can increase by almost 15% at lower T_{amb}, such as -7 °C, compared to a warmer T_{amb} like 25 °C, in city driving [68]. This is because the engine has to work harder to maintain optimal operating temperature, and other factors, such as longer warm-up times, can also negatively affect fuel efficiency.

On the other hand, for EVs, energy consumption can increase by approximately 39% in mixed city and highway driving at lower T_{amb} [68]. This is because the battery has to work harder to maintain its operating temperature and provide power to the electric motor. Additionally, using the vehicle's heating system to warm the cabin can increase energy consumption in cold weather.

The ROI of the Ford Escape PHEV based on mileage for Auto EV, EV Now, and EV Later powertrain modes appear in Figure 4.42.

The ROI was determined by considering the increase in energy consumption of the conventional gasoline and PHEV vehicles at lower T_{amb}. According to Figure 4.42, for EV Now mode, the ROI based on mileage according to the maximum gas price was around 82,000 km to 86,000 km in the tested T_{amb} range, while it was between

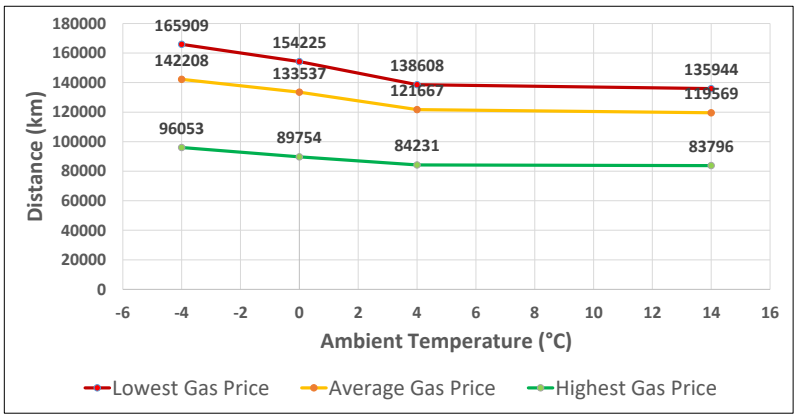

(a) Auto EV mode

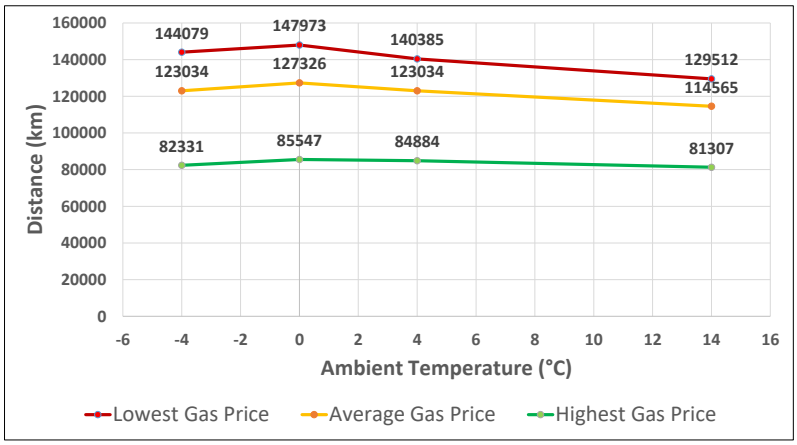

(b) EV Now mode

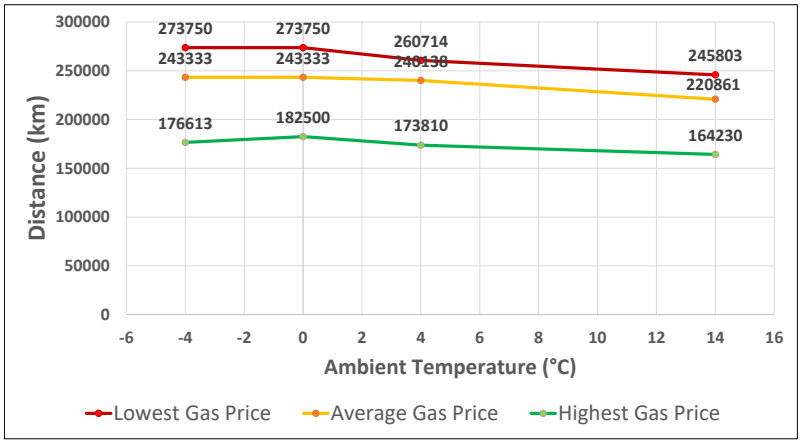

(c) EV Later mode

Figure 4.42: The ROI of the Ford Escape PHEV based on distance

130,000 km to 148,000 km based on the minimum gas price.

This indicates the price of gas had the most significant effect on ROI. Also, it can be concluded that the powertrain modes with higher utilization of the electric motor required lower mileage for ROI by comparing the EV Now mode mileage with EV Later mode, which employed both ICE and electric motor.

The fuel consumption and costs for Ford F-150 XLT with ICE are shown in Table 4.24.

Table 4.24: Fuel consumption [67] and costs of F-150 XLT with ICE at T_{amb} of -7 °C and 25 °C for urban cycles

T_{amb} (°C)	**Fuel Consumption (L/100km)**	**Based on Min Gas Price (¢/km)**	**Based on Ave Gas Price (¢/km)**	**Based on Max Gas Price (¢/km)**
-7	16.6	21.0	23.3	31.5
25	13.8	17.5	19.4	26.2

The energy consumption and costs for F-150 Lightning XLT are shown in Table 4.25.

Table 4.25: Energy consumption [67] and costs of F-150 Lightning XLT at T_{amb} of -7 °C and 25 °C for city cycles

Driving Cycle/ T_{amb} (°C)	**Consumption (Wh/km)**	**Cost (¢/km)**
Urban / -7	382	3.8
Urban / 25	275	2.8

Table 4.26 shows the energy costs for the F-150 Lightning XLT and F-150 XLT with ICE at T_{amb} of -7 °C and 25 °C.

The ROI for the Ford F-150 Lightning XLT based on distance, considering the maximum, average, and minimum gas prices of the previous year in Edmonton, for city driving cycles at T_{amb} of -7 °C and 25 °C are shown in Figure 4.43

Table 4.26: The energy costs of the F-150 Lightning XLT and F-150 XLT at T_{amb} of -7 °C and 25 °C

T_{amb} (°C)	Cost Based on Min Gas Price (¢/km)	Cost Based on Ave Gas Price (¢/km)	Cost Based on Max Gas Price (¢/km)
-7	17.2	19.5	27.6
25	14.8	16.7	28.7

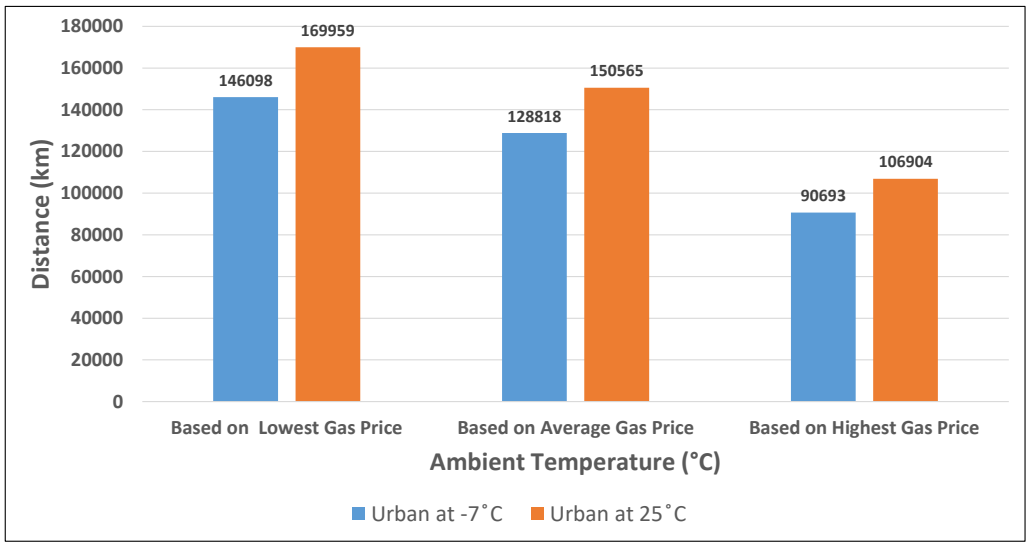

Figure 4.43: The ROI for the Ford F-150 Lightning XLT based on distance

According to Figure 4.43, it is evident that the ROI for the Ford F-150 Lightning XLT is considerably less in T_{amb} of -7 °C with 91,000 km compared to T_{amb} of 25 °C with, 107,000 km for urban, which shows almost an 18% difference. Therefore, the F-150 Lightning XLT is more cost-efficient in T_{amb} of -7 °C due to the higher energy consumption of the Ford F-150 XLT at lower T_{amb}.

The ROI Based on Application of the University of Alberta Fleet Vehicles

The annual average mileage of the UAlberta fleet vehicles based on vehicle type is revealed in Figure 4.44.

The ROI for the Ford Escape PHEV and Ford F-150 Lightning based on the UAlberta fleet application mileage was investigated. This part of the study is based

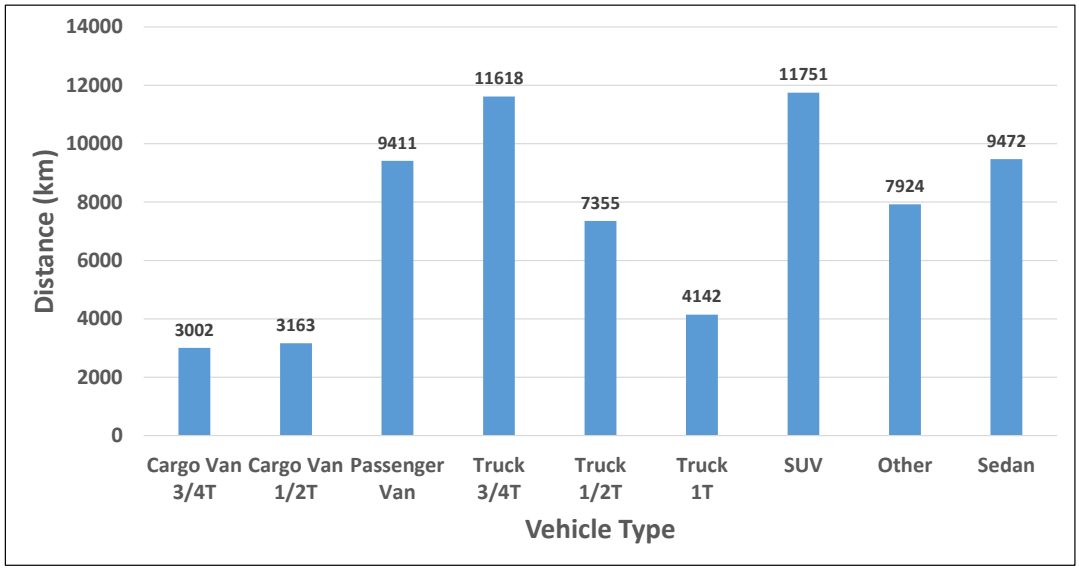

Figure 4.44: The University of Alberta fleet annual average mileage by vehicle type

on the University of Alberta fleet's vehicle mileage data for 2019 - 2020 (Before the Covid-19 pandemic).

The annual average mileage for 1/2 tonne trucks of the UAlberta fleet vehicles based on application is shown in Figure 4.45.

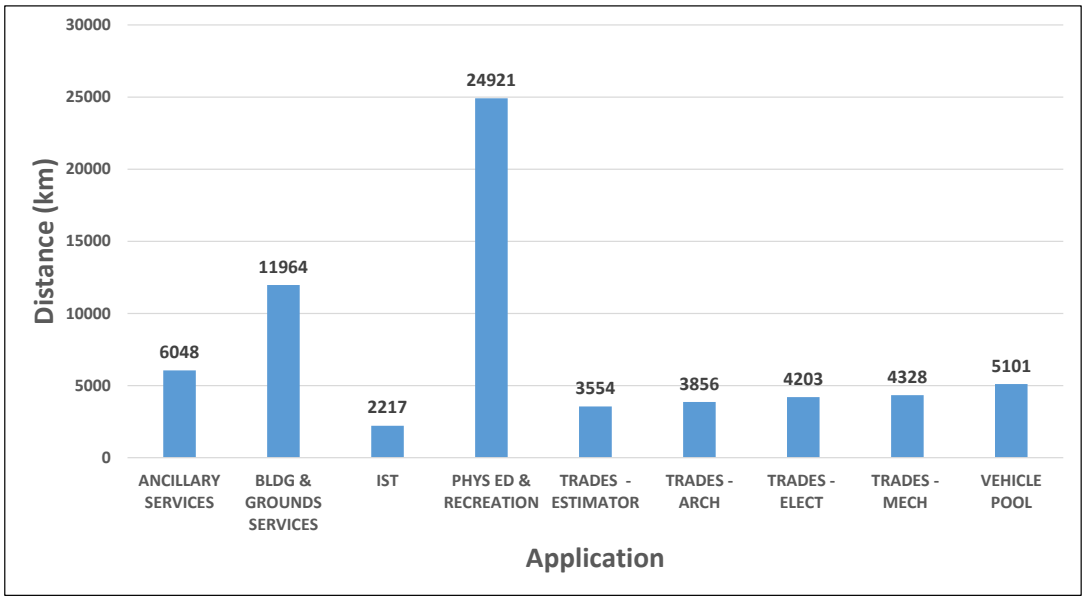

Figure 4.45: The annual average mileage of 1/2 tonne trucks of the University of Alberta fleet by application

Based on the data presented in Figure 4.45, the ROI for the Ford F-150 Lightning for different applications and gas prices at the T_{amb} of 25 °C and -7 °C are shown in Figures 4.46 and 4.47 respectively.

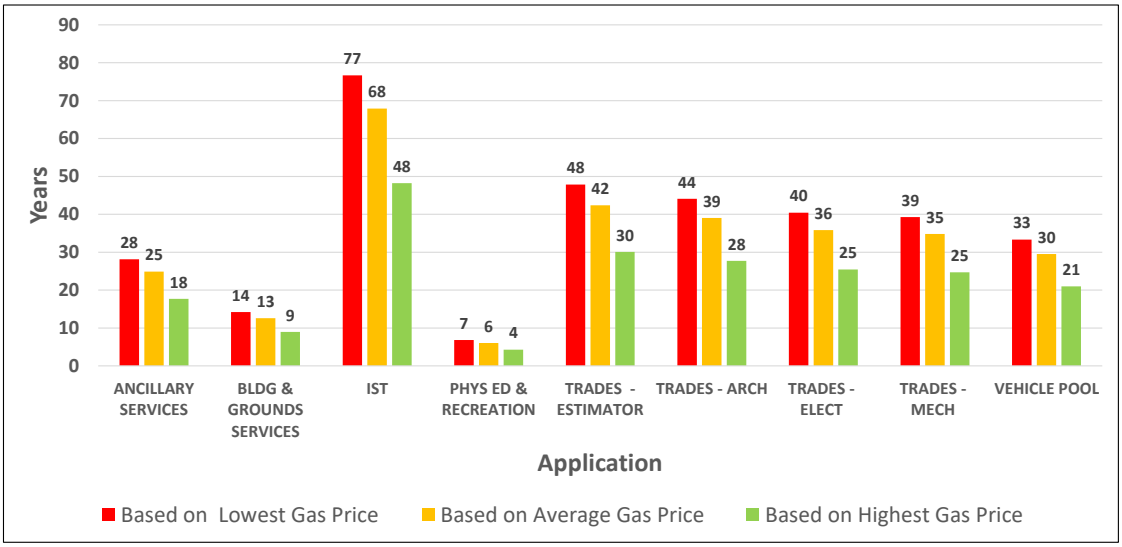

Figure 4.46: The ROI for Ford F-150 Lightning by year, based on the annual average mileage of the UAlberta fleet applications at T_{amb} 25 °C

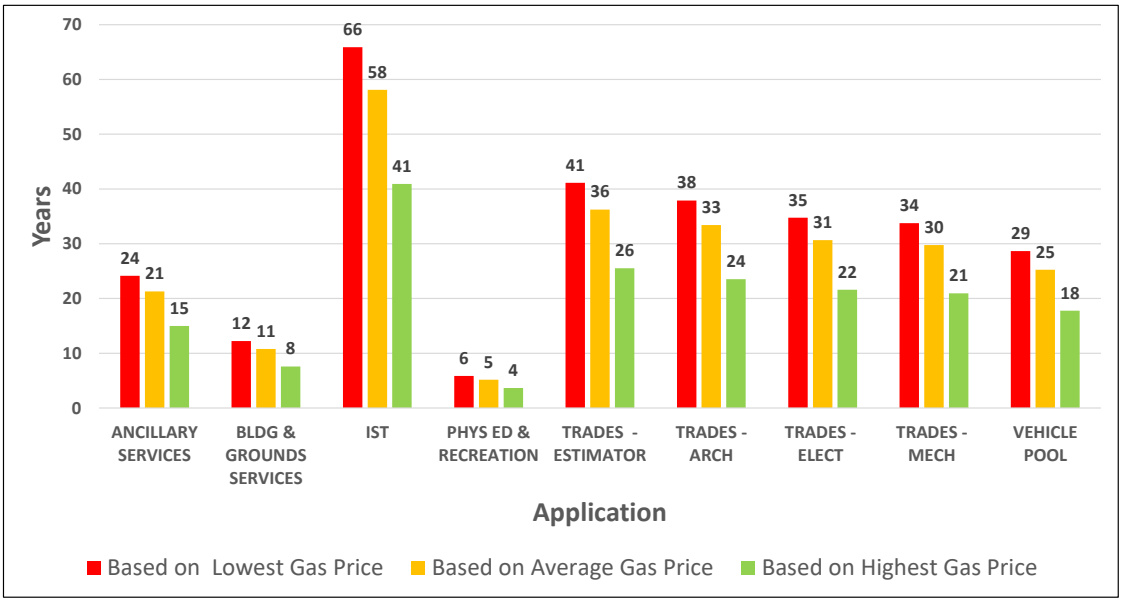

Figure 4.47: The ROI for Ford F-150 Lightning by year, based on the annual average mileage of the University of Alberta fleet applications at T_{amb} -7 °C

Based on the analysis, the ROI for the Ford F-150 Lightning was reasonable for

applications such as PHYS ED and RECREATION, which involved a higher annual mileage than other applications. However, the ROI was less beneficial for applications with lower annual mileage.

The annual average mileage for SUVs of the UAlberta fleet vehicles based on application is shown in Figure 4.48.

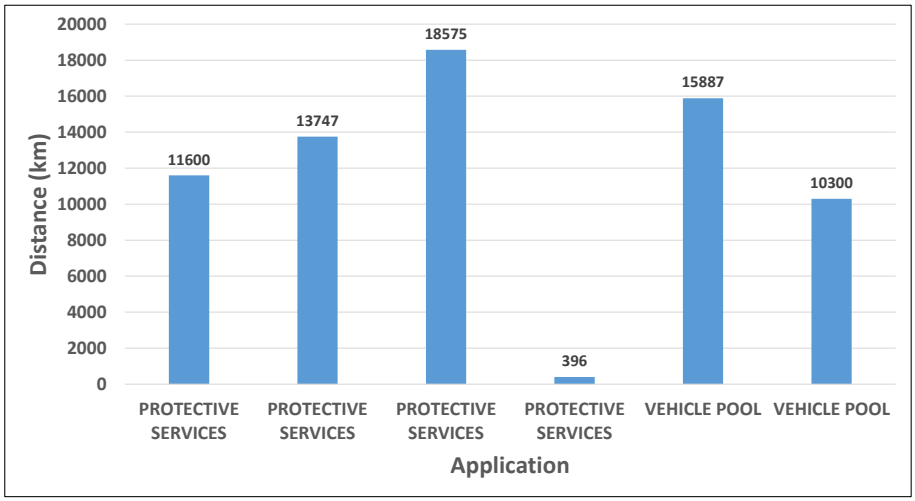

Figure 4.48: The annual average mileage of the SUVs of the University of Alberta fleet by application

The ROI for Ford Escape PHEV by year, based on the annual average mileage of the UAlberta vpool (13,100 km) and protective services vehicles (11,100 km) at T_{amb} of -4 °C, 0 °C, 4° C, and 14 °C (± 1 °C for all) for EV Now, Auto EV, and EV Later modes are shown in Figures 4.49 and 4.50 respectively.

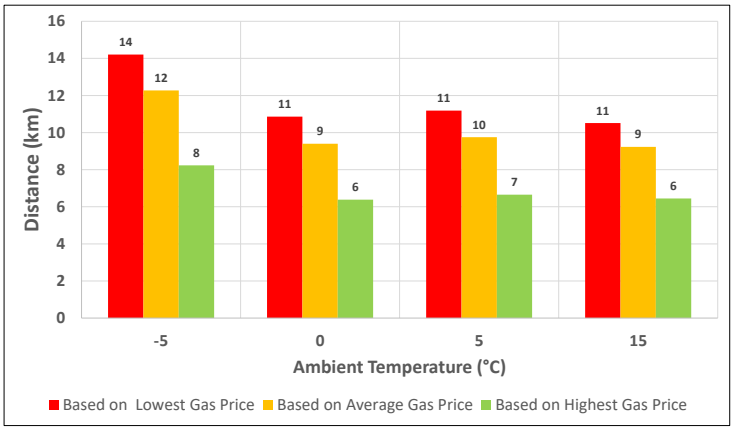

(a) Auto EV mode

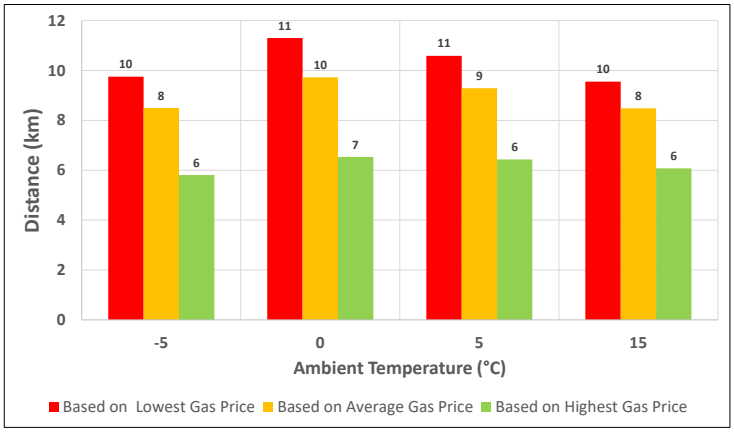

(b) EV Now mode

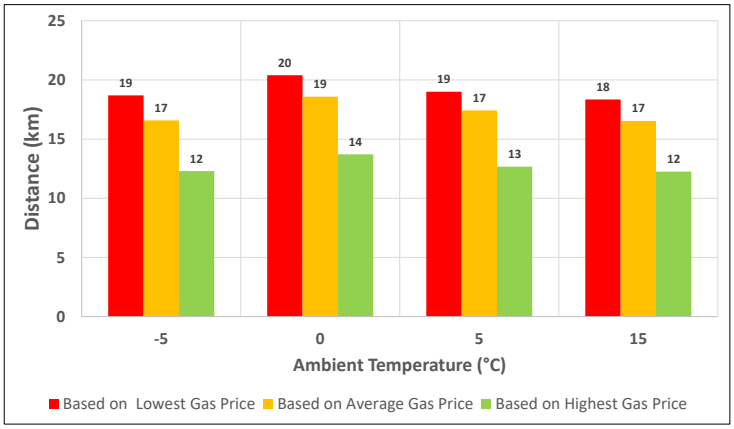

(c) EV Later mode

Figure 4.49: The ROI for the Ford Escape PHEV by year, based on the annual average mileage of the University of Alberta vpool vehicles

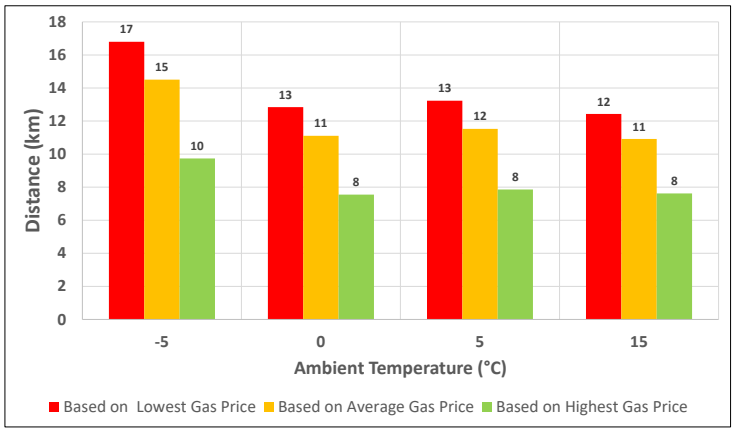

(a) Auto EV mode

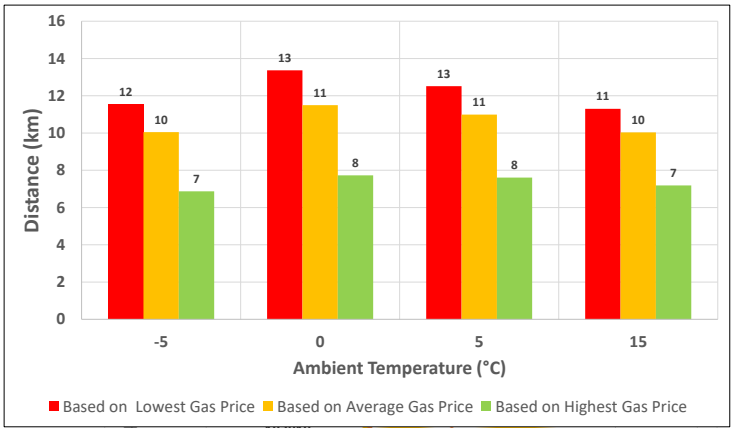

(b) EV Now mode

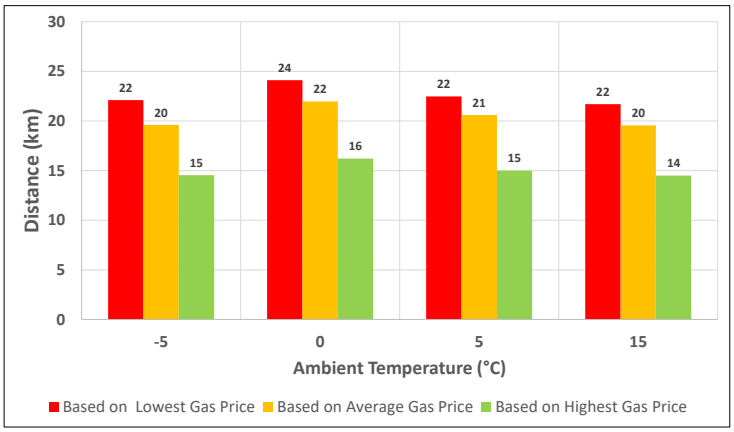

(c) EV Later mode

Figure 4.50: The ROI of the Ford Escape PHEV by year, based on the annual average mileage of the University of Alberta protective services (UAPS) vehicles

The ROI Based on Natural Resources Canada (NRCan) Annual Average Mileage

Based on NRCan, the annual average mileage for passenger vehicles in Canada is approximately 20,000 kilometers per year [69]. Based on this, the ROI for the Ford F-150 Lightning at T_{amb} of -7 °C and 25 °C for city routes was calculated (Figure 4.51).

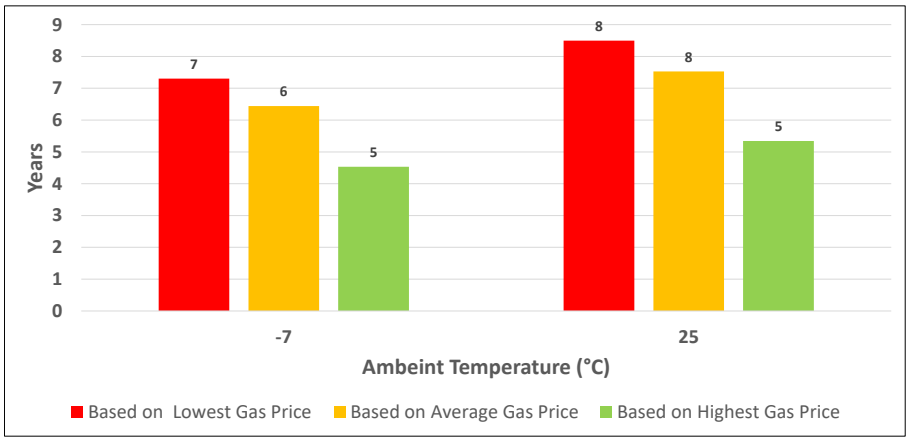

Figure 4.51: The ROI of the Ford F-150 Lightning for city routes at T_{amb} -7 °C and 25 °C based on NRCan, 20,000 km annual mileage

The ROI of Ford Escape PHEV by year, based on 20,000 km annual mileage at the T_{amb} of -4 °C, 0 °C, 4 °C, and 14 °C (± 1 °C for all) for Auto EV, EV Now, and EV Later modes are shown in Figure 4.52.

According to the results, The ROI for EVs and HEVs is influenced by factors such as the cost difference between conventional and electric/hybrid vehicles, annual average mileage, fuel/electricity prices, maintenance costs, and T_{amb}. These factors can vary based on location, usage, and other individual characteristics and should be considered when evaluating the ROI for a specific vehicle and use case. It should be noted that these calculations are based on the assumption of previous gas prices and do not consider the potential impact of future gas price fluctuations. Additionally, the measures only assume the financial aspect of the decision and do not account for other factors, such as environmental impact and operational requirements.

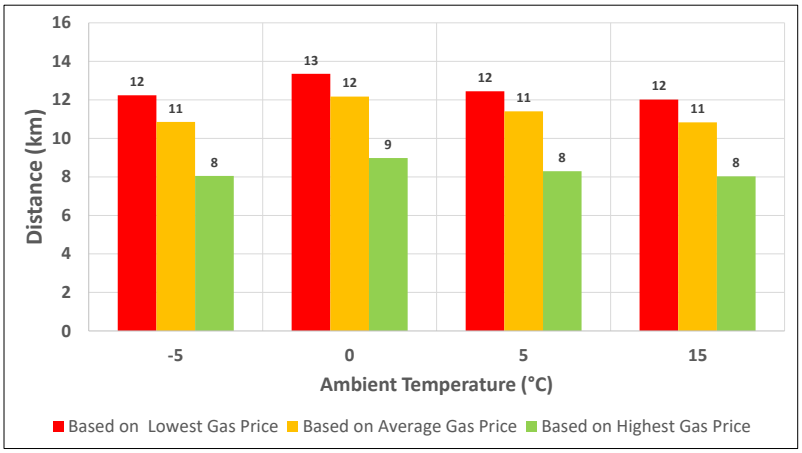

(a) EV Later mode

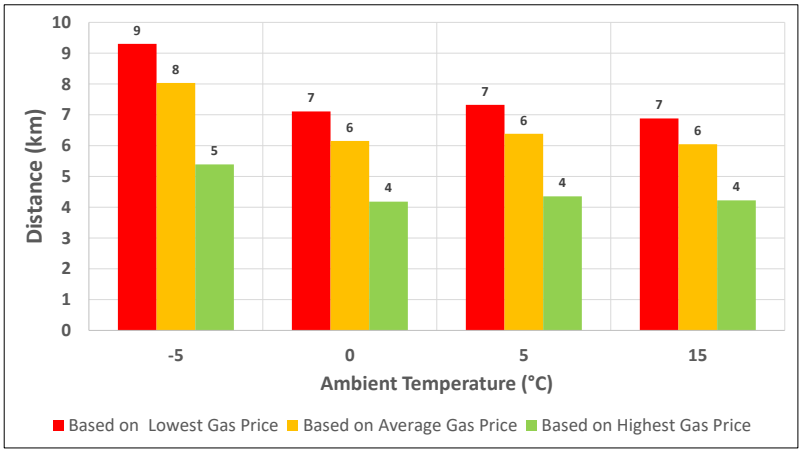

(b) Auto EV mode

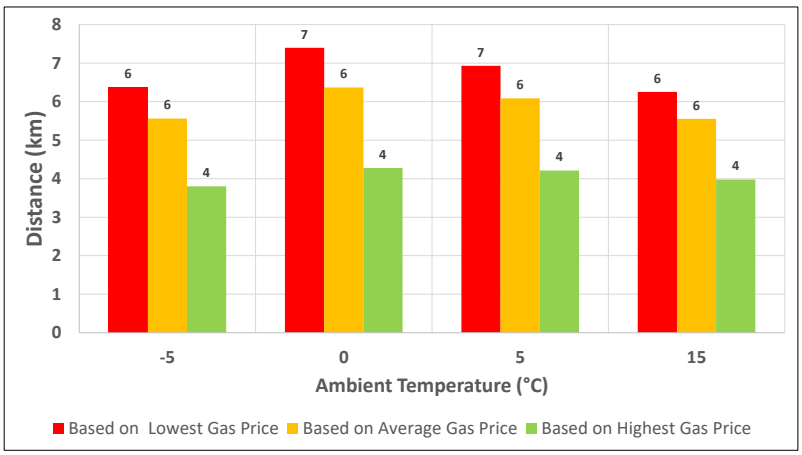

(c) EV Now mode

Figure 4.52: The ROI for the Ford Escape PHEV based on NRCan, 20,000 km annual mileage

Chapter 5

The Effect of Start-Stop Technology on Energy Consumption and Costs

This chapter investigates the effect of using start-stop technology for the University fleet vehicles. To this end, a test procedure is designed, and vehicle fuel saving is determined based on vehicle testing and driving cycles for each application area of university vehicles.

5.1 Introduction

Start-stop technology is part of the automotive industry's efforts to improve the fuel economy of vehicles and reduce emissions in response to environmental concerns and stricter regulations. One example of innovative engineering solutions is the start-stop technology, also called "idle stop-start" or "auto stop-start". This technology is designed to save fuel and decrease emissions by automatically turning off the engine when the vehicle stops, such as at traffic lights or in heavy traffic. The engine will only restart when the driver releases the brake pedal, engages the clutch (in manual transmission vehicles), or when the vehicle wants to accelerate. This technology ensures that vehicles are more environmentally friendly without compromising their performance or the driver's comfort.

One of the advantages of start-stop technology is that it can be easily integrated

into traditional powertrain systems without requiring significant changes or modifications to the engine or transmission. This means it can be implemented relatively quickly and at a lower cost than other technologies, such as hybrid or electric powertrains.

However, it's important to note that the effectiveness of start-stop technology depends on various factors such as driving conditions, vehicle size, and the specific implementation of the technology. In some cases, fuel consumption and emissions savings may be less significant, especially if the vehicle is frequently in motion and has low idle time. Additionally, the frequent stopping and starting of the engine can lead to increased wear on the starter and battery, which may require more frequent maintenance or replacement.

5.1.1 How Start-Stop Technology Works

Figure 5.1 shows the schematic of the Start-stop technology. The system uses sensors such as brake pedal position, clutch position, engine coolant temperature, and battery voltage to determine when the vehicle is stationary and when the engine can be safely turned off. When the vehicle comes to a complete stop, and certain conditions are met, like engine coolant temperature is within a specific range and the battery has sufficient charge, the system automatically shuts off the engine. While the engine is off, the system monitors various parameters to ensure that restarting the engine will not harm the components and that the vehicle can move safely.

The system uses sensors such as brake pedal position, clutch position, engine temperature, and battery voltage to determine when the vehicle is stationary and the engine can be safely turned off. When the vehicle comes to a complete stop, and certain conditions are met, like engine coolant temperature is within a specific range and the battery has sufficient charge, the system automatically shuts off the engine. While the engine is off, the system monitors various parameters to ensure that restarting the engine will not harm the components and that the vehicle can move safely.

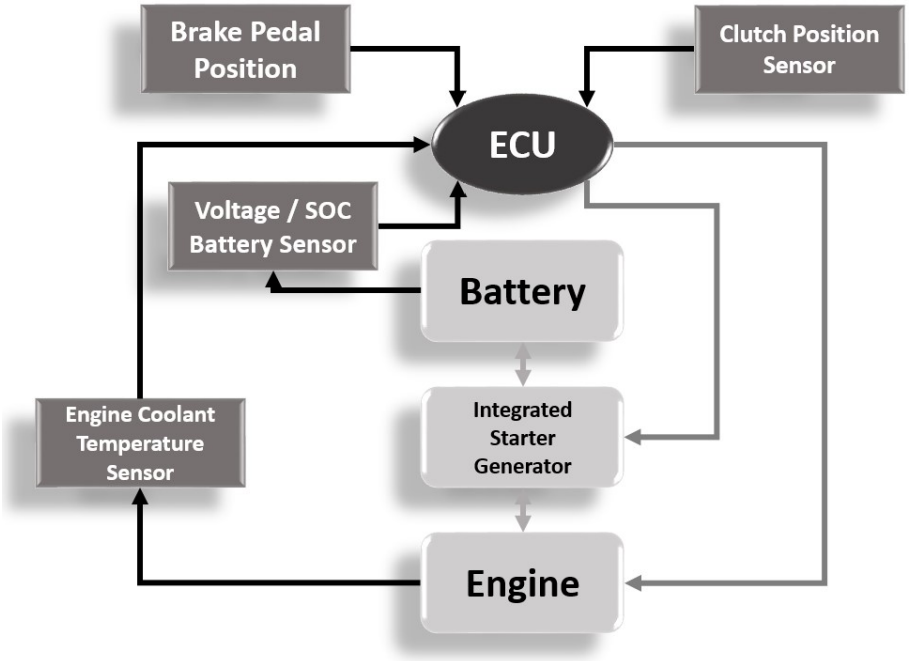

Figure 5.1: The schematic of the Start-stop technology data flow along with ECU

As soon as the driver releases the brake pedal or, engages the clutch in manual transmission, or intends to accelerate, the system quickly restarts the engine, allowing the vehicle to resume motion without delay. The technology is designed to operate smoothly and gradually to avoid the driver discomfort. The vehicle's electrical system typically powers the cabin accessories, AC, infotainment, and lights while the engine is off, ensuring driver comfort and safety; thus, highly durable 12V Absorbed Glass Mat (AGM) batteries are a distinctive battery variant that is frequently utilized in start-stop applications due to their extended cycle life in comparison to Enhanced Flooded Battery (EFB). Research has demonstrated that AGM batteries can endure twice as long as EFB batteries when employed in start-stop applications [70].

5.1.2 Advantages of Start-Stop Technology

The main advantages of start-stop technology are:

i) Fuel Saving: Reducing idling time leads to better fuel economy, especially in city driving conditions where stop-and-go traffic is expected.

ii) Emissions Reduction: Less idling means less emissions of pollutants like CO_2 and nitrogen oxides (NO_x), contributing to cleaner air and reduced greenhouse gas emissions.

iii) Noise Reduction: With engines automatically turning off during stops, the auditory experience for drivers and passengers improves. Quieter surroundings, when the engine is turned off, contribute to enhanced comfort during idling periods.

5.1.3 Drawbacks of Start-Stop Technology

Here are the main drawbacks of using start-stop technology in vehicles:

i) The increased number of engine restarts places greater demands on the vehicle's battery. Manufacturers address this concern by employing advanced batteries capable of handling the additional load.

ii) Some drivers may find the engine restarting and stopping somewhat noticeable or annoying, especially in stop-and-go traffic.

iii) Due to the added components, vehicles equipped with start-stop technology will have a slightly higher capital cost.

Looking ahead, the evolution of start-stop technology is poised to be an integral part of the broader shift toward electrification and hybridization. As hybrid and electric vehicles become more prevalent, start-stop technology will serve as a bridge, easing the transition for drivers accustomed to ICE.

5.1.4 Test Procedure

Three university vehicles were tested to evaluate the effectiveness of start-stop technology on fuel consumption and emissions. A Ford Escape S, Chevrolet Silverado 1500, and Ford Econoline 450 were chosen for the test. The specifications of the Ford Escape S were shown previously in Chapter 4, Table 4.14. The Chevrolet Silverado 1500 and the Ford Econoline 450 specifications are shown in Tables 5.1 and 5.2, respectively.

Table 5.1: Specifications of the Chevrolet Silverado 1500 used in this study

Vehicle Specification	
Model Year	2016
Vehicle Body Style	Truck 1/2T
Fuel Type	Gasoline
Engine Type	4.3 L
Engine Rated Power	213 kW @ 5,300 RPM
Engine Torque	414 N.m @ 3,900 RPM
Compressor Ratio	11.0:1
Induction System	Atmospheric
Transmission Type	6-speed Automatic
Vehicle Base Curb Mass	3,402 kg
Fuel Consumption Rate	12.4 L/100 km city/hwy combined

Table 5.2: Specifications of the Ford Econoline 450 used in this study

Vehicle Specification	
Model Year	2018
Vehicle Body Style	Bus – 28 Passenger
Fuel Type	Gasoline
Engine Type	6.8 L
Engine Rated Power	227 kW @ 6,000 RPM
Engine Torque	569 N.m @ 3,250 RPM
Compressor Ratio	9.2:1
Induction System	Atmospheric
Transmission Type	6-Speed Automatic
Vehicle Base Curb Mass	6,577 kg
Fuel Consumption Rate	7.8 L/100 km city/hwy combined

Five routes were selected for the study in this chapter. These routes were selected

according to four vehicle applications used for the UAlberta fleet and also the test route used for fuel tests of this thesis in Chapter 4.

The fuel test route was the same 20.0 km city route used for the fuel tests in Chapter 4 (Figure 4.4). The reason for choosing this route was that it covered a wide range of driving conditions, similar to most of UAlberta's fleet vehicles. The test route map for UAPS was not provided as GPS data was not collected from this application's vehicles due to security concerns.

The University of Alberta's trade vehicles mainly run near the university campus. The test route used for this application was about 6.3 km (Figure 5.2).

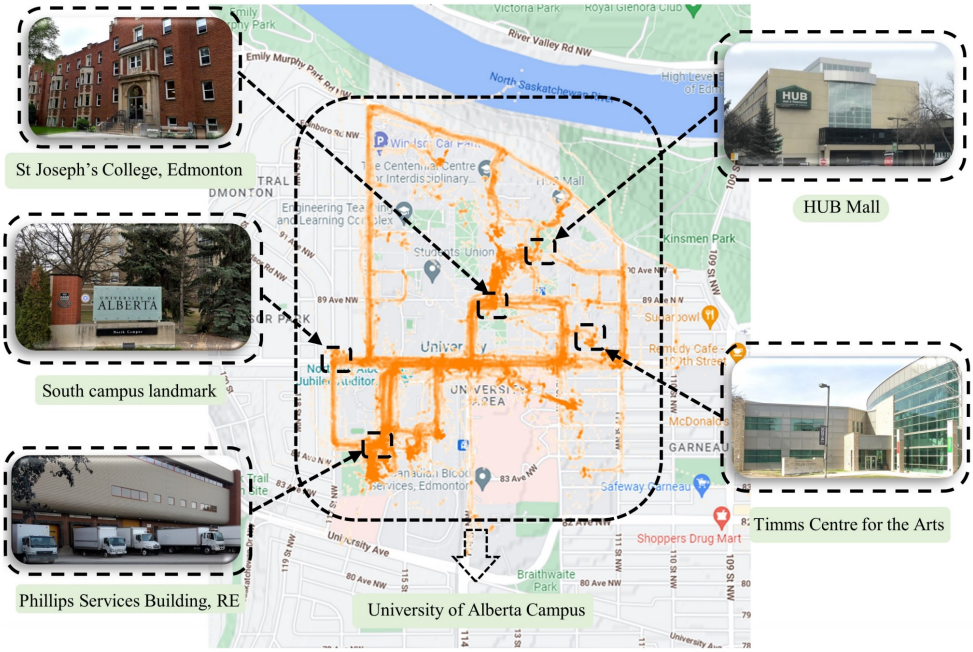

Figure 5.2: The GPS route map for the tested utility and trade vehicles. Data in the figure is from Aug. 17, 2021 to Jan. 20, 2022 data collection [71]

The shuttle minibus traveled from the University of Alberta's North Campus to Campus Saint-Jean (CSJ). The test route from the University of Alberta's North campus to the CSJ was 6.1 km, and the distance from CSJ to the North Campus was 6.3 km, as shown in Figure 5.3.

The test route used for the casual rental vehicle application, shown in Figure 5.4, was about 144.4 km. The casual rentals category mostly ran on highways.

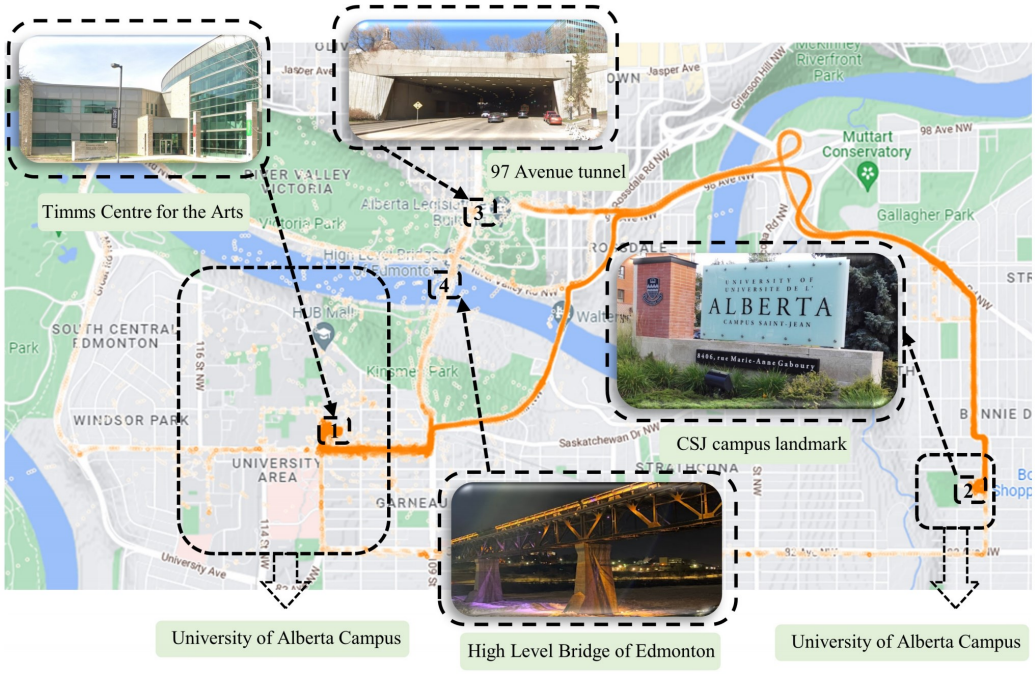

Figure 5.3: The GPS route map for the tested shuttle minibus. Data in the figure is from vehicle testing from Apr. 4, 2022 to Apr. 21, 2022 [71]

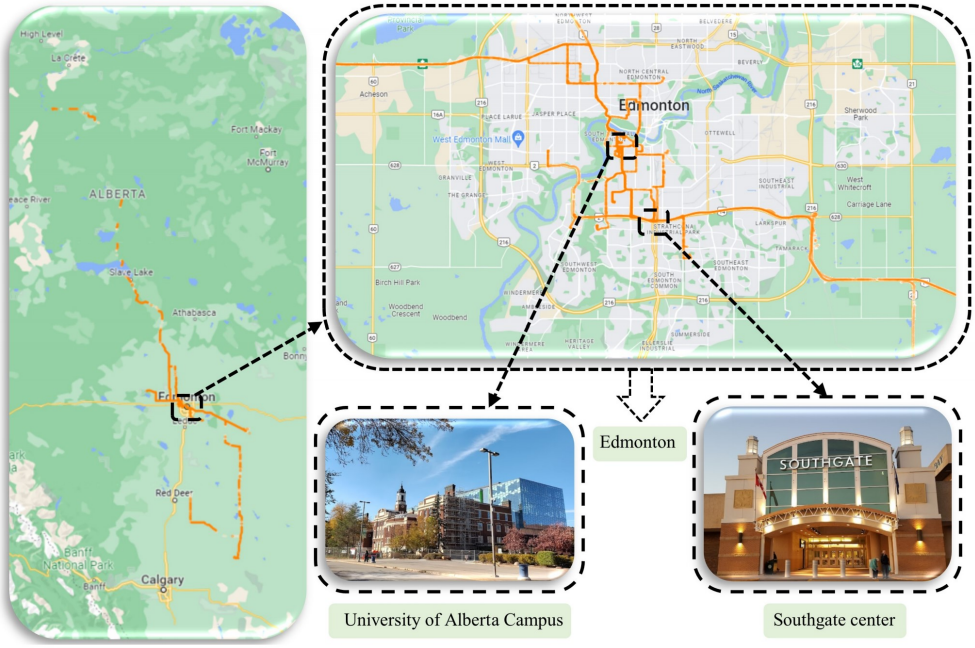

Figure 5.4: The GPS route map for the tested casual rental vehicles. Data in the figure is from May. 12, 2022 to Sep. 14, 2022 [71]

The cycle time for the fuel test route (Figure 5.5) was 2,257 seconds. The idle drive state time accounted for 21.7% of the total time. Thus, the duration of idling

for the test loop was 490 seconds. The Ford Escape S with an engine speed of 750 RPM during idling (fully warmed up) was selected for this test route. The vehicle consumed 0.302 mL/sec during idling, resulting in a total fuel consumption of 147.980 mL during the test.

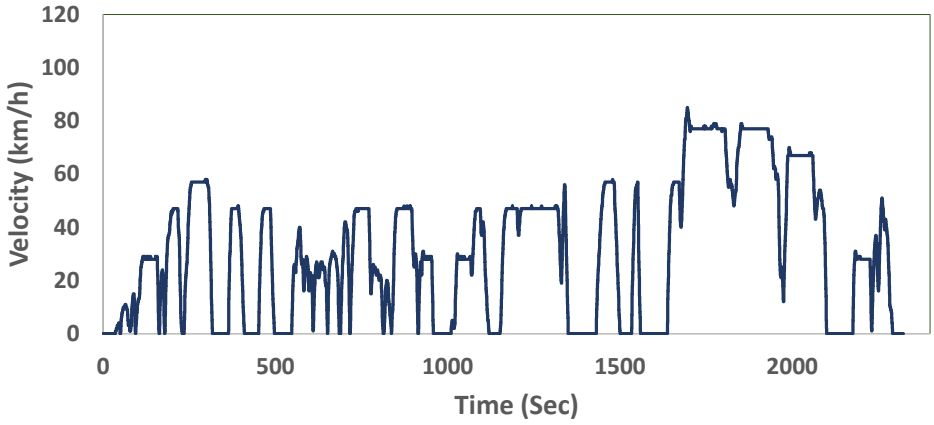

Figure 5.5: The driving cycle for the fuel test route (Figure 4.4)

Figures 5.6, 5.7, 5.8, and 5.9 show the driver test cycles for each of the university vehicle applications. These drive cycles are based on an extensive study done by Liu Yang (See MSc thesis [71]). These cycles are presented in this chapter to extract the percentage of idling time in each university fleet application. Thus, the potential for fuel saving by removing idling via start-stop technology can be determined.

The cycle time for utility and trade vehicles Figure 5.6 was 1,761 seconds. The idle drive state time accounted for 33.7% of the total time. Thus, the duration of idling for the Trade vehicles was 594.6 seconds. The Chevrolet Silverado 1500 had a larger engine compared to the Ford Escape S. With an idling engine speed of 550 RPM and an idling fuel consumption rate of 0.369 mL/sec, the total fuel consumed during idling was approximately 219.407 mL during the test.

The cycle time for the shuttle minibus (Figure 5.7) was 980 seconds. The idle driving state time accounted for 24.7% of the total time, which means 242 seconds for this case. The Shuttle minibus drive cycle test is based on the Ford Econoline 450, which had the largest engine compared to other tested vehicles. With an engine

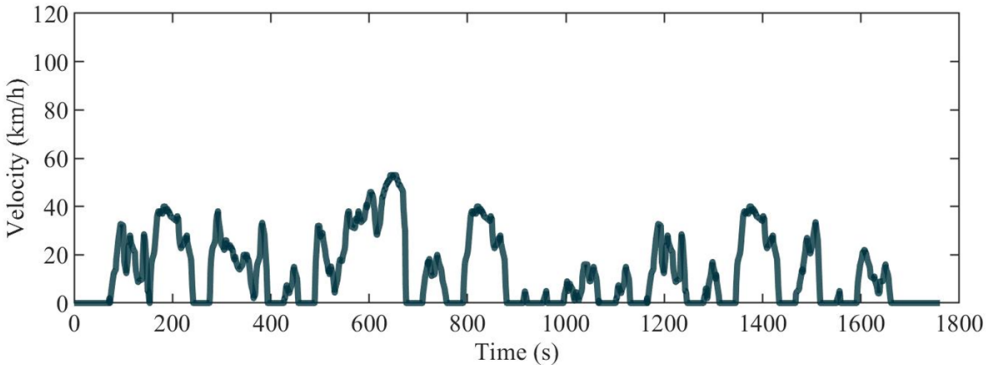

Figure 5.6: The driving cycle for the UAlberta trade vehicles [71]

idling speed of 730 RPM and an idling fuel consumption rate of 0.652 mL/sec, the total fuel consumed during the idling of the test was approximately 157.784 mL.

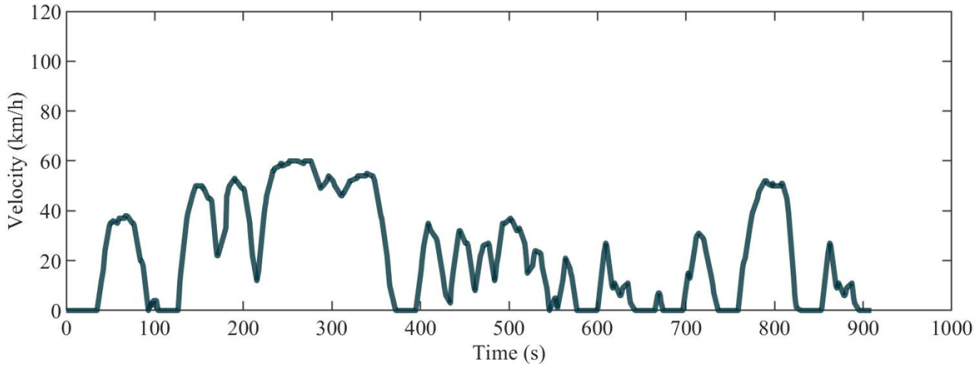

Figure 5.7: The driving cycle for the UAlberta shuttle minibuses [71]

The cycle time for casual rental vehicles in Figure 5.8 was 9,136 seconds. The idle drive state time accounted for 17.6% of the total time. Thus, the idling duration for the causal rental vehicles was 1,607 seconds. The Chevrolet Silverado 1500 was used for the casual rental drive cycle test. With an idling fuel consumption rate of 0.369 mL/sec, the total fuel consumed during idling was approximately 592.983 mL.

The cycle time for UAPS vehicles (Figure 5.9) was 1,221 seconds. The idle drive state time accounted for 41.1% of the total time. Thus, the duration of idling for the Trade vehicles was 502 seconds. The Ford Escape S was used for the UAPS drive cycle test. With an idling fuel consumption rate of 0.302 mL/sec, the total fuel consumed during idling was approximately 151.604 mL during the test.

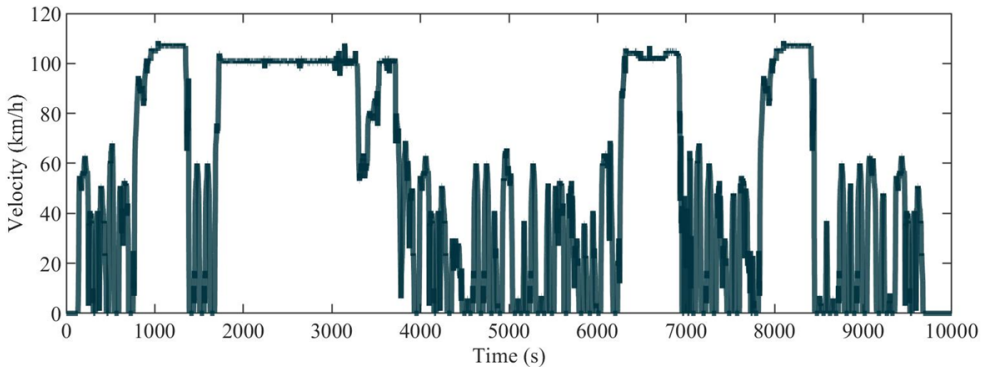

Figure 5.8: The driving cycle for the UAlberta casual rental vehicles [71]

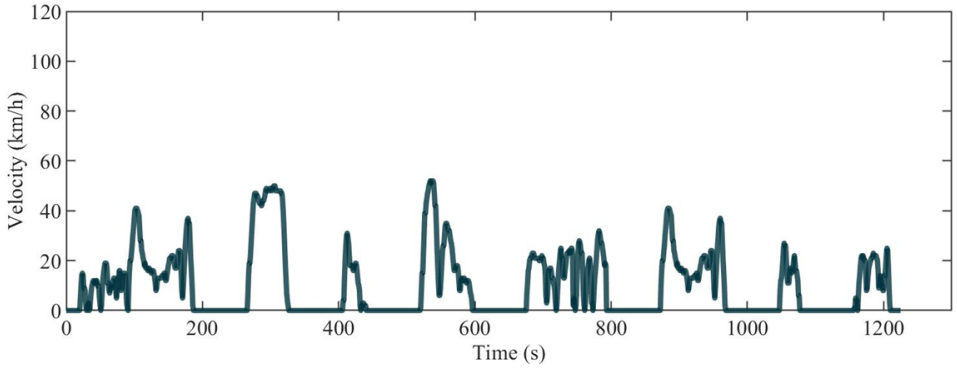

Figure 5.9: The driving cycle for the UAlberta UAPS [71]

The cycle time and idle driving state time for each application of UAlberta fleet vehicles are summarized in Table 5.3.

Table 5.3: The cycle time and idle driving state time based on UAlberta fleet vehicles drive cycles [71] for different applications

Application	**Cycle (km)**	**Cycle Duration (Sec)**	**Idling Duration (Sec)**	**Idle Time Driving State (%)**
Fuel Test	20	2,257	490	21.7
Utility & Trade	6.3	1,761	594.6	33.7
Shuttle Minibus	6.1 - 6.3	980	242	24.7
Casual Rental	144.4	9,136	1,607	17.6
UAPS	3.5	1,221	502	41.1

Based on the data provided in Table 5.3, it can be inferred that UAPS vehicles exhibited the longest idling state time, making up almost 41.1% of the total cycle time. In contrast, casual rental vehicles had the shortest idling state time, constituting only 17.7% of the cycle time.

The effect of start-stop technology on saving the cost of fuel during each second of idling for the three tested vehicles is shown in Table 5.4. The gas prices of $1.267 to $1.900 per liter were used in this study based on Edmonton's regular gas price in 2022.

Table 5.4: The rate of fuel consumption and costs for three sample fleet vehicles

Vehicle	**Fuel Consumption Rate (mL/s)**	**Min Gas Price (126.7¢/L)**	**Ave Gas Price (140.6¢/L)**	**Max Gas Price (190¢/L)**
Ford Escape S	0.302	0.038 (¢/s)	0.042 (¢/s)	0.057 (¢/s)
Chevrolet Silverado 1500	0.369	0.047 (¢/s)	0.052 (¢/s)	0.071 (¢/s)
Ford Econoline 450	0.652	0.083 (¢/s)	0.092 (¢/s)	0.124 (¢/s)

According to Table 5.4, the Ford Econoline 450 had the highest fuel consumption during idling compared to the other two vehicles. This is due to its larger engine size. Specifically, the Ford Econoline 450 consumed 0.652 mL/s, which is almost twice the amount of fuel consumed by the Ford Escape S. By implementing the start-stop technology in Ford Econoline 450 and considering the average gasoline prices in Edmonton, during 10 minutes of idling, a savings of 55.2 ¢can be achieved.

The fuel efficiency and cost savings of UAlberta fleet vehicles were assessed across five different applications using the Ford Escape S, Chevrolet Silverado 1500, and Ford Econoline 450. Tables 5.5, 5.6, 5.7, 5.8, and 5.9 present the results for the fuel test route, UAlberta shuttle minibus, utility & trade, casual rental, and UAPS

applications respectively.

Table 5.5: Total fuel and cost saving for one drive cycle based on fuel test route (Figure 4.4)

Vehicle	**Fuel Saving (mL)**	**Min Gas Price (126.7¢/L)**	**Ave Gas Price (140.6¢/L)**	**Max Gas Price (190¢/L)**
Ford Escape S	147.980	18.75 ¢	20.81 ¢	28.12 ¢
Chevrolet Silverado 1500	180.810	22.91 ¢	25.42 ¢	34.35 ¢
Ford Econoline 450	319.480	40.48 ¢	44.92 ¢	60.70 ¢

Table 5.6: Total fuel and cost saving for one drive cycle based on shuttle minibus application

Vehicle	**Fuel Saving (mL)**	**Min Gas Price (126.7¢/L)**	**Ave Gas Price (140.6¢/L)**	**Max Gas Price (190¢/L)**
Ford Escape S	73.084	9.26 ¢	10.28 ¢	13.89 ¢
Chevrolet Silverado 1500	89.298	11.31 ¢	12.56 ¢	16.97 ¢
Ford Econoline 450	157.784	19.99 ¢	22.18 ¢	29.98 ¢

According to the test results, the Ford Econoline 450 had the greatest fuel cost savings for all applications. Specifically, based on cycle length, this vehicle could save 1,047.764 mL of gasoline for driving one drive cycle based on the casual rental application, amounting to nearly 147 ¢based on Edmonton's average gas price. Based on idling time, the UAPS application had the highest fuel savings of 41.1% of the cycle time, resulting in a gasoline saving of 327.304 mL (costing 46.02 ¢) for the Ford Econoline 450 for driving a 3.5-km drive cycle.

The findings from this chapter can aid UAlberta's fleet management in selecting the

Table 5.7: Total fuel and cost saving for one drive cycle based on utility & trade application

Vehicle	**Fuel Saving (mL)**	**Min Gas Price (126.7¢/L)**	**Ave Gas Price (140.6¢/L)**	**Max Gas Price (190¢/L)**
Ford Escape S	179.569	22.75 ¢	25.25 ¢	34.19 ¢
Chevrolet Silverado 1500	219.407	27.80 ¢	30.85 ¢	41.69 ¢
Ford Econoline 450	387.679	49.12 ¢	54.51 ¢	73.66 ¢

Table 5.8: Total fuel and cost saving for one drive cycle based on casual rental application

Vehicle	**Fuel Saving (mL)**	**Min Gas Price (126.7¢/L)**	**Ave Gas Price (140.6¢/L)**	**Max Gas Price (190¢/L)**
Ford Escape S	485.314	61.49 ¢	68.24 ¢	92.21 ¢
Chevrolet Silverado 1500	592.983	75.13 ¢	83.37 ¢	112.67 ¢
Ford Econoline 450	1,047.764	132.75 ¢	147.32 ¢	199.08 ¢

Table 5.9: Total fuel and cost saving for one drive cycle based on UAPS application

Vehicle	**Fuel Saving (mL)**	**Min Gas Price (126.7¢/L)**	**Ave Gas Price (140.6¢/L)**	**Max Gas Price (190¢/L)**
Ford Escape S	151.604	19.21 ¢	21.32 ¢	28.80 ¢
Chevrolet Silverado 1500	185.238	23.47 ¢	26.04 ¢	35.20 ¢
Ford Econoline 450	327.304	41.47 ¢	46.02 ¢	62.19 ¢

most suitable vehicles for various purposes, considering the engine size of the vehicles and the effects of start-stop technology. Such an approach will undoubtedly reduce fuel consumption by the university fleet vehicles, minimize expenses, and decrease CO_2 emissions.

Chapter 6

Conclusions and Future Works

The transportation sector is a major contributor to greenhouse gas (GHG) emissions, and vehicles are a significant source of GHG emissions. Carbon dioxide (CO_2) is the most prominent GHG produced by vehicles. Thus, reducing fuel/energy consumption of fleet vehicles is important to reduce GHG emissions by the University of Alberta (UAlberta) fleet vehicles. This thesis focused on (i) creating an online platform for collecting data from UAlberta fleet vehicles to monitor their operating conditions, (ii) analysis of the UAlberta fleet vehicles, (iii) developing machine learning models to estimate fuel consumption based on real-time On-Board Diagnostic (OBD) data, (iv) studying the effect of cold climate on electrified and conventional vehicles, and (v) analyzing the effect of start-stop technology on energy consumption and CO_2 emissions of the UAlberta fleet vehicles. The findings from this thesis can help reduce energy consumption and operational costs of the university vehicles and help the fleet manager make informed decisions by identifying areas for improvement.

6.1 Main Contribution from this Thesis

The main contributions of this thesis are:

- **Experimental setup design and implementation:** A combined hardware and software platform was created to collect real-time OBD data from individual university vehicles. The data was transmitted through a cellular network,

stored, and organized in a data server accessible through the university network. The platform was tested for seven simultaneous vehicle data collections. The Freematics data loggers were used to collect data from UAlberta's fleet vehicles and store them in a database. The platform was used for real-time performance monitoring of the UAlberta fleet vehicles. The collected data includes information such as vehicle speed, engine speed, fuel level, and many other relevant Parameter Identifications (PIDs) of the vehicle provided via the OBD Controller Area Network (CAN) bus.

- **Fuel consumption modeling:** Two machine learning algorithms, random forest (RF) and artificial neural network (ANN), were designed for estimating instantaneous fuel consumption using OBD data. This will allow an understanding of how and where the highest fuel consumption and CO_2 emissions occur for each vehicle's operation. It also allows to identify vehicles with high fuel consumption compared to benchmark data. The resulting models can also be used to create fuel consumption and GHG CO_2 reports for the UAlberta fleet vehicles to monitor the university's progress towards increasing sustainability in the university operation.

- **Cold climate effects:** The effect of ambient temperature (T_{amb}) on energy consumption of internal combustion engine (ICE), hybrid electric, and fully electric operation of a vehicle was studied via extensive on-road testing including 213 loops and 4300 km. This allowed the understanding of the rate of energy increase as a function of T_{amb} reduction during winter conditions. This paints a picture of how electrified powertrain technology performs in a cold climate and has a realistic estimate of winter energy consumption and calculation of the payback period for the university vehicles by investing on electrified vehicles.

- **Start-stop technology effects:** This thesis investigated the impact of start-stop technology on energy savings and costs using three vehicles for five driving

cycles based on the UAlberta fleet vehicles' applications. The start-stop technology in the UAlberta fleet is advantageous for applications that involve a higher range of idling, such as UAPS or Utility and Trade applications. However, for applications that are mostly driven on highways with less idling time, such as Casual Rental applications, it is not required to consider vehicles equipped with start-stop technology.

6.2 Conclusions

The main findings from this thesis include:

- The designed data collection platform, utilizing available OBD provided by vehicles, presents an interactive platform that allows users to track the location of vehicles and access relevant information for (i) energy use pattern recognition and (ii) driving cycle extraction and optimization using collected data. Furthermore, the platform can display specific vehicle data (e.g., vehicle speed, location, engine speed, etc) to concentrate on specific data or vehicles of interest. This provides a complete overview of real-time data collected from the vehicles. By analyzing this information, the University of Alberta's fleet management can develop targeted vehicle usage and maintenance strategies to reduce energy consumption, CO_2 emissions, and operating costs.

- The data logger records 2 MB of data per hour per vehicle. At the University of Alberta, with almost 180 vehicles operated for 4 hours each day, the total data generated daily is approximately 1.5 GB. The available PIDs for a vehicle depend on factors like make, model, year of manufacture, and OBD scanner type. The Freematics data logger was able to collect up to 21 PIDs at 1 Hz sampling frequency. Adding more PIDs lowers the sample frequency. The maximum number of 54 PIDs was collected from the UAlberta fleet vehicles.

- Using ANN and RF algorithms was shown to be accurate in estimating fuel consumption for various vehicles. The ANN algorithm has an accuracy of 97% for the Ford F-350 and 96% for the Ford Escape PHEV, while the RF algorithm has an accuracy of 100% for the Ford F-350 and 99% for the Ford Escape PHEV. These algorithms are ideal for calculating fuel usage for fleet vehicles. By utilizing these estimated fuel consumption along with machine learning methods, fuel consumption patterns can be identified, and areas for improvement can be specified, ultimately leading to energy-saving strategies.

- In order to have an accurate fuel consumption model, it was essential to cover a wide range of engine speeds and loads in the training data. The Ford Escape PHEV was equipped with a gasoline engine and an electric motor. It operates on electric power in some conditions, limiting the range of data points and engine operating conditions. Meanwhile, the Ford F-350, powered exclusively by a gasoline engine, has a broader engine operating range, covering a more comprehensive range of driving conditions than the Ford Escape PHEV.

- During the testing of the Ford Escape PHEV's EV Later mode, the engine load was found to be in the range of 40% to 80% at -23 °C and 60% to 80% at T_{amb} 28 °C. This indicates that at higher T_{amb}, the engine load range became narrower, reaching almost 20%. However, there were no significant changes in the engine load for the EV Charge mode across the minimum and maximum tested T_{amb}.

- The Ford Escape PHEV had a 14.4 kWh hybrid battery. A full charge of the hybrid battery with a current 3.2 kW power from zero% state of charge (SOC) to 100% was 12.02 kWh, which was the usable capacity of the battery equivalent to 84% of the total capacity of the hybrid battery. This information needs to be taken into consideration when calculating the vehicle's all-electric range (AER).

- In T_{amb} below 0 °C, when the electric motor powers the vehicle, the positive temperature coefficient (PTC) electric heater uses energy to warm up the cabin, which increases energy consumption using the battery power. On the other hand, warming up the cabin for the EV Charge mode does not significantly impact energy consumption because waste heat from the engine coolant is used to warm up the cabin, reducing the need for additional energy for cabin heating.

- When the ICE is turned on, the coolant and the exhaust three-way catalyst (TWC) temperatures begin to rise. The TWC temperature increased faster than the engine coolant temperature, which is expected since the coolant has a larger thermal mass. For the cold start tests, in which the ICE was not constantly active, the vehicle didn't fully warm up until the end of the test. The T_{amb} impacted the warm-up duration. The engine coolant took twice as long to warm up at T_{amb} below 0 °C (around 800 compared to 400 seconds see in Figure 4.10b). On the other hand, at very low T_{amb} (e.g., -20 °C), the cooling down process of a warmed-up vehicle was relatively long, i.e., more than 6 hours.

- The performance of vehicles with different levels of electrification was affected by T_{amb}. A Ford Escape PHEV was tested in different weather conditions in the T_{amb} rating from -24 °C to 32 °C. During cold start tests, energy consumption was higher than during warm start tests. For instance, in EV Now mode at T_{amb} of -13 °C for cold starts, energy consumption was 664 Wh/km while it was 460 Wh/km at T_{amb} -22 °C for warm starts. EV Charge mode had the highest energy consumption in both scenarios, with 889 Wh/km in T_{amb} -6 °C for cold starts and 1,017 Wh/km in T_{amb} -24 °C for warm starts.

- During cold start tests, EV Now mode consumed over five times more energy when T_{amb} decreased from 29 °C to -13 °C. Auto EV mode consumed about 479% more energy when the T_{amb} decreased from 25 °C to -18 °C. The energy

consumption of the EV Later mode almost doubled by decreasing the T_{amb} from 26 °C to -13 °C. The energy consumption of the EV Charge mode remained almost constant at around 900 Wh/km.

- During warm start tests, changing T_{amb} from 29 °C to -24 °C increased Auto EV mode's energy consumption by 4.5 times. EV Now mode's energy consumption increased threefold by decreasing T_{amb} from 28 °C to -22 °C. EV Later mode's energy consumption doubled by reducing T_{amb} from 28 °C to -23 °C. No significant changes were observed for EV Charge mode. A 107% increase was observed by decreasing T_{amb} from 32 °C to -24 °C.

- The average fuel conversion efficiency for the EV Later mode was 39.9% when the T_{amb} was -23 °C, but it increased to 42.4% at 28 °C. This represented an increase of 5.8% in the average fuel conversion efficiency. Similarly, for the EV Charge mode, the average fuel conversion efficiency at T_{amb} of -24 °C was 40.4%, while it increased to 41.8% at 32 °C. This indicated a 3.5% increase in the average fuel conversion efficiency.

- Increasing the T_{amb} increased fuel conversion efficiency for both EV Later and EV Charge modes. The range of 35% - 40% fuel conversion efficiency at T_{amb} of -23 °C was the most extended duration for the EV later mode of the Ford Escape PHEV. At 28 °C, the highest duration was observed in the range of 40% - 45%. For the EV Charge mode, the peak fuel conversion efficiency was between 35% - 40% at T_{amb} -24 °C and between 40% - 45% at 32 °C.

- Using the ICE engine results in higher energy costs compared to the electric motor due to higher gasoline costs. The cost of the EV charge mode with the most extended active ICE duration was the highest at T_{amb} -24 °C, costing 15.9 ¢/km. EV Later mode with a combination of ICE and the electric motor was the second rank, with the energy cost nearly doubled from 6.1 ¢/km to 11.3

¢/km as the T_{amb} dropped from 28 °C to -23 °C. The EV Now mode was the most efficient at T_{amb} 29 °C, costing only 1.3 ¢/km. During severe cold weather, the cost increased 3.5 times. The Auto EV mode had the highest increase in energy cost, rising from 1.5 ¢/km to 9.4 ¢/km.

- Lowering the T_{amb} resulted in CO_2 emissions increase for all powertrain modes based on Alberta CO_2 intensity value that was used from [25]. The highest recorded emissions occurred during Auto EV mode at T_{amb} -24 °C (231 g/km), while the lowest occurred during EV Now mode at T_{amb} 29 °C (58 g/km). Switching to EV Now mode with T_{amb} at -22 °C increased emissions by almost 3.5 times. Similarly, in EV Later mode, reducing T_{amb} from 28 °C to -23 °C almost doubled CO_2 emissions from 101 g/km to 188 g/km. However, the impact of T_{amb} on CO_2 emissions was minimal in EV Charge mode, with only a 12% increase as it relies more on ICE to run the vehicle and charge the battery.

- PHEVs' CO_2 emissions depend on the CO_2 intensity of the electricity generated. Using clean energy sources, including solar, wind, hydroelectric, and nuclear power, can significantly reduce the environmental impact of transportation. At the time of this study, Manitoba had the highest proportion of clean energy sources. The CO_2 intensity of electricity in Manitoba was 1.2 gCO2/kWh. Based on Manitoba's CO_2 intensity Value, the lowest CO_2 emissions were during the Auto EV and EV Now modes, regardless of T_{amb}, which was extremely cold or warm. However, the highest CO_2 emissions were observed when using the EV Charge mode, followed by the EV Later mode.

- Energy consumption of Ford Escape S was significantly impacted by T_{amb} during both cold and warm starts. For cold starts, energy consumption increased by 12% from T_{amb} 4 °C (792 Wh/km) to 0 °C (888 Wh/km) due to increased rolling resistance and decreased engine efficiency at colder T_{amb}. For warm starts, energy consumption increased by 15% from T_{amb} 14 °C (706 Wh/km) to

-4 °C (814 Wh/km).

- Comparing the energy consumption of the Ford Escape S (i.e., conventional ICE) with PHEV, the energy consumption of the model S was similar to that of the EV Charge mode of the PHEV at lower T_{amb}. Still, at higher T_{amb}, the PHEV consumed more energy than the model S. While the other powertrain modes of the PHEV consumed less energy than the model S, especially at higher T_{amb}, due to the PHEV's electric motor high efficiency.

- Comparing the energy cost of the Ford Escape S with the PHEV, the energy costs for the Ford Escape S were between 15.1 ¢/km to 16.9 ¢/km. In comparison, it was 1.6 ¢/km to 3.6 ¢/km for the EV Now mode, and 2 ¢/km to 5.5 ¢/km for the Auto EV mode, and 8.4 ¢/km to 10.7 ¢/km for the EV Later mode of the Ford Escape PHEV.

- Comparing the CO_2 emission of the Ford Escape S with PHEV, the T_{amb} had a significant impact on CO_2 emissions in the Auto EV and EV Now modes of the PHEV, but a lesser effect on the EV Later and EV Charge modes. While the model S changed slightly with the change of T_{amb}.

- To calculate the return on investment (ROI) of sustainable fleet operations, it is essential to consider various factors such as conventional and PHEV vehicle costs, yearly mileage, fuel/electricity prices, and T_{amb} of vehicle operation. This analysis will assist fleet managers in determining potential savings and cost reductions that can be achieved by implementing energy-efficient strategies. For the case of considering the Ford F-150 Lightning, it was found that the ROI period would be reasonable (4 to 6 years) for high annual mileage applications such as Physical Education and Recreation. This is in contrast to other UAlberta fleet vehicle applications, such as the Information Service and Technology (IST) application, which has a much longer duration of 41 to 66 years (as shown

in Figure 4.46).

- Assigning vehicles for the application based on engine capacity and start-stop tech can improve fuel economy, increase saving costs for fuel, and reduce fleet CO_2 emissions. The effect of start-stop technology on fuel and cost savings was investigated. To this end, three university vehicles, including the Ford Escape S, Chevrolet Silverado 1500, and Ford Econoline 450, were used from the UAlberta fleet vehicles. Four driving routes from the UAlberta fleet vehicle applications were selected, including shuttle minibus, utility & trade, casual rental, UAlberta protection service (UAPS), and the test route used for fuel test. By use of the start-stop system, the Ford Escape S with an idling consumption rate of 0.302 mL/sec, the Chevrolet Silverado 1500 with a rate of 0.369 mL/sec, and the Ford Econoline 450 with a rate of 0.652 mL/sec saved 0.042 ¢/sec, 0.052 ¢/sec, 0.092 ¢/sec respectively, based on average gas price in Edmonton in 2022.

- The fuel test route took 2,257 seconds, with 490 seconds spent idling (21.7%). The utility and trade vehicles had a cycle time of 1,761 seconds, with 594.6 seconds of idling (33.7%). The shuttle minibus had a cycle time of 980 seconds, with 242 seconds spent in an idle driving state (24.7%). The cycle time for casual rental vehicles was 9,136 seconds, with 1,607 seconds of idling (17.6%). The UAPS vehicles had a cycle time of 1,221 seconds, with 502 seconds of idling (41.1%).

- The Ford Econoline 450 had the highest fuel cost savings for casual rentals based on distance and idling time. For a 144.4-km route with a duration of 9,136 seconds, the vehicle saved 1,047.764 mL of gasoline, which cost nearly 147¢based on Edmonton's average gas price in 2022. The UAPS application had the highest fuel savings of 41.1% of the cycle time, resulting in a gasoline saving of 327.304 mL (costing 46.02 ¢for 3.5 km) for the Ford Econoline 450.

6.3 Future Works

There are several ways that this study can be extended for the development of an effective fleet management system for the University of Alberta's fleet vehicles:

- UAlbetra fleet renewal plan for different GHG reduction scenarios can be created by considering findings from this thesis, including ROI, Start-stop saving effect, and vehicle energy consumption based on T_{amb} data.

- The RF and ANN models can be added to the Freematics HUB Graphic User Interface (GUI). These models can be used to monitor the real-time fuel consumption of the vehicles in the UAlberta fleet. By analyzing the collected data and fuel consumption patterns, the operation of the university fleet vehicles can be optimized. This optimization can lead to more efficient and effective use of resources, resulting in the improved overall performance of the UAlberta fleet.

- UAlberta's fleet assignment for daily tasks can be optimized by considering vehicle powertrain technology and findings from this thesis.

- Monitoring driver behavior, such as speeding, harsh braking, and rapid acceleration, can help fleet managers identify areas for improvement in driver training and behavior. This can reduce energy consumption, improve safety, and lower maintenance costs.

- This thesis did not consider/measure slip in winter driving and also the difference between winter vs summer driving. Further studies can be conducted to characterize these effects on vehicle energy consumption as a function of vehicle powertrain (e.g., Hybrid Electric Vehicle (HEV), Electric Vehicle (EV)) and drive train (e.g., All-Wheel Drive (AWD) vs Front-Wheel Drive (FWD)) for winter versus summer driving.

Bibliography

[1] H. Abediasl, A. Ansari, V. Hosseini, C. R. Koch, and M. Shahbakhti, "Real-time fuel consumption estimation using machine learning and on-board diagnostics data," *Proceedings of the Institution of Mechanical Engineers, Part D: J. of Automobile Engineering*, vol. 70, pp. 1–15, 2023. DOI: 10.1177/09544070231185609.

[2] A. Ansari, H. Abediasl, and M. Shahbakhti, "Ambient temperature effects on energy consumption and CO_2 emissions of a plug-in hybrid electric vehicle," *To be submitted to Energies Journal*, pp. 1–23, 2024.

[3] A. Ansari, H. Abediasl, P. R. Patel, V. Hosseini, C. R. Koch, and M. Shahbakhti, "Estimating instantaneous fuel consumption of vehicles by using machine learning and real-time on-board diagnostics (OBD) data," *Canadian Society of Mechanical Engineers (CSME) 2022 International Congress*, pp. 1–6, Jun. 5-8, 2022, Edmonton, AB, Canada.

[4] Y. Liu, A. Ansari, and M. Shahbakhti, "Identification of the driving cycle for university fleet vehicles," *Canadian Society of Mechanical Engineers (CSME) 2022 International Congress*, pp. 1–6, Jun. 5-8, 2022, Edmonton, AB, Canada.

[5] Y. Liu, H. Abediasl, A. Ansari, and M. Shahbakhti, "Characterizing driving behavior and link to fuel consumption for university campus shuttle minibuses," *Canadian Society of Mechanical Engineers (CSME) 2023 International Congress*, pp. 1–6, May 28-31, 2023, Sherbrooke, QC, Canada.

[6] A. Ansari, H. Abediasl, and M. Shahbakhti, "Effect of cold climate on energy consumption of a plug-in hybrid electric vehicle," *Canadian Society of Mechanical Engineers (CSME) 2022 International Congress*, p. 1, Jun. 5-8, 2022, Edmonton, AB, Canada.

[7] U.S. Energy Information Administration (EIA). "Annual energy outlook." (2022), [Online]. Available: https://www.eia.gov/outlooks/aeo/ (visited on 10/15/2022).

[8] M. Muratori, M. Alexander, D. Arent, M. Bazilian, P. Cazzola, E. M. Dede, J. Farrell, C. Gearhart, D. Greene, and A. Jenn, "The rise of electric vehicles—2020 status and future expectations," *J. of Progress in Energy*, vol. 3, no. 2, pp. 1–35, 2021.

[9] G. Rémy, S. Mehar, T. Sophy, S.-M. Senouci, F. Jan, and Y. Gourhant, "Green fleet management architecture: Application to economic itinerary planning," *2012 IEEE Globecom Workshops*, pp. 369–373, 2012, Anaheim, CA, USA.

[10] J. C. Molina, I. Eguia, J. Racero, and F. Guerrero, "Multi-objective vehicle routing problem with cost and emission functions," *J. of Procedia - Social and Behavioral Sciences*, vol. 160, pp. 254–263, 2014.

[11] S. Shahid, A. Minhans, and O. C. Puan, "Assessment of greenhouse gas emission reduction measures in transportation sector of Malaysia," *J. of Teknologi*, vol. 70, no. 4, pp. 1–8, 2014.

[12] H. Tong, W. Hung, and C. S. Cheung, "On-road motor vehicle emissions and fuel consumption in urban driving conditions," *J. of the Air & Waste Management Association*, vol. 50, no. 4, pp. 543–554, 2000.

[13] A. Schoen, A. Byerly, B. Hendrix, R. M. Bagwe, E. C. dos Santos, and Z. B. Miled, "A machine learning model for average fuel consumption in heavy vehicles," *J. of IEEE Transactions on Vehicular Technology*, vol. 68, no. 7, pp. 6343–6351, 2019.

[14] F. Perrotta, T. Parry, and L. C. Neves, "Application of machine learning for fuel consumption modelling of trucks," *2017 IEEE International Conference on Big Data (Big Data)*, pp. 3810–3815, 2017, Boston, MA, USA.

[15] Z. Xu, T. Wei, S. Easa, X. Zhao, and X. Qu, "Modeling relationship between truck fuel consumption and driving behavior using data from internet of vehicles," *J. of Computer-Aided Civil and Infrastructure Engineering*, vol. 33, no. 3, pp. 209–219, 2018.

[16] S. Wickramanayake and H. D. Bandara, "Fuel consumption prediction of fleet vehicles using machine learning: A comparative study," *2016 Moratuwa Engineering Research Conference (MERCon)*, pp. 90–95, 2016, Moratuwa, Sri Lanka.

[17] T. Wu, X. Han, M. M. Zheng, X. Ou, H. Sun, and X. Zhang, "Impact factors of the real-world fuel consumption rate of light duty vehicles in china," *J. of Energy*, vol. 190, pp. 1–12, 2020.

[18] S. Shaw, Y. Hou, W. Zhong, Q. Sun, T. Guan, and L. Su, "Instantaneous fuel consumption estimation using smartphones," *2019 IEEE 90th Vehicular Technology Conference (VTC2019-Fall)*, pp. 1–6, 2019, Honolulu, HI, USA.

[19] A. Pereira, M. Alves, and H. Macedo, "Vehicle driving analysis in regards to fuel consumption using fuzzy logic and OBD-II devices," *2016 8th Euro American conference on telematics and information systems (EATIS)*, pp. 1–4, 2016, Cartagena, Colombia.

[20] X. Shan, P. Hao, X. Chen, K. Boriboonsomsin, G. Wu, and M. J. Barth, "Vehicle energy/emissions estimation based on vehicle trajectory reconstruction using sparse mobile sensor data," *J. of IEEE Transactions on Intelligent Transportation Systems*, vol. 20, no. 2, pp. 716–726, 2018.

[21] P. Borgstedt, B. Neyer, and G. Schewe, "Paving the road to electric vehicles–a patent analysis of the automotive supply industry," *J. of Cleaner Production*, vol. 167, pp. 75–87, 2017.

[22] J. Pielecha, K. Skobiej, and K. Kurtyka, "Exhaust emissions and energy consumption analysis of conventional, hybrid, and electric vehicles in real driving cycles," *J. of Energies*, vol. 13, no. 23, pp. 1–21, 2020.

[23] Center for Sustainability and the Global Environment (SAGE). "Average annual temperature." (2023), [Online]. Available: https://sage.nelson.wisc.edu/data-and-models/atlas-of-the-biosphere/mapping-the-biosphere/ecosystems/average-annual-temperature/ (visited on 02/11/2023).

[24] ECOpoint Inc. "Dieselnet: Emission test cycles." (2023), [Online]. Available: https://dieselnet.com/standards/cycles/index.php (visited on 02/24/2023).

[25] ElectricityMaps. "Live 24/7 CO_2 emissions of electricity consumption." (2022), [Online]. Available: https://app.electricitymaps.com/zone/CA-AB (visited on 12/11/2022).

[26] Idoho National Laboratory (INL). "Comparing energy costs per mile for electric and gasoline-fueled vehicles." (2023), [Online]. Available: https://avt.inl.gov/sites/default/files/pdf/fsev/costs.pdf (visited on 03/21/2023).

[27] N. Shidore, E. Rask, R. Vijayagopal, F. Jehlik, J. Kwon, and M. Ehsani, "Phev energy management strategies at cold temperatures with battery temperature rise and engine efficiency improvement considerations," *SAE International J. of Engines*, vol. 4, no. 1, pp. 1007–1019, 2011.

[28] A. Ghobadpour, S. Kelouwani, A. Amamou, K. Agbossou, and N. Zioui, "A brief review of plug-in hybrid electric vehicles operation in cold climates," *2019 IEEE Vehicle Power and Propulsion Conference (VPPC)*, pp. 1–5, 2019, Hanoi, Vietnam.

[29] R. Suarez-Bertoa, J. Pavlovic, G. Trentadue, M. Otura-Garcia, A. Tansini, and B. Ciuffo, "Effect of low ambient temperature on emissions and electric range of plug-in hybrid electric vehicles," *J. of ACS Omega*, vol. 4, no. 2, pp. 3159–3168, 2019.

[30] J. R. D. Reyes, R. Hoemsen, and R. V. Parsons, "Cold weather travel range and energy consumption of the Chevrolet Volt PHEV," *2015 IEEE Vehicle Power and Propulsion Conference (VPPC)*, pp. 1–6, 2015, Winnipeg, Canada.

[31] I. Koncar and I. S. Bayram, "A probabilistic methodology to quantify the impacts of cold weather on electric vehicle demand: A case study in the uk," *J. of IEEE Access*, vol. 9, pp. 88 205–88 216, 2021.

[32] C. Yu, G. Ji, C. Zhang, J. Abbott, M. Xu, P. Ramaekers, and J. Lu, "Cost-efficient thermal management for a 48v li-ion battery in a mild hybrid electric vehicle," *J. of Automotive Innovation*, vol. 1, pp. 320–330, 2018.

[33] M. Sarmiento-Carnevali, A. Fly, and P. Piecha, "Electric vehicle cold start range estimation through battery-in-loop simulations within a virtual driving environment," 2020, SAE Technical Paper 2020-01-0453.

[34] H. C. Frey, X. Zheng, and J. Hu, "Variability in measured real-world operational energy use and emission rates of a plug-in hybrid electric vehicle," *J. of Energies*, vol. 13, no. 5, pp. 1–23, 2020.

[35] B. Roşca and S. Wilkins, "Enhanced battery model including temperature effects," *2013 World Electric Vehicle Symposium and Exhibition (EVS27)*, pp. 1–8, 2013, Barcelona, Spain.

[36] X. Gong, H. Wang, M. R. Amini, I. Kolmanovsky, and J. Sun, "Integrated optimization of power split, engine thermal management, and cabin heating for hybrid electric vehicles," *2019 IEEE Conference on Control Technology and Applications (CCTA)*, pp. 567–572, 2019, Hong Kong, China.

[37] D. Kum, H. Peng, and N. K. Bucknor, "Optimal energy and catalyst temperature management of plug-in hybrid electric vehicles for minimum fuel consumption and tail-pipe emissions," *J. of IEEE Transactions on Control Systems Technology*, vol. 21, no. 1, pp. 14–26, 2011.

[38] Power Electronic Tips / Schweber, Bill. "Understanding stop/start automobile-engine design, part 1: The idea." (2023), [Online]. Available: https://www.powerelectronictips.com/understanding-stop-start-automobile-engine-design-part-1-idea-faq/ (visited on 03/25/2023).

[39] S. Qiao, Y. Yanding, L. Yinghao, Y. Zhi, W. Zhen, Z. Xiaoyun, and Z. Xuan, "Application of engine intelligent start-stop system in technology of vehicle fuel saving," *2014 Sixth International Conference on Measuring Technology and Mechatronics Automation*, pp. 128–131, 2014, Zhangjiajie, China.

[40] Z. Ma, T. Fu, Y. Wang, W. Zhao, and L. Zhang, "Research on the effects of idling start-stop function on light vehicles fuel consumption and emission under different cycle conditions," *2020 6th International Symposium on Vehicle Emission Supervision and Environment Protection (VESEP2020)*, pp. 1–6, 2021, Tianjin, China.

[41] X. Zhang, H. Liu, C. Mao, J. Shi, G. Meng, J. Wu, and Y. Pan, "The intelligent engine start-stop trigger system based on the actual road running status," *J. of Plos One*, vol. 16, no. 6, pp. 1–16, 2021.

[42] M. Abas, W. W. Salim, M. Ismail, S. Rajoo, and R. Martinez-Botas, "Fuel consumption evaluation of si engine using start-stop technology," *J. of Mechanical Engineering and Sciences*, vol. 11, no. 4, pp. 1–13, 2017.

[43] I. Hascic, F. P. de Vries, N. Johnstone, and N. Medhi, "Effects of environmental policy on the type of innovation: The case of automotive emissions control technologies," *J. of OECD: Economic Studies*, vol. 2009, no. 1, pp. 49–66, 2008.

[44] M. Comes, P. Drumea, M. Blejan, I. Dutu, and A. Vasile, "Ultrasonic flowmeter," *2006 29th International Spring Seminar on Electronics Technology*, pp. 1–4, 2006, St. Marienthal, Germany.

[45] Oak Ridge National Laboratory. "Compare side-by-side." (2023), [Online]. Available: https://www.fueleconomy.gov/feg/Find.do?action=sbs&id=43912 (visited on 02/11/2023).

[46] Oak Ridge National Laboratory. "Detailed test information." (2023), [Online]. Available: https://www.fueleconomy.gov/feg/fe_test_schedules.shtml (visited on 02/20/2023).

[47] J. Ali, R. Khan, N. Ahmad, and I. Maqsood, "Random forests and decision trees," *International J. of Computer Science Issues (IJCSI)*, vol. 9, no. 5, pp. 1–7, 2012.

[48] P. Daponte and D. Grimaldi, "Artificial neural networks in measurements," *J. of Measurement*, vol. 23, no. 2, pp. 93–115, 1998.

[49] H. Abediasl, N. B. Meresht, H. Alizadeh, M. Shahbakhti, C. R. Koch, and V. Hosseini, "Road transportation emissions and energy consumption in cold climate cities," *Urban Climate*, vol. 52, pp. 1–23, 2023.

[50] P. Phlips, T. Megli, and W. Ruona, "Unified power-based analysis of combustion engine and battery electric vehicle energy consumption," *J. of Advances and Current Practices in Mobility*, 202, SAE Technical Paper 2022-01-0532.

[51] D. Basciotti, D. Dvorak, and I. Gellai, "A novel methodology for evaluating the impact of energy efficiency measures on the cabin thermal comfort of electric vehicles," *J. of Energies*, vol. 13, no. 15, pp. 1–16, 2020.

[52] M. V. Prati, M. A. Costagliola, R. Giuzio, C. Corsetti, and C. Beatrice, "Emissions and energy consumption of a plug-in hybrid passenger car in real driving emission (rde) test," *J. of Transportation Engineering*, vol. 4, pp. 1–12, 2021.

[53] Y. Wang, Y. Wen, Q. Zhu, J. Luo, Z. Yang, S. Su, X. Wang, L. Hao, J. Tan, and H. Yin, "Real driving energy consumption and CO_2 & pollutant emission characteristics of a parallel plug-in hybrid electric vehicle under different propulsion modes," *J. of Energy*, vol. 244, pp. 1–11, 2022.

[54] Y. Al-Wreikat, C. Serrano, and J. R. Sodré, "Driving behaviour and trip condition effects on the energy consumption of an electric vehicle under real-world driving," *J. of Applied Energy*, vol. 297, pp. 1–8, 2021.

[55] H. Ribberink, A. Loiselle-Lapointe, and A. Conde, "Chevrolet volt on-road test programs in canada. part 2: Evaluation of gasoline displacement and extreme weather performance in comparison with other vehicles types," *J. of World Electric Vehicle*, vol. 7, no. 1, pp. 154–165, 2015.

[56] H. Lohse-Busch, M. Duoba, E. Rask, K. Stutenberg, V. Gowri, L. Slezak, and D. Anderson, "Ambient temperature (20 °F, 72 °F and 95 °F) impact on fuel and energy consumption for several conventional vehicles, hybrid and plug-in hybrid electric vehicles and battery electric vehicle," 2013, SAE Technical Paper 2013-01-1462.

[57] World Nuclear Association. "Heat values of various fuels - world nuclear association." (2023), [Online]. Available: https://www.world-nuclear.org/information-library/facts-and-figures/heat-values-of-various-fuels.aspx (visited on 07/05/2023).

[58] P. Bielaczyc, A. Szczotka, and J. Woodburn, "The effect of a low ambient temperature on the cold-start emissions and fuel consumption of passenger cars," *Proceedings of the Institution of Mechanical Engineers, Part D: J. of Automobile Engineering*, vol. 225, no. 9, pp. 1253–1264, 2011.

[59] M. Duoba, T. Bohn, and H. Lohse-Busch, "Investigating possible fuel economy bias due to regenerative braking in testing HEVs on 2WD and 4WD chassis dynamometers," *J. of Fuel and Lubricant*, vol. 114, pp. 324–334, 2005.

[60] A. Doyle and T. Muneer, *Traction energy and battery performance modelling*, 2017. DOI: 10.1016/b978-0-12-803021-9.00002-1.

[61] Akins Ford. "How long does it take to charge the ford escape plug-in hybrid?" (2020), [Online]. Available: https://www.akinsford.com/blog/how-long-does-it-take-to-charge-the-ford-escape-plug-in-hybrid/ (visited on 12/03/2022).

[62] GasBuddy-LLC. "Canada national gas station price charts." (2022), [Online]. Available: https://www.gasbuddy.com/charts (visited on 12/10/2022).

[63] GasBuddy-LLC. "Canada national gas station price heat map." (2022), [Online]. Available: https://www.gasbuddy.com/gaspricemap?lat=53.5460983&lng=-113.4937266&z=13 (visited on 12/10/2022).

[64] PlugShare. "University of alberta stadium station." (2022), [Online]. Available: https://www.plugshare.com/location/89039 (visited on 12/11/2022).

[65] Canada Energy Regulator. "Heat values of various fuels - world nuclear association." (2022), [Online]. Available: https://www.cer-rec.gc.ca/en/data-analysis/energy-markets/provincial-territorial-energy-profiles/provincial-territorial-energy-profiles-alberta.html (visited on 12/10/2022).

[66] Natural Resources Canada. "Understanding the tables." (2022), [Online]. Available: https://natural-resources.canada.ca/energy-efficiency/transportation-alternative-fuels/personal-vehicles/choosing-right-vehicle/buying-electric-vehicle/understanding-the-tables/21383 (visited on 12/12/2022).

[67] Oak Ridge National Laboratory. "Compare cars." (2022), [Online]. Available: https://www.fueleconomy.gov/feg/Find.do?action=sbs%5C%5C&id=44878 (visited on 11/19/2022).

[68] Oak Ridge National Laboratory. "Fuel economy in cold weather." (2022), [Online]. Available: https://www.fueleconomy.gov/feg/coldweather.shtml (visited on 11/17/2022).

[69] Natural Resources Canada. "Auto*mart*." (2022), [Online]. Available: https://www.nrcan.gc.ca/sites/nrcan/files/oee/pdf/transportation/fuel-efficient-technologies/autosmart_factsheet_9_e.pdf (visited on 12/15/2022).

[70] P. J. Kollmeyer and T. M. Jahns, "Aging and performance comparison of absorbed glass matte, enhanced flooded, PbC, NiZn, and $LiFePO_4$ 12V start stop vehicle batteries," *J. of Power Sources*, vol. 441, pp. 1–10, 2019.

[71] Y. Liu, "Driving cycle and driver behavior analysis for University of Alberta fleet vehicles," 2023, MSc.Thesis, University of Alberta.

Appendix A: Thesis Publications and Presentations

A.1 Peer Reviewed Journal Papers

1. H. Abediasl, A. Ansari, V. Hosseini, C. R. Koch, and M. Shahbakhti, "Real-time fuel consumption estimation using machine learning and on-board diagnostics data," Proceedings of the Institution of Mechanical Engineers, Part D: J. of Automobile Engineering, vol. 70, pp. 1–15, 2023. doi: 10.1177/09544070231185609.

2. A. Ansari, H. Abediasl, and M.Shahbakhti, "Ambient temperature effects on energy consumption and CO_2 emissions of a plug-in hybrid electric vehicle," To be submitted to Energies Journal, pp. 1–23, 2024.

A.2 Refereed Conference Proceeding Papers

1. A. Ansari, H. Abediasl, P. R. Patel, V. Hosseini, C. R. Koch, and M. Shahbakhti, "Estimating instantaneous fuel consumption of vehicles by using machine learning and real-time on-board diagnostics (OBD) data," Canadian Society of Mechanical Engineers (CSME) 2022 International Congress, pp. 1–6, Jun. 5-8, 2022, Edmonton, AB, Canada.

2. Y. Liu, A. Ansari, and M. Shahbakhti, "Identification of the driving cycle for university fleet vehicles," Canadian Society of Mechanical Engineers (CSME) 2022 International Congress, pp. 1–6, Jun. 5-8, 2022, Edmonton, AB, Canada.

3. Y. Liu, H. Abediasl, A. Ansari, and M. Shahbakhti, "Characterizing driving behavior and link to fuel consumption for university campus shuttle minibuses," Canadian

Society of Mechanical Engineers (CSME) 2023 International Congress, pp. 1–6, May 28-31, 2023, Sherbrooke, QC, Canada.

A.3 Technical Presentation Papers

1. A. Ansari, H. Abediasl, and M. Shahbakhti, "Effect of cold climate on energy consumption of a plug-in hybrid electric vehicle," Canadian Society of Mechanical Engineers (CSME) 2022 International Congress, p. 1, Jun. 5-8, 2022, Edmonton, AB, Canada.

Appendix B: Data Collection and Fuel Measurement Equipment Specifications

B.1 Test Tools Catalogue

B.1.1 Freematics ONE+ Model B Data Logger

Freematics ONE+ Model B integrates ESP32 MCU, 4G LTE-M cellular module and 10Hz GNSS module and some useful peripherals into a OBD dongle that directly plugs into a car's OBD port.

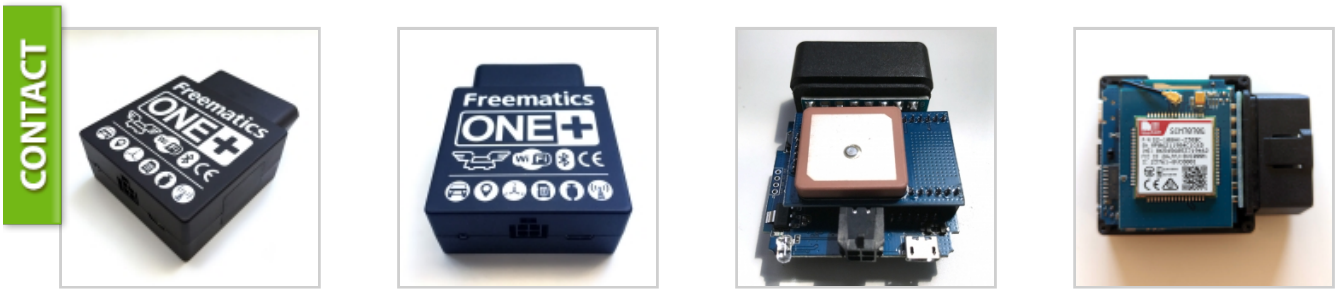

Features

- Dual-core Arduino programmable SoC with built-in WiFi and Bluetooth
- Access to all standard OBD-II PIDs, DTC, VIN from vehicle ECU
- CAN bus data sniffing
- High update rate and accuracy GNSS geolocation
- G-force measurement and motion detection
- Car battery voltage reading
- Massive data storage (microSD up to 32GB)
- Real-time data transmission over WiFi and cellular network
- Configuring and monitoring from mobile device app via BLE

Hardware Facts

Specifications

- Espressif ESP32 with 4MB or 16MB Flash, 8MB PSRAM, 32K RTC
- Built-in 802.11 b/g/n Wi-Fi and dual mode Bluetooth (classic and BLE)
- Integrated ICM-42627 motion sensor
- Integrated u-blox M10 GNSS module and antenna
- Integrated SIM7070G global LTE-M cellular module
- Integrated buzzer
- Enclosure dimensions: 60x48x20mm

Physical Interfaces

- OBD-II male connector
- microUSB port
- microSD card slot
- SIM card slot
- GPIO socket (Molex)

OBD-II Compatibility

CONTACT

ematics ONE+ plugs into the OBD port usually located under the steering column. To check if your hicle is OBD-II certified, open your hood and find the sticker that looks like this:

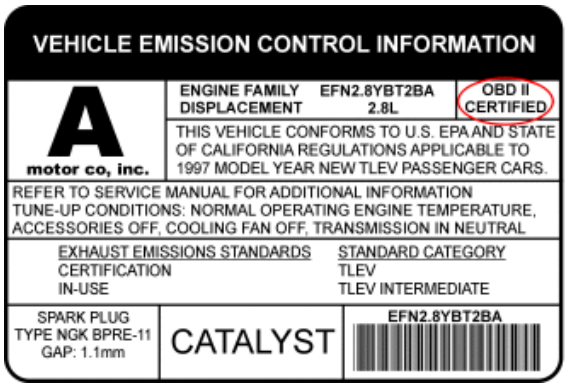

Vehicles using following vehicle protocols are supported.

- CAN 500Kbps/29bit
- CAN 250Kbps/29bit
- CAN 500Kbps/11bit
- CAN 250Kbps/11bit
- KWP2000 Fast
- KWP2000 5Kbps

External I/O

B.1.2 CANedge2 Data Logger

CANedge2 Docs

Specification

CAN-bus (x2)

- Physical
  - Two physical CAN-bus interfaces
  - Industry standard DB9 (D-sub9) connectors
- Transceiver
  - Compliant with CAN Protocol Version 2.0 Part A, B and ISO 11898-1
  - Compliant with ISO CAN FD and Bosch CAN FD
  - Common mode input voltage: ±30V
  - Data rates up to 5Mbps
- Controller
  - 128 standard CAN ID + 64 extended CAN ID filters (per interface)
  - Supports all CAN based protocols (J1939, CANopen, OBD2, NMEA 2000, ...)

Logging

- Extractable industry grade micro SD-card (8-32GB)
- Standard FAT file system (can be read directly by a PC)
- Logging to industry standard `.MF4` (ASAM MDF4) file format
- Log file splitting based on file size or time

Electrical

- Device supply
  - Channel 1 voltage supply range: +7.0V to +32V DC
  - Consumption:
    - CANedge2: 1W
- Secondary port output supply

  Configurable output supply on connector 2 (`CH2`), fixed 5V up to 1.5A

Mechanical

- Dimensions: 50.2 x 83.4 x 24.5 mm (L x W x H)
- Weight: 100g
- Operating temperature: -25 degC to +70 degC

Connector

The CANedge uses two D-sub9 connectors for supply, 2 x CAN, 2 x LIN and a 5 V Supply Output.

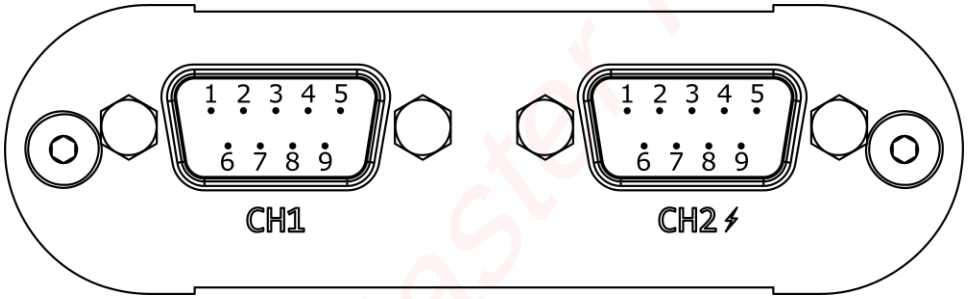

LED

The LEDs are located at the back of the device as illustrated below.

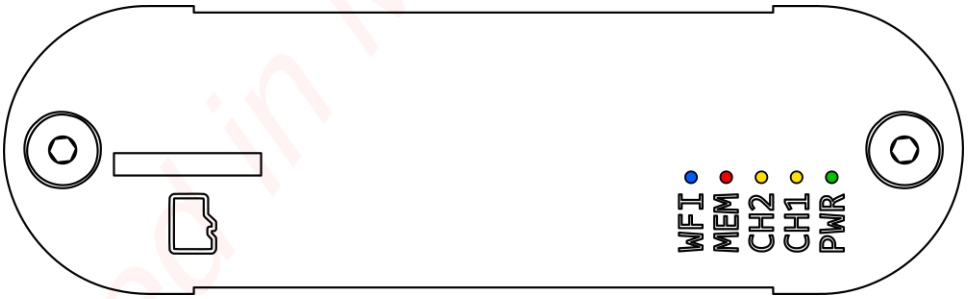

Overview

LED Short Name	LED Color	Main Function
PWR	Green	Power
CH1	Yellow	Bus activity on connector 1 (CH1)
CH2	Yellow	Bus activity on connector 2 (CH2)
MEM	Red	Memory card activity
WFI	Blue	WiFi connected

B.1.3 FlowSonic LF Low-Flow Sensor

FlowSonic® LF Low-Flow Sensor

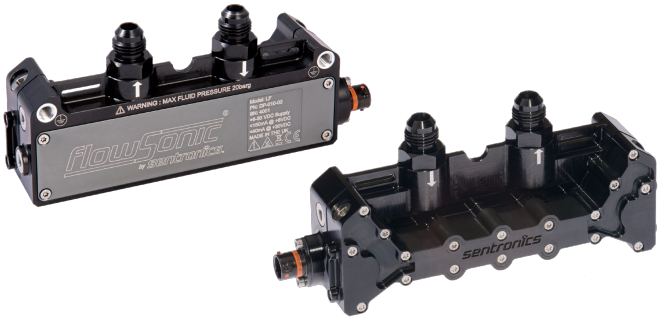

The FlowSonic® LF ultrasonic sensor from Sentronics™ represents a breakthrough in fuel flow measurement technology for automotive engines of every type. The FlowSonic LF has been designed for the ultra low-volume fuel flow conditions found in today's high-efficiency road car engines, making it an ideal tool for R&D as well as emissions testing to the new RDE and WLTP standards. Key features and advantages include:

- Compact, lightweight, no moving parts
- Highly accurate and repeatable
- -40°C to +120°C temperature range
- Fast measurement rate for dynamic flows
- Class-leading ultrasonic turndown ratio
- Easily installed on test bench or vehicle
- Extremely robust and vibration-tolerant
- Internal processing and diagnostics
- CAN, TTL pulse, analog output formats
- Minimal operating and maintenance cost

FlowSonic® LF Dimensions (mm)

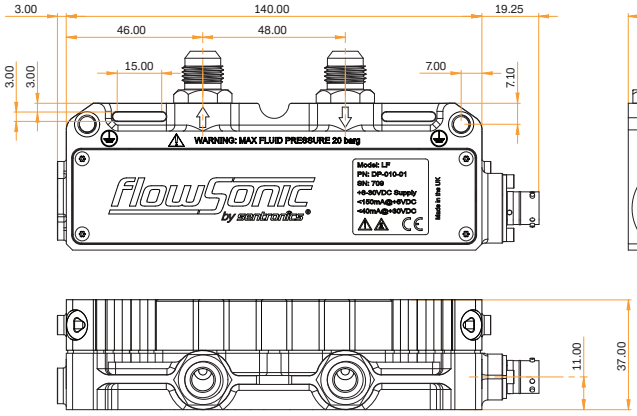

Complete general assembly drawing and CAD data available for download at www.sentronics.com

FlowSonic® LF Pin Out Functions

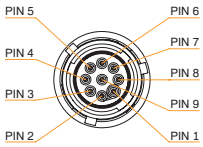

Deutsch ASDD006-09PC-HE Sensor Connector	
Pin 1	Supply +
Pin 2	CAN High
Pin 3	CAN Low
Pin 4	TTL Pulse Output
Pin 5	Analog Output
Pin 6	Comms A
Pin 7	Comms B
Pin 8	CAN Select
Pin 9	Ground (GND)

FlowSonic® LF Specifications and Features DP-010-02

Flow Measurement	
Repeatability	+/- 0.15% of reading
Uncertainty*	+/- 0.5% of reading
Turndown ratio	500:1
Operating flow range	+/- 0-4000 ml/min
Measurement flow range	8-4000 ml/min
Measurement rate	2.2 kHz
Maximum operating pressure	20 barg (2000 kPag)
Pressure drop at maximum flow	< 20 kPa (4000 ml/min for pump petrol @ 20°C)
Fluid temperature range	-20°C to +120°C
Ambient temperature range	-40°C to +120°C
Temperature Measurement	2 x 1000 Ohm RTD (1/3 DIN standard)
Mechanical	
Dry weight	330 g
Fluid capacity	15 ml
Wetted materials	FPM, anodised aluminium alloy, stainless steel
Fuel line connection	-6AN fittings 9/16-inch UNF thread
Deutsch sensor connector	ASDD006-09PC-HE
Deutsch mating connector	ASDD606-09SC-HE
Environmental	
Storage temperature	-40°C to 85°C
External pressure rating	300 kPa
Environmental protection	IP69K (when mated to connector)

** Calculated according to ISO/TR using root-sum square method yielding 95% confidence*

Electrical Supply	
Voltage	8V to 30V DC
Current	< 70 mA @ +12V DC
Voltage protection	Over-voltage 45V DC, reverse polarity -45V DC
CAN Communications	
Design standard	ISO 11898-2 (high-speed applications)
Message format	2.0A (11-bit identifier)
Baud rate	1 Mbit/sec
CAN termination resistor	No
TTL Pulse Output	
Voltage output range	0-5V
Pulses per cc	3000 (fully configurable)
Duty cycle	50%
Output resistance	1.0 kOhm
Analog Output	
Voltage output range	0-10V DC
Resolution	16-bit
Output resistance	47.0 Ohm
Load resistance	> 1.0 kOhm
Configuration Interface	3.3V serial interface
Fuel Compatibility	Petrol, diesel, bio-diesel, ethanol, methanol *please contact us about other fluids*

Specifications subject to change without prior notice

Sentronics Limited
Unit 40, Downton Business Centre
Downton, Salisbury
Wiltshire SP5 3HU England

Telephone +44 (0)1725 513703
Fax +44 (0)1725 513399
Email info@sentronics.com
Web www.sentronics.com

Document LF-DS-02
Issue 0318A

sentronics™

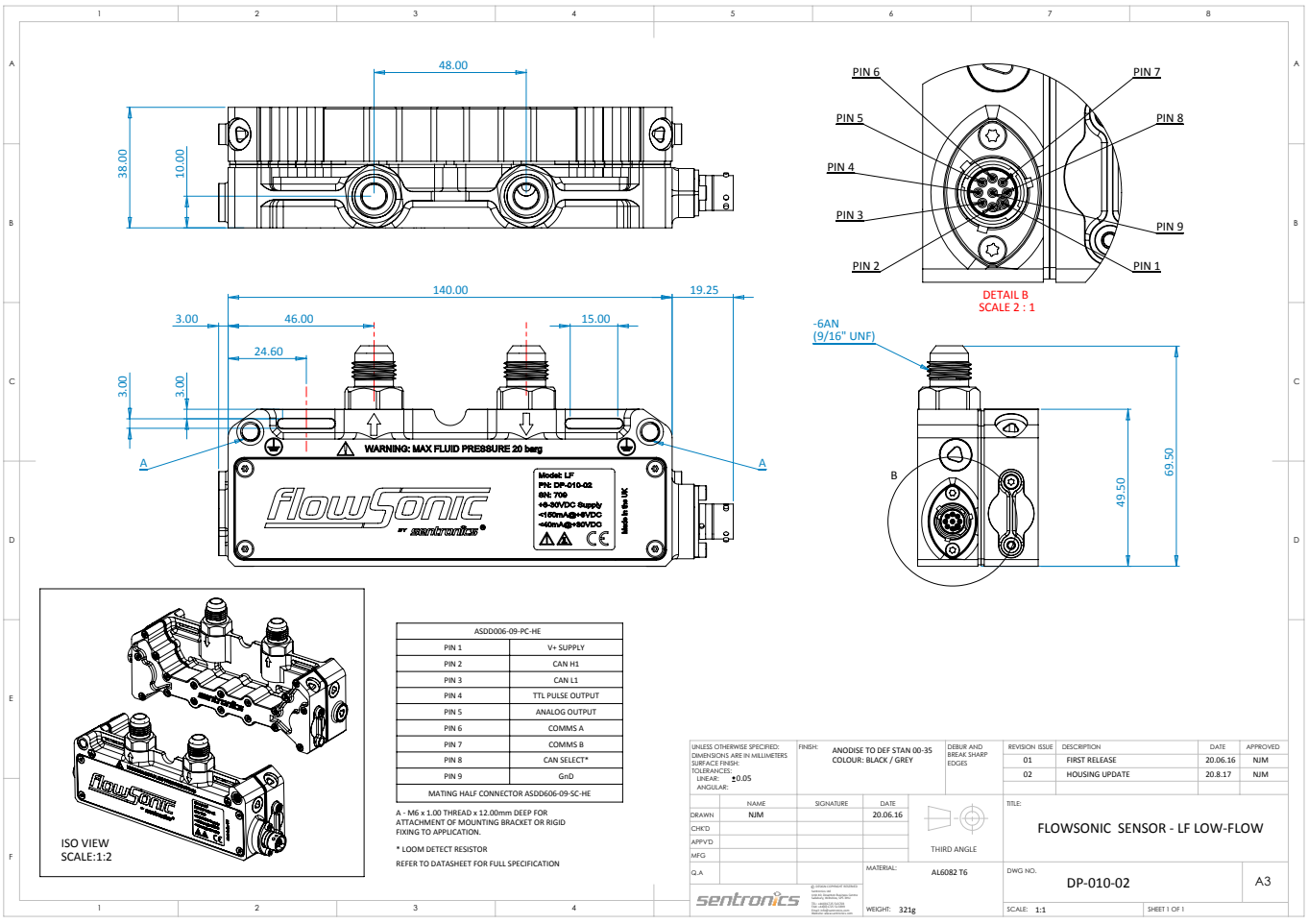

ASDD006-09-PC-HE	
PIN 1	V+ SUPPLY
PIN 2	CAN H1
PIN 3	CAN L1
PIN 4	TTL PULSE OUTPUT
PIN 5	ANALOG OUTPUT
PIN 6	COMMS A
PIN 7	COMMS B
PIN 8	CAN SELECT*
PIN 9	GnD
MATING HALF CONNECTOR ASDD606-09-SC-HE	

A - M6 x 1.00 THREAD x 12.00mm DEEP FOR ATTACHMENT OF MOUNTING BRACKET OR RIGID FIXING TO APPLICATION.

* LOOM DETECT RESISTOR

REFER TO DATASHEET FOR FULL SPECIFICATION

UNLESS OTHERWISE SPECIFIED: DIMENSIONS ARE IN MILLIMETERS SURFACE FINISH: TOLERANCES: LINEAR: ±0.05 ANGULAR:

FINISH: ANODISE TO DEF STAN 00-35 COLOUR: BLACK / GREY

DEBUR AND BREAK SHARP EDGES

REVISION ISSUE	DESCRIPTION	DATE	APPROVED
01	FIRST RELEASE	20.06.16	NJM
02	HOUSING UPDATE	20.8.17	NJM

	NAME	SIGNATURE	DATE
DRAWN	NJM		20.06.16
CHK'D			
APP'VD			
MFG			
Q.A			

THIRD ANGLE

TITLE: FLOWSONIC SENSOR - LF LOW-FLOW

MATERIAL: AL6082 T6

DWG NO. DP-010-02

A3

WEIGHT: 321g

SCALE: 1:1

SHEET 1 OF 1

sentronics

B.2 Test Tools Setup

In order to set up CANedge2, users must do so through the (https://canlogger.csselectronics.com/simple-editor/) website. The configuration settings should be defined using the website's tools, and the resulting configuration should be saved as a JavaScript Object Notation (JSON) file. This JSON file should then be copied to the SD card of the 2x CAN Bus Data Logger device.

Appendix C: Thesis Files

C.1 Program and Data File Summary

The following files were used in this thesis.

C.1.1 Chapter 1

Table C.1: Chapter 1 Figure files

File Name	File Description
Chart1.jpg	Figure 1.1
Light-duty vehicle sales.jpg	Figure 1.2
Global average temperature.jpg	Figure 1.3
Comparing energy costs per mile.png	Figure 1.4
Average energy consumption of top-selling vehicles.jpg	Figure 1.5
Start-stop system components.jpg	Figure 1.6

C.1.2 Chapter 2

Table C.2: Chapter 2 Figure files

File Name	File Description
OBD Protocols.jpg	Figure 2.1
Freematics CAN data logger One+ Model B.jpg	Figure 2.2(a)
Freematics connected.jpg	Figure 2.2(b)
Sample rate of data collection.pdf	Figure 2.3
Freematics CAN data logger connected.jpg	Figure 2.4(a)
Scheme of data collection.jpg	Figure 2.4(b)
Scheme of the data collection platform.jpg	Figure 2.5
Scheme of back-end process.jpg	Figure 2.6
Server IP filtering.jpg	Figure 2.7
Back end of data collection platform.jpg	Figure 2.8
Freematics Hub interface.jpg	Figure 2.9
Scheme of data collection by the CANedge2.png	Figure 2.10
Sentronics flowSonic LF ultrasonic flow meter.jpg	Figure 2.11
Fuel flow meter installed on Chevrolet Silverado 1500.jpg	Figure 2.12a
Fuel flow meter installed on Ford Expedition.jpg	Figure 2.12b
Fuel flow meter installed on Ford Fusion.jpg	Figure 2.12c
Fuel flow meter installed on Ford F-150.jpg	Figure 2.12d

Table C.3: Chapter 2 Figure files

File Name	File Description
Fuel flow meter installed on Ford S.jpg	Figure 2.13a
Fuel flow meter installed on Ford F-350.jpg	Figure 2.13b
Fuel flow meter installed on Ford PHEV.jpg	Figure 2.13c
CSS electronics CANedge2.jpg	Figure 2.14
Asammdf.jpg	Figure 2.15
Ford Escape PHEV FC.jpg	Figure 2.16
Ford Escape S FC.jpg	Figure 2.17
Ford F-350 FC.jpg	Figure 2.18

Table C.4: Chapter 2 data files

File Name	File Description
Ford Escape PHEV.xlsx (Include vehicle's OBD and Sentronics fuel flowmeter collected data)	Figure 2.16
Ford Escape S.xlsx (Include vehicle's OBD and Sentronics fuel flowmeter collected data)	Figure 2.17
Ford F-350.xlsx (Include vehicle's OBD and Sentronics fuel flowmeter collected data)	Figure 2.18

C.1.3 Chapter 3

Table C.5: Chapter 3 Figure files

File Name	File Description
UAlberta South campus transportation service.jpg	Figure 3.1
Ford F-350.jpg	Figure 3.2
Ford Escape PHEV.jpg	Figure 3.3
Route Map1.jpg	Figure 3.4
Scheme of fuel consumption data collection process.jpg	Figure 3.5
EV Charge engine map.jpg	Figure 3.6(a)
Ford F-350 engine map.jpg	Figure 3.6(b)
Time series of speed and fuel consumption PHEV.jpg	Figure 3.7(a)
Time series of speed and fuel consumption F-350.jpg	Figure 3.7(b)
ANN-PHEV.jpg	Figure 3.8(a)
ANN-F-350.jpg	Figure 3.8(b)
RF-PHEV.jpg	Figure 3.9(a)
RF-F-350.jpg	Figure 3.9(b)
Comparing the estimation models for PHEV.jpg	Figure 3.10(a)
Comparing the estimation models for F-350.jpg	Figure 3.10(b)

Table C.6: Chapter 3 python script files

File Name	File Description
Sampling.py	Table 3.7 & Table 3.8 & Table 3.9 & Figure 3.9 & Figure 3.10 & Figure 3.11
Model Selection ANN.py	Table 3.7 & Table 3.8 & Table 3.9 & Figure 3.9 & Figure 3.10 & Figure 3.11
Model Selection RF.py	Table 3.7 & Table 3.8 & Table 3.9 & Figure 3.9 & Figure 3.10 & Figure 3.11
Validation and test ANN.py	Table 3.7 & Table 3.8 & Table 3.9 & Figure 3.9 & Figure 3.10 & Figure 3.11
Validation and test RF.py	Table 3.7 & Table 3.8 & Table 3.9 & Figure 3.9 & Figure 3.10 & Figure 3.11

Table C.7: Chapter 3 data files

File Name	File Description
Ford Escape PHEV EV Charge Map.xlsx (Include Ford Escape PHEV EV Charge mode's OBD record data)	Figure 3.7(a) & Figure 3.8(a) & Table 3.7 & Table 3.8 & Table 3.9 & Figure 3.9(a) & Figure 3.10(a) & Figure 3.11(a)
Ford F-350 Map.xlsx (Include Ford F-350's OBD record data)	Figure 3.7(b) & Figure 3.8(a) & Table 3.7 & Table 3.8 & Table 3.9 & Figure 3.9(b) & Figure 3.10(b) & Figure 3.11(b)

C.1.4 Chapter 4

Table C.8: Chapter 4 Figure files

File Name	File Description
Major factors on energy consumption, and CO2.jpg	Figure 4.1
Recording from the vehicle's instrument cluster display.jpg	Figure 4.2
Button for changing powertrain mode.jpg	Figure 4.3
Ford PHEV instrument cluster display.jpg	Figure 4.4(a)
Route Map2.jpg	Figure 4.4(b)
PHEV SOC status shown on vehicle's display.jpg	Figure 4.5(a)
PHEV Charging details.jpg	Figure 4.5(b)
PHEV Status Shown on Vehicle's Display	Figure 4.5(c)
Energy consumption of Auto EV.pdf	Figure 4.6(a)
Energy consumption of EV Now.pdf	Figure 4.6(b)
Energy consumption of EV Later.pdf	Figure 4.6(c)
Energy consumption of EV Charge.pdf	Figure 4.6(d)
Energy consumption of all modes.pdf	Figure 4.7
TWC warming up time for Auto EV.jpg	Figure 4.8(a)
TWC warming up time for EV Now.jpg	Figure 4.8(b)
TWC warming up time for EV Later.jpg	Figure 4.9(a)
TWC warming up time for EV Charge.jpg	Figure 4.9(b)
Engine coolant warm-up duration for Auto EV.jpg	Figure 4.10(a)
Engine coolant warm-up duration for EV Now.jpg	Figure 4.10(b)
Engine coolant warm-up duration for EV Later.jpg	Figure 4.11(a)
Engine coolant warm-up duration for EV Charge.jpg	Figure 4.11(b)
Cold energy consumption for Auto EV.pdf	Figure 4.12(a)
Cold energy consumption for EV Now.pdf	Figure 4.12(b)
Cold energy consumption for EV Later.pdf	Figure 4.12(c)
Cold energy consumption for EV Charge.pdf	Figure 4.12(d)

Table C.9: Chapter 4 Figure files

File Name	File Description
Cold energy consumption of all modes.pdf	Figure 4.13
Warm energy consumption for Auto EV.pdf	Figure 4.14(a)
Warm energy consumption for EV Now.pdf	Figure 4.14(b)
Warm energy consumption for EV Later.pdf	Figure 4.14(c)
Warm energy consumption for EV Charge.pdf	Figure 4.14(d)
Warm energy consumption of all modes.pdf	Figure 4.15
EV Later -23 engine map.jpg	Figure 4.16(a)
EV Later 28 engine map.jpg	Figure 4.16(b)
EV Charge -24 engine map.jpg	Figure 4.17(a)
EV Charge 32 engine map.jpg	Figure 4.17(b)
EV Later -23 efficiency.jpg	Figure 4.18(a)
EV Later 28 efficiency.jpg	Figure 4.18(b)
EV Charge -24 efficiency.jpg	Figure 4.19(a)
EV Charge 32 efficiency.jpg	Figure 4.19(b)
Duration of fuel efficiency of EV Later -23.jpg	Figure 4.20(a)
Duration of fuel efficiency of EV Later 28.jpg	Figure 4.20(b)
Duration of fuel efficiency of EV Charge -24.jpg	Figure 4.21(a)
Duration of fuel efficiency of EV Charge 32.jpg	Figure 4.21(b)
110V charger.jpg	Figure 4.22(a)
220V charger1.jpg	Figure 4.22(b)
220V charger2.jpg	Figure 4.22(c)
Edmonton's regular gas price summary.jpg	Figure 4.23
12-month average retail regular gas price.jpg	Figure 4.24
Edmonton retail regular gas price.jpg	Figure 4.25
Commercial charge station in Edmonton.jpg	Figure 4.26
Energy cost of Auto EV.pdf	Figure 4.27(a)

Table C.10: Chapter 4 Figure files

File Name	File Description
Energy cost of EV Now.pdf	Figure 4.27(b)
Energy cost of EV Later.pdf	Figure 4.27(c)
Energy cost of EV Charge.pdf	Figure 4.27(d)
Energy cost of all modes.pdf	Figure 4.28
Emissions Intensity of Electricity Generation.png	Figure 4.29
CO2 intensity for Alberta.pdf	Figure 4.30
CO2 Auto EV Alberta.pdf	Figure 4.31(a)
CO2 EV Now Alberta.pdf	Figure 4.31(b)
CO2 EV Later Alberta.pdf	Figure 4.31(c)
CO2 EV Charge Alberta.pdf	Figure 4.31(d)
CO2 all modes Alberta.pdf	Figure 4.32
CO2 all modes Manitoba.pdf	Figure 4.33
S vs. PHEV.jpg	Figure 4.34
Ford Escape S engine.jpg	Figure 4.35(a)
Fuel flow meter installed on Ford S.jpg	Figure 4.35(b)
Cold energy consumption of S.pdf	Figure 4.36(a)
Warm energy consumption of S.pdf	Figure 4.36(b)
Energy consumption of Ford Escape S Vs. PHEV.pdf	Figure 4.37
Energy cost of Ford Escape S vs. PHEV.pdf	Figure 4.38
Ford Escape S Vs. PHEV CO2 emission.pdf	Figure 4.39
ROI of PHEV based on distance Auto EV.pdf	Figure 4.40(a)
ROI of PHEV based on distance EV Now.pdf	Figure 4.40(b)
ROI of PHEV based on distance EV Later.pdf	Figure 4.40(c)
ROI for F-150 Lightning XLT based on distance.pdf	Figure 4.41
UAlberta fleet annual average mileage by vehicle.pdf	Figure 4.42
Annual average mileage of trucks.pdf	Figure 4.43

Table C.11: Chapter 4 Figure files

File Name	File Description
ROI of F-150 Lightning by year UAlberta 25.pdf	Figure 4.44
ROI of F-150 Lightning by year UAlberta -7.pdf	Figure 4.45
Annual average mileage of the SUVs of UAlberta.pdf	Figure 4.46
ROI of Ford Escape PHEV by year Vpool Auto EV.pdf	Figure 4.47(a)
ROI of Ford Escape PHEV by year Vpool EV Now.pdf	Figure 4.47(b)
ROI of Ford Escape PHEV by year Vpool EV Later.pdf	Figure 4.47(c)
ROI of Ford Escape PHEV by year PTS Auto EV.pdf	Figure 4.48(a)
ROI of Ford Escape PHEV by year PTS EV Now.pdf	Figure 4.48(b)
ROI of Ford Escape PHEV by year PTS EV Later.pdf	Figure 4.48(c)
ROI of F-150 Lightning by year NRC.pdf	Figure 4.49
ROI for PHEV based on NRCan EV Later.pdf	Figure 4.50(a)
ROI for PHEV based on NRCan Auto EV.pdf	Figure 4.50(b)
ROI for PHEV based on NRCan EV Now.pdf	Figure 4.50(c)

Table C.12: Chapter 4 data files

File Name	File Description
Ford Escape Short Route.xlsx (Include Ford Escape PHEV all tests overview data)	Table 4.4 & Table 4.7
Ford Escape PHEV Data 1.xlsx & Ford Escape PHEV Data 2.xlsx (Include Ford Escape PHEV OBD record data)	Figure 4.6 & Figure 4.7 & Table 4.8 & Figure 4.12 & Figure 4.13 & Table 4.9 & Figure 4.14 & Figure 4.15 & Table 4.10 & Figure 4.27 & Figure 4.28 & Table 4.11 & Figure 4.31 & Figure 4.32 & Table 4.12 & Figure 4.33& Table 4.13 & Figure 4.37 & Table 4.17 & Figure 4.38 & Table 4.18 & Figure 4.39 & Table 4.19 & Table 4.20 & Table 4.21 & Table 4.22 & Table 4.23 & Figure 4.40
Ford Escape S Data.xlsx (Include Ford Escape S all tests overview & OBD record data)	Table 4.15 & Table 4.16 & Figure 4.36 & Figure 4.37 & Table 4.17 & Figure 4.38 & Table 4.18 & Figure 4.39 & Table 4.19 & Table 4.20 & Table 4.21 & Table 4.22 & Table 4.23
Auto EV TWC.xlsx (Include TWC warming up for Auto EV mode data)	Figure 4.8(a)
EV Now TWC.xlsx (Include TWC warming up for EV Now mode data)	Figure 4.8(b)
EV Later TWC.xlsx (Include TWC warming up for EV Later mode data)	Figure 4.9(a)
EV Charge TWC.xlsx (Include TWC warming up for EV Charge mode data)	Figure 4.9(b)
Auto EV Engine Coolant.xlsx (Include engine coolant warming up for Auto EV mode data)	Figure 4.10(a)
EV Now Engine Coolant.xlsx (Include engine coolant warming up for EV Now mode data)	Figure 4.10(b)
EV Later Engine Coolant.xlsx (Include engine coolant warming up for EV Later mode data)	Figure 4.11(a)

Table C.13: Chapter 4 data files

File Name	File Description
EV Charge Engine Coolant.xlsx (Include engine coolant warming up for EV Charge mode data)	Figure 4.11(b)
EV Later 2-2 -23.xlsx (Include EV Later mode OBD record data at T_{amb} of -23 °C)	Figure 4.16(a) & Figure 4.18(a) & Figure 4.20(a)
EV Later 27-7 28.xlsx (Include EV Later mode OBD record data at T_{amb} of 28 °C)	Figure 4.16(b) & Figure 4.18(b) & Figure 4.20(b)
EV Charge 21-2 -24.xlsx (Include EV Charge mode OBD record data at T_{amb} of -24 °C)	Figure 4.17(a) & Figure 4.19(a) & Figure 4.21(a)
EV Charge 28-7 32.xlsx (Include EV Charge mode OBD record data at T_{amb} of 32 °C)	Figure 4.17(b) & Figure 4.19(b) & Figure 4.21(b)
2019-2020 Vehicle Annual Mileages (Include UAlberta fleet vehicles annual mileages for 2019-2020)	Figure 4.42 & Figure 4.43 & Figure 4.44 & Figure 4.45 & Figure 4.46 & Figure 4.47 & Figure 4.48 & Figure 4.49 & Figure 4.50

Table C.14: Chapter 5 Figure files

File Name	File Description
Scheme of Start-Stop Technology.jpg	Figure 5.1
Trade vehicles map.jpg	Figure 5.2
Shuttle minibus map.jpg	Figure 5.3
Casual rental vehicles map.jpg	Figure 5.4
Ford Escape S driving cycle.pdf	Figure 5.5
Trade vehicles driving cycle.png	Figure 5.6
Shuttle minibus driving cycle.png	Figure 5.7
Casual rental vehicles driving cycle.png	Figure 5.8
UAPS driving cycle.png	Figure 5.9

Table C.15: Chapter 5 data files

File Name	File Description
Ford Escape S Fuel consumption.xlsx (Include Ford Escape S fuel consumption)	Figure 5.5
Ford Econoline 450 Fuel Consumption.xlsx (Include Ford Econoline 450 fuel consumption)	Table 5.4 & Table 5.5 & Table 5.6 & Table 5.7 & Table 5.8 & Table 5.9
Ford Escape S Idle Fuel Consumption.xlsx (Include Ford Escape S idling fuel consumption)	Table 5.4 & Table 5.5 & Table 5.6 & Table 5.7 & Table 5.8 & Table 5.9
Chevy Silverado Idling Fuel Consumption.xlsx (Include Chevy Silverado 1500 idling fuel consumption)	Table 5.4 & Table 5.5 & Table 5.6 & Table 5.7 & Table 5.8 & Table 5.9
UAlberta Application Driving Cycles (Include UAlberta fleet vehicles' application driving cycles)	Table 5.5 & Table 5.6 & Table 5.7 & Table 5.8 & Table 5.9